



**This electronic thesis or dissertation has been  
downloaded from Explore Bristol Research,  
<http://research-information.bristol.ac.uk>**

*Author:*

**Turner, Andrew David**

*Title:*

**Recognition of photic zone anoxia from LC-MS studies of porphyrin distributions in  
ancient sediments.**

**General rights**

Access to the thesis is subject to the Creative Commons Attribution - NonCommercial-No Derivatives 4.0 International Public License. A copy of this may be found at <https://creativecommons.org/licenses/by-nc-nd/4.0/legalcode>. This license sets out your rights and the restrictions that apply to your access to the thesis so it is important you read this before proceeding.

**Take down policy**

Some pages of this thesis may have been removed for copyright restrictions prior to having it been deposited in Explore Bristol Research. However, if you have discovered material within the thesis that you consider to be unlawful e.g. breaches of copyright (either yours or that of a third party) or any other law, including but not limited to those relating to patent, trademark, confidentiality, data protection, obscenity, defamation, libel, then please contact [collections-metadata@bristol.ac.uk](mailto:collections-metadata@bristol.ac.uk) and include the following information in your message:

- Your contact details
- Bibliographic details for the item, including a URL
- An outline nature of the complaint

Your claim will be investigated and, where appropriate, the item in question will be removed from public view as soon as possible.

**RECOGNITION OF PHOTIC ZONE ANOXIA  
FROM LC-MS STUDIES  
OF PORPHYRIN DISTRIBUTIONS  
IN ANCIENT SEDIMENTS**

By

**Andrew David Turner**

October 1998

This thesis is submitted to the Faculty of Science of the University of Bristol, U.K.  
In fulfillment of the requirements for the degree of Doctor of Philosophy

Page  
numbering as  
original

## Declaration

I hereby certify that the work described herein is my own, except where otherwise stated, and has not been submitted for any degree at this, or any other university

A handwritten signature in black ink, reading "Andrew Turner". The signature is written in a cursive style with a long, sweeping horizontal line extending to the right.

Andrew D. Turner



**Dedicated to Mum and Dad**

**Also to the memories of  
Muriel Turner  
Ben and Muriel Morris**

## PREFACE

This thesis is submitted to the Faculty of Science of the University of Bristol, U.K.

In fulfillment of the requirements of the degree of Doctor of Philosophy.

The thesis comprises seven chapters describing work carried out between 1994-1997.

Chapters 2-6, preceded by a general introduction, are the central part of the thesis, which are the analytical studies of porphyrin distributions present in a wide range of sedimentary rock samples.

The experimental work was performed in the laboratories of the organic geochemistry unit (OGU), University of Bristol, England.

The study was performed with Prof. J.R. Maxwell as advisor and was conducted with funding from the Petroleum Research Fund (PRF) of the American Chemical Society.

Parts of this work have been presented earlier:

Results from chapters 2, 3 and 5 were presented orally at the 18<sup>th</sup> International Meeting on Organic Geochemistry in Maastricht, Netherlands (September, 1997) and also at the 9<sup>th</sup> Meeting of the British Organic Geochemical Society (BOGS) in Newcastle, England (July, 1997).

# **CONTENTS**

ACKNOWLEDGEMENTS	i
ABSTRACT	ii
ABBREVIATIONS	iv
NOMENCLATURE	vi

## CHAPTER ONE : INTRODUCTION

SEDIMENTARY PORPHYRINS	1
General	1
<i>Alkyl porphyrins</i>	1
<i>Porphyrin carboxylic acids</i>	3
<i>Bound porphyrins</i>	3
Structural types	4
<i>Cycloalkanoporphyrins (CAPs)</i>	6
<i>Aetioporphyrins (Aetios)</i>	6
<i>Bicycloalkanoporphyrins (BiCAPs)</i>	7
<i>Benzocycloalkanoporphyrins (BenzoCAPs)</i>	7
<i>CAPs with rearranged exocyclic ring</i>	8
Isolation, separation and structure determination	8
Chlorophylls	12
<i>General</i>	12
<i>Bacteriochlorophylls</i>	13
<i>Green Sulphur Bacteria</i>	14
Biomarkers of Green Sulphur Bacteria	15
<i>Porphyrins</i>	15
Other biomarkers	17
<i>Aryl isoprenoids</i>	17
<i>Maleimides</i>	18
Present study	19

## CHAPTER TWO : INITIAL PORPHYRIN LC-MS STUDIES

INTRODUCTION	21
Kupferschiefer	21
General	21
Previous biomarker studies of Kupferschiefer from the Lower Rhine Basin	21
<i>Porphyryns</i>	21
<i>Other biomarkers</i>	23
<i>Kupferschiefer core samples</i>	24
Serpiano oil shale	24
Previous porphyrin studies	25
RESULTS AND DISCUSSION	25
LC-MS coinjection studies	25
Kupferschiefer core	34
LC-MS studies of Serpiano oil shale	43

## CHAPTER THREE : LC-MS STUDIES OF PORPHYRINS FROM TERTIARY EVAPORITIC MARLS

INTRODUCTION	45
Mulhouse Basin	46
General	46
Depositional setting	46
<i>Marls</i>	46
<i>Evaporites</i>	49
Biomarkers of photic zone anoxia	50
<i>Porphyryns</i>	50
<i>Aryl isoprenoids</i>	51
Vena del Gesso	51
General	51
Pigment distributions	52
<i>Porphyryns</i>	52
<i>Carotenoids</i>	54
<i>Stratigraphic analysis</i>	54
RESULTS AND DISCUSSION	55

Mulhouse Basin	55
Vena del Gesso	64
<i>Stratigraphic analysis</i>	68

## CHAPTER FOUR : LC-MS STUDIES OF PORPHYRINS DEPOSITED DURING THE CENOMANIAN/TURONIAN OCEANIC ANOXIC EVENT

INTRODUCTION	73
Composition and occurrence of black shales	73
Accumulation of organic matter	75
<i>Productivity</i>	76
<i>Preservation</i>	77
Present day depositional environments	78
<i>Deep stratified anoxic basin</i>	78
<i>Oxygen minimum zone</i>	80
Mesozoic oceanic black shales	82
Oceanic Anoxic Events	84
Cenomanian/Turonian anoxic event	88
<i>This study</i>	89
Tethyan margin	90
<i>Central Italy "Livello Bonarelli"</i>	90
<i>Tunisia "Oued Bahloul"</i>	96
North Atlantic	97
<i>Circulation of the mid-Cretaceous Atlantic</i>	100
<i>Supply of organic matter</i>	102
RESULTS – LIVELLO BONARELLI	103
General	103
Contessa Gorge Quarry	105
<i>Porphyrin distributions</i>	105
<i>HMW CAPs</i>	107
Bottacione Gorge	124
<i>Porphyrin distributions</i>	124
Monte Petrano, Cagli	127

<i>Porphyrin distributions</i>	127
Moria	129
<i>Porphyrin distributions</i>	131
Fosto	131
<i>Porphyrin distributions</i>	133
Gorgo A Cerbara – Torrente Candigliano	137
DISCUSSION – LIVELLO BONARELLI	137
General	137
Variations in depositional conditions	140
Palaeoenvironment	142
RESULTS – OUED BAHLOUL	146
RESULTS – SOUTHERN NORTH ATLANTIC	150
Porphyrin distributions	151
HMW CAP distributions	153
DISCUSSION – SOUTHERN NORTH ATLANTIC	155
Discussion - CAPs	158
<i>Organic richness and sulphur content</i>	158
<i>Porphyrin metallation</i>	158
CONCLUSIONS	162

## CHAPTER FIVE : LC-MS STUDIES OF PORPHYRINS DEPOSITED DURING THE APTIAN AND TOARCIAN OCEANIC ANOXIC EVENTS

INTRODUCTION	166
General	166
Aptian OAE:- “Livello Selli”	166
Toarcian OAE	169
Southern European sections	170
<i>Belluno</i>	170
<i>Valdorbia</i>	172
Northern European sections	173
<i>Paris Basin (Semécourt and Colombotte)</i>	174
<i>SW German Basin (Holzmaden)</i>	174

RESULTS AND DISCUSSION – APTIAN	176
RESULTS – TOARCIAN	182
Tethyan continental margins	182
<i>Valdorbia</i>	182
<i>Belluno</i>	185
North European Epicontinental Seas	187
<i>Paris Basin</i>	187
<i>Holzmaden</i>	189
DISCUSSION – TOARCIAN	189

## CHAPTER SIX : OVERVIEW AND FUTURE RECOMMENDATIONS

OVERVIEW	195
FUTURE WORK	204

## CHAPTER SEVEN : EXPERIMENTAL

GENERAL	207
Solvents and Glassware	207
Extraction	207
Fractionation	207
<i>Column chromatography</i>	207
<i>Gel Permeation Chromatography (GPC)</i>	208
INSTRUMENTATION	209
Ultraviolet/visible (Uv/vis) Spectrophotometry	209
High Performance Liquid Chromatography (HPLC)	209
Liquid Chromatography-Atmospheric Pressure Ionisation-Mass Spectrometry (LC-APCI-MS)	209
Demetallation of metallo porphyrins	210
APPENDICES	
Appendix A	212
Appendix B	212
Appendix C	215
STRUCTURES	216
REFERENCES	225



## LISTS OF FIGURES

### Chapter one

1.1 Transformation pathways for chl <i>a</i> to DPEP	2
1.2 Examples of alkyl porphyrin structural types	5
1.3 Alkyl bacterioporphyrins from diagenetic transformation of bacteriochls <i>c</i> , <i>d</i> and <i>e</i>	16

### Chapter two

2.1 Palaeogeography of the Lower Rhine Basin, NW Germany	22
2.2 Partial LC-APCI-MS chromatogram of ex-iron porphyrin fraction of Kupferschiefer, with carbon numbers of major peaks labelled	27
2.3 Mass chromatograms of high molecular weight components in Kupferschiefer using HPLC conditions shown in program 2	28
2.4 Mass chromatograms of high molecular weight CAP components in ex-iron porphyrin fraction of Kupferschiefer using modified HPLC conditions shown in program 3	29
2.5 Partial mass chromatograms for HMW components of ex-iron fraction (a) before coinjection of standards (b) after coinjection of C <sub>34</sub> <i>n</i> -Pr Et (34b) and (c) of C <sub>34</sub> <i>i</i> -Bu Me (33) standards	31
2.6 Partial mass chromatograms for HMW components of ex-iron fraction after coinjection of (a) C <sub>34</sub> non-PZA (46a,b) standard (b) C <sub>35</sub> <i>i</i> -Bu Et (34c) standard and (c) C <sub>33</sub> Et Et (34a) standard	32
2.7 Partial mass chromatograms for HMW CAPs showing with shaded peaks showing components co-eluting with porphyrins from the bacteriochlorophyll <i>d</i> series	33
2.8 Partial mass chromatograms for early eluting CAPs (C <sub>32</sub> -C <sub>36</sub> ) from Kupferschiefer bulk sample	35
2.9 Partial mass chromatograms showing HMW CAP (C <sub>33</sub> -C <sub>35</sub> ) components for ex-Ni porphyrins in selected samples (1,3,5,10,15&20)	36
2.10 Plot of C <sub>34</sub> (peak c) component / C <sub>32</sub> (DPEP) through core	38
2.11 Plot of Me <i>i</i> -Bu / Me Et maleimides through core	39

2.12 Plot of major C <sub>35</sub> component / C <sub>32</sub> (DPEP) through core	41
2.13 Plot of bacteriochl <i>d</i> C <sub>33</sub> component / C <sub>32</sub> (DPEP) through core	42
2.14 Partial mass chromatograms showing HMW CAPs present in ex-vanadyl porphyrin fraction from Serpiano oil shale	44

### Chapter three

3.1 Tertiary evaporite basins of the Upper Rhine Graben, showing location of Mulhouse Basin	47
3.2 Stratigraphy of the Mulhouse Basin showing depth and organic matter type (A, B or C)	48
3.3 HPLC distribution of ex-nickel porphyrins from "FMM" bed showing elution range of collected fractions	50
3.4 Schematic representation of lithological succession showing horizons I to XVI	53
3.5 Partial mass chromatograms of HMW CAPs with shaded peaks showing components co-eluting with bacteriochl <i>d</i> -derived porphyrins	57
3.6 Mass spectra of selected HMW CAP components (i) C <sub>33</sub> (ii) C <sub>34</sub> (iii) C <sub>35</sub> from Mulhouse Basin (a) bacteriochl <i>d</i> -derived (b) early eluting (c) late eluting	58
3.7 Partial mass chromatograms for HMW CAPs with shaded peaks showing components co-eluting with bacteriochl <i>d</i> -derived porphyrins	59
3.8 Plots of peak areas of HMW CAPs / C <sub>32</sub> (DPEP) through Salt IV section (a) C <sub>34</sub> (peak c) component (b) C <sub>35</sub> (with same retention as bacteriochl <i>d</i> -derived standard)	61
3.9 Plot of peak areas of early and late eluting HMW CAPs / DPEP through Salt IV section	62
3.10 Partial mass chromatograms for CAPs (C <sub>31</sub> -C <sub>36</sub> ) from selected sub-samples within VDG horizon IV	65
3.11 Partial mass chromatograms for CAPs (C <sub>31</sub> -C <sub>36</sub> ) from selected samples within VDG	66
3.12 Partial mass chromatograms for early eluting CAPs (C <sub>31</sub> -C <sub>36</sub> ) from (a) Kupferschiefer bulk sample (b) VDG IV-4 (c) VDG VI	67
3.13 Depth profiles through marl IV of (a-b) C <sub>34</sub> CAPs (c-e) C <sub>35</sub> CAPs (f) C <sub>36</sub> CAPs vs. C <sub>32</sub> CAP	69

3.14 Depth profiles through VdG (II to XI) of (a-b) C <sub>34</sub> CAPs (c-e) C <sub>35</sub> CAPs (f) C <sub>36</sub> CAPs vs. C <sub>32</sub> CAP	70
3.15 Depth profile of isorenieratene (a) through marl horizon IV (b) through marls II to XI	72

## Chapter four

4.1 Schematic diagrams showing five generalised modern day environments favouring accumulation of organic-rich sediments	79
4.2 Present day map showing Gubbio and Oued Bahloul localities together with highly schematic cross-sections for the Cen/Tur	91
4.3 Map showing positions of Umbrian Cen/Tur sampling locations	93
4.4 Palaeogeography of North Atlantic Ocean during Cen/Tur times with circles indicating positions of investigated sites.	98
4.5 Lithological section of the Cen/Tur Livello Bonarelli at the Contessa Gorge site showing the stratigraphic positions of the studied samples	106
4.6 Partial HPLC-MS base peak chromatogram of demetallated vanadyl fraction with carbon numbers of major peaks labelled	108
4.7 Partial mass chromatograms for HMW components of ex-vanadyl fraction (a) before co-injection of standards (b) after co-injection of C <sub>34</sub> <i>n</i> -Pr Et (34b) and (c) of C <sub>34</sub> <i>i</i> -Bu Me (33) standards	109
4.8 Partial mass chromatograms for HMW components of ex-vanadyl fraction after co-injection of (a) C <sub>34</sub> non-PZA (46a,b) standard (b) C <sub>35</sub> <i>i</i> -Bu Et (34c) and (c) C <sub>33</sub> Et Et (34a) standards	110
4.9 Partial mass chromatograms for CAPs of CGQ1, with shaded peaks showing components co-eluting with porphyrins derived from bacteriochl <i>d</i> series	112
4.10 Partial mass chromatograms for HMW CAPs in Livello Bonarelli samples from Contessa Gorge Quarry (CGQ)	113
4.11 Partial mass chromatograms of CAPs in Contessa Gorge samples (a) "CG" ex nickel (b) "CG" ex vanadyl (c) CGQ1 ex-nickel	114
4.12 Lithological sections of the Cen/Tur Livello Bonarelli at (a) Bottacione Gorge, Gubbio (b) Fosto	115

4.13 Lithological sections of the Cen/Tur Livello Bonarelli at (a) Moria (b) Monte Petrano (Cagli area)	123
4.14 Partial mass chromatograms of CAPs in demetallated nickel porphyrins from Bottacione Gorge, Gubbio (BG1-4)	125
4.15 Partial mass chromatograms of CAPs in demetallated vanadyl porphyrins from Bottacione Gorge, Gubbio (a-c) BG1-3 (d) GU1	126
4.16 Partial mass chromatograms of HMW CAPs ( $C_{33}$ - $C_{35}$ ) from demetallated nickel porphyrins from Monte Petrano (MP0-MP5)	128
4.17 Mass chromatograms of HMW CAPs from (a) demetallated vanadyl porphyrin fraction from Monte Petrano (b) demetallated nickel porphyrin fraction of MP4 with shaded peaks showing early eluting components	130
4.18 Partial mass chromatograms of CAPs ( $C_{32}$ - $C_{35}$ ) in Moria section	132
4.19 Partial mass chromatograms of CAPs ( $C_{32}$ - $C_{35}$ ) from demetallated vanadyl porphyrin fractions from Fosto section (FOS1-4)	134
4.20 Mass chromatograms showing CAP components eluting in F1 demetallated iron porphyrin fraction	135
4.21 HPLC-MS of vanadyl CAPs obtained from Fosto (F1) Bonarelli sample ( $C_{32}$ - $C_{44}$ )	139
4.22 Depth plots of $C_{34}$ peak c component vs. DPEP through Livello Bonarelli sections (a) Monte Petrano (b) Bottacione Gorge	145
4.23 Section of the Bahloul Formation at Oued Bahloul, Tunisia, showing positions of samples containing porphyrins	147
4.24 Partial mass chromatograms of CAPs in demetallated nickel porphyrins from Oued Bahloul (Tunisia)	149
4.25 Partial HPLC-MS base peak chromatogram of demetallated vanadyl fraction of 367-02 with carbon numbers of major peaks labelled	152
4.26 Partial mass chromatograms of CAPs ( $C_{32}$ - $C_{35}$ ) in ex-vanadyl porphyrins from Southern North Atlantic (a) 367-18 (b) 368-63 (c) 144-03 (d) 144-02	154
4.27 Relationship between PZA, TOC (%) and (a) Sulphur (b) Ni/(Ni+VO) porphyrin ratio	159
4.28 Ni/(Ni+VO) ratio vs. peak area ratio of $C_{34}$ peak c to DPEP in PZA samples	161
4.29 Schematic model of deposition of Cenomanian/Turonian black shales (a)	164

Chapter five

5.1 Map of Italy showing locations of Toarcian samples	171
5.2 Palaeogeographic reconstruction of Southern Alps of N. Italy (W to E) during Toarcian	171
5.3 Lithological section of Livello Selli at Gorgo a Cerbara nr. Piobbico, Umbria showing samples taken 1996	177
5.4 Base peak chromatogram of ex-nickel porphyrins in Livello Selli sample GAC1	178
5.5 Partial mass chromatograms of CAPs ( $C_{32}$ - $C_{35}$ ) in Livello Selli samples from Gorgo a Cerbara	179
5.6 Plot of ratio of $C_{34}$ peak c to DPEP in samples from Livello Selli section at Gorgo a Cerbara	181
5.7 Base peak chromatogram of ex-nickel porphyrins in Toarcian sample VAL4 from Valdorbis	183
5.8 Partial HPLC-MS chromatograms of CAPs ( $C_{32}$ - $C_{35}$ ) in ex-nickel Toarcian samples from Valdorbis	184
5.9 Partial mass chromatograms of ex-vanadyl HMW CAPs from Toarcian samples from Belluno (BL)	186
5.10 Partial HPLC-MS chromatograms of demetallated porphyrins from Paris Basin	188
5.11 Mass chromatograms of ex-vanadyl CAPs ( $C_{32}$ - $C_{35}$ ) from Toarcian Holzmaden samples	190
5.12 Peak area $C_{34}$ peak c / DPEP for Toarcian samples (a) Valdorbis (b) Belluno (c) epicontinental sea samples	191
5.13 Sketches of depositional models within the Belluno Basin during the Toarcian	192

Chapter six

6.1 Schematic representation of (a) $C_{34}$ and (b) $C_{35}$ CAP components eluting in porphyrin fractions analysed during this study	201
--	-----

## **LIST OF TABLES**

### **Chapter four**

4.1 TOC and Sulphur data for Cen/Tur Livello Bonarelli samples collected June 1996	105
4.2 Identification of PZA in Livello Bonarelli sediments	141
4.3 Bulk geochemistry for Oued Bahloul samples	146
4.4 Details of North Atlantic DSDP samples	150
4.5 Bulk geochemical data for DSDP North Atlantic samples containing porphyrins	150

### **Chapter five**

5.1 TOC and S and porphyrin data for Livello Selli samples (GAC1-6)	176
5.2 TOC, S and Ni-porphyrin data for Valdorbia sediments	182

### **Chapter seven**

7.1 Solvent composition for gradient elution program 1 during normal-phase semi-preparative isolation of HMW CAP-containing fraction	209
7.2 Details of normal phase HPLC solvent programs utilised during LC-APCI-MS of free base porphyrins	210

## ACKNOWLEDGEMENTS

I firstly wish to thank Prof. James Maxwell F.R.S for his overall supervision and valuable time and help spent during the project and the discussion of this thesis.

Dr. Toni Rosell-Melé is thanked for the initial laboratory supervision, provision of some samples, and for the time and help spent discussing some of the fundamental concepts of this work.

The PRF of the American Chemical Society is thanked for the provision of a studentship and the funds for the trips to Central Italy and the EAOG conference in Maastricht, Netherlands.

Dr. Hugh Jenkyns is thanked for his supervision during the field trip to Central Italy. His geological expertise and menu translation skills were particularly welcomed.

Dr. Brendan Keely, Dr. Paul Farrimond and Paul Barrett are thanked for the provision of some samples.

Jim Carter and Andy Gledhill are thanked for their valuable assistance with the TSQ HPLC-MS and DEC workstation, plus their good sport whilst losing at squash.

A big thank you to Sue Trott and to all members of the OGU, past and present for their friendship, help and support, and for all the laughs along the way.

Dr. to be, Neil "Cheggs" Crawford is particularly thanked for his unique approach to work and life and for the lengthy discussions/arguments/laughs we have had over the past few years concerning porphyrins, maleimides, OAEs and the rise and fall of LFC/NUFC respectively.

I would like to thank all the friends and space cadets outside the department who I feel very lucky to have, and have more than helped and encouraged me in everything I have done since I came to Bristol ten (!) years ago. In particular, Alison Orbaum, who put up with me for an amazing seven whole years; time for which I am eternally grateful.

Finally, the love and encouragement from my family is something that cannot be expressed adequately here. Without their support in many different ways, this work would not have been possible.

## ABSTRACT

The distributions of sedimentary porphyrins are typically dominated by DPEP, a C<sub>32</sub> cycloalkanoporphyrin (CAP) diagenetic product of the major chlorophyll, chlorophyll *a* (chl *a*). The bacteriochls *c*, *d* and *e* series are present in the green sulphur bacteria (Chlorobiaceae) which are strict anaerobes; by analogy with the chl *a* to DPEP relationship, members of these series give rise to  $\geq$  C<sub>33</sub> components (HMW CAPs).

Previous work isolated from the Permian Kupferschiefer a series of such CAPs derived from the bacteriochls *d*, providing evidence for the occurrence of photic zone anoxia (PZA) in the depositional setting. In the present study, these and other  $\geq$  C<sub>33</sub> CAPs have been used as co-injection standards to develop an HPLC-MS approach for the routine recognition of PZA by way of CAP components derived from the bacteriochls *d*. This approach extends earlier studies covering the entire deposition of Kupferschiefer in the Lower Rhine Basin, and has confirmed evidence for PZA from the Triassic Serpiano oil shale and marls from the Eocene Mulhouse Basin; no bacteriochl *d*-derived CAPs were found in marls from the Miocene Vena del Gesso Basin, although other HMW CAPs of bacteriochl origin may be present.

Porphyrin distributions in a suite of black shales deposited at different locations around the Cenomanian/Turonian (Cen/Tur) boundary have been compared with maleimide distributions (Crawford, personal communication). This period is a major example of an "Oceanic Anoxic Event" (OAE). Evidence shows that PZA existed along the continental margins of the western Tethys, so an existing model of an expanded oxygen minimum zone (OMZ) to explain black shale deposition now has to take into account extension of anoxic conditions into the photic zone. Temporal and lateral variations show that PZA was a periodic occurrence, with local factors imparting a significant effect. High abundances of bacteriochl *d*-derived components in Atlantic Cen/Tur black shales reveal a strong PZA signal in parts of the southern North Atlantic during this OAE.

Aptian and early Toarcian OAE sediments deposited along the continental margins of the Tethys also reveal the occurrence of PZA. The periodic appearance of this phenomenon is again thought to result from the fluctuating intensity of an expanded OMZ. Toarcian sediments from the northern epicontinental seas of France and Germany were found, however, to contain a more intense signal for PZA, most probably as a result of the nature of these restricted basinal settings.



All the Cen/Tur samples containing a Ni/(Ni+VO) porphyrin ratio  $< 0.81$  were found to contain biomarkers for PZA, but this relationship was not apparent in the Tethyan Toarcian and Aptian samples. The complexity of the porphyrin distributions means that a large number of HMW CAP components remain of unknown origin and may or may not be related to the bacteriochls of Chlorobiaceae.

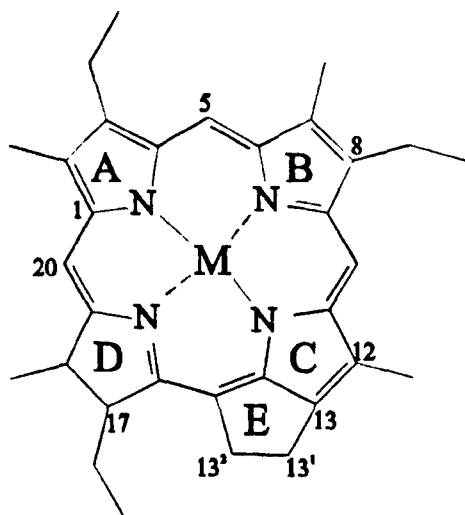
## ABBREVIATIONS

Aetio	Aetioporphyrin
APCI	Atmospheric pressure chemical ionisation
Bacteriochl	Bacteriochlorophyll
BenzoCAP	Benzononcycloalkanoporphyrin
BiCAP	Bicycloalkanoporphyrin
Bu	Butyl
CAP	Cycloalkanoporphyrin
CCD	Carbonate compensation depth
Cen/Tur	Cenomanian/Turonian boundary
Chl	Chlorophyll
DCM	Dichloromethane
DPEP	Desoxophylloerythroaetioporphyrin
DSDP	Deep Sea Drilling Project
EI	Electron ionisation
Et	Ethyl
Eh	Redox potential
eV	Electron volts
GC	Gas chromatography
GC-MS	Gas chromatography-mass spectrometry
GPC	Gel permeation chromatography
HMW	High molecular weight
HPLC	High performance liquid chromatography
HPLC-MS	High performance liquid chromatography-mass spectrometry
<i>i</i>	iso
LC	Liquid chromatography
<i>m/z</i>	Mass to charge ratio
Me	Methyl
MeOH	Methanol
min	Minutes
MPMP	Modified porphyrin maturity parameter
MS	Mass spectrometry

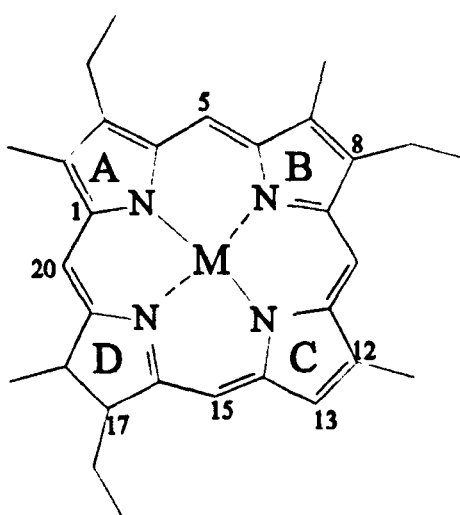
MSA	Methane sulphonic acid
Myr	Million years
n.O.e	Nuclear Overhauser effect
NMR	Nuclear magnetic resonance
OAE	Oceanic anoxic event
OEP	Octaethylporphyrin
OM	Organic matter
OMZ	Oxygen minimum zone
PDA	Photodiode array detector
Pent	Pentyl
Porph	Porphyrin
Pr	Propyl
Pr/Ph	Pristane/Phytane ratio
PZA	Photic zone anoxia
<i>sec</i>	Secondary
S/N	Signal to noise ratio
TCA	Tricarboxylic acid
TLC	Thin layer chromatography
TOC	Total organic carbon
$t_R$	Retention time
UV/vis	Ultraviolet/visible (spectrophotometry)
Vanadyl	Oxovanadium (IV)
VdG	Vena del Gesso
WSBW	Warm saline bottom water
Wt.	Weight

## NOMENCLATURE

The I.U.P.A.C. numbering system, as shown below, has been used throughout this thesis for the nomenclature of porphyrins.



Cycloalkanoporphyrin (CAP)



Aetioporphyrin (Aetio)

# **CHAPTER ONE**

## **INTRODUCTION**

## INTRODUCTION

### SEDIMENTARY PORPHYRINS

#### General

##### *Alkyl porphyrins*

So called petroporphyrins were the first biomarkers identified in sedimentary organic matter, so have been the subject of much investigation since their discovery in a variety of shales and oils (Treibs 1934, 1936). Treibs proposed that these red pigments were metallo complexes of the alkyl porphyrins desoxophylloerythroaetioporphyrin (DPEP; 1) and aetioporphyrin-III (2), which could be related, *via* a hypothetical defunctionalisation pathway to chlorophyll *a* (Chl *a*) (3) and haeme (4) respectively. Chls comprise one of the most important groups of natural products as they are responsible for harvesting solar energy and converting it into chemical energy in the form of sugars. The reactions originally proposed to explain the transformation of the most abundant photosynthetic pigment, chl *a*, include 1) demetallation, *i.e.* loss of  $Mg^{2+}$ , 2) phytyl ester hydrolysis, 3) decarbomethoxylation, 4) vinyl reduction, 5) chlorin ring aromatisation, 6) keto group reduction, 7) decarboxylation and 8) metal ion insertion (*c.f* Fig. 1.1). Further evidence, giving the scheme in Fig. 1.1, arose from the discovery of the minimum number of intermediates in the chl *a* to DPEP pathway in one recent lake (Priest Pot) and two highly immature older lake sediments (Marau shale and Willershausen; Keely *et al.*, 1990). The scheme shown is partly one of convenience with respect to the order of the reactions, but the first three definitely occur in the water column. Indirect evidence that the aromatisation step does indeed occur comes from the identification in the Eocene Messel oil shale of specific bacterially-derived porphyrin acids (Ocampo *et al.*, 1985a and 1985b; see below). Metallation enhances the stability of porphyrins but it is unclear at what depositional stage metal insertion takes place (Quirke, 1987; Callot, 1991). Sedimentary metallo porphyrins occur predominantly as vanadium (IV) and nickel (II) complexes, *i.e.* as vanadyl ( $VO^{2+}$ ) and nickel ( $Ni^{2+}$ ) species (e.g. Maxwell *et al.*, 1980). The predominance of these species is thought to be related to several factors, including 1) their thermodynamic and kinetic stability over geological time (Lewan and Maynard, 1982; Quirke, 1987), 2) stability in contact with clay minerals (Bergaya and Van Damme, 1982), 3) abundance and availability of metal ions to chelate with the

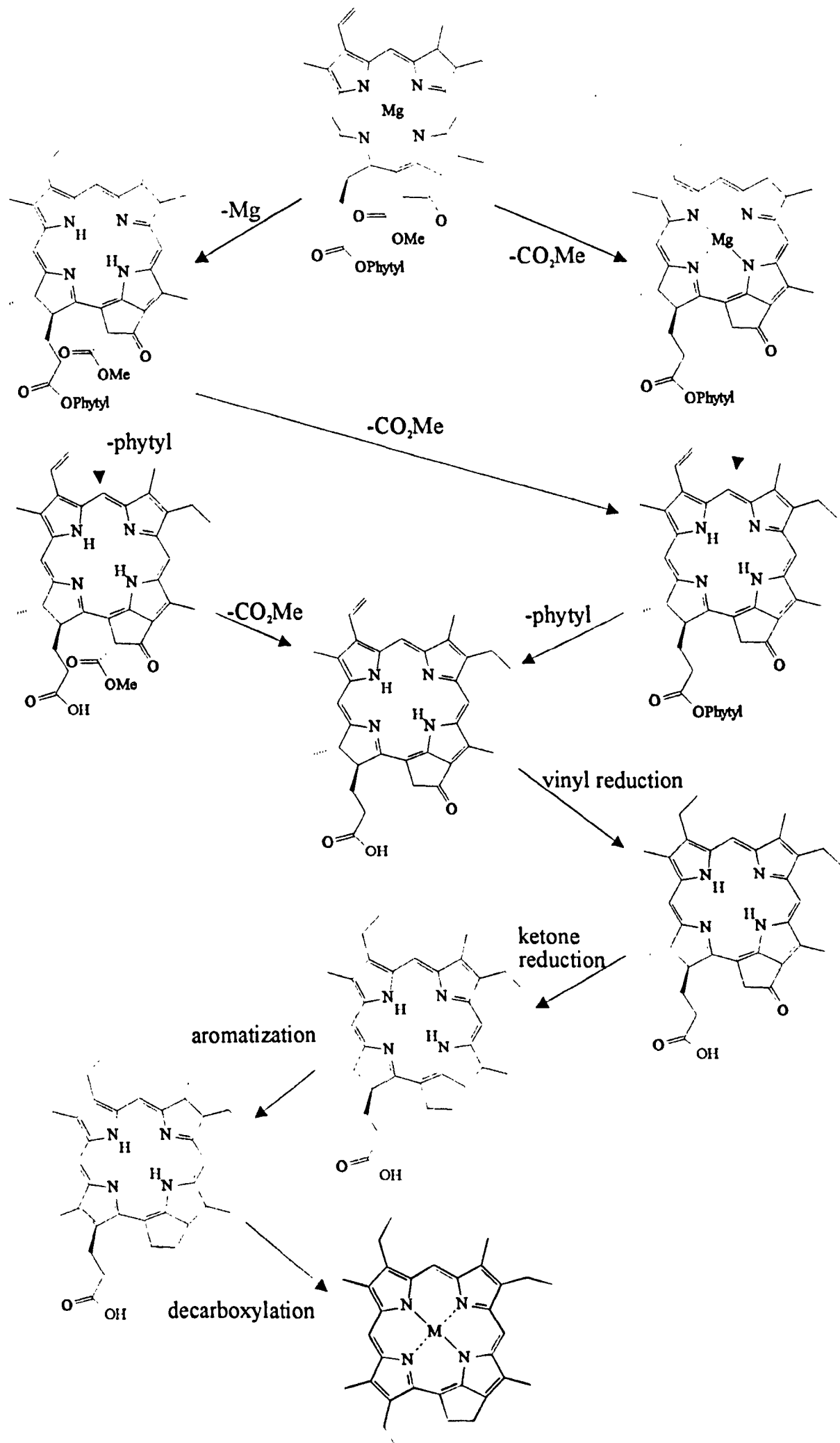


Figure 1.1. Transformation pathways for chl *a* to DPEP (Modified from Keely *et al.*, 1990.)

macrocycle (Quirke, 1987) which can depend upon redox conditions, presence of sulphide and sedimentation rate (Lewan, 1984; Sundararaman *et al.*, 1993). Other complexes ( $\text{Mn}^{2+}$ ,  $\text{Fe}^{3+}$  and  $\text{Ga}^{3+}$ ) have been detected in low concentrations in coals (Bonnett and Czechowski, 1980; Bonnett and Czechowski, 1981; Bonnett *et al.*, 1983) along with high concentrations of iron porphyrins in the Permian Kupferschiefer (Eckardt *et al.*, 1989) and copper ( $\text{Cu}^{2+}$ ) complexes in immature ocean sediments (e.g. Palmer and Baker, 1978). Free base alkyl porphyrins have also been reported in immature sulphur-rich marls (Schaeffer *et al.*, 1993) and marine and lake sediments (Baker and Louda, 1983; Keely *et al.*, 1994). For convenience, M in the structures shown below is  $\text{Ni}^{2+}$  and/or  $\text{VO}^{2+}$  and/or 2H.

#### *Porphyrin carboxylic acids*

Solvent extractable alkyl porphyrins appear to occur more widely in sediments than their carboxylic acid counterparts, although porphyrin acids have been found in a number of recent and immature sediments. A variety of structural classes of nickel porphyrins have been isolated from the immature lacustrine Messel oil shale (Ocampo *et al.*, 1992), including components which could be assigned to specific precursor chlorophylls. These include acids (5) related to the bacteriochls *d*(6) of the green sulphur bacteria (see below), a range of components with an exocyclic ring attached to C-15 and C-17, most likely derived from the chl *c* of brown algae, dinoflagellates and diatoms (Ocampo *et al.*, 1987) and a group of aetio-type components (see below) whose presence suggested a possible haeme-type input from bacterial cytochromes. Other non-specific acids included two C-3  $\beta$ -unsubstituted components (7,8) and the  $\text{C}_{33}$  acid counterpart of DPEP (9), which has also been found in the immature lacustrine Willershausen (Pliocene) sediment (Keely *et al.*, 1994).

#### *Bound porphyrins*

Over recent years it has become apparent that a significant proportion of the organic matter in sulphur-rich sediments can occur as macromolecular material containing components linked by (poly) sulphide bonds (Sinninghe Damsté and de Leeuw, 1990; Kohnen *et al.*, 1991a and 1991b). Studies have involved the use of Raney nickel, MeLi/MeI or nickel boride to cleave (poly)sulphide bonds, followed by determination of the distributions of the hydrocarbons liberated (e.g. Schmid *et al.*, 1987; Sinninghe Damsté & de Leeuw, 1990; Kohnen *et al.*, 1991b; Back *et al.*, 1992). Interest in such



chemical degradation comes from the fact that the bound components appear to be better preserved than their free counterparts, so they can provide more information with respect to source inputs and hence palaeoenvironmental assessment (*e.g.* Kohnen *et al.*, 1991a; Adam *et al.*, 1993; Sinnighe Damsté *et al.*, 1988). Little attention, however, has been paid to porphyrins, although Schaeffer *et al* (1993) showed that significant amounts of alkyl porphyrins could be liberated by Raney Nickel treatment of the polar fraction of the extract of an immature sulfur-rich marl (Gibellina, Italy, Late Miocene). It was found that the bound porphyrins exceeded the “free” (solvent extractable) porphyrins by a factor of 7. The distribution also showed major differences to that of the free porphyrins, although some components were present in both fractions. In this case the pigments were released as free bases and it was thought that the metals normally available for chelation had been quenched as sulphides during early diagenesis. The major components liberated were porphyrins with a fused 5+7 membered exocyclic ring system (see below), including two unsaturated components (10a,b), which seemed to suggest attachment of sulphur at C-15<sup>1</sup> or 15<sup>2</sup>. Later characterisation of the major porphyrin released by deuteriated nickel boride, showed a pattern of D labelling indicating attachment of a precursor (*e.g.* 13''-17'''-cyclopheophorbide enol *a*) with a C-15<sup>2</sup> ketone as a precursor bound to the macromolecular material (Schaeffer *et al.*, 1994).

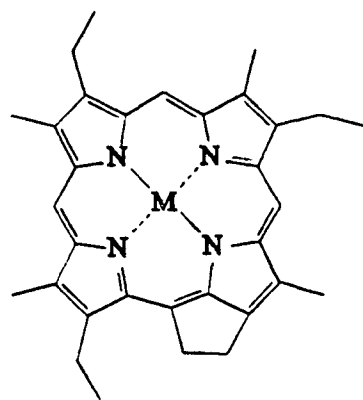
The presence of kerogen-bound alkyl porphyrins has also been shown in the Messel oil shale by Huseby and Ocampo (1995). Components released by hydrous pyrolysis of the extracted kerogen were more abundant than the free components and had a different distribution. These ester-bound species, also released by both acid and base hydrolysis, included high abundances of both mono- (*e.g.* 11a) and di- carboxylic acids (*e.g.* 11b) with possible origins from chlorophylls and bacterial cytochromes respectively.

### **Structural types (Fig. 1.2)**

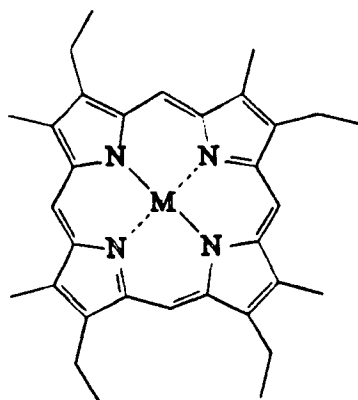
#### *General*

Probe MS first showed that sedimentary alkyl porphyrins were not single compounds *i.e.* aetioporphyrin III and DPEP as first believed by Treibs (1934, 1936). Molecular ion distributions for both metallo porphyrins and free-bases in the C<sub>27</sub>-C<sub>34</sub> range (Dean and Whitehead, 1963; Thomas and Blumer, 1964) showed the mixtures to be complex,

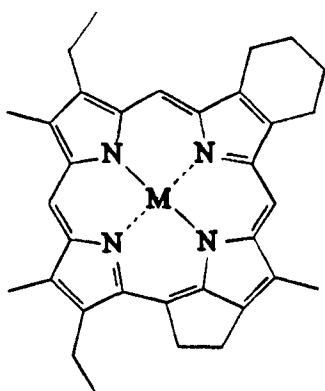
Fig 1.2 Examples of porphyrin structural types



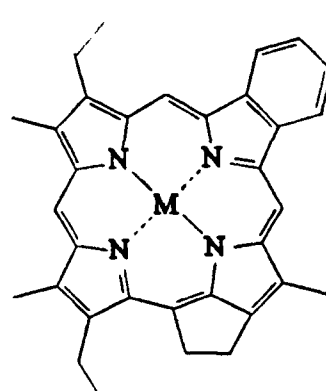
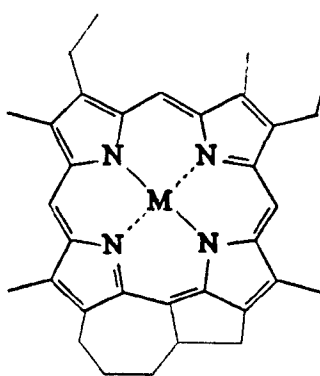
a. CAP



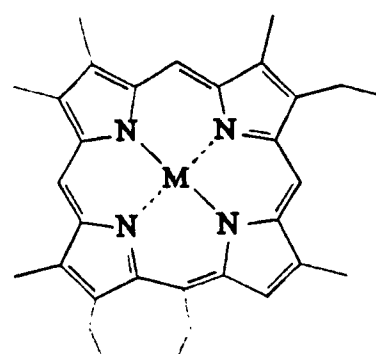
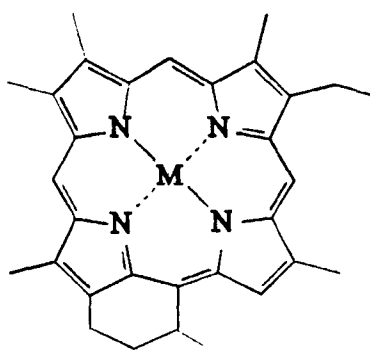
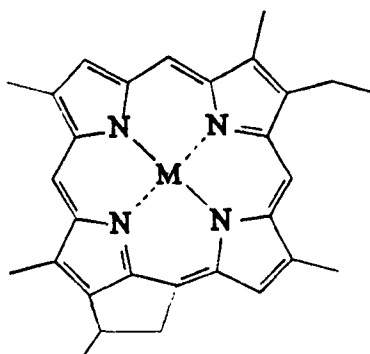
b. Aetio



c. BiCAPs



d. BenzoCAP



e. CAPs with rearranged exocyclic ring

incorporating several structural types based on the number of degrees of unsaturation, which have now been confirmed by structural studies (see below); representative examples of the major types are shown in Fig 1.2.

The occurrence of these and related components and their possible origins has been reviewed recently in detail (Callot, 1991), so is not discussed further here, except to mention that the cycloalkanoporphyrin (CAP) and aetio components are the two major families, each comprising a mixture of homologues. Other types recognised were the di-DPEP type (BiCAPs), rhodo-DPEP type (now known as benzo-CAPs) and rhodo-aetio (now known as benzo-aetios) (Baker *et al.*, 1967; Yen *et al.*, 1969; Rankin and Czernuszewicz, 1993).

#### *Cycloalkanoporphyrins (CAPs)*

These are the most directly related to chlorophylls, one type possessing a five-membered exocyclic ring attached to ring C at C-13,15. The C<sub>32</sub> CAP, DPEP (1), is typically the most abundant and is most likely to derive from chl *a* (3) as it has the same carbon skeleton and chl *a* is the most abundant chlorophyll. There are, however, other possible minor contributors to DPEP as it shares the same carbon skeleton with other chlorophylls, including chl *b* (12) and bacteriochl *a* (13). Other CAPs which are non-specific biomarkers include for example a C<sub>31</sub> component with an unsubstituted C-7 position (14), which may have either a chl *b* or chl *c*<sub>3</sub> (15c) origin (Chicarelli and Maxwell, 1984; Verne-Mismer *et al.*, 1990)

#### *Aetioporphyrins*

One example is the first isolated sedimentary porphyrin, aetioporphyrin III (2). Several possibilities exist for the source of aetioporphyrins, although a specific origin usually remains open due to the lack of structural specificity. One possible source of aetioporphyrin III, as proposed initially by Treibs (1934, 1936), is the haeme from animals. Corwin (1960) later proposed that it was a thermal degradation product of DPEP and hence was also derived from chlorophylls although preferential thermal cleavage of the C-13<sup>2</sup>, C-15 bond in DPEP seems unlikely (Barwise, 1987). The occurrence in recent aquatic environments and immature sediments of oxidised products of chl *a*, such as purpurin-18 (16) and purpurin-7 phytol ester (17) (Baker and Louda, 1980; Louda *et al.*, 1980; Naylor, 1997; Naylor and Keely, 1997; Wooley *et al.*, 1997), in which ring E has been opened, does suggest, however, the possibility

of a chlorophyll contribution to aetioporphyrins *via* defunctionalisation. On the other hand, evidence for a mixed or different biological source for aetioporphyrin III in the Lower Cretaceous Julia Creek oil shale was obtained from stable carbon isotopic data (Boreham *et al.*, 1989; Ocampo *et al.*, 1989) which showed that it was depleted in  $^{13}\text{C}$  by 4‰ relative to  $\text{C}_{32}$  DPEP. This suggested an origin in the haeme groups present in bacterial cytochromes rather than haeme in animals, given the ratio of contributions of animals and plants to organic matter in living systems is *ca.* 1 to  $10^5$ .

#### *Bicycloalkanoporphyrins (BiCAPs)*

These components can either occur as species with a six membered ring on ring B at C-7,8 (*e.g.* **18**) and related to the benzo-CAPs (**20a,b**, see below) or with a 5+7 fused ring system (*e.g.* **19a,b**).

The former type has been identified in the Maastrichtian Timahdit oil shale (Verne-Mismer *et al.*, 1987) and the similar substitution pattern (C-13 to C-17) indicates a chlorophyll origin. Likewise, a possible relationship to chl *c* (**15**) has been postulated for component (**18**) with a rearranged five membered ring. The mechanism to form the six membered ring and the stage at which it occurs is, however, still uncertain (Callot, 1991). Component (**19b**) with a fused ring system has been observed in the Late Cretaceous El Lajun shale (Prowse *et al.*, 1987) as well as in the immature Late Pliocene Willershausen lake sediment (Keely *et al.*, 1994) and in the desulphurisation products of the macromolecular material from the Miocene, Gibellina marl (see above). Such porphyrins have also been detected as minor components in several other sediments (Chicarelli and Maxwell, 1986; Verne-Mismer *et al.*, 1987). Chlorins with the same carbon skeleton have been found in diatoms (Watanabe *et al.*, 1993), a sponge (Karuso *et al.*, 1986) and a clam (Sakata *et al.*, 1990), so may be porphyrin precursors. Stable carbon isotope compositions of the major Willershausen BiCAP (**19b**) and DPEP were similar, suggesting a diatom chl *a* origin for both (Keely *et al.*, 1994). Similar measurements made on the same components in the Julia Creek oil shale showed only a slight difference (0.9‰) compared with DPEP (Boreham *et al.*, 1990), again suggesting a diatom source for such BiCAPs to be the most likely.

#### *Benzocycloalkanoporphyrins (BenzoCAPs)*

These components, present as minor constituents in some samples, are characterised by the “rhodo-type” electronic spectrum (Smith, 1975). The structural type was

originally postulated from probe-mass spectrometry, with later confirmation of a benzo-structure coming from comparison of electronic spectra of isolated fractions with those of synthetic rhodo aetioporphyrins (Clezy and Mirza, 1982) and from the distribution of maleimide oxidation products (Barwise and Whitehead, 1980). They are now known to have the benzene ring at C-7,8 (**20a,b**) (Kaur *et al.*, 1986; Verne-Mismer *et al.*, 1987;1988; Quirke *et al.*,1990). Again, the mechanism to form the benzene ring and the stage at which it occurs is uncertain (Callot, 1991).

#### *CAPs with rearranged exocyclic ring*

Major components possessing a 5-membered rearranged exocyclic ring have been found in the Eocene Messel oil shale (e.g. **21**; Ocampo *et al.*, 1984), the Maastrichtian Oulad Abdoun oil shale (Verne-Mismer, 1988) and more recently in the Permian Kupferschiefer marl (Gibbison, 1996). Such components almost certainly arise from chl *c* (**15**) by rearrangement of the C-17 propenoic substituent (Callot, 1991 and references therein). Components with a 6 and a 7-membered ring have also been identified (Chicarelli *et al.*, 1984; Wolff *et al.*, 1983; Hayes *et al.*, 1987; Boreham *et al.*, 1990), although assigning origins is difficult. For instance, a <sup>13</sup>C enrichment in a 7-membered ring (butano) alkyl-porphyrin (**22**) relative to DPEP was observed in the Serpiano (Chicarelli *et al.*, 1993), Messel (Hayes *et al.*, 1987) and Julia Creek oil shales (Boreham *et al.*, 1990). Cyclisation of a propionic side chain to the C-15 position, probably induced enzymatically during deposition, has been suggested (Keely *et al.*, 1994).

#### **Isolation, separation and structure determination**

Porphyrin fractions are typically isolated using column chromatography and/or TLC, although gel permeation chromatography (GPC) has also been occasionally used (Blumer and Snyder, 1967; Rosell-Melé & Maxwell, 1996 and references therein). Interestingly, there is an early example of the use of TLC to isolate a C<sub>32</sub> (**2**) porphyrin component in sufficient purity for structure determination (Quirke and Maxwell, 1980).

The application of electron ionisation mass spectrometry (EI-MS) to the study of porphyrin fractions (Baker *et al.*, 1967) gave early evidence for the great complexity of their distributions. The technique provided useful characterisation, giving information on molecular masses and carbon number ranges (e.g. Baker and Palmer,

1978). Later application of gas-chromatography and mass spectrometry (GC and GC-MS) to the derivatised petroporphyrins (as their more volatile bis-(trimethylsiloxy)-silicon complexes; Boylan *et al.*, 1969; Alturki *et al.*, 1972 and Eglinton *et al.*, 1984) and to the metallo complexes and free bases (Blum *et al.*, 1988 and 1989; Blum and Eglinton, 1989 and Blum *et al.*, 1990) clearly demonstrated the advantage of a routine combined separation-detection method for analysis of such complex mixtures. Indeed, GC-MS with full scan and selected ion monitoring (SIM) indicated that these mixtures can be among the most complex of any sedimentary biomarker type (Gill *et al.*, 1986 and references therein).

Early studies also indicated the suitability of normal-phase high performance liquid chromatography (HPLC) for the separation of free-base alkyl porphyrins obtained from demetallation of the metallo complexes (Hajibrahim *et al.*, 1978; Quirke *et al.*, 1979; Eglinton *et al.*, 1980; Brassell *et al.*, 1980; Hajibrahim, 1981). Likewise, reversed phase HPLC allows separation within the vanadyl (Sundararaman, 1985) and nickel (Habermehl and Springer, 1982; Fookes, 1983) fractions. These studies, along with improvements in resolution and with solvent programming for the free bases (Barwise *et al.*, 1986, Chicarelli *et al.*, 1986) allowed isolation of individual components. Following isolation of normally 150-500 µg of a component, <sup>1</sup>H Fourier Transform-Nuclear Magnetic Resonance (<sup>1</sup>H-FT-NMR) spectrometry has enabled elucidation of many components, as the free bases or nickel species. In order to determine the position of the substituents on the macrocycle for full structural elucidation, the nuclear Overhauser effect (n.O.e) is typically used (e.g. Quirke *et al.*, 1980b; Krane *et al.*, 1983) and more than fifty components have been elucidated (reviewed by Callot, 1991). Iron porphyrins in a coal have been characterised using paramagnetic shift effects by forming complexes with the high crystal field strength ligand, cyanide (Bonnett *et al.*, 1990). The spin state and oxidation state, set as low-spin iron (III) dicyanide, enables the resulting paramagnetically shifted <sup>1</sup>H NMR spectra to provide structural information without the need for demetallation. The <sup>1</sup>H-NMR approach requires, however, relatively large amounts of a component in >90% purity for unambiguous assignment. Furthermore, many of the more interesting components, from a palaeoenvironmental assessment standpoint, are present in much lower concentrations, making isolation tedious.

Although  $^1\text{H}$ -NMR has become the preferred means of structure determination, a few early studies used crystallographic methods. X-ray analysis of the major metalloporphyrin from Julia Creek oil shale showed it to be vanadyl-DPEP (Ekstrom *et al.*, 1983). This technique, however, is limited to large samples as high quantities of crystals of sufficient purity need to be obtained. Other X-ray crystallographic work has identified the nickel complex of desoxophylloerythrin (**23**) (Habermehl *et al.*, 1984), although the OH substituent is probably an artefact introduced during isolation, since it is known that hydroxylation of C-13<sup>2</sup> in some CAPs can occur during TLC on silica (Ponomarev and Shul'Ga, 1982).

The development of a suitable HPLC-MS interface has long been viewed as a desirable development for the analysis of complex porphyrin mixtures, since the resolution is probably better than the resolution obtained by GC-MS.

Chlorophyll and chlorin distributions have been obtained by HPLC-MS techniques using either continuous flow fast-atom bombardment (FAB; van Breemen *et al.*, 1991) or by the use of a thermospray interface (Eckardt *et al.*, 1990). Such techniques, however, were not found to be suitable for the analysis of porphyrins as, for example, porphyrin precipitation was found to occur at the tip of the thermospray interface probe, resulting in a low detection sensitivity (Eckardt *et al.*, 1990). The application of a moving belt interface was demonstrated for the analysis of the petroporphyrins of Boscan 9K3 oil and the La Luna Marl oil shale (McFadden *et al.*, 1979). In this approach, the first commercially available HPLC-MS system, the eluent is deposited on to a moving belt which transports the sample into the ion source through a series of vacuum locks. The solvent is removed by infra-red heaters, leaving the sample as a residue. Within the mass spectrometer, the sample is flash-vapourised into the ion source. Ion chromatograms obtained showed the presence of homologous series of porphyrins of both CAP and aetio types in the carbon number range C<sub>28</sub> to C<sub>35</sub>. A particle beam interface has also been used for the analysis of sedimentary vanadyl porphyrins (Sundararaman and Vestel., 1993). In this technique, the eluent is pneumatically nebulised, forming a fine mist of droplets. The solvent is then removed in a heated chamber and analyte particles enter the ion source. The sensitivity was reported to be a factor of 3 times higher than that obtained using the thermospray interface.

The recent development of HPLC-atmospheric pressure ionisation (API)-MS has

allowed the on-line separation and detection of individual free-base porphyrin components present in complex mixtures (Rosell- Melé *et al.*, 1996). The API interface can be operated in two modes, pneumatically assisted electrospray ionisation (ESI), also known as ion spray, or atmospheric pressure chemical ionisation (APCI). Due to the high proton affinity of free-base porphyrins, ionisation occurs in both modes by gas-phase ion-molecule reactions (Ikonomu *et al.*, 1991). In ESI an electrostatic spray is formed by applying a potential of several thousand volts between the eluent capillary and a counter electrode. Sample molecules are simultaneously nebulised and ionised at atmospheric pressure. The gas phase ions formed then pass through a two stage momentum separator into the mass analyser at high vacuum. APCI involves the spraying of eluent through a high temperature vaporiser where the combination of heat and gas flow desolvates the nebulised droplets, producing a dry vapour of solvent and analyte molecules (Covey *et al.*, 1986). Ionisation occurs in a corona discharge region created by a high voltage (Duffin *et al.*, 1992). This region provides a source of high-energy electrons, ionising the nearby gases which in turn undergo ion-molecule reactions with air and solvent molecules producing reactive intermediate ions ( $R^+$ ; Huang *et al.*, 1990). Analyte molecules (M) within the corona region react with these intermediate ions resulting in “soft” atmospheric chemical ionisation of the analyte with the formation of protonated molecules ( $MH^+$ ). The chemistry occurring within the APCI source is very complex, which with the high reactivity of the ions and high concentration of gas-phase molecules results in the formation of adduct or cluster ions of air and water over a large mass range (Mitchum and Korfmacher, 1983). Such cluster ions produce a high chemical background if they are mass analysed, so any water molecules clustered to the analyte are removed by drying gases before the ions enter the mass analyser.

In the study of Rosell-Melé *et al.* (1996), the APCI spectra of free-base porphyrins showed, apart from  $MH^+$ , the presence of ions at  $[MH+53]$ . These, found to occur in all solvent types, are thought to arise from the formation of iron complexes ( $[M-2H+^{56}Fe]^+$ ) during the ionisation process, where the iron may arise from the corona discharge electrode (Rosell-Melé *et al.*, 1996). The APCI mode was preferred to the ESI due to the more stable and reproducible response obtained, even though ESI appeared to be slightly more sensitive with respect to the limit of detection. In addition, HPLC peak tailing occurred during ESI operation, probably resulting from



adsorption on to the unheated capillary (Rosell- Melé *et al.*, 1996), resulting in some loss of chromatographic resolution. The HPLC-APCI-MS system was also used to compare the normal phase analysis of free-base porphyrins with the reversed phase analysis of both vanadyl and nickel porphyrins. The sensitivity for the free base porphyrins was found to be greater than for the metallo complexes, with the Ni species giving a poorer analytical selectivity for mixtures due to the abundant isobaric ions resulting from the greater number of metal isotopes (Rosell- Melé *et al.*, 1996). Furthermore, the HPLC resolution of free base porphyrins under normal phase conditions is significantly better than that obtained for the metallo porphyrins under reversed phase conditions (Sundararaman, 1985; Verne-Mismer *et al.*, 1990b; Barwise *et al.*, 1986; Chicarelli *et al.*, 1986). HPLC-APCI-MS is therefore a valuable tool in the analysis of the complex mixtures of free base porphyrins obtained from geological samples. Mass chromatography in particular enables the detection of components present in very low abundance, for instance high molecular weight (>C<sub>33</sub>) CAPs resulting from diagenesis of the bacteriochls present in green sulphur bacteria, *i.e.* can provide information relevant to the assessment of the redox conditions within ancient water columns (Rosell- Melé *et al.*, 1996).

## **Chlorophylls**

### *General*

The occurrence, role and distribution of chlorophylls have been reviewed in detail (Scheer, 1991), so only a few points relevant to the present work are mentioned here. Chl *a* (3), the most abundant, is present in all oxygenic photosynthetic organisms. Photons of light are captured by chlorophyll-protein complexes in order to convert carbon dioxide into carbohydrates. Intense absorption of chl *a* occurs in narrow parts of the visible region and the absorption range of the antenna complexes is enhanced by the presence of accessory light-harvesting pigments which include carotenoids along with a variety of chlorophylls. There is a fairly wide structural variation in the elements of the chlorophyll macrocycle, such that about 25 or so basic structures are known. Chlorophyll (and carotenoid) compositions therefore enable various photosynthetic organisms to be differentiated. The majority of eukaryotes (both terrestrial and aquatic) contain chl *b* (12) along with chl *a*. Cyanobacteria, however, do not contain any chl *b*, so have been a ready source of chl *a* for reference purposes. In some

divisions of the Protista kingdom, such as Phaeophyta (brown algae), Chrysophyta (diatoms and golden-brown algae), Pyrrophyta (dinoflagellates) and Cryptophyta, chl *a* is accompanied by varying abundances of one or more of the chls *c* (15a-c). Chl *d* (24) has been found in Rhodophyta (red algae) although it may be formed from Chl *a* oxidation during isolation and work up (e.g. Jackson, 1976). [8-vinyl]-chl *a*, often referred to as divinyl chl *a*, was first found in greening cucumber seedlings and has since been found in a number of different tissues, including marine phytoplankton. Divinyl chl *b* has been identified in *Zea mays* seedlings.

### **Bacteriochlorophylls**

Photosynthetic bacteria contain bacteriochls. These prokaryotic chlorophylls show a greater structural diversity than the eukaryotic chls. Bacteriochl *a* (13) is often the primary photosynthetic pigment with other bacteriochls (and carotenoids) acting as accessory pigments. With the notable exception of the green sulphur bacteria, bacteriochl *b* (25) is present in most photosynthetic bacteria as the major accessory pigment. For example, the purple sulphur bacteria (Chromatiaceae) contain both bacteriochls *a* and *b*. Bacteriochl *a* also acts as a secondary pigment in the Chlorobiaceae- the green sulphur bacteria. The primary chlorophylls of Chlorobiaceae consist of 3 homologous series of the bacteriochls *c* (26), *d* (6) and *e* (27). These lack the 13<sup>2</sup> carbomethoxy group and bear an  $\alpha$ -hydroxyethyl substituent at C-3. Pigments of the *c* and *e* series differ from the *d* series by the presence of a C-20 methyl substituent and the bacteriochls *e* have a formyl group at C-7 like chl *b*. An important structural feature of the three series is the additional alkylation which occurs at C-8 and C-12 in certain members. Previous work (Smith and Bobe, 1987) has shown these homologues are enzymatically methylated (S-adenosyl methionine, which also provides the C-20 methyl in the *c* and *e* series) in a physiological response to lowered light availability. This alters the nature of the pigment aggregation and therefore the light absorptivity of the organism. Further variations are seen in the nature of the esterifying alcohol. Phytol is the major alcohol by far in eukaryotic chlorophylls (except in the chls *c* which lack an esterifying alcohol) whereas other alcohols such as geranylgeraniol (bacteriochl *a*) and farnesol (bacteriochlorophylls of Chlorobiaceae) are more frequently found as well as other alcohols (e.g. in Chlorobiaceae bacteriochlorophylls).

## Green Sulphur Bacteria

The role of bacteria in sedimentary environments is complex. Some bacteria are limited to very specific, sometimes extreme environments, whilst others can grow in both aerobic and anaerobic environments, carrying out more than one primary bacterial function. Bacterial community composition is dependent not only on oxygen levels, but also on levels of salinity, acidity and temperature. A common feature of bacterial communities is the reliance of one bacterial group on the products of another group, so different communities living in aerobic and anaerobic environments can actually be interdependent. In certain environments, such as in a stable, stratified water column, specific ecological niches exist along the gradients of oxygen, light and temperature. Where anoxic bottom waters develop and sulphate is present in sufficient amounts, sulphate reducing bacteria can thrive, resulting in the accumulation of sulphide. (N.B. In stratified freshwater lakes, a low sulphate concentration ( $<0.3$  mM) can result in low production of sulphide). As such sulphide-containing environments are often in close contact with oxidised environments, migration tends to occur between the two. Hence, a sulphide gradient may exist, with the concentration decreasing nearer the surface waters. Sulphide ions may, however, extend high enough so they coincide with the lower limit of dissolved oxygen. This "chemocline" zone can support communities of photosynthetic bacteria if it occurs sufficiently high in the water column to receive light. Under such conditions purple sulphur bacteria (Chromatiaceae) can occur within the chemocline, growing beneath algae and cyanobacteria. They utilise  $H_2S$  for anaerobic photosynthesis, which they are also able to store as sulphur within their cells (and which can be further oxidised to sulphate when sulphide concentrations are very low; de Wit, 1992), but they can tolerate low levels of oxygen.

Green sulphur bacteria, Chlorobiaceae, are incapable of growing in the presence of oxygen so exist lower in the water column. Also, the energy required, related to the minimum amount of light needed to maintain cell integrity in the absence of other energy sources, is about 10 times lower than for purple sulphur bacteria. Therefore the green sulphur bacteria grow at lower light intensities (de Wit, 1992 and references therein). They exist as two strains- the green-coloured and the brown-coloured. The green strains contain bacteriochls *d* and usually *c* as the major chlorophylls, plus bacteriochl *a* as an accessory pigment and an accessory carotenoid pigment, either

chlorobactene (28) or  $\gamma$ -carotene (29). The bacteriochls *c* and *d* strongly absorb light in the 440–450 nm visible region which is not absorbed by Chromatiaceae (Montesinos *et al.*, 1983). Therefore, the green Chlorobiaceae thrive in anaerobic layers just below the purple sulphur bacteria. The brown strains contain bacteriochl *e* along with bacteriochl *a* and the major accessory pigment isorenieratene (30). Small quantities of  $\beta$ -isorenieratene (31),  $\beta$ -carotene (32) and chlorobactene are also found in some strains. In the brown Chlorobiaceae, the carotenoid : bacteriochl ratio is about four times higher than in the green strains (de Wit and Caumette, 1995) giving rise to the brown colour. It has been shown that brown Chlorobiaceae do not occur below a plate of Chromatium purple sulphur bacteria (de Wit, 1992). However, the carotenoids in the brown Chlorobiaceae have a broader absorption band (450–550nm), so are especially adapted to allow effective absorption of radiation in the deeper layers of the water column with extremely low light intensities, most probably beneath abundant growth of phytoplankton (Pfennig, 1989) where growth of Chromatium is not supported (de Wit, 1992). Another major difference between the green and purple sulphur bacteria is their use of different pathways for carbon fixation. The Chromatiaceae, along with cyanobacteria and algae, fix carbon *via* the strongly  $^{13}\text{C}$ -discriminating  $\text{C}_3$  pathway whereas Chlorobiaceae uniquely use the energy-efficient, reversed tricarboxylic acid cycle (TCA) cycle for carbon metabolism (Sirevåg and Ormerod, 1970), which results in less discrimination against  $^{13}\text{C}$  relative to the  $\text{C}_3$  route (Quandt *et al.*, 1977; Sirevåg *et al.*, 1977).

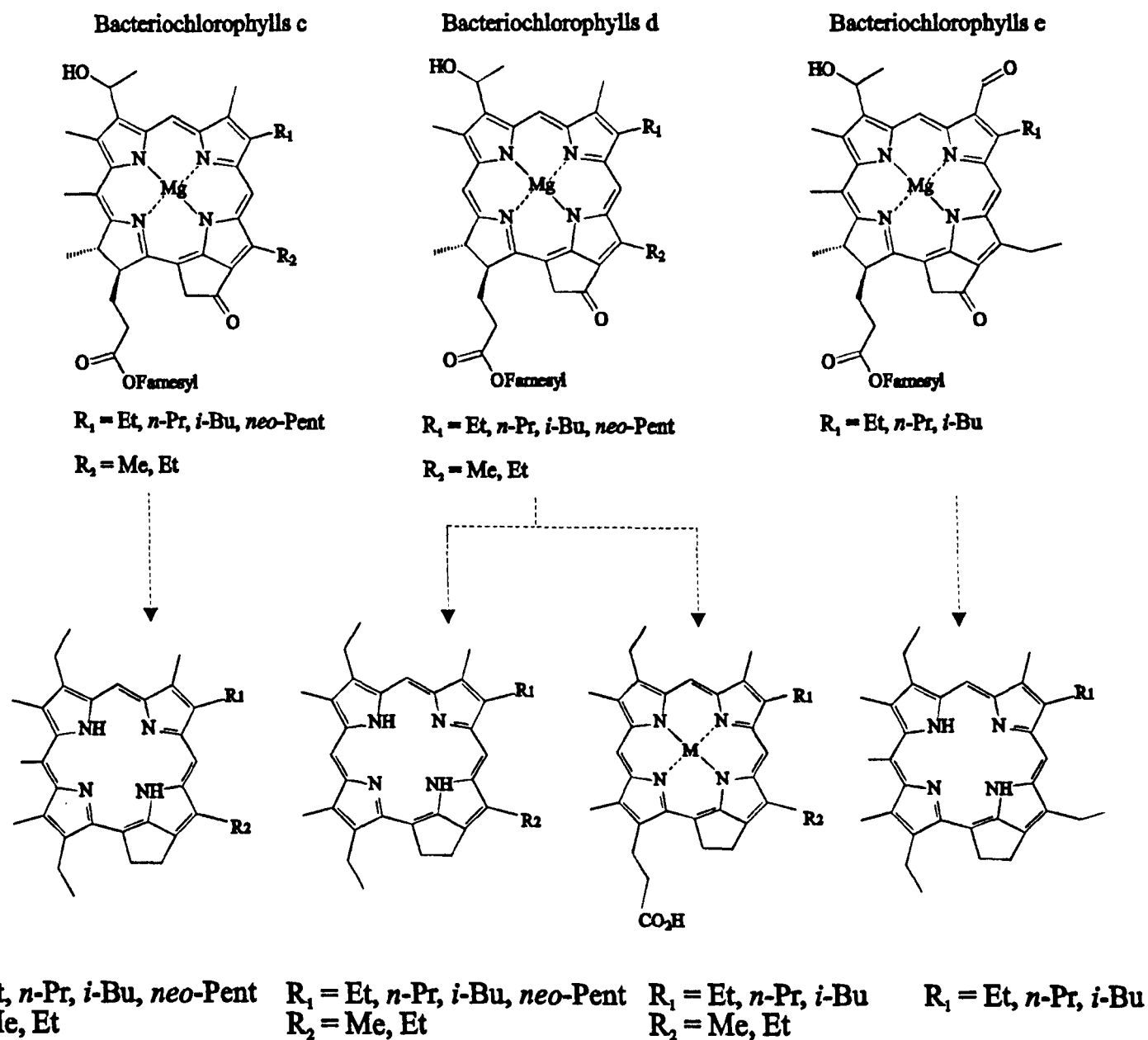
### **Biomarkers for Green Sulphur Bacteria**

The diagenetic transformation products of Chlorobiaceae pigments provide biomarkers for the presence of such bacteria in the original depositional setting. Identification of these specific biomarkers in geological samples provides evidence for the presence of green sulphur bacteria and hence the extension of anoxic conditions in to the photic zone of the palaeo water column.

#### ***Porphyrins***

By analogy with the chl *a*/DPEP precursor/product relationship (Fig. 1.1), the bacteriochlorophylls of Chlorobiaceae would be expected to follow an analogous transformation pathway of defunctionalisation and give rise to alkyl bacterioporphyrins with identical carbon skeletons (Fig. 1.3). Porphyrins specifically derived from these

Figure 1.3. Alkyl bacterioporphyrins from diagenetic transformation of bacteriochls *c*, *d* and *e*.



bacteriochlorophylls might therefore be expected to show components with extended alkylation at C-8 (up to *neo*-pentyl in the *c* and *d* series; *i*-Bu in the *e*-series), C-12 (Me,Et) and a C-20 Me substituent in the *c* and *e* series (Fig. 1.3).

The first structural evidence for components derived from Chlorobiaceae came from the presence of a minor series of porphyrin carboxylic acids (C<sub>34</sub>-C<sub>36</sub>; **5**) in the lacustrine Messel oil shale (Ocampo *et al.*, 1985a; 1985b), these components having the same carbon skeleton as members of one of the bacteriochl *d* (**6**) series (Fig. 1.3) with an Et substituent at C-12 and Et, *n*-Pr and *i*-Bu at C-8. Further evidence, using HPLC coinjection of a synthesised standard, came from the occurrence in the evaporitic Mulhouse Basin marls of a C<sub>34</sub> CAP (**33**) derived from a bacteriochl *d* of the second series with a Me substituent at C-12 (Keely *et al.*, 1993). Gibbison *et al.* (1996) reported the presence of a series of three high molecular weight CAPs (**34a-c**), from the demetallated porphyrin fraction of the Permian Kupferschiefer marl from the Lower Rhine Basin. The presence of Et, *n*-Pr and *i*-Bu substituents at C-8 and an Et substituent at C-12 again indicated that bacteriochl *d*-containing green sulphur bacteria existed in the palaeo water.

Interestingly, no alkyl porphyrins or porphyrin acids from the bacteriochlorophyll *c* or *e* have been reported in sediments although their occurrence would be expected by analogy with bacteriochl *d* derived biomarkers (Fig. 1.3).

### **Other biomarkers**

#### *Aryl isoprenoids*

The intact diaromatic carotenoid isorenieratene from the brown strains of Chlorobiaceae has been found in Holocene Black Sea sediments and in some older immature sediments (Repeta, 1993; Brassell *et al.*, 1983; Cardoso *et al.*, 1978; Sinninghe Damsté *et al.*, 1993; Keely *et al.*, 1995). The first report of a diagenetic product came from the identification of isorenieratane (**35**), in the Toarcian of the Paris Basin (Schaefflé *et al.*, 1977) and it has since been reported in a variety of samples, including Paleozoic source rocks and oils (*e.g.* Requejo *et al.*, 1992; Sinninghe Damsté and Köster, 1998). Diagenetic alteration of isorenieratene and of chlorobactene (**28**) gives rise to a series of aryl isoprenoids, *i.e.* 1-alkyl-2,3,6-trimethylbenzenes (*e.g.* **36**). Summons and Powell (1987) first identified such a series in oils and sediments of Silurian and Devonian age. MS and comparison with standards

I confirmed the characteristic 2,3,6 tri-methyl substitution pattern indicative of a green sulphur bacterial origin.

A similar series of compounds co-occurring with related di- (e.g. 37) and tri- (e.g. 38) components have now been reported in a variety of samples (Clark and Philp, 1989; Schwark and Puttmann, 1990; Clayton *et al.*, 1992; Requejo *et al.*, 1995; Hartgers *et al.*, 1994a; Guthrie and Pratt, 1995; Grice *et al.*, 1996b; Koopmans *et al.*, 1996 and references therein; Sinninghe Damsté and Köster, 1998). Where measured, the  $\delta^{13}\text{C}$  values are appropriately heavy ( $\delta^{13}\text{C} -13.4\text{‰} \pm 1.0$  to  $-21.3\text{‰} \pm 1.2$ ) for operation of the reversed TCA cycle (Grice *et al.*, 1996b; Koopmans *et al.*, 1996 and references therein). There have also been several studies of components released from macromolecular material by desulphurisation. For example, work on recent Black Sea sediments showed that the proportion of isorenieratene incorporated into sulphur-rich geomacromolecules increases with burial depth (Sinninghe Damsté *et al.*, 1993; Repeta, 1993; Wakeham *et al.*, 1995). This sequestration has been observed elsewhere, with the identification of a variety of diaryl isoprenoids, including isorenieratane, released from sulphur-rich macromolecular material (e.g. Kohnen *et al.*, 1991a,b). More detailed recent work has revealed an even wider range of products in sediments ranging from Ordovician to Miocene in age (Koopmans *et al.*, 1996). These include polyaromatics with up to three (e.g. 39) or four additional aromatic rings (e.g. 40), other  $\text{C}_{32}$  and  $\text{C}_{33}$  components with a variety of aromatic substitution patterns (e.g. 41) and shorter chain components containing sulphur (e.g. 42) and/or with additional aromatic ring patterns (e.g. 43). Again, heavy  $\delta^{13}\text{C}$  values for these components confirm their derivation from Chlorobiaceae. Indeed, isotopic measurements are essential for studies of such components as recent work on the Eocene Green River Shale has shown the potential formation of isorenieratane from the aromatisation of  $\beta$ -carotene (Koopmans *et al.*, 1997).

### *Maleimides*

Maleimides (1-*H*-pyrrole-2,5-diones) are oxidation products of cyclic tetrapyrrolic pigments. After the death of phytoplankton the pigments are susceptible to photo-oxidation (Jen and MacKinney, 1970a) in the euphotic zone, where they probably break down to maleimides. Indeed, the formation of methyl ethyl (Me Et) maleimide (44) by solar irradiation of chl *a* in synthetic seawater has been reported (Rontani *et*

*al.*, 1991). Such products may also be formed in the laboratory by oxidation of chlorophylls or their tetrapyrrolic degradation products using an oxidising agent such as chromic acid (Ellsworth and Aronoff, 1968; Ellsworth, 1970). Indeed, chromic acid oxidation (Didyk *et al.*, 1975; Hodgson *et al.*, 1971) or photo-oxidation (Crawford, personal communication) of sedimentary alkyl porphyrin fractions gives mixtures of alkyl maleimides which retain some information about the side chains present in the original chls. As expected, Me Et maleimide is the dominant product but the presence of extended chain maleimides (e.g. Me *i*-Bu maleimide, (45)), related to the extended alkylation in the bacteriochls *c*, *d* and *e*, provides evidence for the presence of green sulphur bacteria in the palaeo water column (Quirke *et al.*, 1980a; Grice *et al.*, 1996b). Maleimides also occur as such in sediments, presumably formed at the time of deposition (Grice *et al.*, 1997; Crawford, personal communication) and their distribution provides analogous information to that obtained by oxidation of co-occurring alkyl porphyrin fractions. Furthermore, where  $\delta^{13}\text{C}$  values can be determined for certain of the extended chain maleimides (*i.e.* Me *n*-Pr and Me *i*-Bu) relative to Me Et maleimide of mainly phytoplanktonic origin, and a significant enrichment observed, this provides further evidence for the existence of episodes of photic zone anoxia (Grice *et al.*, 1996b, 1997). Stable isotope studies are particularly important here with respect to Me *n*-Pr maleimide. Recent isotope work has shown that this component can also have a phytoplanktonic chlorophyll origin (Crawford, personal communication).

### **Present study**

High molecular weight ( $>\text{C}_{32}$ ) extended chain CAPs can be biomarkers for Chlorobiaceae. The present work involves the determination of the porphyrin distributions in a large range of sediment samples using an HPLC-PDA-APCI-MS approach, with the aim of recognising the presence or not of porphyrins derived from the green sulphur bacteria. Recognition of such components provides palaeoenvironmental information relating to the redox conditions within the water column by way of providing evidence for the presence of anoxia within the photic zone.

The specific aims of this work were:

1. (a) Assignment of HMW CAP structural isomers in the demetallated iron (ex-Fe)



porphyrins in Kupferschiefer marl by co-injection studies, extending this to a stratigraphic study of the porphyrin distributions in a core covering the entire Kupferschiefer deposition (Chapter 2).

(b) Extension of the approach to the demetallated porphyrins of Serpiano oil shale and sequences in Tertiary evaporitic marls (Vena del Gesso and Mulhouse basin) (Chapter 3).

2. Similar studies of the porphyrins in black shales deposited at different locations during the specific time period known as the Cenomanian/Turonian “oceanic anoxic event” (OAE) (Schlanger and Jenkyns, 1976). These comprise a suite of samples taken from outcrops from Italy and a section from Tunisia (Oued Bahloul), plus a range of DSDP core samples from the Atlantic (Chapter 4).
3. A study of the porphyrins in sediments deposited during other OAEs (*i.e.* Toarcian and Aptian) (Chapter 5).

Appropriate reference is also made to the distributions of free maleimides and/or those from oxidation of the porphyrin fractions. The maleimide studies have been carried out by a colleague (Crawford, personal communication).

## **CHAPTER 2**

# **INITIAL PORPHYRIN LC-MS STUDIES**

## INTRODUCTION

### Kupferschiefer

#### General

Kupferschiefer is the basal unit of the Upper Permian Zechstein evaporites and the horizon occupies a huge area from N.E. England across the N. Sea through Holland, Germany and Poland (Wedepohl, 1964, 1971; Ziegler, 1982; Vaughan *et al.*, 1989). It was deposited in anoxic bottom waters of the shallow epicontinental Zechstein Sea (Paul, 1982), as indicated by the presence of fine laminations, occurrence of well preserved fish and plant remains and an absence of benthic activity. The samples studied here come from a core (Rheinberger Heide) from the Lower Rhine Basin (Fig. 2.1), where a small (*ca.* 40x80km) lagoon existed (Eckardt, 1989; Grice *et al.*, 1996). Kupferschiefer from the basin is a typical black shale with an average TOC of *ca.* 4% (Püttmann and Eckardt, 1989). The lagoon is thought to have been between 50 and 80m deep and was periodically connected to the Southern Permian Basin over two palaeohighs (Schwark, 1992; Fig. 2.1).

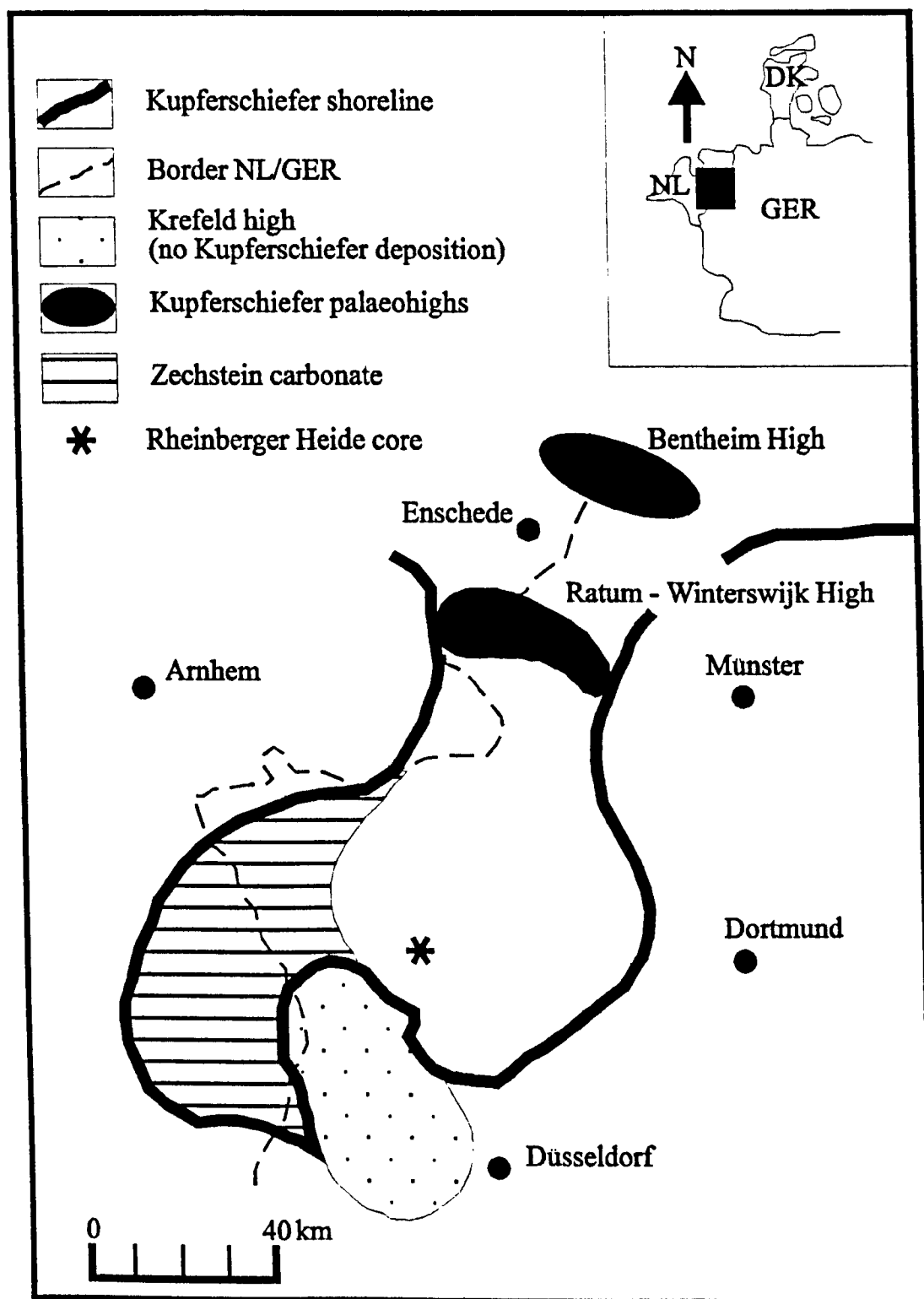
For the initial LC-MS study, an aliquot of an extract obtained previously from a bulk sample covering the first 60cm of the core, taken a few kilometres from the original shoreline, was used (Grice *et al.*, 1996a; Gibbison *et al.*, 1996; Schwark and Püttmann, 1990; Schwark, 1992). Aliquots of extracts of a suite of 20 samples were also examined, taken from the whole 2 metre length of the same core, covering the entire Kupferschiefer deposition (*c.f.* Grice *et al.*, 1996a).

#### Previous biomarker studies of Kupferschiefer from the Lower Rhine Basin

##### *Porphyrins*

High concentrations of alkyl porphyrins have been observed in bulk samples (Eckardt *et al.*, 1989). These were found complexed mainly to nickel (up to *ca.* 3000 µg/g TOC) but with a significant presence of both vanadyl (*ca.* 650 µg/g) and iron (up to *ca.* 400µg/g) porphyrins, the latter previously having only been found in very low concentrations in coals (*e.g.*, Bonnett *et al.*, 1983). Probe EI-MS revealed a carbon number range of C<sub>27</sub>-C<sub>35</sub>, with CAP species dominating the nickel and vanadyl porphyrins, whereas the aetio components were most abundant in the iron porphyrins (Eckardt *et al.*, 1989). LC-MS studies by Gibbison (1996), revealed, however, that higher relative abundances of HMW (≥C<sub>33</sub>) CAPs were present in the demetallated iron fraction (ex-iron). Hence, extensive HPLC isolation work was carried out on the

Fig. 2.1. Palaeogeography of the Lower Rhine Basin, NW Germany  
(Modified from Schwark, 1992)



ex-iron fraction (from the extract of 16 kg sample) to isolate minor HMW CAP components for structural elucidation. Normal phase HPLC separation initially provided a fraction containing >C<sub>32</sub> CAPs (amongst others). Further fractionation by normal phase and reversed phase HPLC provided six > C<sub>32</sub> components (one C<sub>35</sub>, two C<sub>34</sub> and three C<sub>33</sub> CAPs). <sup>1</sup>H NMR plus n.O.e studies allowed full characterisation of three of these, revealing the presence of a homologous series (34a-c) corresponding to one series of the bacteriochls *d* (6) (Gibbison *et al.*, 1996), with an Et group at C-12 and with an Et, *n*-Pr or *i*-Bu at C-8. Therefore bacteriochl *d*, unique to the green strains of Chlorobiaceae, existed in the water column during sediment deposition, providing direct molecular evidence for the existence of photic zone anoxia (PZA) during Kupferschiefer deposition in the Lower Rhine Basin. <sup>1</sup>H NMR also revealed a C<sub>34</sub> CAP with an Et-substituted 5-membered exocyclic ring with the same HPLC retention time under normal phase conditions as the C<sub>34</sub> porphyrin (34b) of bacteriochl *d* origin. Although the origin of this partially elucidated component is unclear, (46a or b) it is not a biomarker on structural grounds for any of the bacteriochls and therefore is not an indicator for PZA.

LC-MS co-injection studies were undertaken to determine whether the C<sub>34</sub> CAP (33), also of bacteriochl *d* origin, was present. The nickel standard synthesised by Bauder *et al.* (1992) was demetallated and co-injected with the ex-iron porphyrin fraction (Gibbison, 1996). This component co-eluted with the other two major C<sub>34</sub> components present in the HMW CAP region of the fraction. Therefore, under the normal phase analytical scale conditions used (Experimental – program 2) separation of structural isomers was not achieved, so there was no proof as to the presence of C<sub>34</sub> CAP (33) in the ex-iron fraction (Gibbison, 1996).

#### *Other biomarkers*

Recent work in our laboratory has shown the presence of free maleimides in the polar fraction (Grice *et al.*, 1996a). GC-MS showed a simple distribution dominated by Me Et maleimide (44) of mainly phytoplanktonic origin. Other components present in lower abundance were Me *n*-Pr (49) and Me *i*-Bu maleimide (45), derived on structural grounds from the bacteriochls *c*, *d* or *e*. Isotope ratio monitoring (irm) GC-MS showed both to be highly enriched in <sup>13</sup>C relative to Me Et maleimide and lipid biomarkers of phytoplanktonic origin (Chapter 1) and hence provided further evidence in the bulk Kupferschiefer sample for the existence of PZA. This work also showed the presence of complex mixtures of aromatic hydrocarbons with differing degrees of aromatisation,

including isorenieratane (35) diagenetically derived from the diaromatic carotenoid isorenieratene (30) of Chlorobiaceae origin (Grice *et al.*, 1996b). Stable carbon isotope studies of a number of these components, both as the free biomarkers and their S-bound counterparts released by nickel boride treatment of the polar fraction of the extract, also showed them to be significantly enriched. Hence these aromatic isoprenoid hydrocarbons are on structural and isotopic grounds assigned an origin in Chlorobiaceae.

#### *Kupferschiefer core samples*

The 2m core was previously sectioned into 20 samples of *ca.* 10 cm each. Schwark (1992) sub-divided it into four sections (TI, TIIA, TIIB and TIII, top) based on geological and sedimentary data. High hydrogen and low oxygen indices plus high TOC content of sub-section TI indicated that this related to deposition under more oxygen-depleted conditions (Schwark, 1992), probably resulting from higher productivity and better organic matter preservation. The presence of Me *n*-Pr (49) and Me *i*-Bu (45) maleimide together with <sup>13</sup>C-enriched aromatic hydrocarbons derived from isorenieratene throughout the core indicated that the entire deposition was characterised by periods of PZA. In particular, the higher relative abundance of Me *i*-Bu maleimide to Me Et maleimide in sub-section TI indicated that anoxygenic photosynthesis was rapidly established after the initial transgression of the Zechstein Sea, but became less prevalent in the upper core sections, with low abundances of Me *i*-Bu maleimide in samples 19 and 20 at the top of TIII highlighting an upward trend toward more oxygenated conditions, also shown by other biomarker distributions (*e.g.* Grice *et al.*, 1996b), at the end of Kupferschiefer deposition (Schwark, 1992).

#### **Serpiano oil shale**

The Serpiano oil shale from Monte San Giorgio, Switzerland, was deposited during the Mid Triassic (Anisian-Landinian boundary, *ca.* 239 Myr). The geology of the highly bituminous shales in the section (up to 55% TOC) has been discussed previously in detail (Zorn, 1971; Rieber, 1973, 1975 and 1982; Rieber and Sorbini, 1983 and Kuhn-Schnyder, 1974) and they are noted for the presence of very well preserved fossils of marine vertebrates. Serpiano shale was deposited in a shallow (50-100m) reef-bordered basin, approximately 8-10 km in diameter; reduced water circulation and high photic zone productivity resulted in the development of anoxic conditions in the bottom water as evidenced by the lack of bioturbation and benthic fossils (Zorn, 1971; Rieber, 1973 and 1975).

### Previous porphyrin studies

Serpiano contains high abundances of metalloporphyrins (*ca.* 3% of solvent extract) with much higher amounts of vanadyl than nickel species (Chicarelli, 1985). Traces of chlorins have also been found (Blumer, 1950). Various reports have described the porphyrin components, with nine ex-vanadyl components being fully characterised (for details see Chicarelli, 1985; Chicarelli and Maxwell, 1986; Chicarelli *et al.*, 1987; Chicarelli *et al.*, 1993). Although none of these are HMW porphyrins with extended alkylation, probe MS showed the presence of >C<sub>32</sub> CAPs in low abundance (*ca.* 1% of total porphyrins; Chicarelli, 1985). By comparison, the sum of the C<sub>35</sub> (**34c**) and C<sub>34</sub> peak c (**33** and **34b**) components in samples from the TI section of the Rheinberger-Heide Kupferschiefer core amounts to *ca.* 10% of the most abundant porphyrin, DPEP (**1**). Earlier HPLC-MS analysis of the ex-vanadyl porphyrins showed the presence of HMW CAPs, with mass chromatography and mass spectral data confirming that CAP components were present in the carbon number range C<sub>30</sub>-C<sub>35</sub> (Rosell-Melé *et al.*, 1996). The free maleimides and those from oxidation of the ex-vanadyl and nickel porphyrin fractions showed the presence of Me *i*-Bu (**45**) and Me *n*-Pr maleimides (**49**; Grice *et al.*, 1996a). Irm GC-MS analysis of the free maleimides revealed a significant enrichment in <sup>13</sup>C for the Me *n*-Pr component relative to the Me Et component (**44**). Therefore, on both structural and isotopic grounds, the maleimides provide specific evidence for a contribution from the bacteriochls *c* (**26**), *d* (**6**) or *e* (**27**) and hence that the deposition was characterised by periods of PZA within the palaeo water column (Grice *et al.*, 1996a).

## RESULTS AND DISCUSSION

### LC-MS coinjection studies

Previous studies (see above) of the two C<sub>34</sub> CAPs (**33** and **34b**) of bacteriochl *d* origin and the non-PZA C<sub>34</sub> CAP (**46a** or **b**) from the bulk Kupferschiefer sample revealed that under the normal phase HPLC conditions described by Barwise *et al.* (1986) (program 2- Chapter 7), separation of the three structural isomers was not achieved (Gibbison, 1996). This shows that LC-MS recognition alone of HMW CAPs does not provide proof for the presence of bacteriochl *d*-derived porphyrins, as porphyrins related either to other series of bacteriochls (*c* and/or *e*) or indeed to sources other than Chlorobiaceae could be present.

In the present study, the ex-iron fraction was used to investigate further the separation of the HMW CAP components under normal phase conditions. The overall distribution

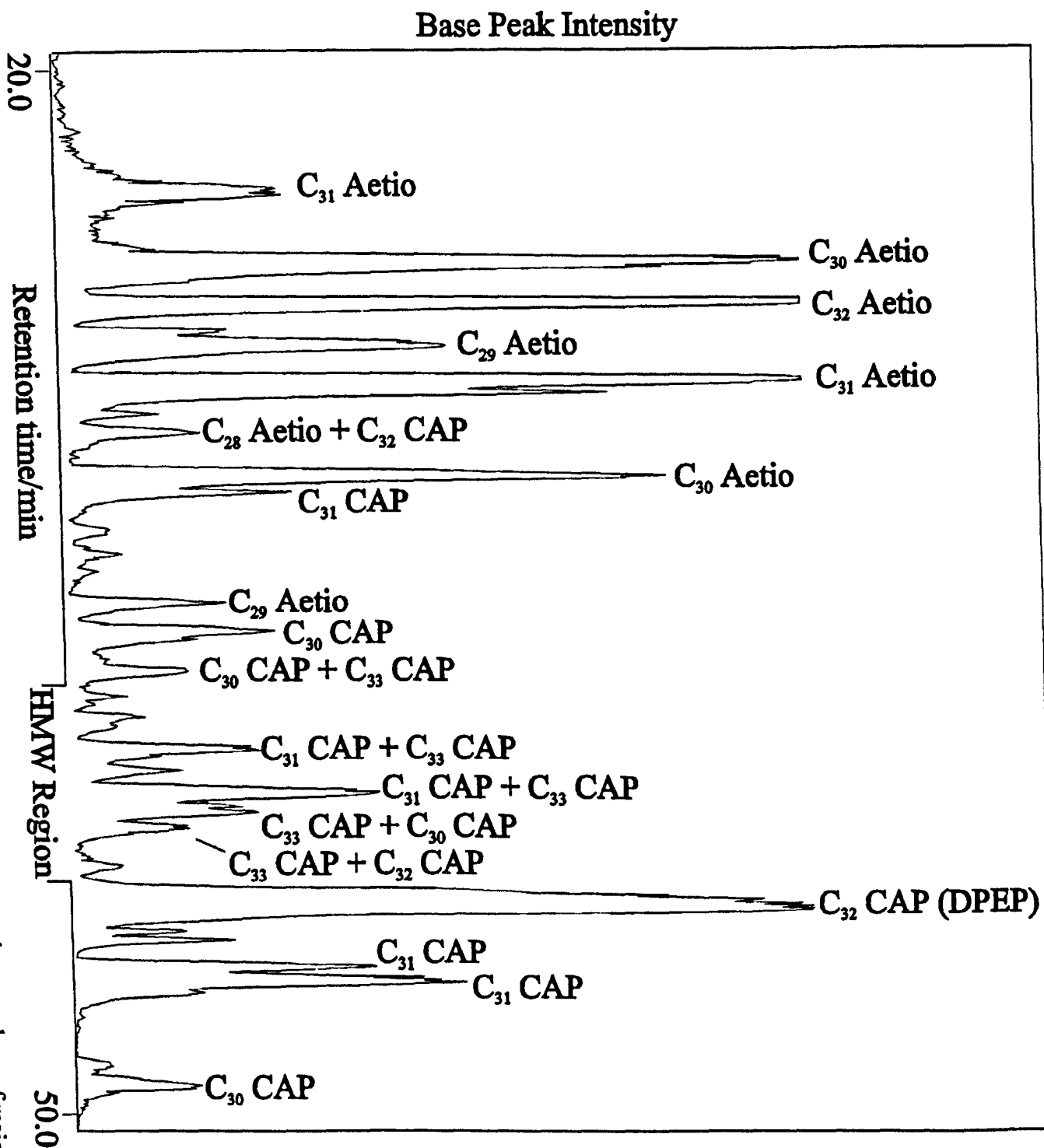
(fig 2.2) is in the form of a base peak chromatogram (*c.f.* Rosell-Melé *et al.*, 1996) based on the intensity of the base peak in the spectra ( $[M+H]^+$ ) and shows the major component to be DPEP (**1**; Gibbison, 1996). Carbon number assignments and structural types relate to the major type (or types when more than one  $[M+H]^+$  ion was present in comparable abundance) from examination of the mass spectra. Other significant peaks correspond to  $C_{31}$  and  $C_{30}$  CAPs ( $m/z$  463 and 449) and aetio-types within the range  $C_{28}$ - $C_{32}$  ( $m/z$  423, 437, 451, 465 and 479) which elute earlier than the CAPs (Chicarelli *et al.*, 1996). The major HMW ( $>C_{32}$ ) components elute within the middle of the chromatogram but it was noted that there are other minor ( $C_{30}$ - $C_{36}$ ) CAPs (see Chapter 3) eluting prior to the “HMW region” together with a pseudohomologous series eluting *ca.* 1 min after the bacteriochl *d* derived CAPs (not shown in the partial mass chromatograms in figs. 2.3 and 2.4., but see below; figs. 2.8 and 2.9). Mass chromatograms reveal the different series of component types, *e.g.* the CAP distributions in figs 2.3 and 2.4, and are a useful tool for recognising components, such as the HMW CAPs, present in relatively low abundance. Unfortunately, some of the chromatograms are noisy because of the extremely low abundance of the HMW CAPs and the DPEP peak is overloaded. A number of adjustments were made to the solvent program in order to obtain improved separation, in particular among structural isomers, resulting in program 3 (Chapter 7). The mass chromatogram corresponding to the  $C_{34}$  CAPs ( $m/z$  505) shows the major component(s) to elute only as a single broad peak in fig 2.3 using program 2 but the peak is resolved into three distinct, partially separated peaks under program 3 (fig 2.4) and the  $C_{35}$  CAP peak becomes a partly resolved doublet, although the  $C_{33}$  CAP region is essentially unchanged. With this improvement, co-injection of the appropriate available standards was carried out with the ex-iron fraction of the bulk sample.

Standards employed were:

1. *n*-Pr, Et  $C_{34}$  CAP (**34b**) – PZA biomarker, isolated from Kupferschiefer (Gibbison *et al.*, 1996);
2.  $C_{34}$  CAP with rearranged exocyclic ring (*e.g.* **46a** or **b**)– non-PZA marker, isolated from Kupferschiefer (Gibbison, 1996);
3. *i*-Bu, Me  $C_{34}$  CAP (**33**) – PZA biomarker, synthesised by Bauder *et al.* (1992);
4. *i*-Bu, Et  $C_{35}$  CAP (**34c**) – PZA biomarker, isolated from Kupferschiefer (Gibbison, *et al.*, 1996);



Figure 2.2 Partial LC-APCI-MS chromatogram of ex-iron porphyrin fraction of Kupferschiefer with carbon numbers of major peaks labelled.



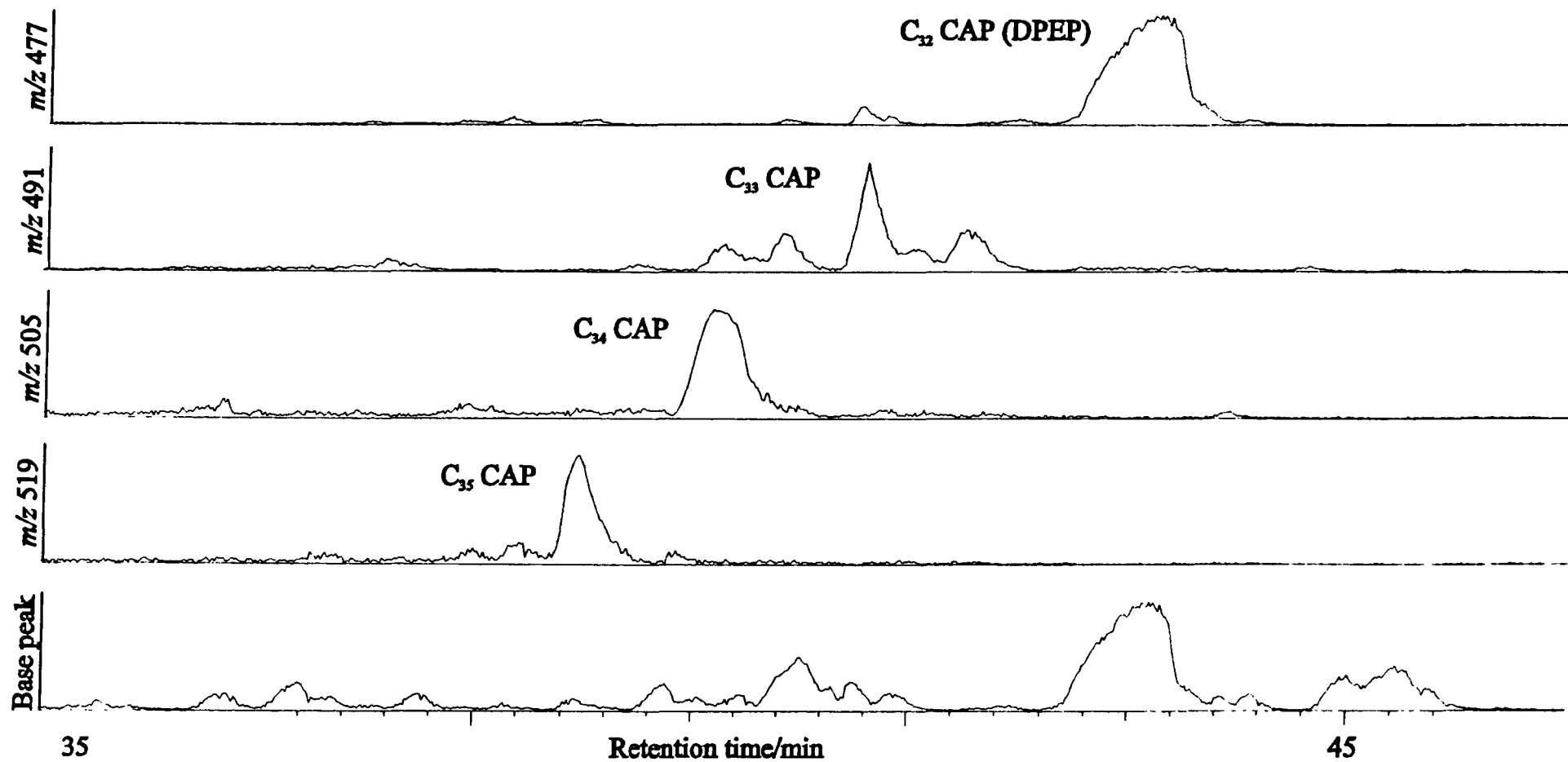


Figure 2.3 Mass chromatograms of high molecular weight components in Kupferschiefer using HPLC conditions shown in program 2.

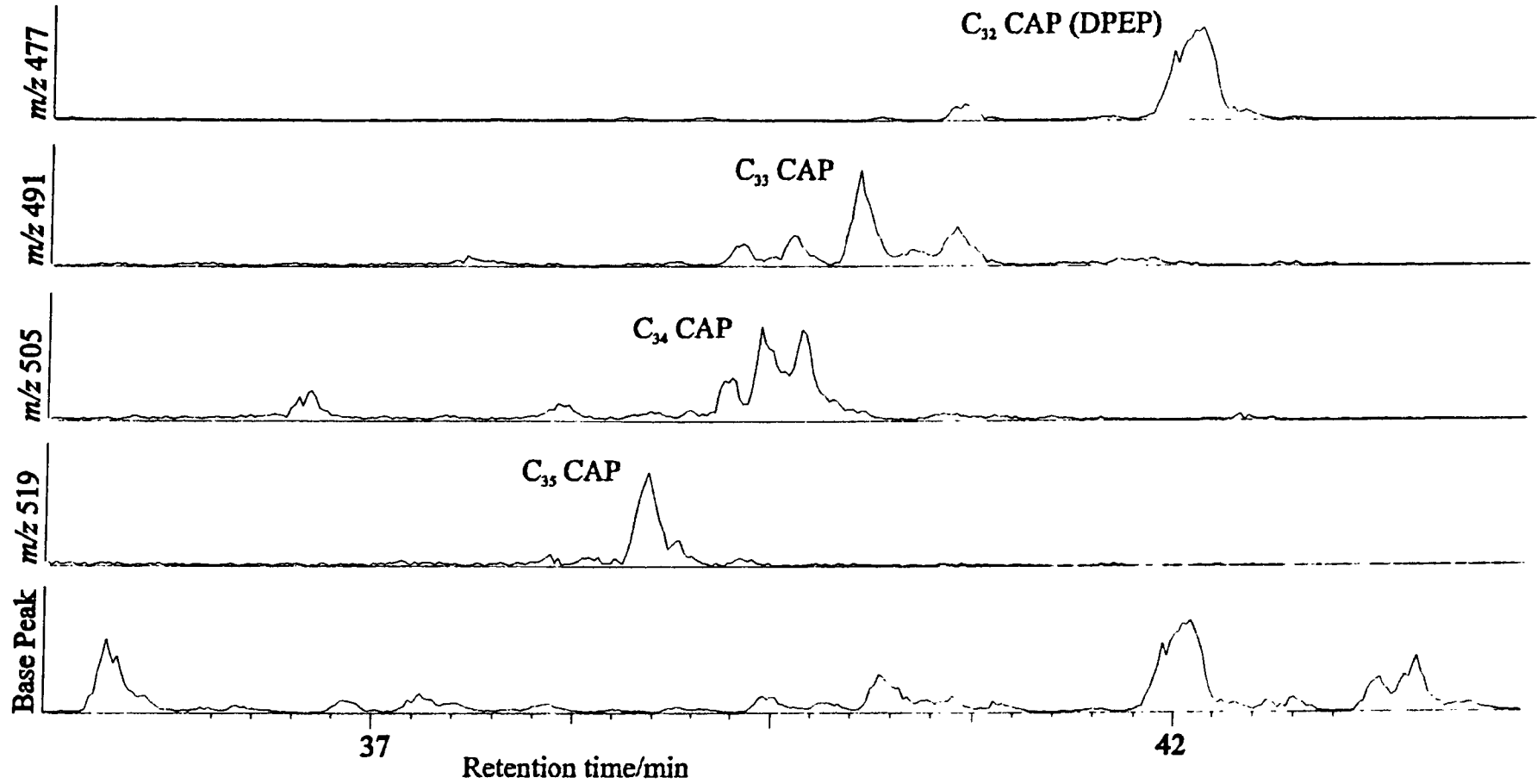


Fig 2.4 Mass chromatograms of high molecular weight CAP components in ex-iron porphyrin fraction of Kupferschiefer utilising modified HPLC conditions shown in program 3

5. Et, Et C<sub>33</sub> CAP (34a) – PZA biomarker, isolated from Kupferschiefer (Gibbison, 1996).

Fig 2.5a again shows the appropriate mass chromatograms with fig 2.5b showing the same fraction co-injected with the *n*-Pr, Et C<sub>34</sub> (34b) PZA standard. The *m/z* 505 chromatogram shows the familiar three major peaks distribution within the “HMW region”, with the third (peak c) enhanced after co-injection of 34b. Fig 2.5c shows the results of the co-injection of the C<sub>34</sub> *i*-Bu, Me CAP PZA standard (33) and also shows an enhancement of peak c. However, co-injection of the non-PZA C<sub>34</sub> CAP (46a,b) shows enhancement of peak b (fig 2.6a). It is therefore apparent that the two specific C<sub>34</sub> CAP biomarkers of the bacteriochls *d* still coelute with peak c within the characteristic distribution, whereas the C<sub>34</sub> CAP with the rearranged exocyclic ring coelutes with peak b. It is tempting to suggest, therefore, that with the modified solvent conditions and the careful use of retention time comparison, peak c in the C<sub>34</sub> mass chromatogram could be used as an indicator for the presence of bacteriochl *d*-derived porphyrins whereas peak b is an indicator of C<sub>34</sub> porphyrin(s) derived from other sources. However, it is important to note that the presence of porphyrins derived from bacteriochls *c* (26) or *e* (27) is also possible and these could in theory co-elute with any of peaks a-c, although the presence of a methyl at C-20 in such components would be expected to significantly alter the HPLC retention times. If this is the case, some of the early eluting CAPs or the pseudohomologous series of CAPs observed eluting *ca.* 1 min after the bacteriochl *d*-derived components (fig. 2.9), may be derived from either or both the bacteriochls *c* and *e* (Chapter 3). Unfortunately, with the absence of C-20 methyl substituted porphyrin standards, it is not possible to directly test this theory. The *m/z* 519 chromatograms before (fig. 2.6a) and after (fig. 2.6b) co-injection of the *i*-Bu, Et C<sub>35</sub> CAP clearly show an enhancement of the major C<sub>35</sub> CAP peak. Likewise, the Et, Et C<sub>33</sub> CAP coelutes with one of the later eluting major *m/z* 491 peaks (fig. 2.6a and c).

In summary, fig 2.7 shows the mass chromatograms of the CAPs (C<sub>32</sub>-C<sub>35</sub>) resulting from the LC-MS analysis of the ex-iron porphyrin fraction of the bulk Kupferschiefer sample. The shaded peaks correspond to components which co-elute with the available standards derived from the bacteriochl *d* series and taken together, their occurrence can therefore be used as evidence for the presence of components derived from Chlorobiaceae and thereby for the existence of PZA during sediment deposition. Kupferschiefer also contains a series of mono aromatic 2,3,6- substituted isoprenoids

Figure 2.5 Partial mass chromatograms for HMW components of ex-iron fraction

(a) before co-injection of standards (b) after co-injection of  $C_{34}$  *n*-Pr Et (34b) and (c) of  $C_{34}$  *i*-Bu Me (33) standards

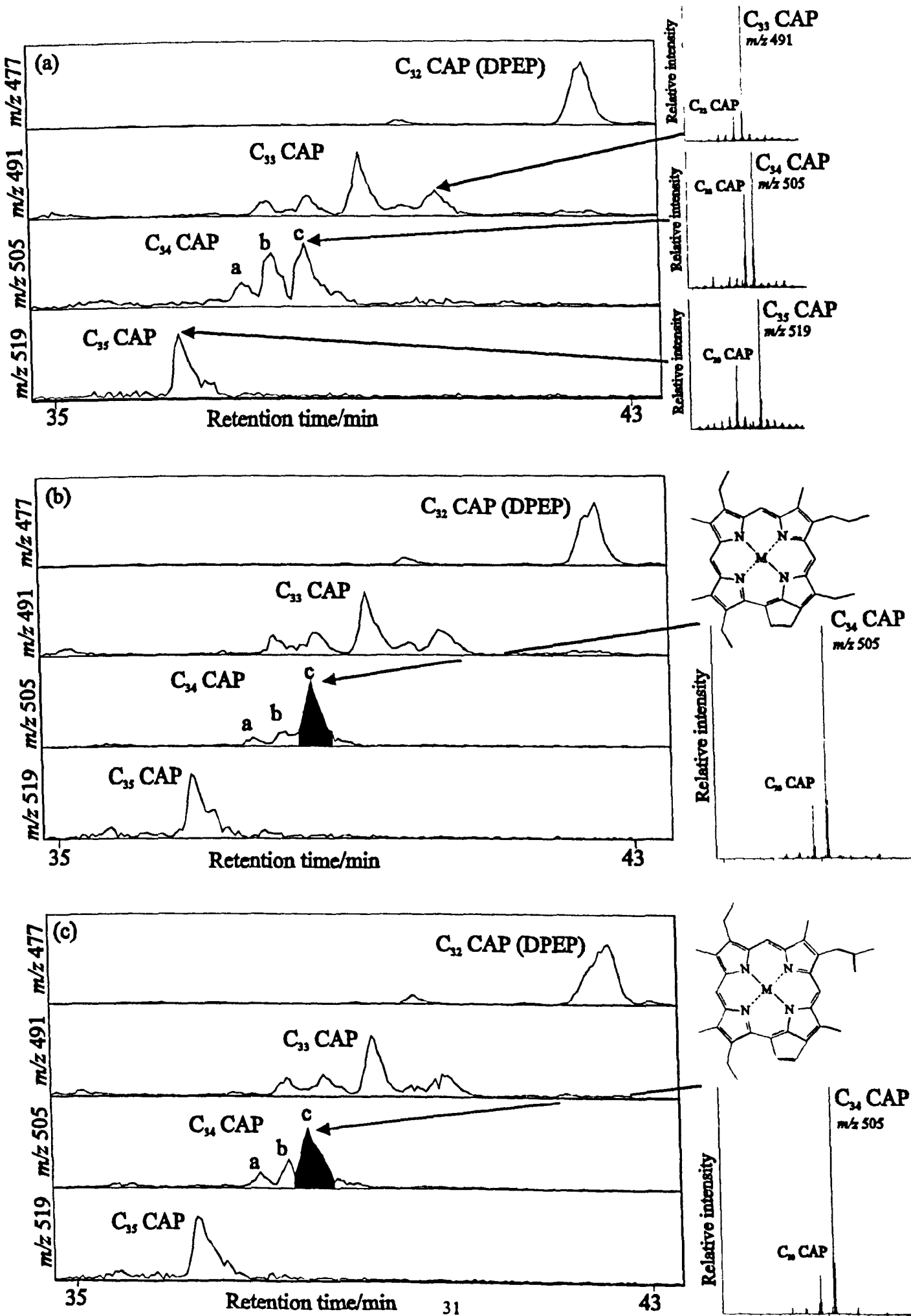
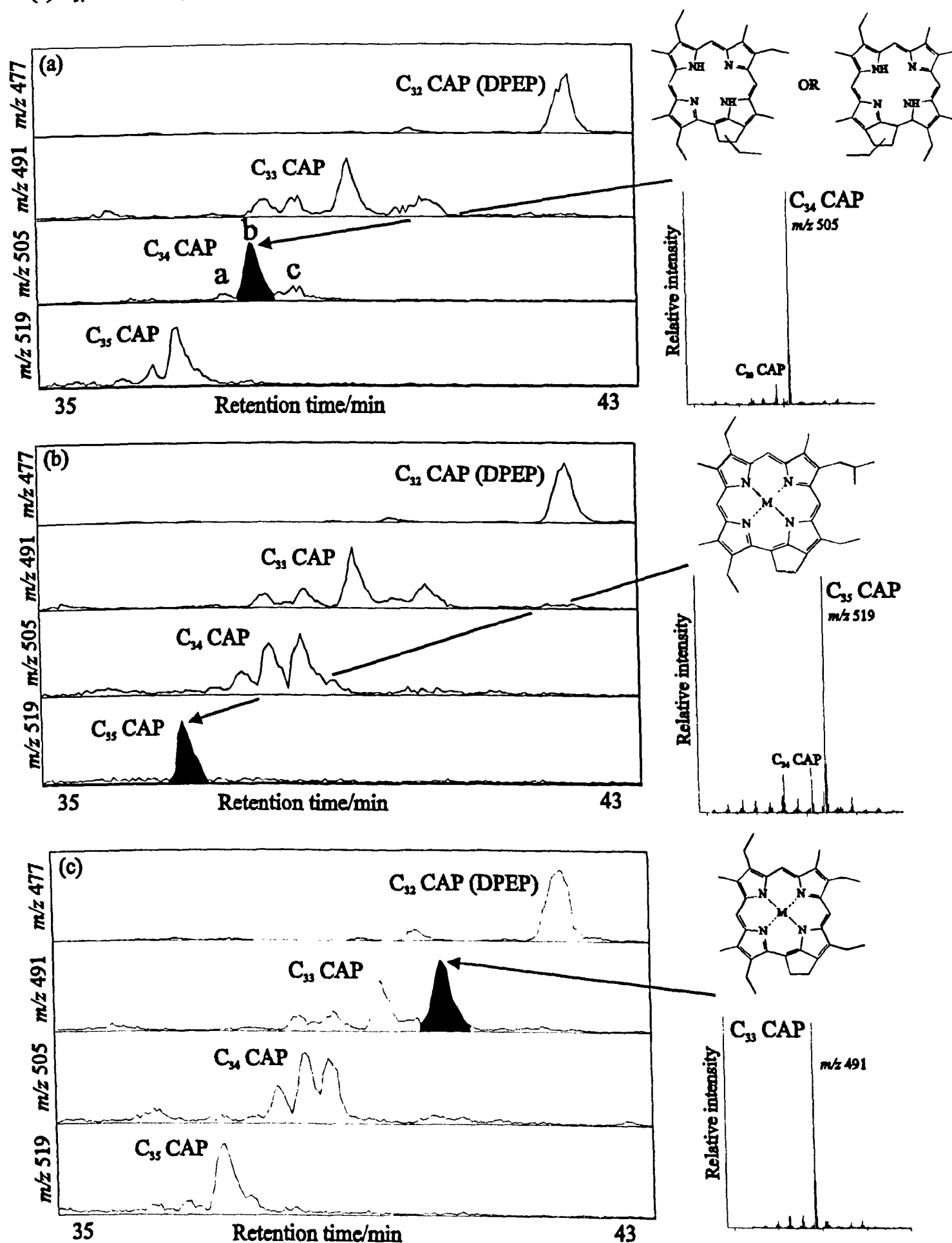


Figure 2.6 Partial mass chromatogram for HMW components of ex-iron fraction after co-injection of

(a)  $C_{34}$  non-PZA (46a,b) standard (b)  $C_{35}$  *i*-Bu Et (34c) standard and (c)  $C_{33}$  Et Et (34a) standard



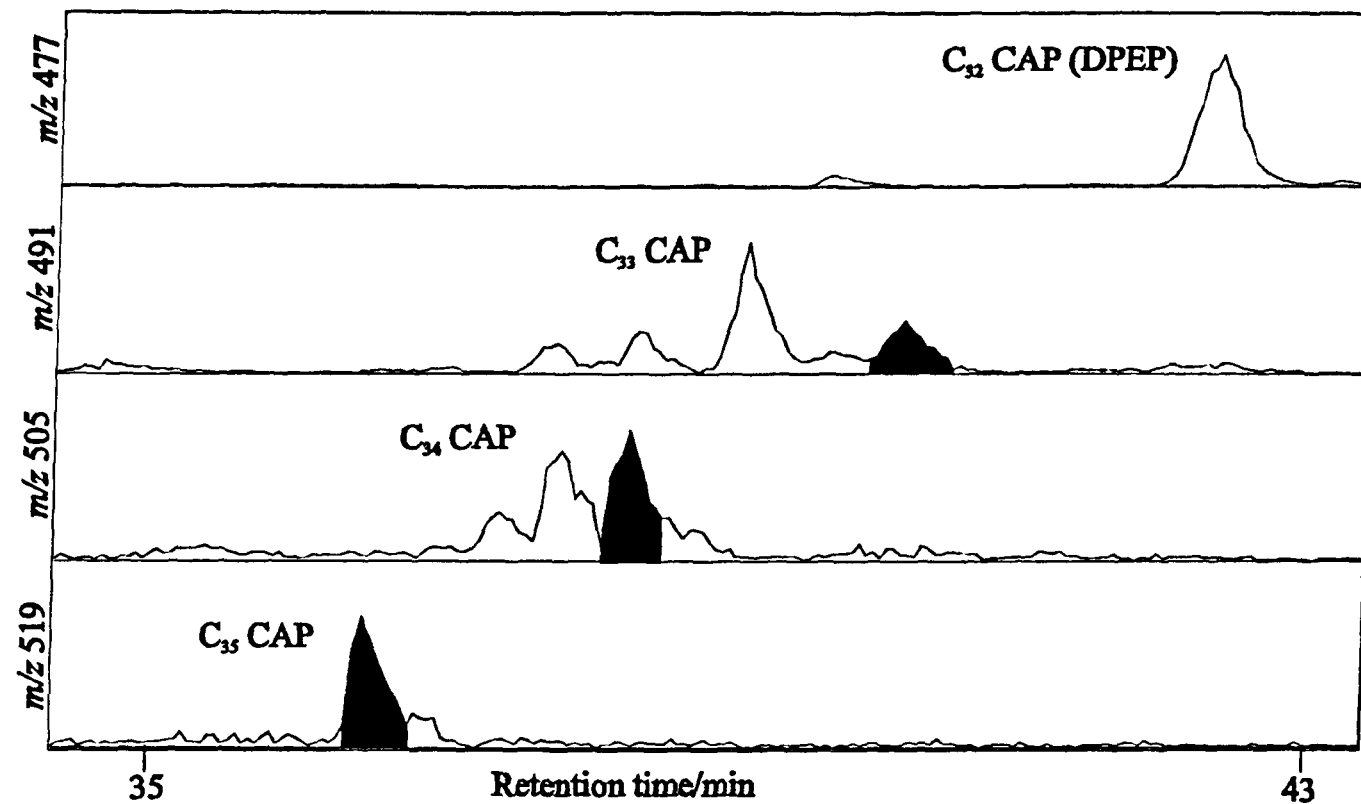


Figure 2.7 Partial mass chromatograms for HMW CAPs with shaded peaks showing components co-eluting with porphyrins derived from bacteriochlorophyll *d* series

derived from the green strains of Chlorobiaceae together with abundant diaryl isoprenoids diagenetically derived from isorenieratene from the brown strains (Grice *et al.*, 1996b, 1997). So both green and brown strains of Chlorobiaceae were present in the palaeowater column of the Kupferschiefer depositional setting, suggesting that there were periods when the chemocline existed at different depths (de Wit, personal communication). LC-MS has also shown the existence of at least two series of unidentified HMW CAPs, confirmed by their mass spectra, eluting both earlier and later than the bacteriochl *d*-derived CAPs (figs. 2.8 and 2.9). It might be expected that since abundant diaromatics from isorenieratene are present, that porphyrins derived from the bacteriochls *e* should also be present. It might also be expected (see above) that the C-20 Me would have a significant effect on retention time, so it is tempting to suggest that some of these other CAPs are derived from either or both the bacteriochls *c* or *e*. If this is the case, it is difficult, however, to explain the presence of the early eluting C<sub>31</sub> and C<sub>32</sub> components from the defunctionalisation of the bacteriochls *c* (26) or *e* (27), if these components are indeed members of the series. It is noted further, that even if some of these early or late eluting components are derived from the bacteriochls *c/e*, there are still other components present which are therefore derived from other unknown sources.

On the other hand, oxidation of a porphyrin fraction (T1+ T3; in which the HMW region had been removed by prep-HPLC) from a Cenomanian/Turonian black shale (chapter 4) containing porphyrin components with the same retention behaviour, revealed the presence of Me *i*-Bu maleimide (45).

### **Kupferschiefer core**

Crude fractions containing nickel porphyrins plus aromatic hydrocarbons obtained from Schwark (1992) for each sample (T1-20) within the core were separated further into hydrocarbon and porphyrin sub-fractions by Grice (1995). The nickel porphyrins were demetallated and the free bases purified and analysed by HPLC-MS. Each sample shows a distribution containing many of the major peaks present in the bulk sample. For example DPEP (1) is present throughout, as are other major CAP species (C<sub>28</sub>-C<sub>31</sub>) and a range of aetio porphyrins (C<sub>28</sub>-C<sub>32</sub>). Each sample contains a varying distribution of HMW CAPs with the characteristic 3 peak C<sub>34</sub> distribution in some samples but with others showing a different distribution. Examples of such changes are shown in fig 2.9, with shaded peaks representing the components which compare exactly with the retention time of the standards derived from bacteriochl *d*. The presence of such



Fig. 2.8. Partial mass chromatograms for early eluting CAPs ( $C_{31}$ - $C_{36}$ ) from Kupferschiefer bulk sample

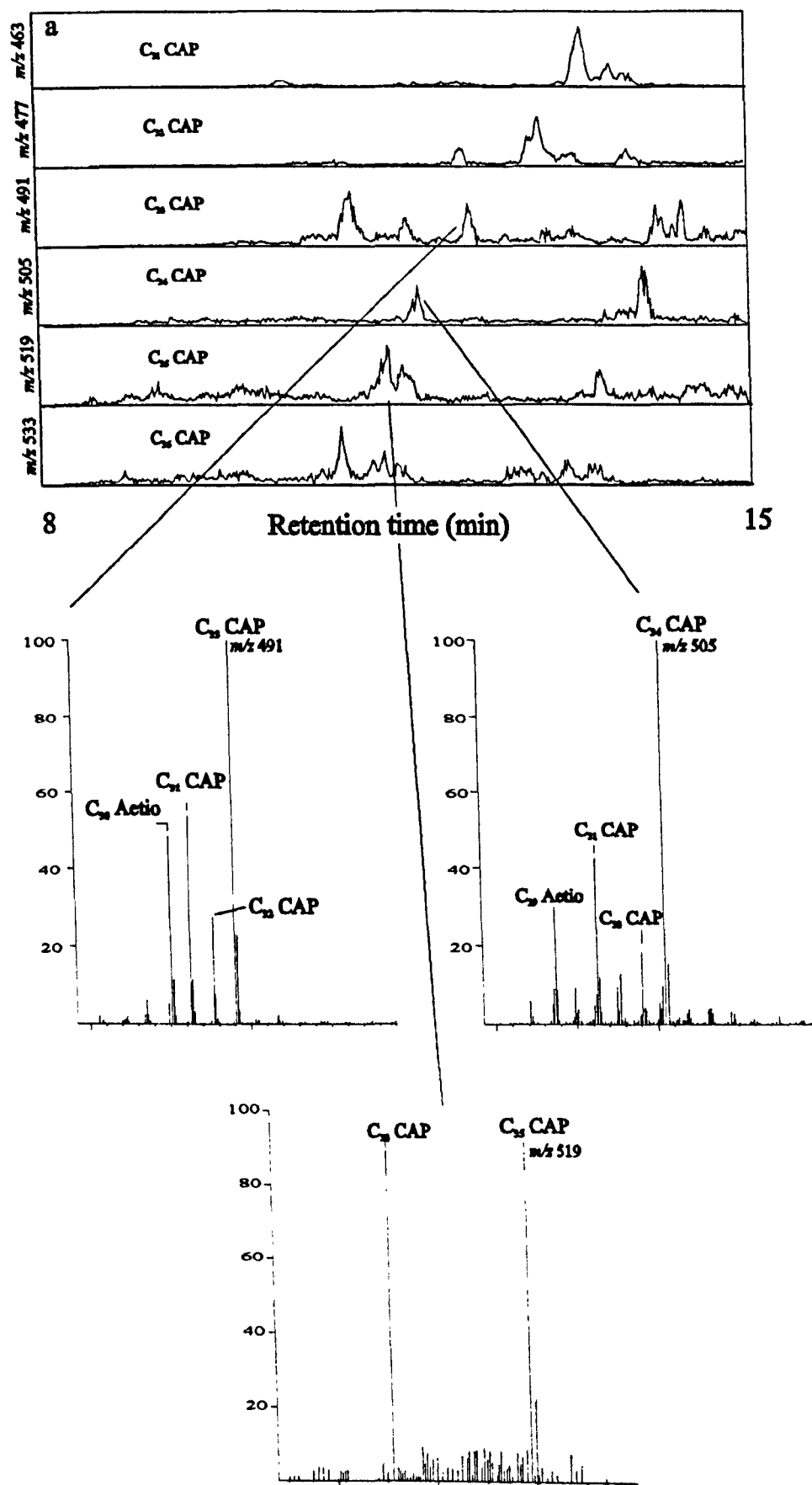
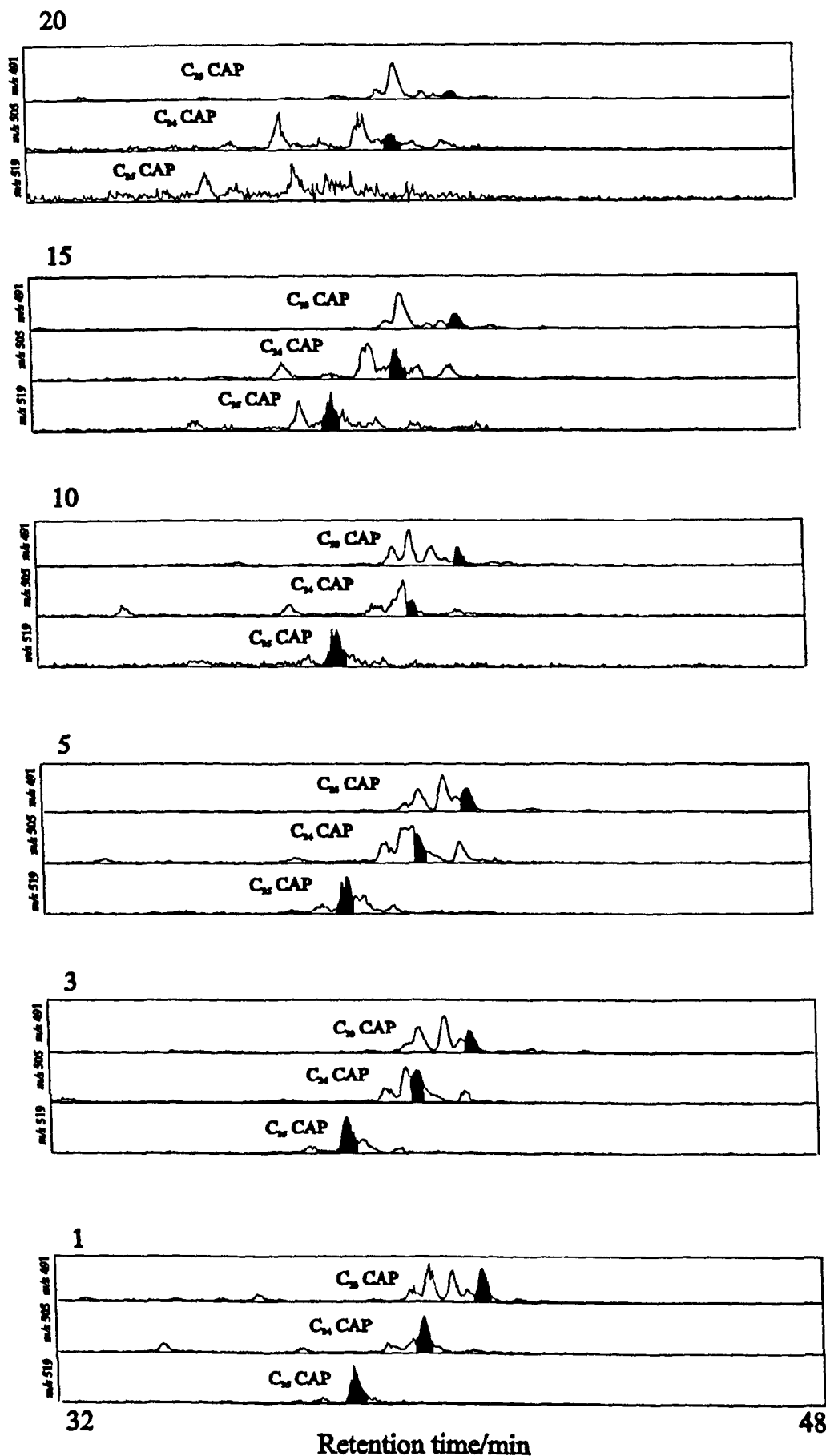


Figure 2.9 Partial mass chromatograms showing HMW CAP components ( $C_{33}$ - $C_{35}$ ) for ex-Ni porphyrins in selected samples (1,3,5,10,15 & 20)

Shaded peaks indicate components co-eluting with porphyrin standards derived from bacteriochl d



porphyrin components with the same retention time as those derived from bacteriochl *d* extends the previous work of Grice *et al.* (1996b) who found Me *i*-Bu maleimide throughout the core, suggesting that the entire deposition of Kupferschiefer in the Lower Rhine Basin was characterised by periods of PZA. The chromatograms show interesting changes, especially between those from the lower section (TI) and those near the middle or at the top (TII, TIII). For example, the C<sub>34</sub> mass chromatogram in sample 1 (TI) at the bottom clearly shows a relatively large peak *c* as compared with sample 3 (TI) which in turn is larger than in the other samples. Likewise, the C<sub>33</sub> peak co-eluting with the bacteriochl *d*-derived porphyrin (34a) is relatively more abundant (compared with the other C<sub>33</sub> components) in sample 1 than in any of the other samples. It is also interesting to note the presence of other HMW CAPs eluting both at earlier and later retention times. For example, the *m/z* 505 chromatograms for samples 1 and 10 clearly show C<sub>34</sub> CAP components, confirmed by the mass spectra, eluting very much earlier (*ca.* *t<sub>R</sub>*=33 to 35 min) than the C<sub>34</sub> CAPs derived from bacteriochls *d*. Other C<sub>34</sub> CAPs are also seen, particularly in the samples from section TIII (*i.e.* 16-20) eluting slightly earlier than peak *c* (*ca.* 1 min earlier; fig. 2.8). The results also show other C<sub>34</sub> CAPs eluting soon after the bacteriochl *d*-derived peak *c* component in most of the samples. Likewise, the multiplicity of C<sub>35</sub> CAPs increases in samples from TIIB upwards (samples 14-20).

The peak area of the C<sub>34</sub> peak *c* components (assumed to be a biomarker for bacteriochl *d*), was compared with the area of the DPEP peak, DPEP being derived mainly from phytoplanktonic sources, *i.e.* mainly from chl *a*. The ratio would be expected to reflect the changes in the relative contribution of bacteriochls of Chlorobiaceae compared with chlorophyll of phytoplanktonic origin. Fig. 2.10 displays the plot of the ratio, which shows initially a relatively high contribution of the peak *c* in samples 1 and 2 in section TI, and decreases towards section TIIA to a value (except for sample 5) which stays more or less constant, with minor fluctuations, until dropping in sample 20 at the top of section TIII. This compares favourably with the Me *i*-Bu/Me Et maleimide ratio used to plot changes in bacteriochl relative to phytoplanktonic chlorophyll input in previous studies (Grice *et al.*, 1996b). The latter plot (fig. 2.11) also shows a maximum abundance of Me *i*-Bu maleimide in samples 1 and 2 in TI which again then drops and remains fairly constant until the top of section TIII. Hence, the C<sub>34</sub> peak *c*/DPEP porphyrin ratio strengthens the suggestion that the conditions of PZA were set up soon after the initial transgression of the Zechstein but that these conditions became less

Figure 2.10 Plot of  $C_{34}$  (peak c) component /  $C_{32}$  (DPEP) through core

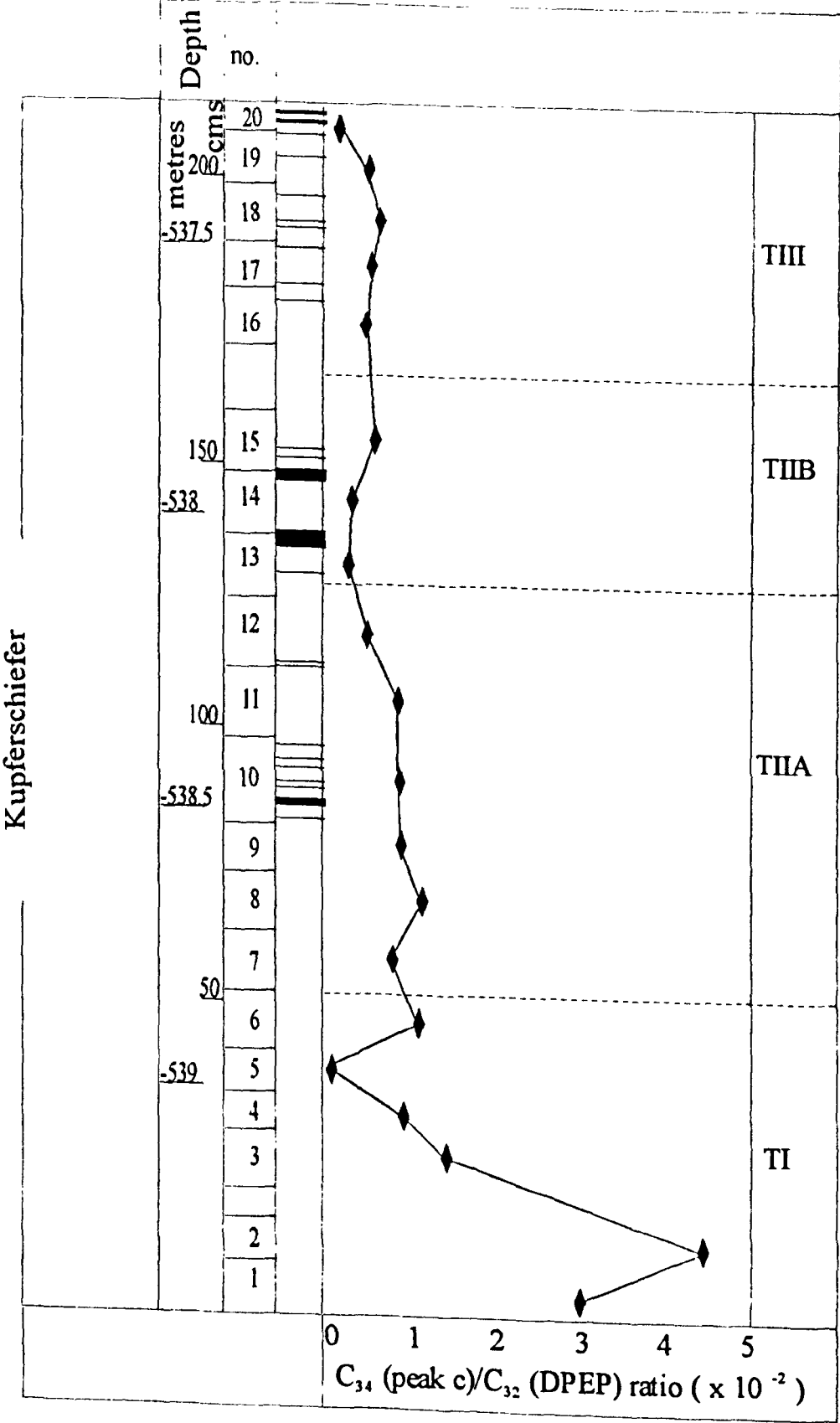
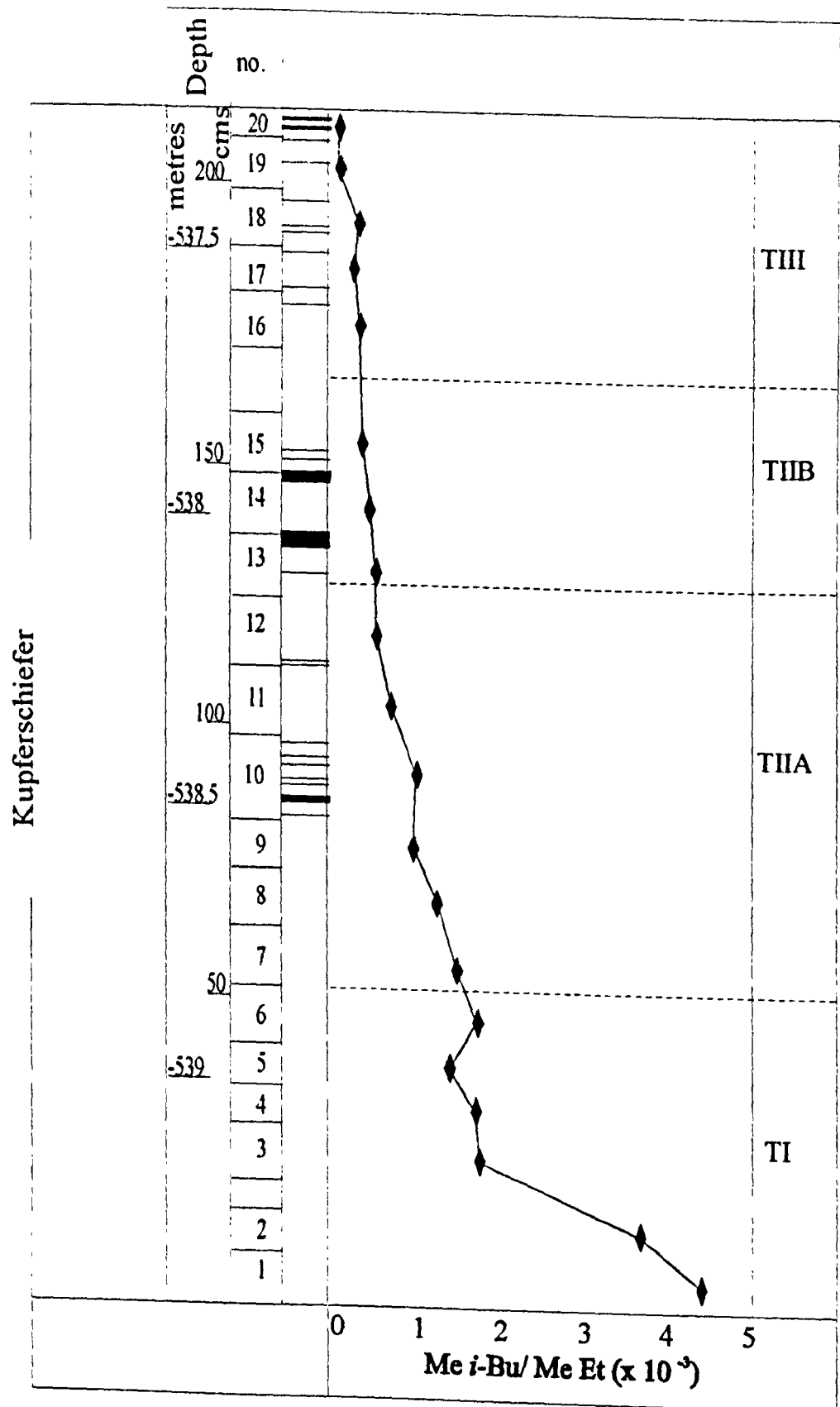


Figure 2.11 Plot of Me *i*-Bu / Me Et maleimides through core



Reproduced from Grice *et al.* (1996b)

prevalent during the deposition of the upper core sections, especially at the top of section TIII where Kupferschiefer deposition precedes deposition of the Zechstein carbonates which were deposited under more oxygenated bottom water conditions (Schwark, 1992). Me *i*-Bu maleimide is assigned an origin from certain of the bacteriochls *c* (26), and/or *d* (6) and/or *e* (27) with an *i*-Bu substituent at C-8, whereas peak *c* in the C<sub>34</sub> mass chromatogram is thought to be bacteriochl *d*-derived. Although the presence of HMW CAPs derived from bacteriochls *c* and *e* and having the same retention time as the peak *c* cannot be completely ruled out, it is perhaps more likely that the C<sub>34</sub> peak *c*/DPEP porphyrin ratio would reflect changes in the contribution from bacteriochl *d* only, whereas the Me *i*-Bu/Me Et maleimide ratio is less specific reflecting changes in input from any of the three bacteriochlorophyll types. Such considerations might explain minor discrepancies between the trends in the two ratios. Figure 2.12 shows the peak area ratio of the C<sub>35</sub> HMW CAP / C<sub>32</sub> DPEP which shows the same general trend as the C<sub>35</sub> plot (figs. 2.10), with higher values for samples 1 and 2, intermediate values in the remainder of section TI and most of section TIIA and lower values within sections TIIB and TIII. There are, however, some differences, for instance the rise within section TIIA. Such fluctuations could be a results of: (1) noise in the C<sub>35</sub> CAP chromatograms (fig. 2.9), as the component(s) is present in much lower abundance than the C<sub>34</sub> CAP peaks, leading to a reduced precision of the calculation of the peak area or (2) varying contributions of C<sub>35</sub> CAPs not of bacteriochl origin. The maleimide distributions show the presence of Me *n*-Bu and Me *sec*-Bu maleimides (Grice, 1995). These extended alkyl substituents could also be present in hypothetical C<sub>35</sub> CAPs such as *n*-Bu Et (47) or *sec*-Bu Et (48); such hypothetical components, if present, might coelute with the C<sub>35</sub> CAP peak in the *m/z* 519 chromatogram, or alternatively might be responsible for some of the other observed C<sub>35</sub> components (see also chapter 4). Fig. 2.13 shows the peak area ratio of the bacteriochl *d*-derived C<sub>33</sub> HMW CAP component / C<sub>32</sub> DPEP which shows some similarities to the other plots, but with greater discrepancies when compared with the maleimide plot in fig. 2.11. For instance, a general decreasing trend is observed within section TIIA as with the maleimides, but significant increases can be seen in sections TIIB and TIII. Again, the maximum ratio is seen in sample 2 as opposed to sample 1 and the increase seen in samples 18-20 is similar to that seen in fig. 2.12 for the C<sub>35</sub> HMW CAP / DPEP ratio. Fig. 2.13 suggests that the C<sub>33</sub> CAP / DPEP ratio seems to be a less precise reflection of the contribution of Chlorobiaceae than the Me *i*-Bu / Me Et maleimide ratio or the

Figure 2.12 Plot of major  $C_{35}$  component /  $C_{32}$  (DPEP) through core

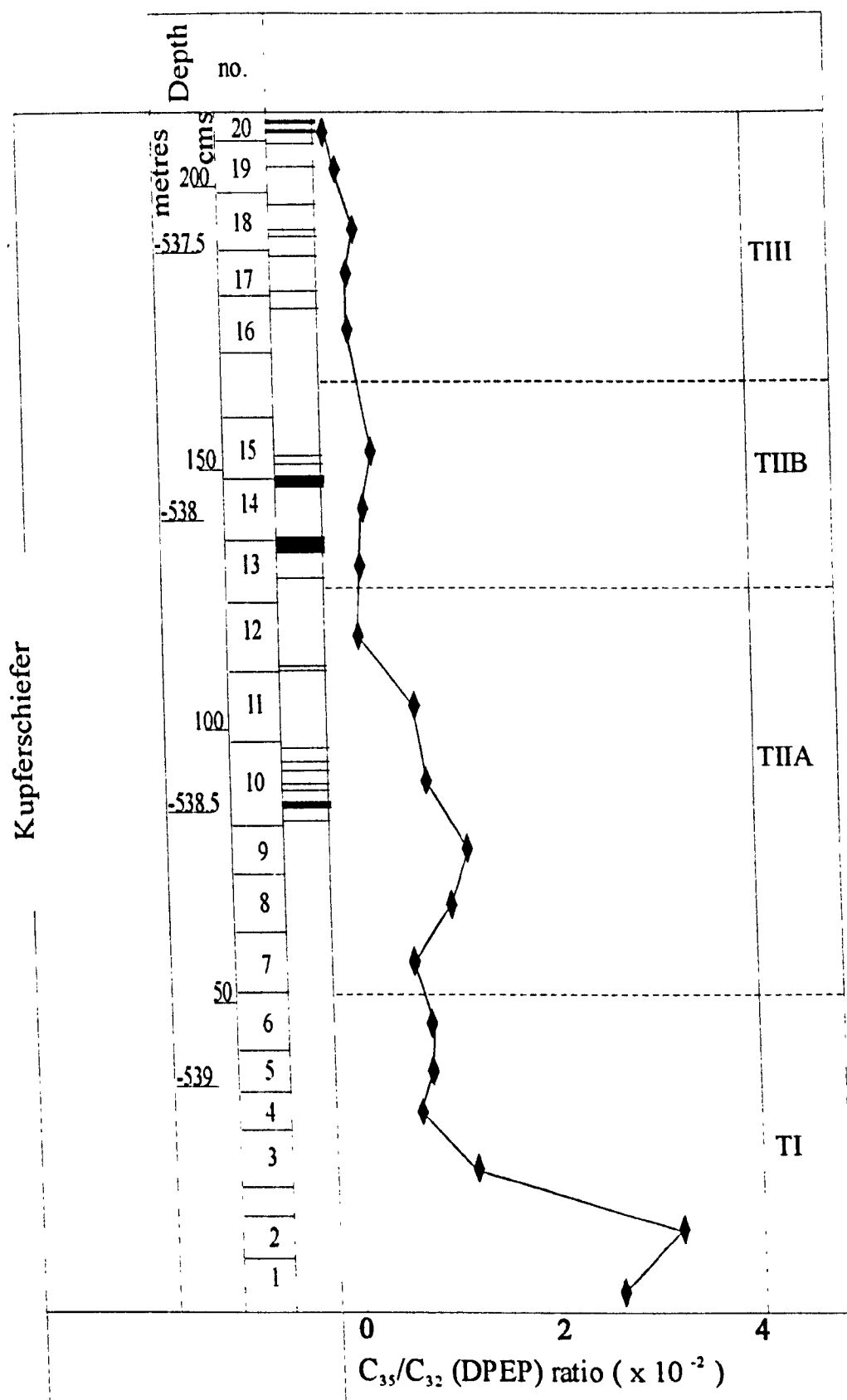
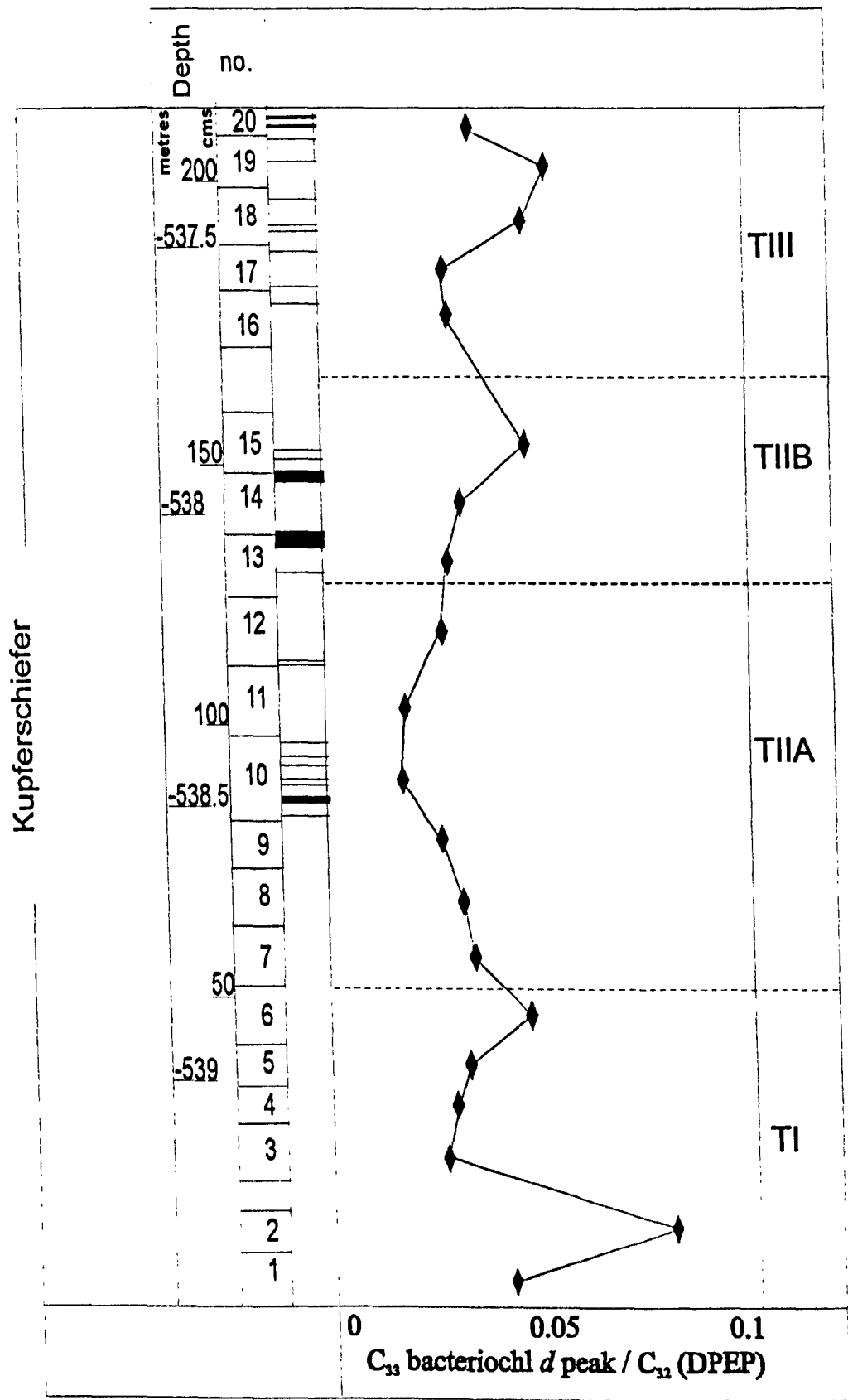


Figure 2.13 Plot of bacteriochl *d* C<sub>33</sub> component / C<sub>32</sub> (DPEP) through core





C<sub>34</sub> peak c / DPEP porphyrin ratio. Although there is a greater peak multiplicity in the C<sub>33</sub> chromatogram, the greater number of hypothetically possible C<sub>33</sub> isomers might result in more than one component contributing to the bacteriochl *d*-derived C<sub>33</sub> CAP peak.

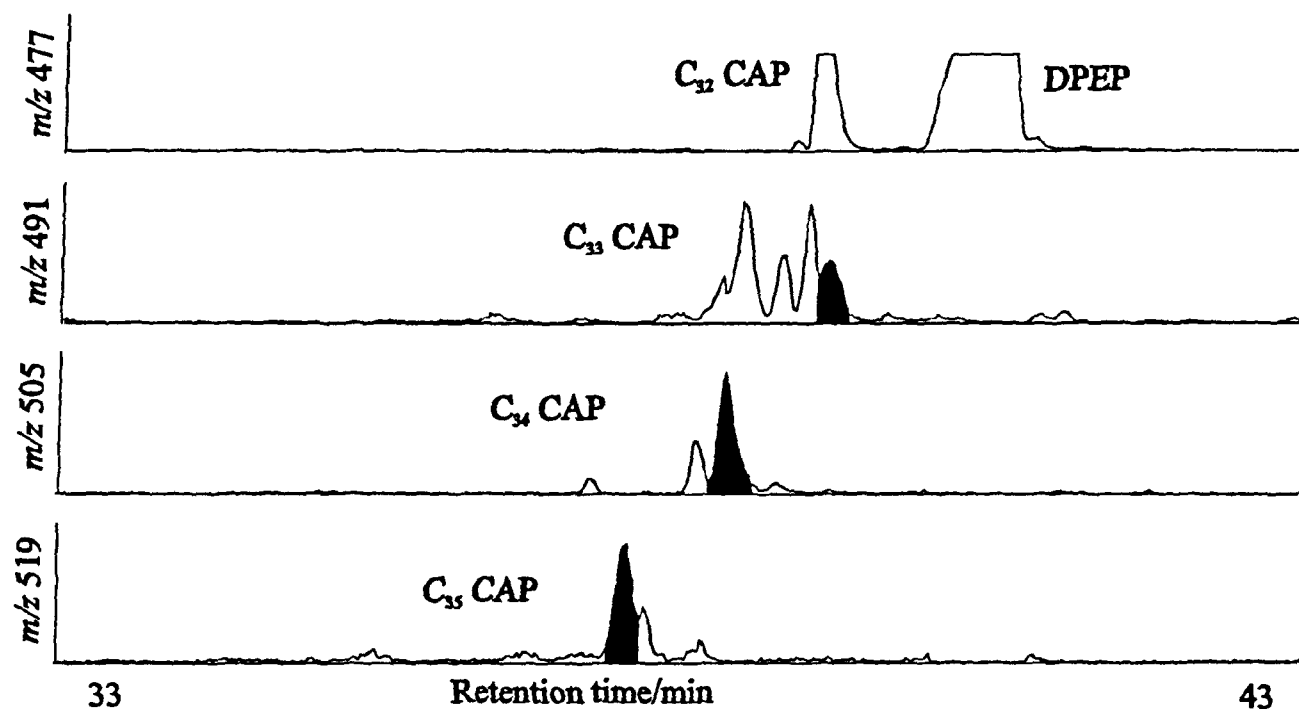
Overall, however, the similarity in the trends of the porphyrin ratios and maleimide ratio observed through the core indicates that porphyrins appear to reveal the presence of changing contributions from the bacteriochls of Chlorobiaceae and hence that the approach can at least be tentatively used for the investigation of the occurrence of PZA, especially if large numbers of samples need to be rapidly screened, and with greater confidence if the distributions of the other PZA biomarkers are also investigated (*i.e.* alkyl maleimides and/or aryl isoprenoids – see introduction).

#### **LC-MS studies of Serpiano shale**

As a further test for the improved solvent programme, the demetallated vanadyl porphyrins were analysed by HPLC-MS. The overall distribution was the same as described by Rosell-Melé *et al.*, (1996), with slight differences in the peak distribution of the HMW CAPs (fig 2.14) as a result of the improved resolution. Figure 2.14 shows the appropriate mass chromatograms with the peaks having the retention times of the bacteriochl *d*-derived standards (C<sub>33</sub>-C<sub>35</sub>) shaded. The major peak in the *m/z* 519 chromatogram corresponds to the (*i*-Bu Et) C<sub>35</sub> CAP standard (34c) and a significant peak in the *m/z* 491 chromatogram to the (Et Et) C<sub>33</sub> standard (34a). The C<sub>34</sub> mass chromatogram shows the presence of two resolved major peaks (peak a absent), the later co-eluting with the two C<sub>34</sub> components of bacteriochl *d* origin (33 and 34b), equivalent to peak c in the Kupferschiefer distribution. The other C<sub>34</sub> peak corresponds in retention time to peak b in the Kupferschiefer distribution and the non-PZA C<sub>34</sub> standard (46a,b).

In summary, the HMW CAP distributions of the ex-vanadyl porphyrins show the presence of peaks corresponding to standards derived from the bacteriochl *d* series. On their own, these results provide reasonable evidence for the presence of Chlorobiaceae chlorophylls in the palaeo water column. Taken with the previous maleimide study discussed above (Grice *et al.*, 1996a) they strengthen the confirmation of the existence of water column stratification and PZA during the deposition of the Serpiano oil shale 239 million years ago in a lagoonal setting.

Figure 2.14 Partial mass chromatograms showing HMW CAPs present in ex-vanadyl porphyrin fraction of Serpiano oil shale



Shaded peaks show components with same retention times as porphyrin standards derived from bacteriochlorophyll *d*

**CHAPTER 3**

**LC-MS STUDIES OF PORPHYRINS FROM**

**TERTIARY EVAPORITIC MARLS**

## INTRODUCTION

Evaporites are typically formed by the precipitation of salts from natural brines during evaporation of lagoons, saline lakes or marginal salt pans. There is much evidence that evaporitic source rocks have contributed to major oil reserves (Palacas, 1984 and references therein) which has led to many studies aimed at developing an understanding of evaporitic source rock formation (Eugster, 1985; Warren, 1986 and Evans and Kirkland, 1988). Evaporites can form in many different environments (*e.g.* Schreiber and Hsü 1980) as evidenced by studies of modern depositional settings in the wide coastal flat areas (sabkhas) of the Persian Gulf (*e.g.* Shearman, 1963; Purser, 1985), continental salt lakes in North America and eastern Africa (Eugster and Hardie, 1978), gypsum lakes in southern Australia (Warren, 1989) and marine settings world-wide (Javor, 1989 and references therein). With such a range of depositional regimes, the extent of organic matter accumulation varies, with the general controls being the extent of primary production, conditions of preservation and inorganic sedimentary dilution effects (*e.g.* Demaison and Moore, 1980; Huc, 1988; see also chapter 4). Although the number of organism species contributing to the organic matter in evaporitic environments is low, decreasing with increasing salinity, the overall level of productivity can be high (*e.g.* Evans and Kirkland, 1988), with the main primary producers being algae and bacteria (Javor, 1989) and with significant contribution of terrigenous organic matter in some settings. Preservation conditions vary widely, but good organic matter preservation is generally found in oxygen-depleted environments (see chapter 4). Reduced oxygen levels may arise by the formation of cyanobacterial mats (*e.g.* Palmisano *et al.*, 1989a,b; Villanueva *et al.*, 1994a) or in hypersaline water bodies with a stable, density-stratified water column. In the latter case, oxygenic primary producers will thrive in a moderately saline upper water body, whose organic matter after death will settle down into an anoxic, highly saline bottom water (brine), where it may be preserved under conditions unsuitable for the existence of benthic, bioturbating organisms (Warren, 1986). Stratigraphic sequences in such evaporitic settings typically consist of alternating layers of marls (fine grained carbonates or shales) containing relatively high levels of organic matter, and evaporite deposits (*e.g.* halite, gypsum) low in organic matter. The fine-grained shales and carbonates are sedimented more slowly than the gypsum, halite and other “higher” salts (*e.g.* sylvite and carnalite), which could explain the differences in TOC, with high dilution of

organic content occurring in the evaporite layers even under conditions of high productivity and good preservation (Schreiber and Hsü, 1980; Hofmann *et al.*, 1993). The sediments from the Mulhouse and Vena del Gesso (VdG) basins were both deposited in hypersaline environments at different times during the Tertiary (Oligocene and Miocene (Messinian) ages respectively), with a prevailing Mediterranean-type climate (Schuler *et al.*, 1991) where restricted circulation led to the development of anoxic conditions (Vai and Ricci Lucchi, 1977; Hofmann *et al.*, 1993).

### **Mulhouse Basin**

#### **General**

The Mulhouse Basin is the southernmost of four sub-basins in the Upper Rhine Graben Tertiary rift segment, a 300km long and 30-40km wide area of the West-European continental rift system, reaching from Basle to Frankfurt (fig. 3.1; Blanc-Valleron, 1991). During the upper Eocene to lower Oligocene period, the basin was an evaporitic lake, resulting in deposition of a 1600m thick evaporitic sequence (Fig. 3.2). The deposits of the Salt IV interval consist of up to 5m-thick marl and anhydrite units alternating with 5 to 20m-thick halite units and also contains extensive potash bearing units (*e.g.* Ci). During deposition of the studied section (from within the lower part of the Salt IV unit, interval S1-T; fig. 3.2) the area was permanently water-filled, with a lake level that varied considerably (Blanc-Valleron, 1991). Beds within this stratigraphic interval are persistent throughout the basin and are believed to be synchronous (Courtot *et al.*, 1972; Maikovsky, 1941; Sturmfels, 1943). The marl samples studied come from cores taken in the central part of the basin.

#### **Depositional setting**

##### **Marls**

The organic matter in the interval S1-T is concentrated in the marl beds, where TOC ranges from 0.3 to 7% (Blanc-Valleron, 1986; Blanc-Valleron *et al.*, 1991; Hofmann, 1992; Hofmann *et al.*, 1993) the values being governed by dilution of organic matter by inorganic sedimentation and hence by sedimentation rate (Hofmann *et al.*, 1993). Well preserved laminations in the marl beds show an absence of bioturbation and hence the presence of anoxic or highly saline bottom water within the lake. These sub-millimetric laminations show alternating layers of carbonate and organic-rich clays which have been interpreted as reflecting variations in sediment input as a result of seasonal climatic cycles with wet winter and dry summer seasons (von Kühn and Roth, 1979; Schuler, 1988). Similar annual deposits have been noted in both modern and

Fig 3.1. Tertiary evaporite basins of the Upper Rhine Graben, showing location of Mulhouse Basin (modified from Blanc-Valleron, 1991).

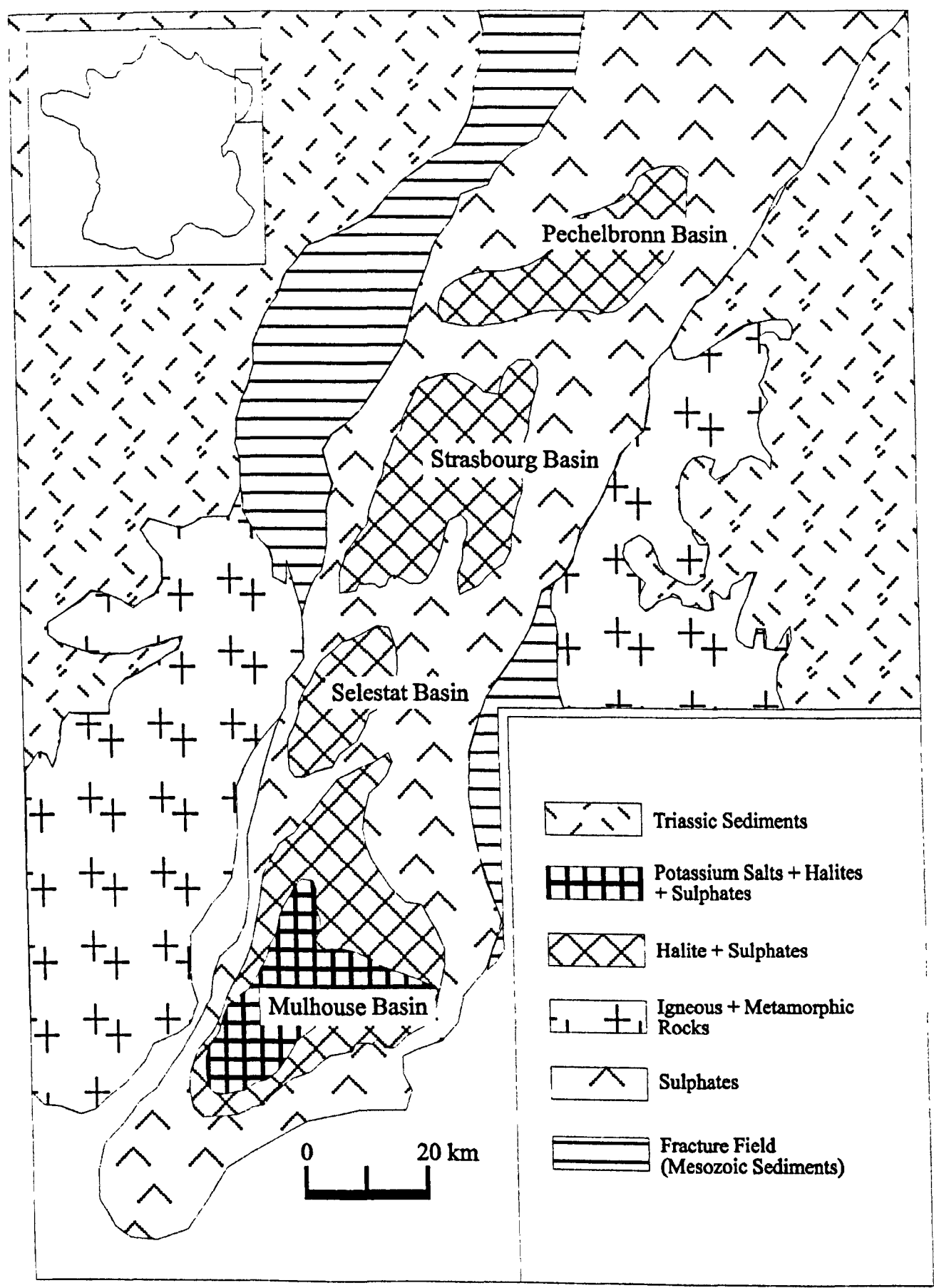
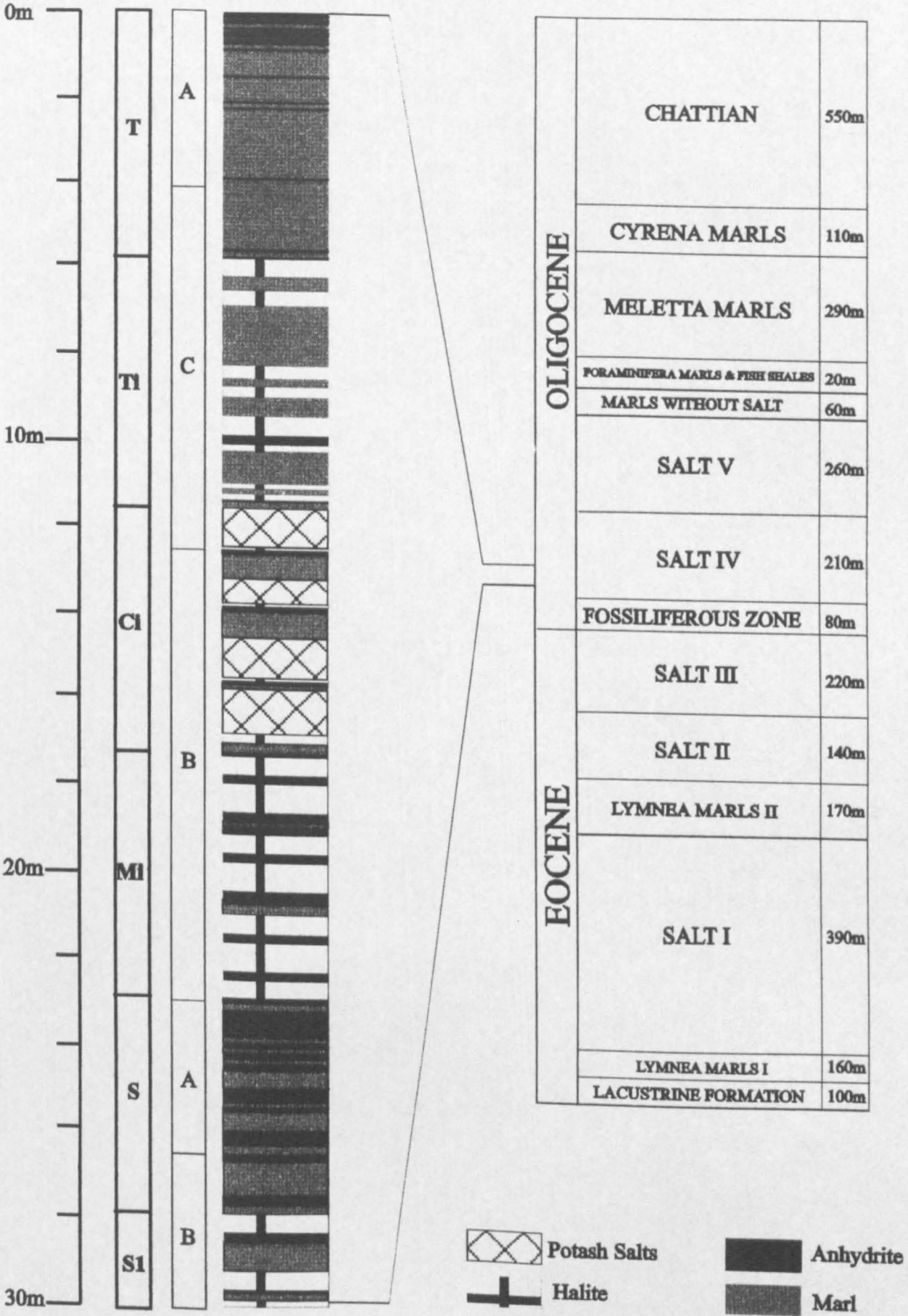


Fig 3.2. Stratigraphy of the Mulhouse Basin showing depth and organic matter type (A, B or C) (modified after Blanc-Valleron *et al.*, 1991)



ancient depositional systems (Kelts and Hsü, 1978; Dickman, 1985; Anderson and Dean, 1988). Indeed, counting the carbonate/clay varves enables determination of sedimentation rate and an estimation for the time period of marl deposition (Hofmann *et al.*, 1993). Organic-rich marls of three types (A, B and C) were deposited in a stratified water body when the lake level was highest and with significant terrigenous input (Hofmann *et al.*, 1993). Deposition of type C marls (associated with the Ti unit) occurred in O<sub>2</sub>-deficient (dysaerobic to anaerobic), highly saline bottom water with good preservation as evidenced by the pristane/phytane ratio (Pr/Ph). The upper part of the stratified water body had restricted connection to the sea and was of moderate to low salinity with a low primary production heavily influenced by bacterial activity (Gely *et al.*, 1993) which, together with a relatively high sedimentation rate, providing a constant influx of clastic sedimentary components and terrigenous-derived organic matter, resulted in type C marls with TOC 0.5 – 1.0%. Deposition of type A marls occurred in strictly anaerobic, highly saline bottom waters, resulting in excellent preservation (low Pristane/Phytane, <0.3) of laminae, with high pyrite and high organic-sulphur content of kerogen inferring the occurrence of sulphate reduction (Sinninghe-Damsté *et al.*, 1993c). Hence, during marl deposition the lake level was at its highest, providing a connection to the sea (evidenced by elevated dinosterane concentrations and high C<sub>27</sub>/C<sub>29</sub> sterane ratios, reflecting a higher marine input; Keely *et al.*, 1993). The upper water was therefore saline with a high nutrient supply, allowing extensive primary production which, combined with low sedimentation rates, resulted in high levels of preserved organic matter (TOC 2 to 4%). In the S and T units (fig. 3.2), laminae of amorphous organic matter are observed of type A. The combination of lower sedimentation rate with a highly saline upper water body may have allowed algal or bacterial mats to thrive at the chemocline as observed in some stratified lakes (Kirkland *et al.*, 1983). Such plates can settle into and be preserved in the sediment, resulting in the formation of laminae of amorphous organic matter. Marls of type B (associated with Mi and Ci) are of a transitional type reflecting the change in conditions of deposition from type A to C.

### *Evaporites*

Organic matter in the associated evaporites is lean (TOC < 0.5%; Hofmann, 1992; Sinninghe Damsté *et al.*, 1993b), being deposited during unstratified lake conditions. Evaporation of the shallow upper water body led to concentration of the brine and precipitation of gypsum, halite and finally sylvite respectively with increasing levels of

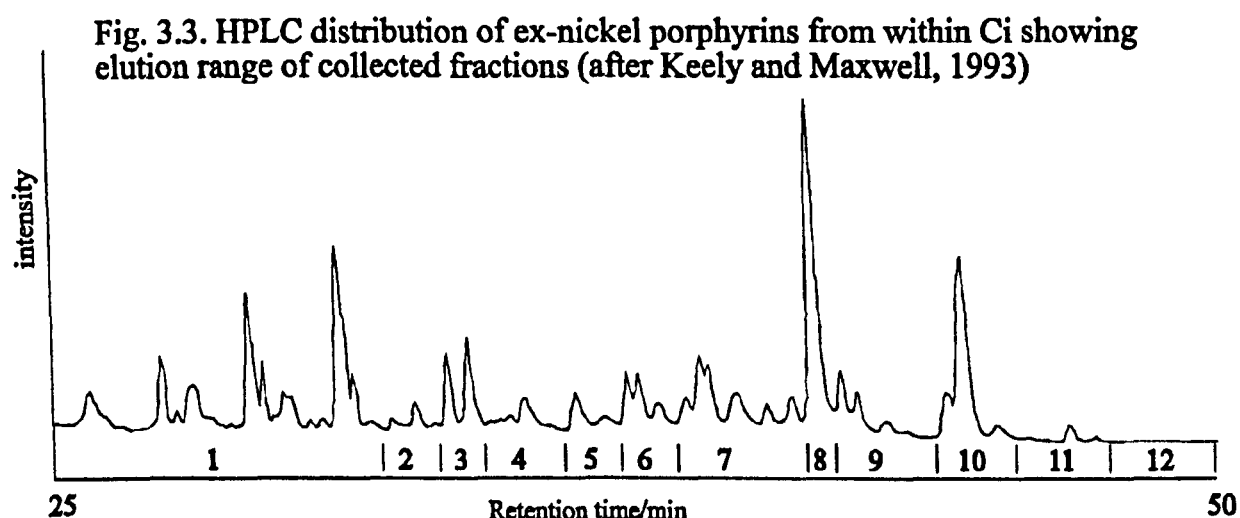


salinity. Stratigraphic variations within the evaporites are a result of periodic changes in brine concentration, as opposed to the stratigraphic variations within the marl beds which represent the conditions within the upper water body during the stratified stages of the lake (*c.f.* Carpentier *et al.*, 1992).

### Biomarkers of photic zone anoxia

#### Porphyryns

Keely and Maxwell (1993) examined alkyl porphyrin distributions in four selected marl samples from horizons located 1.50, 12.63 and 16.92m below the top of the “T” bed (fig. 3.2). Ni (II) porphyrins were found to dominate ( $\text{Ni}/\text{Ni}+\text{VO} = 0.9\text{--}1.0$ ). Probe EI-MS showed the CAP carbon number distributions to be similar in all samples, with the most abundant being either  $\text{C}_{31}$  or  $\text{C}_{32}$ . Probe EI-MS after demetallation produced clearer spectra and showed a range of CAPs from  $\text{C}_{28}$  to at least  $\text{C}_{35}$ , and possibly up to  $\text{C}_{37}$ . HPLC of the sample (16.92m) from the Ci unit allowed trapping of sub-fractions to determine the retention region of the HMW CAPs (fig. 3.3)



Probe MS detected  $>\text{C}_{33}$  components in five fractions (2, 4-7) with especially high abundances of  $\text{C}_{34}$  (fractions 6 and 7),  $\text{C}_{35}$  and  $\text{C}_{36}$  CAPs (fraction 5). In addition, lower abundances of  $\text{C}_{34}\text{--}\text{C}_{37}$  CAPs were present in fractions 2 and 4. Under normal-phase HPLC conditions, higher carbon number CAPs are expected to elute earlier than lower carbon number components of the same pseudohomologous series (Chicarelli *et al.*, 1986). Therefore, the presence of  $\text{C}_{35}\text{--}\text{C}_{37}$  CAPs eluting later in the chromatogram than lower carbon number species inferred the presence of more than one pseudohomologous series of HMW CAPs and gave some evidence for the occurrence of anoxic conditions within the photic zone of the stratified Mulhouse lake at the time

of marl deposition. In addition, co-injection of the C<sub>34</sub> CAP (33) derived from the bacteriochl *d* series with one sample in the “T” bed (1.62m) suggested the presence of a C<sub>34</sub> CAP component with the same retention time, but this can only be considered tentative evidence given the complexity of porphyrin distributions revealed by HPLC-MS (Chapter 2) and the unavailability of HPLC-MS at this time.

### *Aryl isoprenoids*

No diaromatic isoprenoids characteristic of an origin in isorenaratene (30), characteristic of the brown strains of Chlorobiaceae were present in the marls (Sinninghe-Damsté *et al.*, 1993b). The monoaromatic hydrocarbon distributions were dominated by *n*-alkyl-substituted benzenes and toluenes (C<sub>13</sub>-C<sub>37</sub>) and 1-alkyl-2,3,6-trimethyl aryl isoprenoids which could be derived from the chlorobactene (28) of green coloured strains of Chlorobiaceae were absent. Similarly, the low abundance of 1,2,3,4-tetramethylbenzene in the alkylated benzenes of kerogen pyrolysates also argued against the presence of Chlorobiaceae in the water column during marl deposition (Sinninghe Damsté *et al.*, 1993c). There was therefore an apparent contradiction between the porphyrin results and the aromatic hydrocarbon results. It was therefore decided to re-examine the porphyrin distributions in a number of the marls, using HPLC-MS in order to shed further light on the apparent contradiction between the earlier porphyrin and aromatic hydrocarbon data.

## **Vena del Gesso Basin**

### **General**

The Vena del Gesso (VdG) Basin sediments are located in the Periadriatic trough of Northern Italy (see Vai and Ricci Lucchi, 1977) and were deposited during the “Messinian salinity crisis” (Hsü *et al.*, 1973). The Messinian was the final age in the Miocene (upper boundary *ca.* 5.1 Ma, Harland *et al.*, 1982) and was an important stage marked by the deposition of thick evaporite deposits throughout the Mediterranean region. These are thought to indicate that the Straits of Gibraltar were closed *ca.* 6.5-5.1 Ma, controlling the connection to the Atlantic and restricting the whole of the Mediterranean region, reducing it to a series of evaporitic basins (Vai and Ricci Lucchi, 1977). This crisis arose from the combined influence of a major eustatic sea level fall and tectonically-induced basin collapse. During transgressive phases, marine water entered the region over a sill and on its way to the VdG basin the salinity increased as a result of evaporation, so that marine water with salinity above normal

marine levels entered the basin and led to the development of anoxic conditions (Vai and Ricci Lucchi, 1977). Marls were deposited under anoxic conditions, as revealed by presence of fine scale laminations and rare bioturbation, during the filling of a lagoon, with subsequent evaporation and shallowing resulting in the development of algal mats (stromatolites) and eventual precipitation and deposition of gypsum. Repeated evaporative drawdowns and marine transgressions resulted in the cyclicity of the evaporite sediment deposits as shown in fig. 3.4. The sequence is dominated by thick gypsum beds (up to 35m) representing high sedimentation rates over short time periods, with marl and stromatolite beds (up to 2m and 50cm thick respectively) representing longer periods of marine influx with low sedimentation rates. Fourteen marl-gypsum depositional cycles (III-XVI; fig. 3.4) have been identified (Vai and Ricci Lucchi, 1977). Marl layers are relatively high in organic carbon (TOC = 1-2%) and contain organic matter of low thermal maturity with many lipid components being preserved as organic sulphur compounds (Kohnen *et al.*, 1991a, b, 1992a, b).

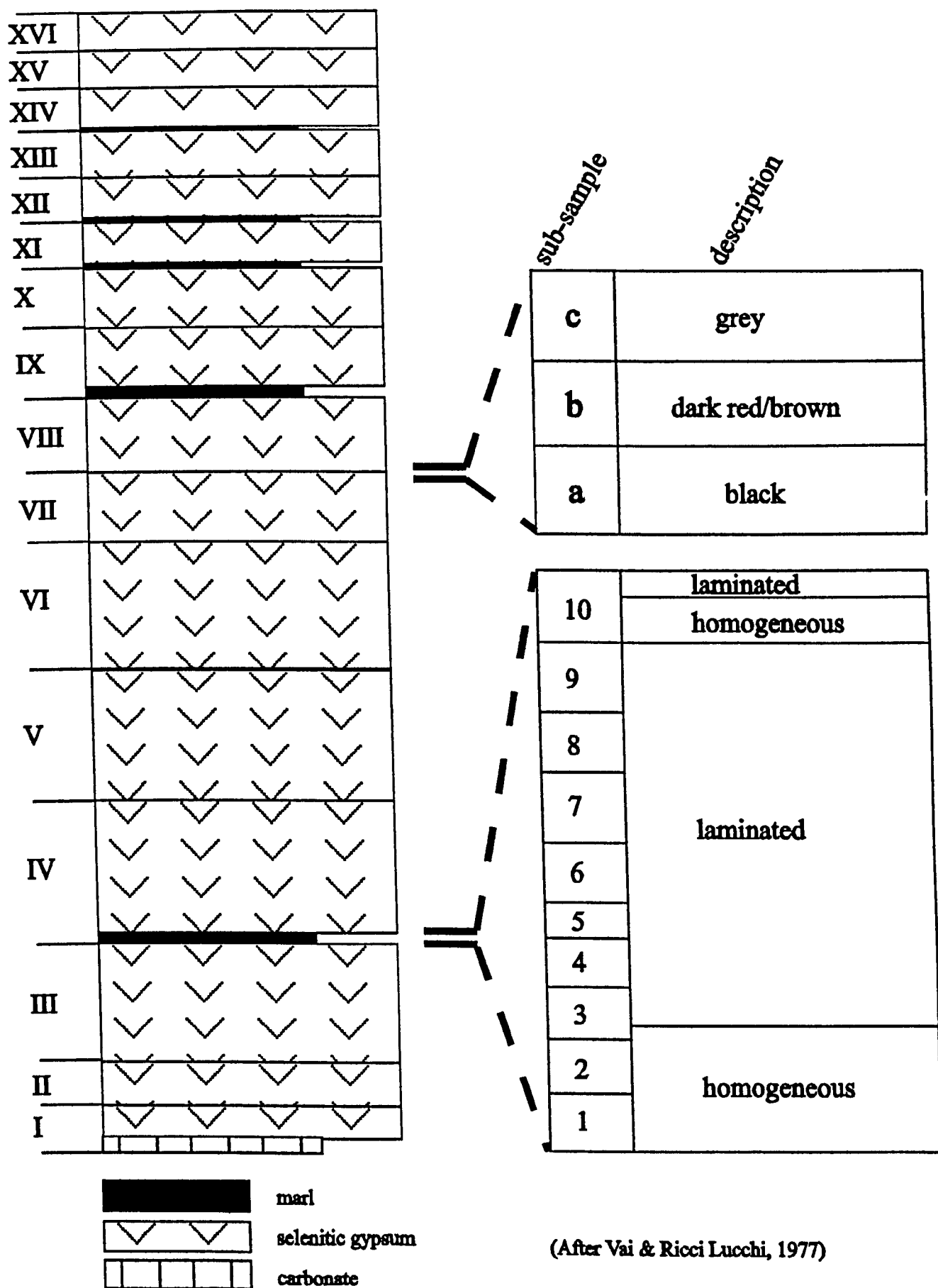
#### **Pigment distributions**

Marl layers have been previously studied in order to trace the variability in pigment compositions (Keely *et al.*, 1995). In particular, cycle IV, exhibiting sub-millimetre laminations (split into 10 sub-samples each representing *ca.* 13 cm of deposition) was examined. Pigment compositions were analysed by UV/vis which showed the presence of free-base porphyrins (*ca.* 20-800  $\mu\text{g g}^{-1}$  organic carbon), chlorins and carotenoids with only minor amounts of metallo porphyrins.

#### ***Porphyrins***

Electrospray and probe EI-MS plus normal phase HPLC analysis of free base porphyrin fractions from samples in cycles III-VII revealed simple distributions over a narrow carbon number range (Keely *et al.*, 1995). C<sub>32</sub> (DPEP; 1) and C<sub>31</sub> CAP components plus a C<sub>33</sub> BiCAP species (19b; structures assigned by HPLC coinjection of standards) dominated the mass spectra with differing relative abundances in each sample or sub-sample. The spectra provided no convincing evidence for the presence of HMW CAP species, although LC-PDA-MS analysis of three sub-samples of IV (*e.g.* IV-1-4) did reveal a C<sub>34</sub> CAP (Keely *et al.*, 1995). This HMW CAP, masked in the probe-MS by the high relative abundance of the major species, was tentatively assigned on purely carbon number grounds as a diagenetic product of the bacteriochl pigments

Fig. 3.4 Schematic representation of lithological succession showing horizons I-XVI



(After Vai & Ricci Lucchi, 1977)

of Chlorobiaceae, although as noted in Chapter 2, such a component may arise from other non-bacteriochl sources (Gibbison *et al.*, 1996).

### *Carotenoids*

Reversed phase HPLC, UV/vis, LC-MS and hydrogenation to isorenieratane (35) revealed the presence of the intact diaromatic carotenoid, isorenieratene (30) and a geometrical isomer (a *cis*-isorenieratene), (Keely *et al.*, 1995; Putschew *et al.*, 1998). Isorenieratane was also present in the products of desulphurisation of the kerogen (Li/EtNH<sub>2</sub>), polar fractions of the extract (nickel boride) and asphaltenes (nickel boride) as was a range of isorenieratene-derived diaryl isoprenoids with 2,3,6-trimethyl substitution (Schaeffer *et al.*, 1995; Kenig *et al.*, 1995). All of these components had heavy  $\delta^{13}\text{C}$  values (ca. 13.7‰). Hence, the structural and isotopic data from the marls therefore gave clear evidence for the presence of brown strains of Chlorobiaceae in the palaeo water column; indeed, the development of anoxygenic photosynthesis was recurrent in the marls throughout the entire evaporitic sequence (Keely *et al.*, 1995; Kenig *et al.*, 1995; Sinnighe-Damsté *et al.*, 1995).

### *Stratigraphic analysis*

Depth profiles of isorenieratene and porphyrin abundances were calculated for samples covering the whole sequence and for sub-samples from horizons IV and VIII (Keely *et al.*, 1995). Porphyrin concentrations, were highest in marl horizon IV, with marls at the top of the sequence also containing significant quantities. The porphyrin profile did not correlate with the abundance of the purely bacterially-derived isorenieratene, presumably because the porphyrins reflect mainly an algal input. Isorenieratene had the greatest concentration in the thickest marl horizons at the base and middle of the sequence, especially IV, with only small amounts present from VII to XI. Within horizon IV, the concentrations indicated that the greatest extent of anoxygenic photosynthesis occurred during deposition in the middle of the horizon (IV-1-3 to IV-1-6). However, the presence of sulphur-bound isorenieratene in samples IV-1-1 to IV-1-3 showed that photic zone anoxia was established earlier in marl IV deposition (Kenig *et al.*, 1995). Lipids thought to be derived from the purple sulphur bacteria (Chromatiaceae) were abundant in samples IV-1-1 and IV-1-2, with reduced levels in IV-1-3. As mentioned earlier, marl deposition was initiated during a transgressive phase when marine waters entered the basin (Vai and Ricci Lucchi, 1977). Samples

containing the highest abundances of free and bound isorenieratene were therefore probably deposited after the initial transgression, when stable anoxic conditions became highly developed and extended into the photic zone. Concentrations then decreased toward the top of the horizon as the water depth decreased, leading to a reduction in the influence of photic zone anoxia. The type of photosynthetic sulphur bacteria which proliferate is dependent on the spectrum and intensity of light reaching the chemocline, which is in turn controlled by the photic zone productivity and chemocline depth (*e.g.* Montesinos *et al.*, 1983). Abundant growth of Chromatiaceae, apparent from IV-1-1 and IV-1-2, implied that a relatively high chemocline existed, whereas from samples IV-1-3 and IV-1-6, reduced Chromatiaceae abundance together with abundant growth of Chlorobiaceae suggested the existence of a deeper chemocline (Kenig *et al.*, 1995). Reduction in the input of Chlorobiaceae in samples IV-1-7 to IV-1-8 reflects the regressive, evaporative phase of the deposition, with the disappearance of <sup>13</sup>C-enriched aryl isoprenoids in samples IV-1-9 and IV-1-10 indicating the cessation of photic zone anoxia. This is thought to have occurred due to the relative sea-level drop, water column mixing and the zone of light penetration reaching the sediment (Keely *et al.*, 1995; Kenig *et al.*, 1995; Sinninghe-Damsté *et al.*, 1995). Depth profiles therefore seem to suggest similarities in extent of photic zone anoxia between deposition of marl IV and of the entire sequence, therefore indicating similarities between the mechanisms causing these changes (Keely *et al.*, 1995).

## RESULTS AND DISCUSSION

### Mulhouse Basin

Eighteen samples of free base porphyrins (from the S, Ci, Ti and T units) were obtained from Dr. Brendan Keely and were chosen to provide a reasonable coverage of the section analysed previously (Keely and Maxwell, 1993; Keely *et al.*, 1993; Sinninghe-Damsté *et al.*, 1993b, d). The HPLC distributions show a wide range of carbon numbers (C<sub>28</sub> to at least C<sub>36</sub>) comprising mainly CAPs, DPEP (1) being the dominant species, with aetio components also present (maximising at C<sub>30</sub> or C<sub>31</sub>), together with a series (C<sub>28</sub> to C<sub>34</sub>) of BiCAPs. Modified porphyrin maturity parameters (MPMP = C<sub>28</sub>A/C<sub>28</sub>A+C<sub>32</sub>D) were calculated for each sample from the peak areas of all C<sub>28</sub> aetio components (C<sub>28</sub>A) and of C<sub>32</sub> DPEP (C<sub>32</sub>D) and are shown in Appendix A. These are based on the vanadyl porphyrin maturity parameter (PMP) of Sundararaman (1992) who compared the relative peak heights of C<sub>28</sub> octa-methyl porphyrin and C<sub>32</sub> DPEP. MPMPs calculated for the immature free base porphyrins of

Mulhouse range from 0 to 0.12 (*c.f.* MPMP Kupferschiefer ex-iron and Serpiano ex-vanadyl of 0.28 and 0.14 respectively). Given the low amounts of available standards, coinjection studies were not carried out. Instead, the bulk Kupferschiefer sample was analysed immediately before the samples, in order to allow for small changes in retention time. Figs. 3.5a-c show the mass chromatograms for HMW CAPs (C<sub>32</sub>-C<sub>36</sub>) for three selected samples in the top unit (T), covering the top three metres of the section. The shaded areas corresponding to the bacteriochl *d*-derived standards are present above background in all three samples as confirmed by the mass spectra (*e.g.* fig. 3.6a). The *m/z* 505 chromatogram for sample T/413-416 shows the familiar three peak distribution with peak **c** having the same retention time as the *n*-Pr Et (**34b**) and *i*-Bu Me (**33**) C<sub>34</sub> CAPs. This is, however, the only sample showing this three peak distribution, with mass chromatograms for most other samples showing small peaks corresponding to bacteriochl *d* CAPs together with either or both an early eluting (fig. 3.6b) and a later eluting (fig. 3.6c) HMW CAP series (see below) as confirmed by the spectra. Hence, it does indeed appear that components derived from bacteriochls *d* are present. Coincidentally, sample T413-416 is the same as that used in previous work (Keely and Maxwell, 1993), where coinjection with the C<sub>34</sub> CAP (**33**) standard was carried out.

Figs. 3.5d and 3.7a show the mass chromatograms from two samples within unit Ti and figs. 3.7b-d for selected samples from Ci and S. The distributions seem to indicate that, overall, the bacteriochl *d* HMW CAPs are most abundant in the T unit, with only very small peaks or peaks around noise level visible in most samples in the remainder of the section. Plots of peak areas of these HMW CAPs vs. DPEP are shown in fig. 3.8. Peak areas are only included in the plots where the height of shaded areas in the mass chromatograms are at least twice the height of the noise level and the mass spectra show M+H<sup>+</sup> ions with a signal intensity at least twice that of the background signal (not including ions from co-eluting peaks). As a result, in some samples with low abundance of components, high noise levels result in a low signal to noise (S/N) ratio and imprecise peak area calculations. Bearing in mind the errors arising from the low S/N ratio, the general trend does imply, however, that the highest levels of the bacteriochl *d*-derived porphyrins are present in the T section, albeit in low abundance, and with very little, if any, components present in the Ti unit. Unfortunately, no maleimide studies have been carried out on these samples to confirm the presence of Chlorobiaceae in the water column. If the HMW CAP components are indeed

Figure 3.5. Partial mass chromatograms for HMW CAPs with shaded peaks showing components co-eluting with bacteriochl *d*-derived porphyrins

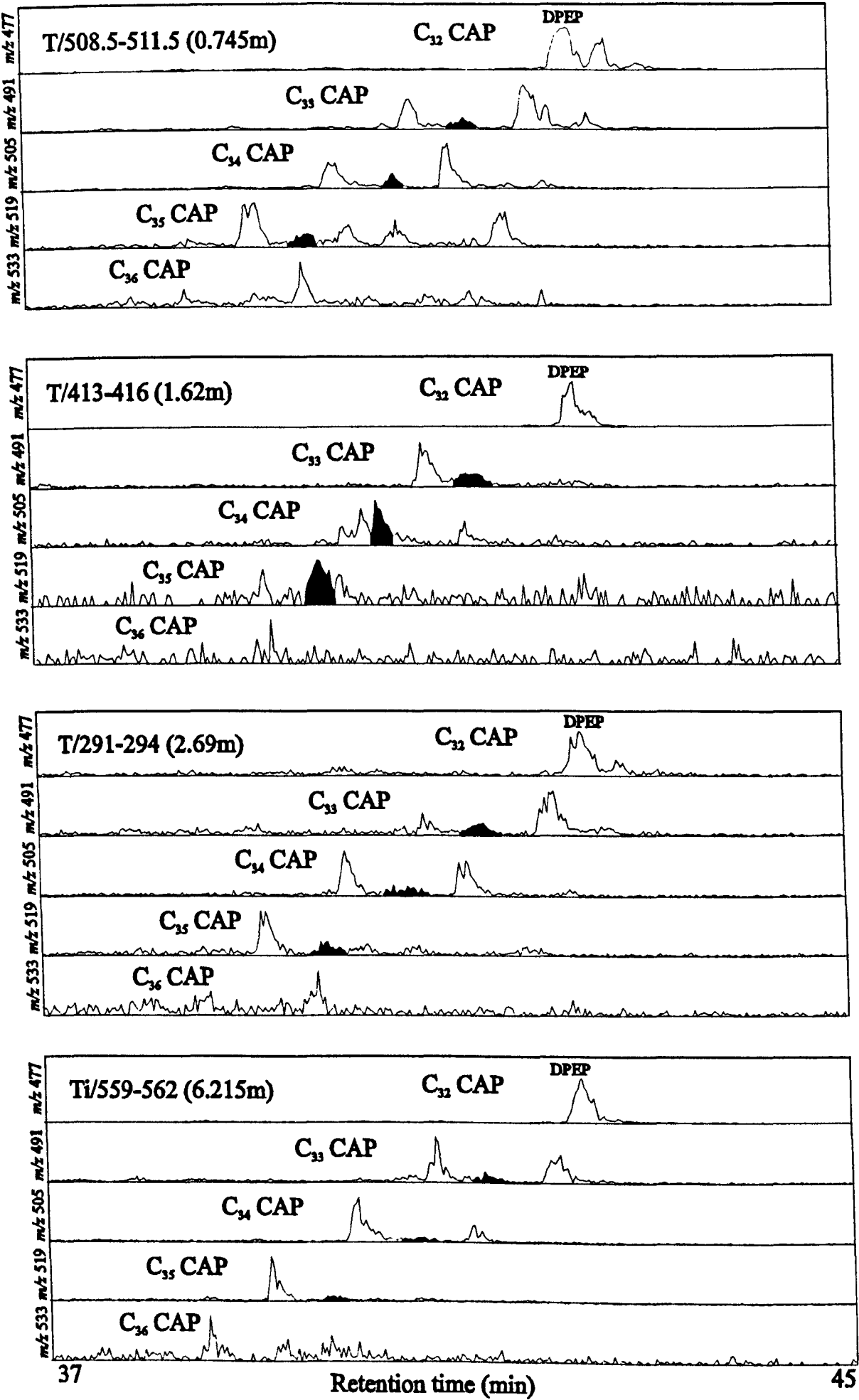




Fig. 3.6. Mass spectra of selected HMW CAP components (i)  $C_{33}$  (ii)  $C_{34}$  (iii)  $C_{35}$  from Mulhouse Basin (a) bacteriochl *d*-derived (b) early-eluting (c) late-eluting

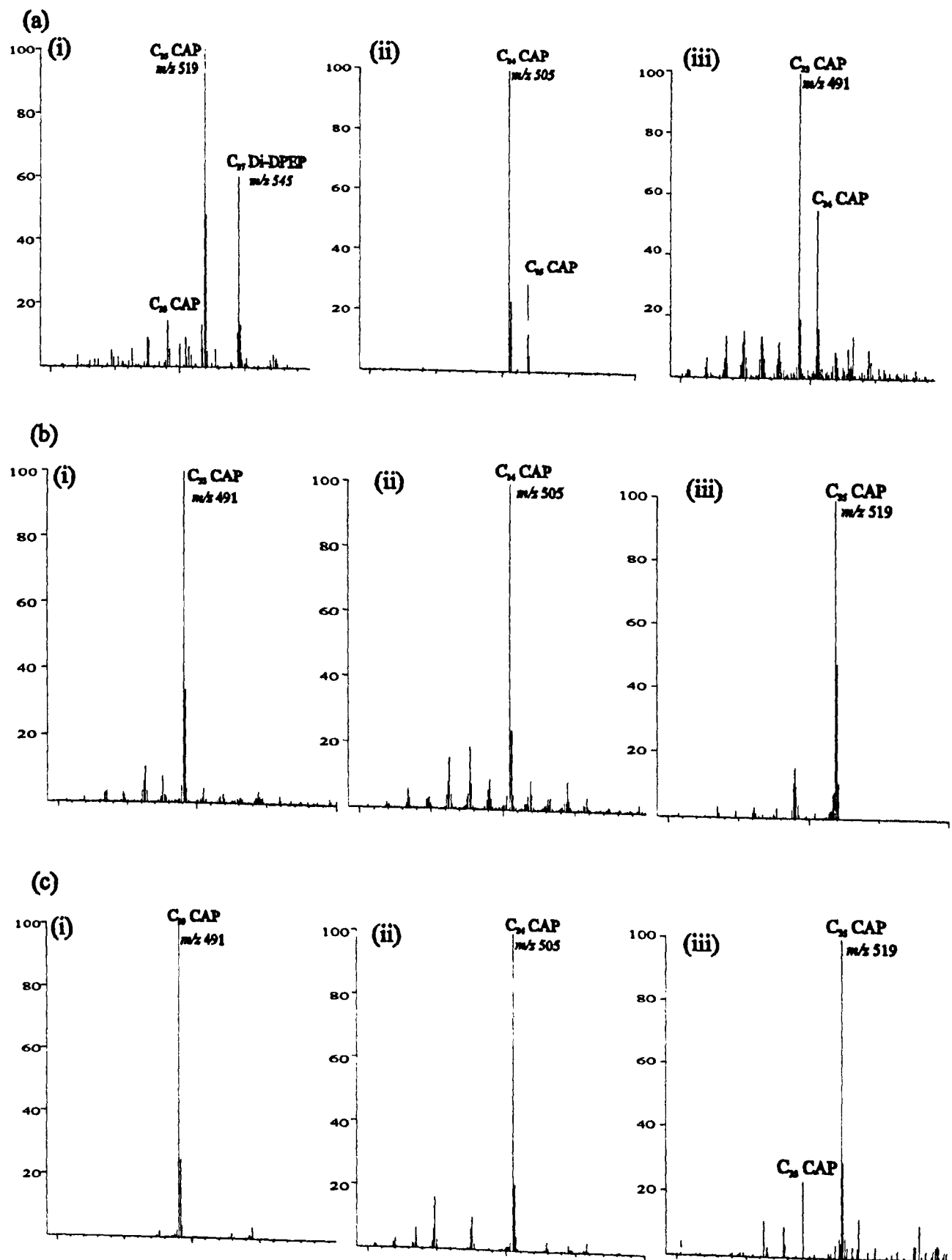
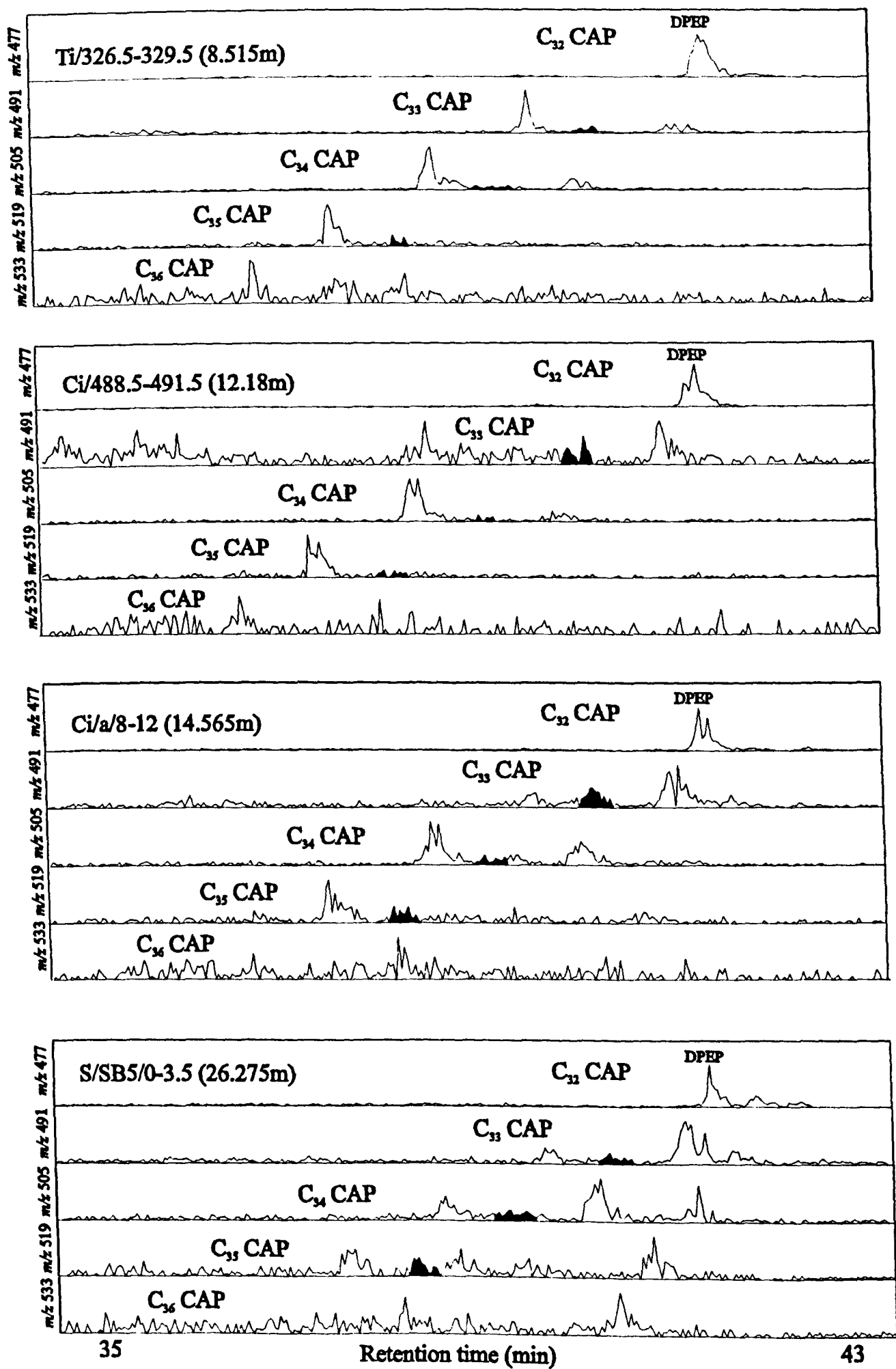


Figure 3.7. Partial mass chromatograms for HMW CAPs with shaded peaks showing components co-eluting with bacteriochl *d*-derived porphyrins.



bacteriochl *d* derived, the absence of aryl isoprenoids (Sinninghe-Damsté *et al.*, 1993b, d) derived from green strains of the bacteria, is difficult to explain. Given the low abundance of the HMW CAPs corresponding to the standards and the fact that chlorobactene is typically in low abundance compared to the bacteriochls *d* (Montesinos *et al.*, 1983; de Wit and Caumette, 1995), it is possible that any aryl isoprenoids derived from chlorobactene were “swamped” by more abundant aromatic hydrocarbons present (Sinninghe-Damsté *et al.*, 1993b, d). On the other hand, the presence of bacteriochl *d*-derived porphyrins would fit with other trends in the marls such as the trends in both TOC values and Pr/Ph ratios (Hofmann *et al.*, 1993b; Keely *et al.*, 1993; see Introduction). Hence, the higher relative abundance of the bacteriochl *d*-derived HMW CAPs are found in the marls with type A organic matter, providing evidence for the presence of green Chlorobiaceae as a result of an increased contribution of marine waters and higher algal productivity leading to generation of anoxic conditions and sulphate reduction.

The uppermost sample (T/508.5-511.5) also clearly shows a series of HMW CAPs (C<sub>33</sub>-C<sub>36</sub>), confirmed by their mass spectra (fig. 3.6b), eluting *ca.* 25-30 seconds earlier than, and more abundant than, the bacteriochl *d*-derived series (*i.e.* several minutes later than the early eluting series seen in the Kupferschiefer samples; fig 2.8). This series is also seen in many of the other samples throughout the section, *e.g.* Ti/559-562 (fig. 3.5d), Ti/326.5-329.5 and Ci/488.5-491.5 (fig. 3.7a,b respectively) and confirms the probe MS data from previous studies (Keely and Maxwell, 1993). The relative peak areas seen in the mass chromatograms clearly indicate that these early eluting species are derived from chlorophylls which were more abundant in the water column of the Mulhouse lake than the bacteriochls *d*. This can also be seen in the plots of the ratio of peak areas of the early eluting C<sub>34</sub> and C<sub>35</sub> components to DPEP (figs. 3.9a, b), which show a maximum C<sub>34</sub>:DPEP ratio of *ca.* 0.7 for the early eluting species. These plots show a general decreasing trend down the section from T to S1 with significant maxima seen in samples T/291-294, Ti/481.5-484.5, Ci/a/8-12 and S/SB5/0-3.5. The uppermost sample (T/508.5-511.5; 0.745m) also clearly shows (fig. 3.5a) a significant presence of later eluting HMW CAPs (C<sub>33</sub>-C<sub>36</sub>), again confirmed by the mass spectra (fig. 3.6c), eluting between 20 and 60 seconds after the bacteriochl *d*-derived species. Such species are also apparent in other samples, mainly in the top unit T and to a lesser extent in units Ci and S, although C<sub>33</sub> and C<sub>34</sub> CAPs are visible above baseline noise within unit Ti in samples Ti/559-562 and Ti/326.5-329.5 (figs. 3.5d and

Figure 3.8. Plots of peak areas of HMW CAPs /  $C_{32}$  (DPEP) through Salt IV section  
 (a)  $C_{34}$  (peak c) component (b)  $C_{35}$  (with same retention as bacteriochl *d*-derived standard)

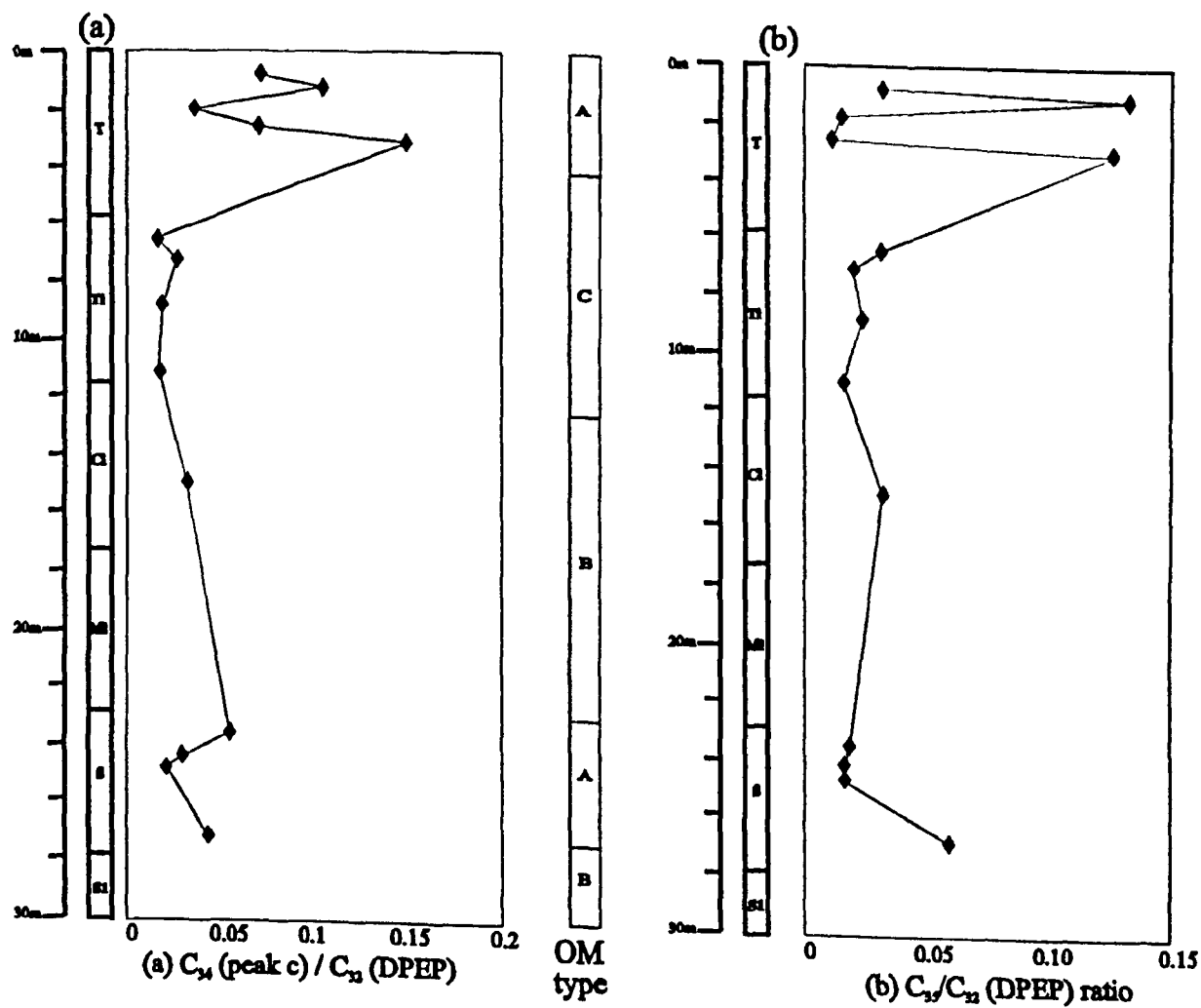
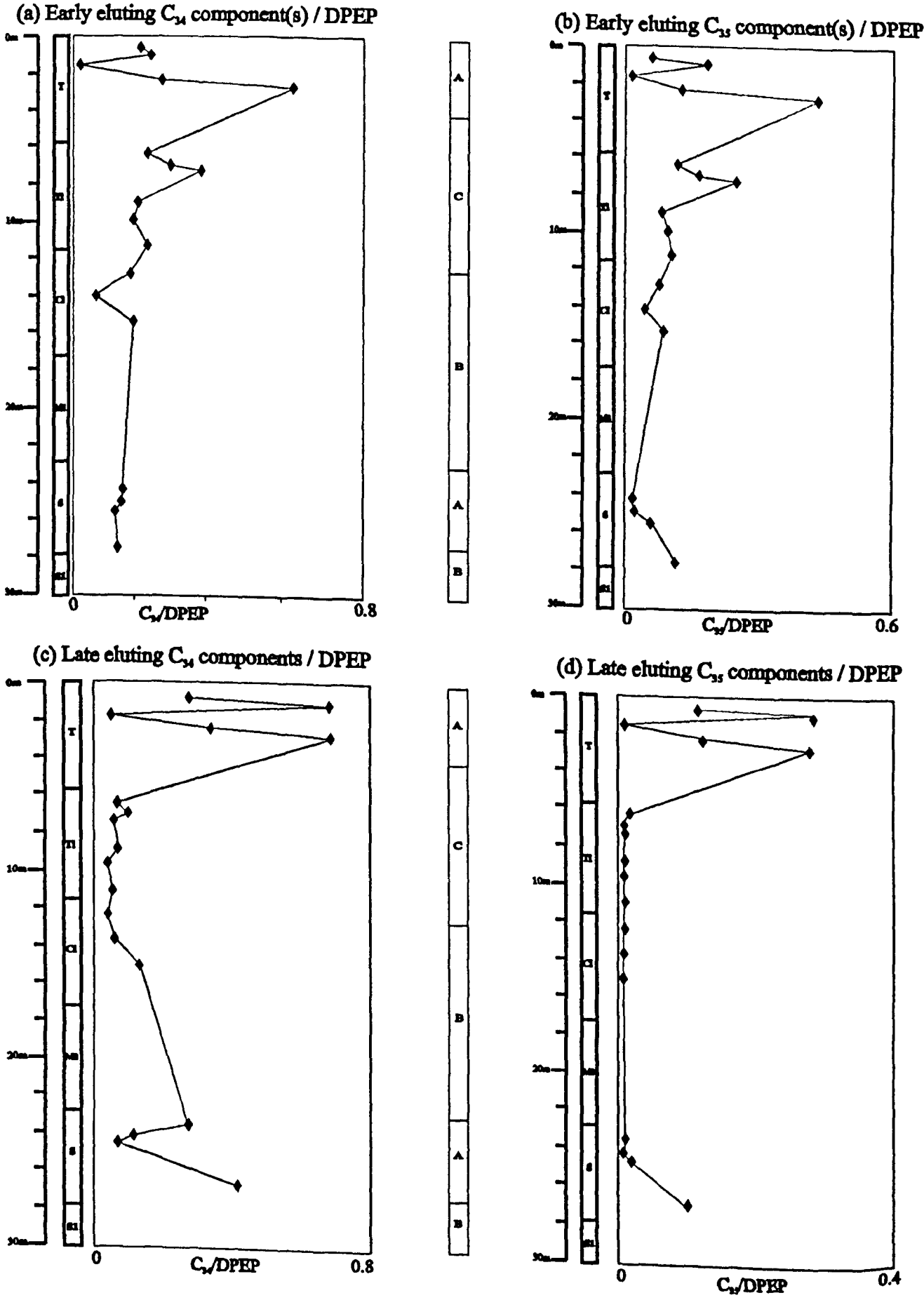


Figure 3.9. Plot of peak areas of early and late eluting HMW CAPs / DPEP through Salt IV section



3.8a respectively). Some of these components are also present, albeit in much lower abundance, in other samples (*e.g.* Kupferschiefer; chapter 2, and some Cen/Tur; chapter 4 and Toarcian samples; chapter 5).

Figs. 3.9c and d plot the ratio of the late eluting C<sub>34</sub> and C<sub>35</sub> CAPs to DPEP and show that the largest proportion of such species is again found in the uppermost unit, T, where the maximum C<sub>34</sub>:DPEP ratio is >0.7, and within the bottom section, S. Whilst mass spectra confirm that these components are indeed HMW CAPs, their structures and origin are unknown. With a similar CAP to DPEP ratio between the early and late eluting species, bearing in mind the errors in peak area measurement associated with low S/N ratios in some of the mass chromatograms, one possibility is that such components may be derived from the same series of chlorophylls. With the relatively high abundance of such species throughout the Salt IV section and indeed the significant proportion of such species in section Ti, associated with high Pr/Ph, lower algal productivity, high bacterial activity and low TOC “type” B/C marls, it seems that such species are derived from chlorophylls in species more adaptable to such environments than the bacteriochls *d* from green Chlorobiaceae whose overall quantitative contribution to the accumulated organic matter was relatively small. Keely and Maxwell suggested, given the absence of aryl isoprenoids derived from the aromatic carotenoids of Chlorobiaceae (see above) and of components enriched in <sup>13</sup>C (Hollander *et al.*, 1993a) that these relatively abundant HMW CAPs might derive from the bacteriochls of multicellular filamentous green bacteria (*Chloroflexus*) which were previously recognised in abundant quantities within benthic calcite/gypsum mats in medium/high salinity (salinity: 100-150 g/L) solar saltern ponds (Villanueva *et al.*, 1994a), which in turn did not contain any isorenieratene or chlorobactene. These bacteria contain bacteriochls *c* as their principal chlorophyll, so it is possible that the more abundant HMW CAPs in the marls could derive from such bacteria. Although not obligate anaerobes, *Chloroflexus* only photosynthesise under anoxic conditions (Trüper and Pfennig, 1992). The occurrence of such CAP components with the same retention behaviour in other samples (see above) seems possible, as the bacteriochls *c* are also present in the green strains of Chlorobiaceae.

In summary, the HPLC-MS studies confirm the presence of HMW CAPs in the Mulhouse marls, especially in unit T and provide further evidence for the presence of green strains of Chlorobiaceae during deposition of the type A marls. Deposition of the

marls appears also to be associated with other unknown and more abundant HMW CAPs which may also derive from bacteriochls.

### Vena del Gesso

A number of free base porphyrin fractions were provided by Dr B.J. Keely. These were taken from marls II to XI inclusive, with further sub-samples IV-2 to IV-10 being taken from marl bed IV. HPLC-MS confirmed the presence of major C<sub>31</sub> and C<sub>32</sub> CAP components plus the C<sub>33</sub> BiCAP component as identified previously in most samples (Keely *et al.*, 1995). As expected, MPMPs are low, ranging from 0 to 0.05 (Appendix A), with the one exception of 0.41 for the lowermost sample, II.

Mass chromatography revealed the presence in most samples of CAPs within the carbon number range C<sub>31</sub> to C<sub>36</sub>. Fig. 3.10 shows the partial mass chromatograms of CAPs (C<sub>31</sub> to C<sub>36</sub>) from selected sub-samples within horizon IV (IV-2, IV-4, IV-6 and IV-8) whilst fig. 3.11 shows the mass chromatograms for the same carbon number range from selected samples within the entire VdG deposition (II, VI, VIIIa and X). Again, comparisons were made with the bulk Kupferschiefer sample which was analysed immediately before the VdG samples. The region within which the bacteriochl *d*-derived CAP components elute is marked. It is clear that no peaks corresponding to the standards are present, so no HMW CAPs derived from the bacteriochls *d* are apparent. Likewise, no monoaromatic 2,3,6 trimethyl aryl isoprenoids, which would be derived from chlorobactene, have been found (Keely *et al.*, 1995; Sinninghe Damsté *et al.*, 1995; Gelin *et al.*, 1995; Kenig *et al.*, 1995; Schaeffer *et al.*, 1995). Hence, there is no evidence for the presence of the green strains of Chlorobiaceae in the water column during marl deposition.

Fig. 3.10c shows the mass chromatograms for sub-sample IV-4 which had previously shown the presence of a C<sub>34</sub> CAP tentatively assigned as a diagenetic product of Chlorobiaceae (Keely *et al.*, 1995). Peaks within the *m/z* 505 C<sub>34</sub> CAP chromatogram, together with both the *m/z* 519 and *m/z* 533 (C<sub>35</sub> and C<sub>36</sub> CAPs respectively) chromatograms, show species eluting both much earlier and later than the expected HMW region. These components appear to be also present in some of the other marl IV samples (*e.g.* IV-6), but not in others (*e.g.* IV-2); the same situation appears to hold for other marls (fig. 3.11). Whilst some of the early eluting components seem to coincide in retention time with some of the early eluting CAPs in Kupferschiefer (fig. 3.12), there seems to be no obvious complete pseudohomologous series in the chromatograms C<sub>34</sub>-C<sub>36</sub>, which may be derived from the bacteriochls *e* series. A number of HMW

Fig. 3.10. Partial mass chromatograms for CAPs ( $C_{31}$ - $C_{36}$ ) from selected sub-samples within VDG horizon IV

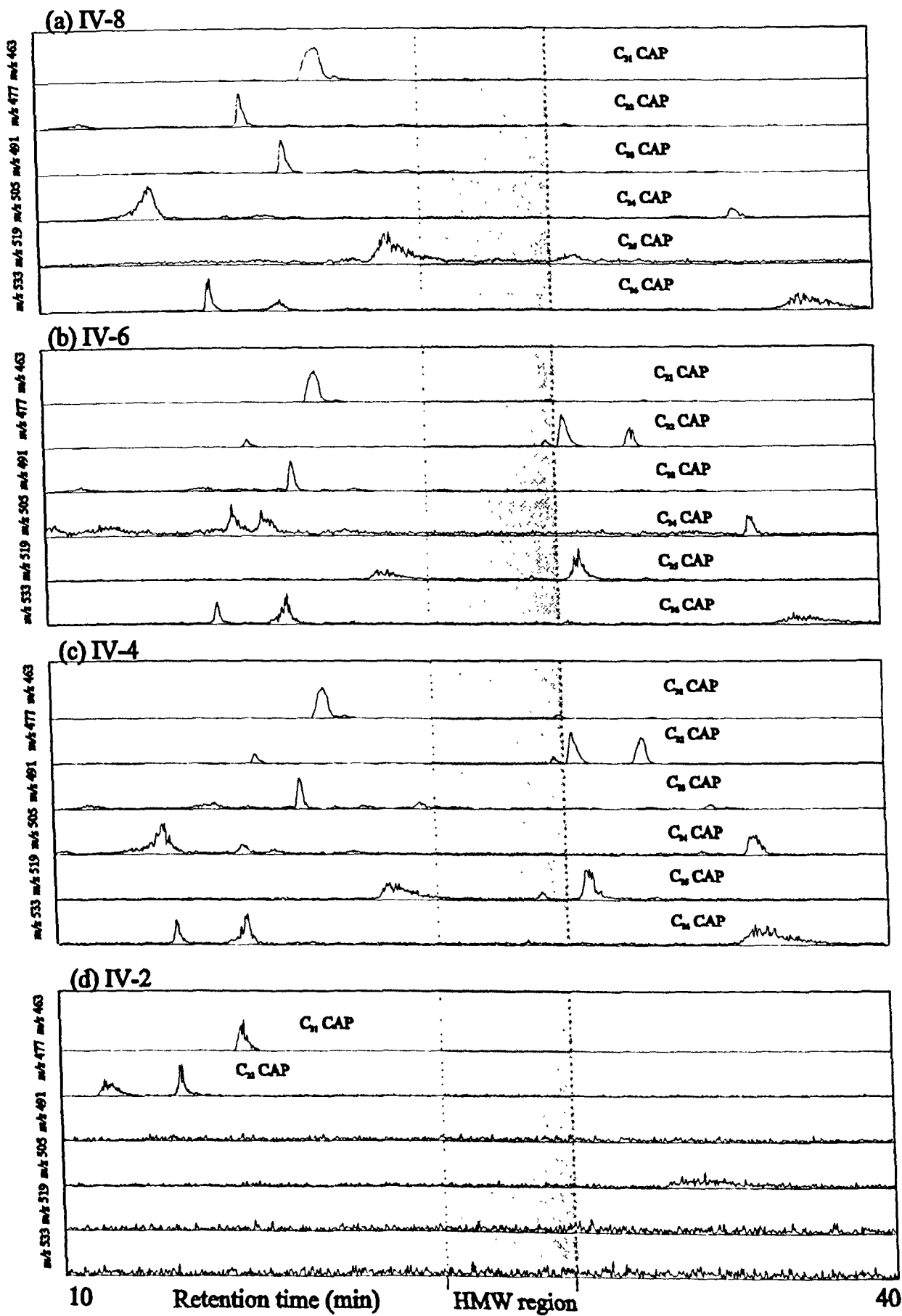




Fig. 3.11. Partial mass chromatograms for CAPs ( $C_{31}$ - $C_{36}$ ) from selected samples within VDG

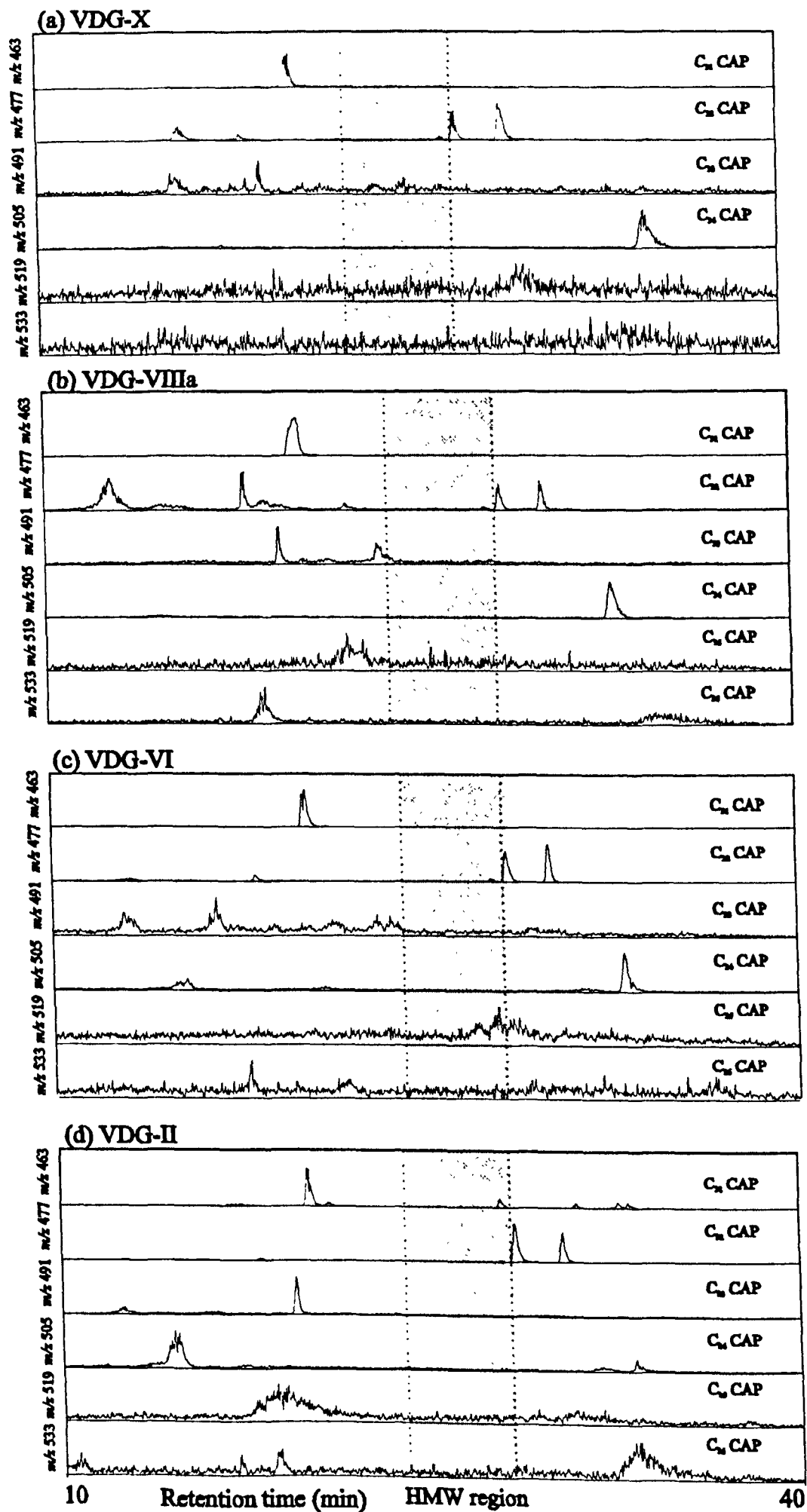
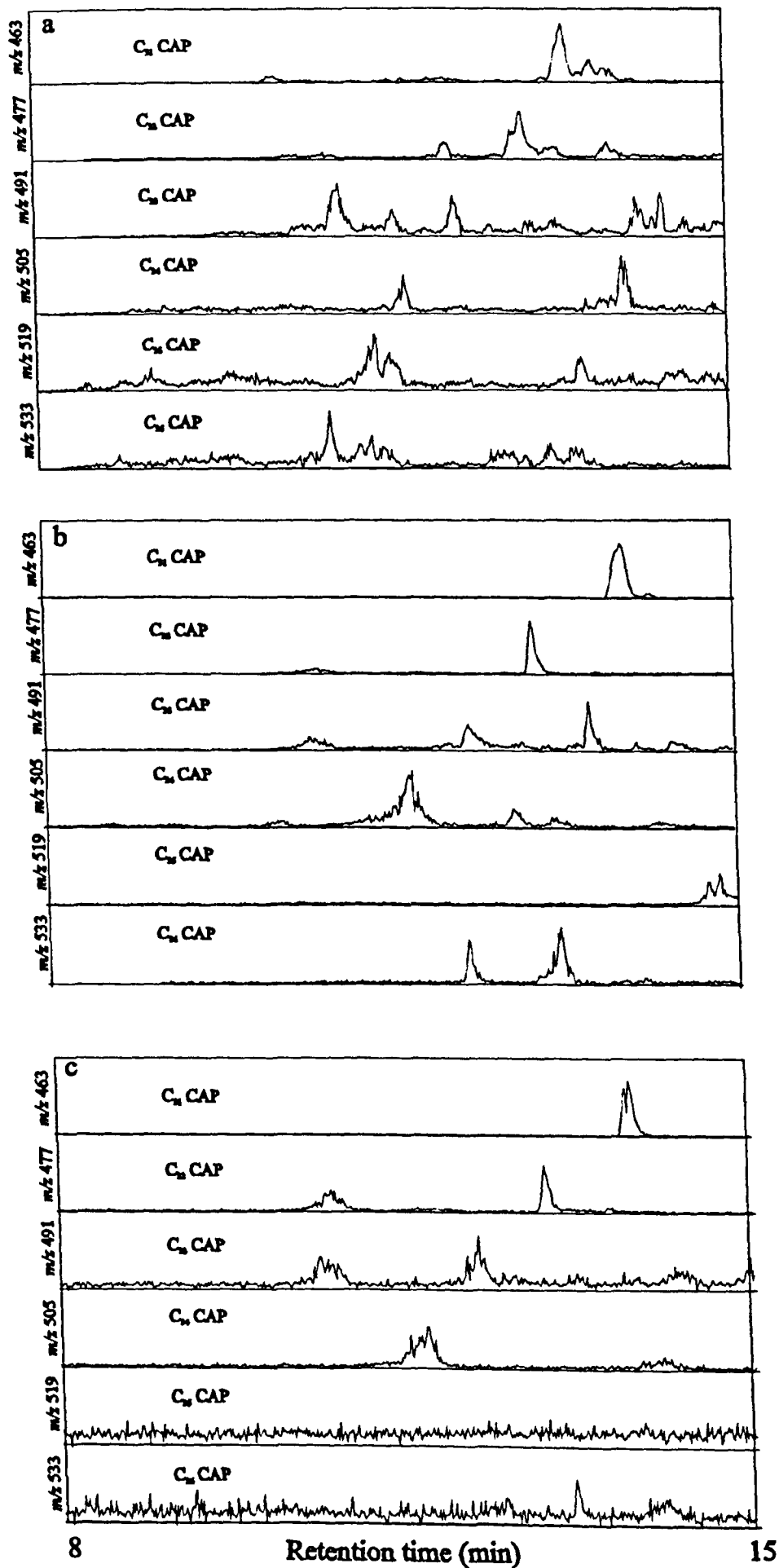


Fig. 3.12. Partial mass chromatograms for early eluting CAPs ( $C_{31}$ - $C_{36}$ ) from (a) Kupferschiefer bulk sample (b) VDG IV-4 (c) VDG VI



CAPs are also seen, eluting after the “HMW region”, but again, the retention positions do not seem to indicate the presence of any pseudohomologous series. The C<sub>35</sub> chromatogram in some of the samples shows the presence of a minor C<sub>35</sub> component eluting within the “HMW region” (e.g. IV-4 and IV-6; fig 3.10b,c), but after the bacteriochl *d*-derived CAP (34c). A similar component is also observed, possibly as part of a series, in another Cen/Tur sample from the North Atlantic (chapter 4), which has recently been found to contain high concentrations of isorenieratene derivatives (Sinninghe Damsté and Köster, 1998). However, this component does not seem to comprise part of any series, as no C<sub>34</sub> or C<sub>36</sub> CAPs are detected within the same region of the chromatogram (fig 3.10). As stated previously, although the structures of such components are unknown, it was tentatively suggested that the HMW components (>C<sub>33</sub>) might be related to a bacteriochl *c* or *e* origin (Chapter 2), with the lower carbon number components in the same region being derived from other sources. This hypothesis is strengthened by other more recent work which has found free maleimides to be present in VDG-IV samples, with samples IV-1 to IV-8 inclusive containing significant amounts of Me *i*-Bu maleimide specifically derived from the bacteriochls of Chlorobiaceae (Magnus, personal communication). It is, however, difficult to see how the CAPs observed, although corresponding in retention time to CAPs present in some other samples, are derived from the bacteriochls when no discernible pseudohomologous series have been observed.

### *Stratigraphy*

Fig. 3.13 shows the individual depth profiles of the early and late eluting C<sub>34</sub> and C<sub>35</sub> CAPs relative to DPEP through the marl IV horizon VdG section. Figs 3.13a and b show the plots for the early and late eluting C<sub>34</sub> CAP components respectively, whilst 3.14c and e show the early and late eluting C<sub>35</sub> components. Fig 3.13d shows the plot for the single C<sub>35</sub> component which elutes within the “HMW region”, but after the bacteriochl *d*-derived CAP, whilst fig 3.13f displays the changes in the relative amounts of any C<sub>36</sub> components present. Figs 3.14a-f show the same ratios for the same components through the VdG marls (II to XI), taking an average value of all the marl IV sub-samples as the overall value for this marl. These can be compared to the depth plot of isorenieratene through the marl IV horizon (fig 3.15a) and through the entire section (II to XI; fig 3.15b; taken from Keely *et al.*, 1995). Fig 3.13a,b and f show some similarities in the depth plots, with maximum values seen at IV-3 in both the C<sub>34</sub> and C<sub>36</sub> porphyrin distributions and the isorenieratene plot. However, the greater

Figure 3.13. Depth profiles through marl IV of (a-b)  $C_{34}$  CAPs (c-e)  $C_{33}$  CAPs (f)  $C_{36}$  CAPs vs.  $C_{32}$  CAP

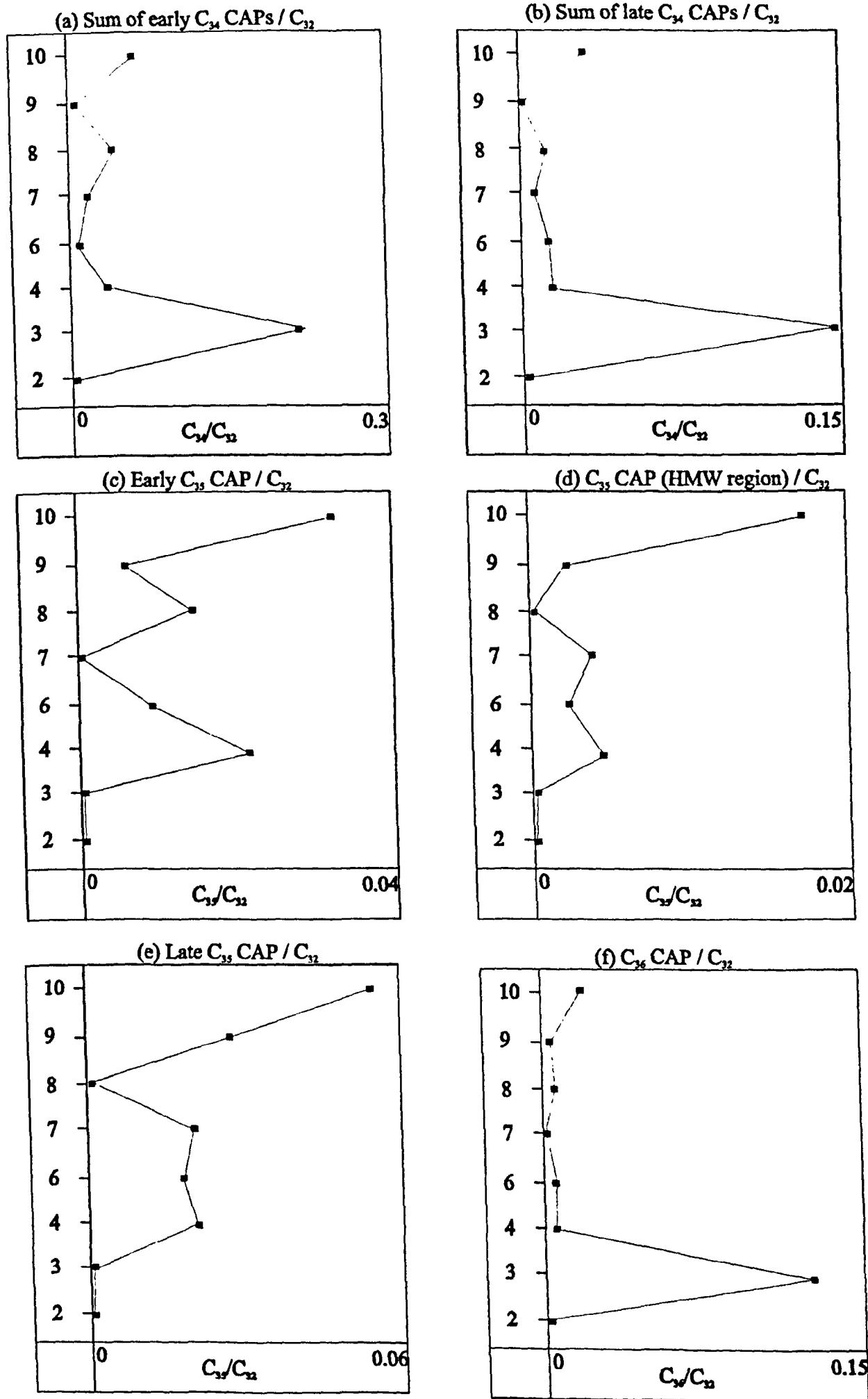
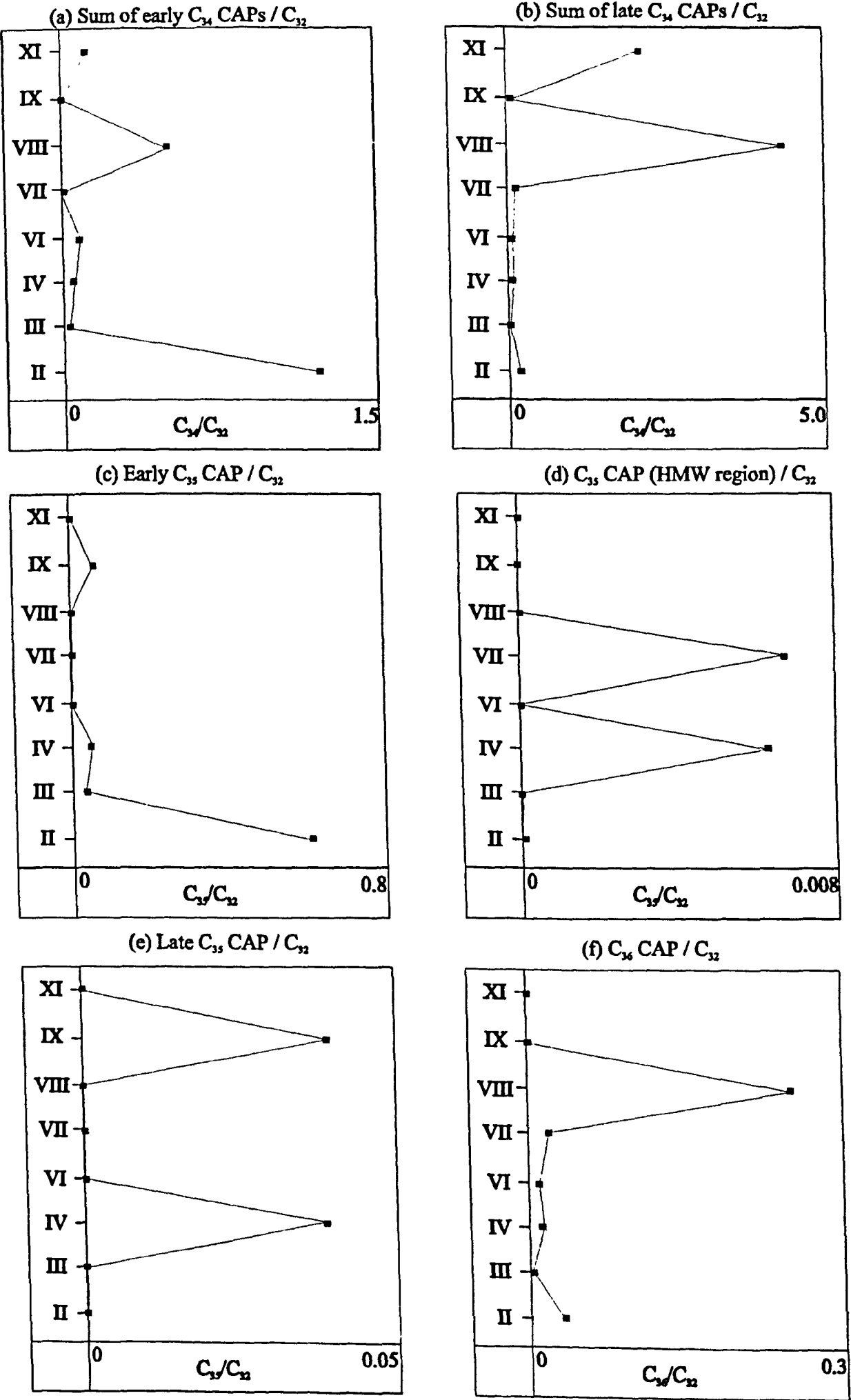


Figure 3.14 Depth profiles through VdG (II to XI) of (a-b)  $C_{34}$  CAPs (c-e)  $C_{35}$  CAPs (f)  $C_{36}$  CAPs vs.  $C_{32}$  CAP

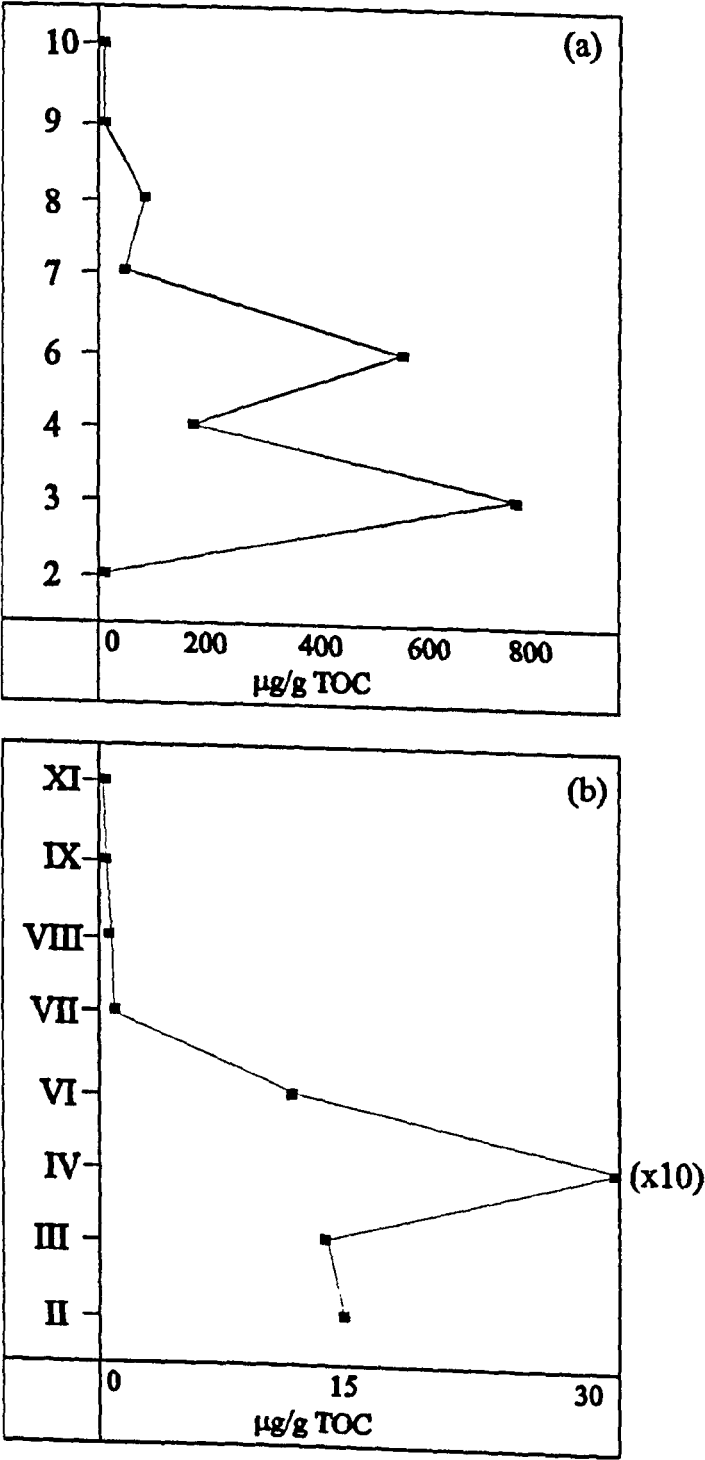


amounts of isorenieratene in IV3-6 as compared with IV-2 and IV7-10 is not generally reflected in any of the porphyrin depth plots of fig 3.13. Furthermore, the great abundance of isorenieratene detected in marl IV, as compared with the other marls (fig 3.15b), is not seen in any of the porphyrin depth profiles in fig 3.14.

In general, therefore, it seems that the depth profiles of the porphyrins and of isorenieratene do not match. Perhaps, the low bacteriochl to carotenoid ratio inherent in the brown Chlorobiaceae, may mean that bacteriochl *e*-derived components are present at too low a concentration for detection.

These results suggest that the early-eluting or late eluting HMW CAPs do not, in this instance, adequately describe the changes in abundance of the brown strains of Chlorobiaceae in the water column during deposition of the VdG marls. This unfortunately does not extend the previous studies showing that the maximum extent of photic zone anoxia was in the middle of the marl horizons (laminated marls) with these conditions being much less developed at the top and bottom of the horizon (homogeneous marls).

Fig 3.15 Depth profile of isorenieratene (taken from Keely *et al.*, 1995)  
(a) through marl horizon IV (b) through marls II to XI



## **CHAPTER 4**

# **LC-MS STUDIES OF PORPHYRINS FROM BLACK SHALES DEPOSITED DURING THE CENOMANIAN/TURONIAN OCEANIC ANOXIC EVENT**



## INTRODUCTION

### Composition and occurrence of black shales

Organic-rich shales, traditionally referred to as black shales or bituminous shales, have been of interest for some time, having a widespread distribution corresponding to certain times together with a recognition of their potential as hydrocarbon source rocks. There are a number of classification patterns for such shales (e.g. Hattin, 1975; Pratt, 1984; Dean *et al.*, 1984) but they are generally marine deposits laid down in oxygen-depleted environments and are rich in OM, often between 4 and 10% TOC, but with some reaching 50% and with a minimum level usually taken as 1% (e.g. Weissert, 1981; Stein *et al.*, 1986; Arthur *et al.*, 1990). Other notable features often include a dark colour, the presence of fine laminations with an absence of benthic fauna, an enrichment in phosphates and in trace elements such as Ni, Cu, V, Cd and U, high content of iron sulphides – usually pyrite, and low carbonate content. There are however exceptions to most of these guidelines. Colour can be influenced by both OM type and maturity as well the overall level of organic carbon. For instance, immature shales are often found to be brown in colour, but shales containing even only minor amounts of mature OM can be blacker (Arthur and Sageman, 1994). The black colour can also be in part due to the presence of fine-grained pyrite, but the presence of significant levels of  $\text{CaCO}_3$  in some cases can impart a lighter colour to shales even highly enriched in OM. The fine laminations, implying varying fluxes of at least two ingredients, have been attributed to various factors, in combination with low oxygen concentrations inhibiting benthic activity. These include seasonal changes in productivity resulting from phytoplankton blooms, bottom-current activity and the periodic colonisation of sediment/water interfaces by sulphide-oxidising bacterial mats (Arthur and Sageman, 1994 and refs. therein). Laminae have also been observed in re-deposited turbidite sediments (e.g. Stow and Dean, 1984) and may also form as secondary structures due to the action of some diagenetic chemical processes (Ricken, 1985; Beiersdorf and Knitter, 1986). A temporary elimination of the *in situ* macrobenthos may also occur for reasons other than oxygen depletion, e.g. a sudden sediment influx, introduction of highly saline bottom waters or toxic plankton production, and could therefore result in a reduction or even elimination in OM recycling. This may then lead to the preservation of thin organic-rich sediments indistinguishable from those deposited under anoxic environments (Funnell, 1987). There are also examples of black shale sections that appear homogenous, as the finely

laminated structures originally deposited may be disturbed by physical processes such as redeposition or bioturbation (Dean and Gardner, 1982; Arthur *et al.*, 1984a), whilst similarly, there are examples of light coloured, organic-poor limestones which are laminated (*e.g.* Robertson and Bliefnick, 1983; De Graciansky *et al.*, 1982). Pyrite, too, cannot be used exclusively as an indicator of anoxic bottom waters, as it may form in oxic sediments that become anoxic after burial, or in anoxic microenvironments within oxic sediments (Waples, 1983). On the other hand, pyrite formation may be inhibited in anoxic sediments if there is a lack of available iron. Black shale sequences are commonly found interbedded with rocks of other lithologies such as marls, limestones or lighter coloured mudstones and shales. These lighter coloured interbeds are generally poor in OM and are bioturbated, indicating deposition under oxygenated conditions (Demaison and Moore, 1980; Schlanger and Cita, 1982; Waples, 1983; Arthur *et al.*, 1984b). Such lithology may be cyclical and in many instances is thought to reflect regular climatic variations (*e.g.* Schwarzacher and Fischer, 1982; de Boer and Wonders, 1984; Herbert and Fischer, 1986), although diagenetic effects together with the influences of turbidite influx, productivity and/or redox change can also result in such cycles of sedimentation.

Since the arrival in 1968 of the Deep Sea Drilling Project (DSDP), black shales have been recovered from all of the world's ocean basins (*c.f.* Weissert, 1981) which, together with a widespread occurrence on land (Jenkyns, 1980), showed the global nature of such sequences and led to extensive studies of black shale deposition.

Although there are a few beds of organic-rich shales that were deposited during the Triassic period (*e.g.* Rieber 1974, 1982), the majority of sections analysed have been found to be deposited during the Jurassic and in particular the Cretaceous period. Such shales are of great economic importance as they are by far the most important source of petroleum, with estimations giving between 70-85% of generated oil being produced by source rocks deposited during the Jurassic and Cretaceous (Irving *et al.*, 1974; Tissot, 1979), with more OM in Cretaceous shales alone than is contained in all the global coal and petroleum reserves (Ryan and Cita, 1977). Well known Jurassic organic-rich shales include those deposited during the Early Toarcian (Falciferum Zone) throughout NW Europe (*e.g.* Posidonienschiefer, Schistes Cartons and Jet Rock in Germany, Paris Basin and north east England respectively), the Middle to Upper Callovian in Southern England (Lower Oxford Clay) and during the late Jurassic (Kimmeridgian to Tithonian age); the type section of the latter is the Kimmeridge Clay, which is generally thought

to be the main source rock for North Sea oil. Cretaceous shales are more widespread, with a succession of local minor OM-enriched deposits seen in the lowermost Cretaceous western North Atlantic followed by the near global distribution concentrated in the mid-Cretaceous between Aptian and Turonian (Schlanger and Jenkyns, 1976; Arthur and Schlanger, 1979; Tissot *et al.*, 1980 and Cool, 1982). For a detailed description of the global distribution of marine black shales throughout the Mesozoic era, see reviews by Jenkyns (1980) and Hallam (1987a).

### **Accumulation of organic matter**

Much discussion has taken place concerning the relative importance of the differing processes involved during the deposition of black shales. Accumulation of OM in deep-water oceanic environments, for example, is in a general sense not favoured due to its degradation and remineralisation whilst settling through an oxygenated water column and within the oxygenated surface sediment. Therefore, the assumption that black shales are primarily deposited under oxygen depleted conditions generally remained unchallenged over the years, although more recently the extent of the importance of this oxygen depletion compared with other factors has been debated (*e.g.* Demaison and Moore, 1980 vs. Pederson and Calvert, 1990). Indeed, this has yet to be answered, as the effects on OM as a result of changes in productivity and levels of dissolved oxygen are difficult to trace in the marine environment, due to the great complexities in oceanic circulation and OM depositional patterns. Many workers accept, however, that bulk sediment accumulation rate is a primary control on organic carbon content in marine sediments (Muller and Suess, 1979; Ibach, 1982; Canfield, 1989; Betts and Holland, 1991); for instance, it is possible that with a high sedimentation rate, abundant OM is buried, despite oxidising conditions in deep water (Summerhays, 1983).

Differing opinions exist, however, concerning the relative importance of the roles of high productivity (contended by Calvert, 1987; Pederson and Calvert, 1987, 1990; Calvert and Pederson, 1992; Calvert *et al.*, 1996) and enhanced OM preservation (Demaison and Moore, 1980; Jenkyns, 1980, 1991; Canfield, 1989; Demaison, 1991; Van Cappellen and Canfield, 1993). Other factors such as water depth and the degree of dilution by other sedimentary components (see above), plus the role of mineral surfaces in the sorptive protection of OM (*e.g.* Hedges and Keil, 1995) and the length of oxygen exposure time (Hartnett *et al.*, 1998) are other important factors which together give rise to conditions which are favourable for organic carbon burial and the subsequent accumulation of shales high in organic carbon.

## *Productivity*

Sources of OM may be typically marine, with varying contributions from terrestrial higher plants. Primary productivity in the marine environment is controlled by levels of light, water temperature (affecting solubility of dissolved CO<sub>2</sub> and O<sub>2</sub>) and nutrient availability (reviews by Berger *et al.*, 1989; Jahnke, 1990; Meyers, 1997).

Phytoplanktonic productivity is confined to the photic zone, which can extend to 150m in clear, open water to only a few metres in more turbid environments. Important nutrients, primarily nitrates, phosphates and silicates, are consumed by phytoplankton, so must be replaced by either vertical mixing or horizontal supply in order to sustain the productivity. Alternatively, nutrients may be supplied to the oceans directly from the land, either during high stands of sea level or *via* terrestrial run-off. Organic debris settling through the water column is bacterially degraded, a process that utilises dissolved oxygen and “remineralises” the OM, returning nutrients to the deeper water layers. These nutrients can then be returned to the surface layers by water column mixing processes induced by either turbulence or upwelling. The latter is often controlled by the prevailing wind action and also Coriolis forces, resulting in the horizontal movement of surface waters, to be replaced by the vertical movement of deeper, more nutrient-rich waters.

The distribution of land masses is also an important factor. For instance, zones of high fertility are often found in eastern boundary coastal regions where trade winds drive away surface waters resulting in coastal upwelling (see also below). This is in contrast to the low production zones in the mid-latitude centres of oceans (gyres), where stable thermal stratification separates the warm surface layer from the deeper, cold, nutrient-rich layers so that wind-driven mixing across the thermocline is the only major means of fertilising the photic zone. Hence, highly productive zones can be found concentrated along continental margins which in turn receive a greater flux of carbon settling to the sea floor at a given depth than in the less productive open ocean zones (*e.g.* Jahnke *et al.*, 1990). In fact, it has been suggested that up to half the world's organic-rich sediments were deposited in upwelling zones (Parrish, 1987), even though these areas constitute only a small surface area of the oceans. As an example, the area along the west coasts of the world's continents constitutes about 0.1% of the ocean, but the resulting coastal upwelling and high productivity produces large fish stocks which comprise 50% of the world's fish market (Ryther, 1969). However, upwelled water is not always nutrient-rich, as off Cabo Frio, Brazil (Fahrbach and Meincke, 1979), being

highly dependent on the nature of the intermediate/deep water masses, and therefore does not necessarily result in higher productivities (Hay and Brock, 1992); it is also noted that a large number of known OM-rich beds are not in areas of predicted upwelling (Arthur *et al.*, 1987).

### *Preservation*

Traditionally, there has been relatively little appreciation on the role of primary productivity in the formation of black shales, with most of the historical focus being on the role of preservation in reducing environments. Indeed, a major assumption made by many workers is that OM is preferentially preserved in environments containing no (anoxic) or low (dysaerobic) concentration levels of dissolved oxygen (*e.g.* Demaison and Moore, 1980; Tyson, 1987; Emerson and Hedges, 1988; Stein, 1991), resulting in sediments high in TOC. Similarly, the presence of significant amounts of porphyrin and chlorin pigments has been used to provide further confirmation of oxygen-depleted conditions (Baker and Louda, 1980; Didyk *et al.*, 1978). In fact, degradation of OM continues after the removal of oxygen from the water column, with nitrates and then sulphates being utilised as oxidants by the appropriate bacterial community, with the latter producing  $H_2S$  as a by-product. The general assumption that this anaerobic degradation proceeds at a lower rate than aerobic degradation has, however, more recently been discussed by a number of workers who seem to show that rates of OM remineralisation under oxic and anoxic conditions are similar (see review by Henrichs and Reeburgh, 1987). Whether or not high OM preservation is a direct result of deposition in anoxic environments, or is more a result of high primary productivity (which in turn can result in a reduction in bottom water or water column oxygenation), it is generally assumed that wherever there are anoxic bottom waters, there will be subsequent significant preservation of OM (Waples, 1983), although the physical characteristics of the local or regional depositional setting provide an important control on the overall extent of the preservation. Other workers have also shown that processes of primary productivity and anoxia are linked in other ways. For instance, phosphorous, an essential nutrient for photosynthetic productivity, has been found to be actively accumulated by bacteria and preserved under aerobic conditions in bioturbated sediments, whereas under anoxic conditions this phosphorous is released from sediments and can be transferred to the ocean surface via upwelling (Ingall and Jahnke, 1994). Hence, intensified oxygen depletion as a result of high productivity may result in the stimulation of benthic phosphorous release which, if allowed to build up, further

stimulates the primary productivity (Van Cappellen and Ingall (1994). However, the authors have shown that these processes are highly dependent on the overall time scale involved, as the build up of regenerated phosphorous in the oceanic reservoir takes a finite amount of time, whereas a reduction in the rate of vertical overturn results in an almost immediate drop in primary productivity due to the consequent reduction in the rate of upwelling. Simulation models in fact suggest that drops in rate of vertical overturn of less than 15,000 years will not be long enough to allow build up of regenerated phosphorous, whereas over longer periods of time, perhaps in certain areas of the ocean during oceanic anoxic events (see below), a longer period of sluggish circulation, *e.g.* in the Cretaceous southern North Atlantic and Tethys Ocean, could easily result in a build up of phosphorous and consequently stimulate the primary productivity to a considerable extent (Van Cappellen and Ingall, 1994).

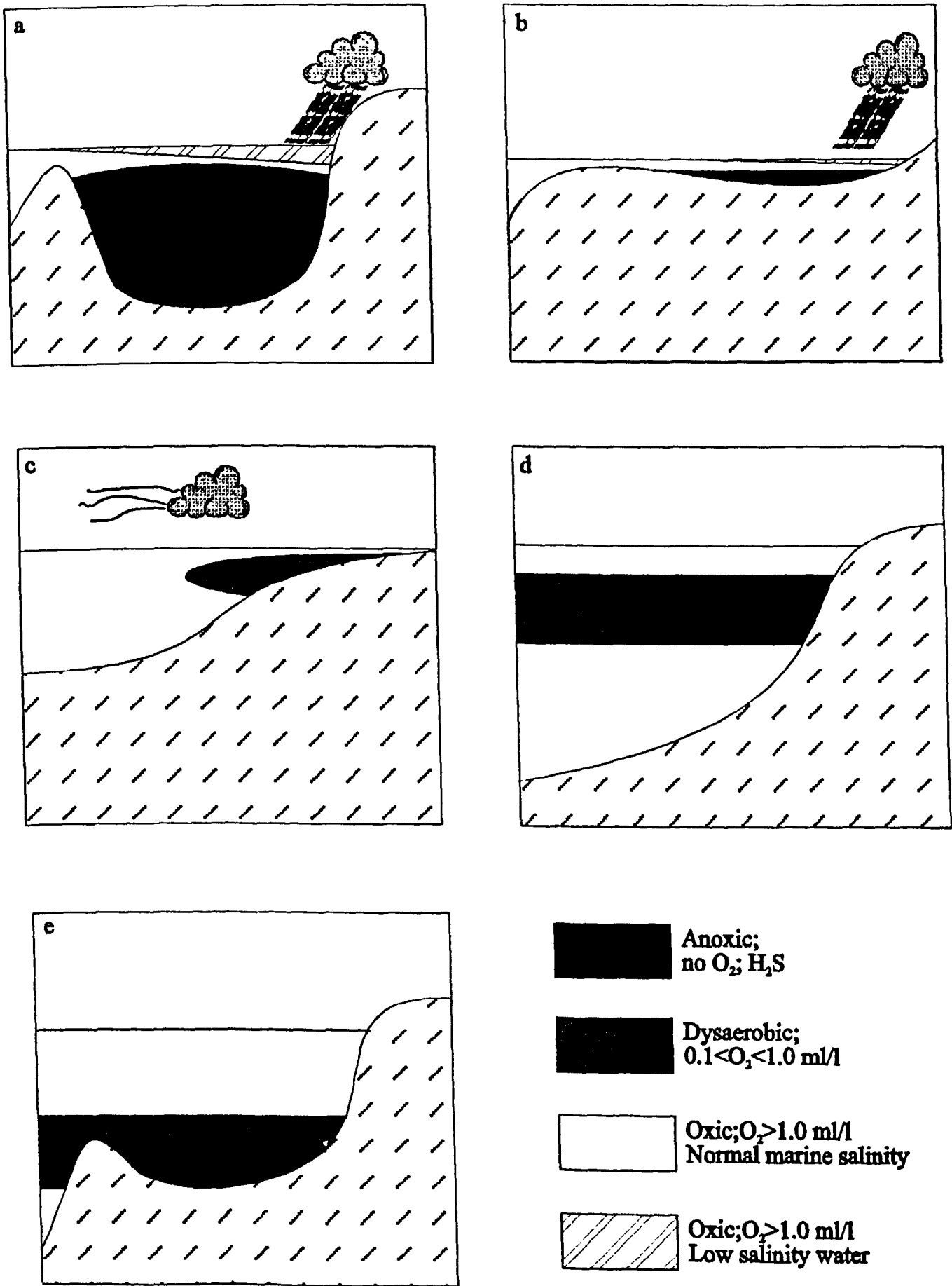
### **Present day depositional environments**

#### *Deep stratified anoxic basin*

Studies of a variety of modern environments where organic carbon-rich sediments accumulate, have strongly influenced the interpretation of ancient black shale deposits. With the Black Sea originally defined as the “type” anoxic basin (*e.g.* Glen and Arthur, 1984) in which organic-rich, laminated sediments have accumulated, the restricted, or stratified basin model (fig. 4.1a) is often cited as one example of a depositional setting which encourages the preservation of OM (Rhoads and Morse, 1971); however, the extent to which this deep basin model remains applicable to Mesozoic marine shales remains questionable (*e.g.* Hallam, 1975). Such an anoxic water body is formed when the supply of dissolved oxygen to the lower waters is less than its rate of consumption and occur where a physical barrier, *e.g.* a sill or ridge, isolates a major body of water from the open ocean. Such a barrier may restrict the circulation of water, in turn limiting the replenishment of dissolved oxygen within the basin. In some scenarios, with microbial oxidation reducing the oxygen levels within the basin, and with a positive water balance maintained (*i.e.* dominance of outflowing less saline water over influx of deeper, saline water) oxygen becomes permanently absent, leading to the development of stratified, anoxic conditions underneath a pycnocline. If this anoxicity is maintained, then euxinic (*i.e.* anoxia + free  $H_2S$ ) conditions may extend into the zone of light penetration, allowing growth of green sulphur bacteria, as in the modern Black Sea (*e.g.* Repeta *et al.*, 1989; Sinninghe Damsté *et al.*, 1993a). Extensive stratification

Figure 4.1 Schematic diagrams showing five generalised modern day environments favouring accumulation of organic-rich sediments.

- (a) Silled deep basin (b) shallow epicontinental sea (c) coastal upwelling zone (d) "anoxic" open ocean (e) deep borderland basin



stratification in such basins results in the trapping of nutrients in the lower levels of the water column so that the overall level of productivity is generally low (*e.g.* Hollander *et al.*, 1993b). Similar conditions and processes give rise to the development of oxygen-depleted conditions within shallow epicontinental seas (fig. 4.1b; *e.g.* Baltic Sea), although the presence of a sill or ridge is not always required for circulation restriction if the sea is shallow and large enough. Density stratification may be reinforced by an influx of low salinity surface water in regions where precipitation is greater than evaporation (*e.g.* Weissert, 1981; Rossignol-Strick *et al.*, 1982; Barron *et al.*, 1985) and/or where there is extensive dissolution of salts or a basinal influx of deeper, more saline, oxygen-poor water, formed on shelves or shallow ocean basins in regions where evaporation exceeds precipitation (*e.g.* Arthur and Natland, 1979).

### *Oxygen minimum zone*

An oxygen minimum zone (OMZ) results from degradation of sinking OM together with its relatively long residence time in waters of intermediate depth. An OMZ can form in upwelling-induced coastal areas of high productivity such as off Namibia and Peru (*e.g.* Thiede and Suess, 1983; fig. 4.1c). Oxygen-deficient depositional conditions develop in regions where such an OMZ impinges upon a continental slope or shelf, such as in the modern Indian Ocean (Thiede and van Andel, 1977; Demaison and Moore, 1980), in which case sediments can be deposited, preserving large quantities of OM (2-25%; Dean *et al.*, 1984; Arthur *et al.*, 1984a, 1987; Schlanger *et al.*, 1987). In the present day Gulf of California, circulation is “estuarine” (after Berger, 1970), *i.e.* deep water inflow and surface water removal by offshore winds, resulting in seasonal upwelling and high plankton productivity (Lisitzin, 1971). An OMZ results, ranging from 300 to 1200m, and laminated organic-rich facies are confined to the area of the slope intersecting this layer, together with alternating clay-rich laminae attributed to the seasonal input of detrital material from rivers draining the Mexican mainland. The deposition of high amounts of OM often results in the near total reduction of sulphate within the sediments, as observed in sediments deposited in the waters under the upwelling areas of Peru (sites 680 and 688), Benguela (SW Africa; site 532) and Oman (Arabian Sea; site 723) (Prell *et al.*, 1989; Suess *et al.*, 1988; Morse and Emeis, 1992), with drilled cores taken from the extensive OMZ in the NE Arabian Sea off Pakistan containing a strong smell of H<sub>2</sub>S (von Rad *et al.*, 1995). However, the waters of most OMZs contain traces of oxygen and are devoid of sulphide, so would not support communities of anaerobic photosynthetic bacteria. Rare present day exceptions include



the OMZ of the Arabian Sea (Deuser, 1975) where nitrogen isotope data (see below) from recent cores has provided evidence for productivity-induced denitrification (Altabet *et al.*, 1995) and from where small amounts of isorenieratane was identified (Hoefs *et al.*, 1995). Also, in the Peru upwelling region during certain conditions (Dugdale *et al.*, 1977; Packard *et al.*, 1978, 1984), a phenomenon known as *aguaje* occurs, where the presence of free sulphide has been detected in waters below the photic zone. Current vector measurements of the Peru-Chile undercurrent, the major source of upwelling water on the coast of Peru, showed that in the early spring of 1976 there was a reversal in flow of the current which resulted in the return of oxygen-depleted water to regions of high marine productivity where it underwent further reduction in oxygen, consequently resulting in sulphate reduction, production of sulphide and subsequent fish kills. *Aguaje* records suggest that such deep water anomalies occur approximately every eight years (Packard *et al.*, 1984). However, analysis of carotenoid distributions in recent sediments deposited in this region found no biomarkers indicative of the green sulphur bacteria (Repeta and Gagosian, 1987; Repeta, 1990). An expanded OMZ may also form at intermediate depths in the open ocean (fig. 4.1d), as seen in the northern Indian Ocean (Didyk *et al.*, 1978) where the occurrence of  $H_2S$  in the water column was also reported (Ivanenkov and Rozanov, 1961), and in the equatorial East Pacific where the effect of the Coriolis force causes vast areas of the ocean to become oxygen depleted (Demaison and Moore, 1980). In some cases, OMZs impinge upon underwater silled basins (fig. 4.1e), such as the borderland of southern California. In these regions, basins, silled below *ca.* 500m depth, contain oxygen depleted waters with reduced circulation, resulting in the preservation of organic-rich sediment. Although the organic geochemistry of a wide variety of modern coastal upwelling systems has been studied, there is as yet no unique set of geochemical biomarkers that can be safely and specifically attributed to such environments (Brassell *et al.*, 1983; Repeta *et al.*, 1992; ten Haven *et al.*, 1992), although with the dominance of diatoms and certain radiolarian species in these areas (Blasco, 1971; Thiede and Jünger, 1992), sedimentary radiolarian abundance is often used as an indicator of fertility changes (Farrimond *et al.*, 1990; Caulet *et al.*, 1992 and refs therein)

A final “oxygen-demand” model involves the preservation of organic-rich sediment in oxygen-deficient areas that form as a result of a high rate of OM deposition (Dean *et al.*, 1984). A sharp redox boundary commonly develops at the sediment-water interface

which may later fluctuate above or below this interface as a result of fluctuations in the rate of supply of OM, hence resulting in increases or decreases in the rate of microbial oxidation. Environments where such black, H<sub>2</sub>S-containing, organic-rich muds are to be found include some large bays, lagoons, tidal flats and intertidal swamps (*e.g.* Rosenberg, 1977; Martens and Klump, 1984).

### **Mesozoic oceanic black shales**

In general, observations of such modern environments in which organic-rich sediments have been found to accumulate have strongly influenced the interpretation of ancient oceanic black shale deposition. However, there is little doubt that at certain times in the past, atmospheric and oceanic conditions were different from those experienced today, so that the widespread deposition of Mesozoic black shales may have been controlled largely by other more significant global and/or local changes which are not experienced to the same extent during the present day in any marine setting. Continental distribution and consequent oceanic and atmospheric circulation, extent of tectonics and volcanism, and global sea levels were certainly very different throughout much of the Mesozoic. For instance, during these less glacial times, *e.g.* Jurassic and Cretaceous periods when polar ice caps were absent (Kemper, 1987), and a closer assembly of continents characterised the land/ocean distribution, a warm, equable climate (Frakes, 1979; Barron and Washington, 1982a; Barron, 1983; Hallam, 1985), with an absence of large-scale continental glaciation, may have resulted in reduced thermohaline global oceanic circulation (driven at present by sinking, cold water in high latitude, polar regions). Models have shown that when the temperature of high latitude water exceeds 10°C, this deep circulation system vanishes (Wilde and Berry, 1982) so that considerably less oxygen can be transported to the deep. Consequently, a warmer deep ocean and thus lower initial oxygen solubility (Sarmiento *et al.*, 1988), together with the occurrence of high density saline shelf waters (Roth, 1978; Arthur and Natland, 1979; Brass *et al.*, 1982) were major factors influencing the widespread depletion of oxygen in deep water and may have allowed the burial and preservation of OM to occur more easily than at present, even with average surface productivities that were lower in some areas than present (de Boer, 1986; Arthur and Sageman, 1994). Some models have suggested that in the absence of the formation of cold polar deep water, the warm saline water formed on low-latitude shelves or in areas with a negative water balance (*e.g.* in more isolated seas in the Mediterranean), was the major source of bottom water (Brass *et al.*, 1982; Wilde and Berry, 1982), giving rise to the notion that circulation in the Cretaceous

oceans was slower (Bralower and Thierstein, 1984) and largely salinity driven. The model of Brass *et al.* (1982) has furthermore shown that the rate of warm saline bottom water (WSBW) formation from such areas would increase during marine transgressions (see below), which, together with the decreased solubility of oxygen, would advect waters containing less dissolved oxygen to the deep water masses of the ocean. Arthur *et al.* (1987) argued that the flooding of low latitude shelves would increase the flux of WSBW and result in upwelling, particularly along continental margins, and in the subsequent formation of an OMZ (Southam *et al.*, 1982, 1984). Models of ancient climate and ocean circulation have also been used to test theories about regions of high productivity associated with wind-induced upwelling (*e.g.* Parish and Curtis, 1982; Scotese and Summerhayes, 1986), coastal upwelling expected from changes in palaeogeography, predicted regions of high precipitation and/or fresh water run-off (thereby providing the potential for salinity stratification; Barron *et al.*, 1985), nutrient concentrations, temperature changes and changes in sea level (both eustatic and tectonic). Atmospheric concentrations of O<sub>2</sub> and CO<sub>2</sub> are also important factors, with some calculations suggesting that atmospheric CO<sub>2</sub> may even have been ten times higher during the Early Cretaceous than at present (Budyko and Ronov, 1979), with even a more moderate estimate of four to eight times present-day CO<sub>2</sub> concentrations (Bernier, 1992) still resulting in a warm, greenhouse climate favouring higher temperature, slow ocean circulation and widespread black shale deposition. Enhanced *p*CO<sub>2</sub> results in greater incorporation of <sup>12</sup>C into marine OM, a pattern which is seen for example in the greater depletion in δ<sup>13</sup>C of OM in Cen/Tur black shales from DSDP sites 367, 530 and 603 and elsewhere, which are mainly marine in origin (Dean *et al.*, 1986), as compared with sediments deposited in a variety of modern environments (Meyers, 1989). High fertility in palaeo oceanic surface waters has been proposed for the formation of Mesozoic black shales based on model predictions, identification of certain nannofossil assemblages enriched in high fertility indicators (Schlanger and Jenkyns, 1976; Thiede and van Andel, 1977; Parrish and Curtis, 1982; Roth, 1986; Hofmann *et al.*, 1997) and, at certain times isotopically heavy δ<sup>13</sup>C excursions (see below), together with a high supply of terrestrial OM during high mid-Cretaceous sea levels (Habib, 1979; Jenkyns, 1980; Stein *et al.*, 1986). However, it has alternatively been proposed that the productivity of the Cretaceous surface waters was moderate (Fischer and Arthur, 1977; Berger, 1979), with even the highest estimates of primary

production in the mid-Cretaceous considerably lower than those measured in high-productivity areas within modern oceans (Bralower and Thierstein, 1987).

In summary, the formation of black shales is complex and it is not yet possible to define fully the exact conditions under which individual ancient black shales were deposited, especially with the lack of precise stratigraphic resolution and because the relative roles of sediment accumulation rates, dissolved oxygen concentrations and levels of productivity are not yet fully understood. Further complications are revealed when comparing the depth distribution of organic carbon accumulation rates between the mid-Cretaceous (Aptian to Cenomanian) and the Holocene (Stein, 1986). There appears to be little correlation between bulk sedimentation rate and organic carbon accumulation rates (from van Andel *et al.*, 1975) and hence between palaeowater depth (from Thierstein, 1979; Roth, 1981) and organic carbon accumulation rates at mid-Cretaceous sites, as opposed to the good correlation between bulk and organic carbon accumulation rates and palaeowater depth observed in sediments deposited above the carbonate compensation depth (CCD, see below) in Holocene oxic deep water environments (Bralower and Thierstein, 1987). This implies that during the mid-Cretaceous, as opposed to the Holocene, anoxic deep water conditions existed so that no correlation existed between sedimentation rate and TOC, as for example in the modern Black Sea (Degens and Ross, 1974; Stein, 1986), *i.e.* factors other than bulk accumulation rate, such as productivity and circulation/ ventilation of bottom waters, were varying through both space and time.

### **Oceanic Anoxic Events**

During the 1970's, a number of workers noted that a large proportion of the widespread deposits of Cretaceous organic-rich black shales were concentrated within specific time intervals (Schlanger and Jenkyns, 1976; Fischer and Arthur, 1977; Thiede and van Andel, 1977; Ryan and Cita, 1977). This indicated the possibility that much of the Cretaceous ocean system was oxygen deficient from around Hauterivian to Santonian times, with much of the marine organic carbon being preserved in sediments, along with a significant proportion of terrestrial OM in many cases. The approximate synchronicity of the stratigraphic occurrences of these shales in a variety of depositional regimes throughout the world led Schlanger and Jenkyns (1976) to term the phrase "Oceanic Anoxic Events" (OAE). This term initially described two time periods, the late Barremian through Albian and the geologically brief late Cenomanian through early Turonian (Cen/Tur; this chapter) when such sediments are concentrated.

Other time periods later added included the third Cretaceous period, Coniacian to Santonian (Ryan and Cita, 1977) and the Jurassic early Toarcian (chapter 5), together with the possible additions of the Ordovician, Silurian and Devonian (Jenkyns, 1980). Subdivision of the Aptian-Albian OAE resulted in three narrower envelopes, or subevents (OAE1a-c), with the earliest interval, OAE1a during the Early Aptian (chapter 5), OAE1b late Aptian/Early Albian, and OAE1c Late Albian (Arthur *et al.*, 1990).

Near-global black shale deposition during these time periods is interesting as it implies that certain global factors were exerting a significant control on production and preservation of OM. However, the exact extent to which this control reaches is still a matter of debate as, due to limits in stratigraphic resolution, there is no demonstration of an exact synchronicity between single black shale layers on a global scale within each of these OAE time periods.

Significant oceanographical events within OAEs are also represented in other ways within the geological record. For instance, during the Cen/Tur OAE, a significant planktonic foraminifera extinction event occurred (see Kuhnt *et al.*, 1986, 1990; Jenkyns, 1985; Thurow *et al.*, 1982; Gale *et al.*, 1993; Erbacher *et al.*, 1996), thought to relate to sea level transgressions, increasing productivity and the resulting wide establishment of intensified oxygen-depleted conditions (Jenkyns, 1985; Erbacher *et al.*, 1996; Erbacher and Thurow, 1997). This occurred together with the extensive burial of large quantities of isotopically light marine OM (depleted in  $^{13}\text{C}$ ), resulting in the oceanic carbon reservoir becoming  $^{13}\text{C}$  enriched in many areas, consequently leading to the biogenic carbonate becoming isotopically heavy, and a positive excursion in the OM ( $\delta^{13}\text{C}_{\text{org}}$ ) and in the  $\delta^{13}\text{C}$  signal in the pelagic carbonates ( $\delta^{13}\text{C}_{\text{carb}}$ ) deposited near-globally (Scholle and Arthur, 1980; Schlanger *et al.*, 1987; Arthur *et al.*, 1988). The inherent complexities of these excursions (in particular a “three peak” excursion is noted) have been measured in less condensed Cen/Tur lithologies (Pratt and Threlkeld, 1984; Thurow *et al.*, 1988), with some authors showing notable similarities between carbon isotopic  $\delta^{13}\text{C}_{\text{carb}}$  profiles in Cenomanian to Turonian shales deposited in different parts of the world (*e.g.* Gale *et al.*, 1993), although the exact synchronicity of such excursions is difficult to prove. This same pattern of carbon isotopic enrichment is seen in some nutrient-enhanced modern lakes, evidenced by enriched  $\delta^{13}\text{C}_{\text{org}}$  in buried OM as a result of the higher productivity (Schelske and

Hodell, 1991). Furthermore, the greater magnitude of  $\delta^{13}\text{C}_{\text{org}}$  compared with the  $\delta^{13}\text{C}_{\text{carb}}$  seen in many Cen/Tur sections is thought to represent the significant drawdown of atmospheric  $\text{CO}_2$  during the Cen/Tur event, as previous work has shown that increased  $p\text{CO}_2$  results in an increased carbon fractionation factor *i.e.* marine OM becomes relatively more enriched in  $^{13}\text{C}$  with lower  $p\text{CO}_2$  (Dean *et al.*, 1986; Freeman and Hayes, 1992). These excursions occur together with an apparent  $\delta^{34}\text{S}$  excursion (Claypool *et al.*, 1980), implying that significant amounts of reduced sulphur were also preserved (*e.g.* Berner and Raiswell, 1983). Some authors have, in the past, inferred that during such periods, global marine water anoxia or even widespread marine water “stagnation” was the major factor resulting in widespread synchronous deposition of black shales in a variety of marine environments (*e.g.* Schlanger and Jenkyns, 1976; Brumsack, 1980; Scholle and Arthur, 1980; de Graciansky *et al.*, 1984, 1986; Zimmerman *et al.*, 1986), especially as many of the Cretaceous black shales seemingly represent slowly accumulating sediments (de Boer, 1986). Workers have also shown the coincidence between these black shale anoxic events and temperature increases (evidenced by oxygen-isotope data; Jenkyns *et al.*, 1994) and with eustatic rises in sea-level (Schlanger and Jenkyns, 1976; Vail *et al.*, 1977; Arthur 1979), caused primarily by increases in spreading rates and the volumes of ocean ridges (Hays and Pitman, 1973; Kominz, 1984). Tissot (1979) noted that 95% of global marine black shales were deposited during times of eustatic high sea level. In fact, the correlation between fast plate spreading rates, which give rise to shallower, broader and thus more voluminous ridges, is reasonably good with the highstands of sea-level of both the Jurassic and Cretaceous periods (Hallam, 1975; Vail *et al.*, 1977; Sheridan, 1987). The absolute vertical extent of these long-term eustatic changes is, however, uncertain, although estimates include those by Hays and Pitman (1973), Pitman (1978) and Watts and Steckler (1979) of 500m, 350m and 150m respectively. As well as possibly affecting ocean circulation patterns (Barron and Peterson, 1989), such transgressions produced wide, productive shelf areas with an influx of terrestrial debris and nutrients, as a result of the mobilisation from coastal lowlands (*e.g.* Thurow *et al.*, 1992; Erbacher, 1994; Jenkyns *et al.*, 1994) and widespread erosion of existing relief near the former coastline (Hilbrecht *et al.*, 1996). The largest increase in nutrient mobilisation, and hence in the resulting enhanced productivity, is thought to coincide with the maximum rate of transgression, rather than the time of highest stand of sea level (Jenkyns *et al.*, 1994).

This is backed up by stratigraphic evidence for the highest marine transgression occurring in Turonian times (*e.g.* Jenkyns, 1991), which is significantly later than the peak in burial of OM around the Cen/Tur boundary event as evidenced by the positive carbon isotope excursion. Increased areas of shallow, epicontinental seas in mid-latitude regions is apparent during much of the mid-Cretaceous compared with the Cenozoic, with an especially large transgression around Cen/Tur time documented globally (*e.g.* Western Interior Seaway of North America; Kauffman, 1977). Some authors describe fertile shelf seas produced by such transgressions that act as sinks for oxygen, with zones of anoxic waters spreading outwards from the shelf seas, across continental margins and into ocean basins, thereby providing a source of oxygen-depleted water to ocean basins where productivity may be low (Jenkyns, 1980). Another potential consequence of such major sea-level fluctuations, is the consequent fluctuation in the CCD as noted by Fischer and Arthur (1977), Berger (1979), Sclater *et al.* (1979) and Tucholke and Vogt *et al.* (1979). This is the depth at which the rate of supply of biogenic carbonate equals the rate of dissolution, so that below the CCD, calcite does not accumulate on the sea bed, leaving siliceous radiolarian and diatom oozes and red or brown clays to form. Thus, an increase in sea level, producing an elevation in the CCD, may have resulted in a reduction in the effects of inorganic dilution, thereby reducing the carbonate contents and enhancing the accumulation rate of OM in sedimentary deposits. A shallow CCD also results in the absence of calcareous fauna/flora which generally provide the best resolution of stratigraphy, thereby making more difficult the precise dating of deeper, mid-Cretaceous North Atlantic sites (Thierstein, 1979).

The increased ocean floor spreading rates during the Cenomanian, together with increased submarine volcanism and hydrothermal activity, as evidenced by the seawater strontium isotope record (Ingram *et al.*, 1994), as well as during the Aptian/Albian (Jones *et al.*, 1994), also resulted not only in an increased sulphidic flux (von Damm *et al.*, 1985), but also in a primary increase in atmospheric CO<sub>2</sub>; this could have caused a greenhouse warming which then resulted in an addition of CO<sub>2</sub> to the atmosphere from the warming ocean (de Boer, 1986). Increased input of this juvenile CO<sub>2</sub> would also raise the acidity of the oceans, making corrosion of calcite more possible, leading to the formation of a shallower CCD (Sheridan, 1986).

Overall, the wide variation in palaeoclimate and palaeoceanographical settings in which certain black shales were distributed infers that no single, simple depositional model

can be used to explain global deposition. For instance, the increased production of WSBW from transgressed low-latitude arid shelf areas (see above) resulting in increased productivity and an intensified OMZ does not explain the apparently synchronous deposition of shales in shallow epicontinental seas at more humid, higher latitudes (*e.g.* Western Interior Seaway). A basic model of periodic stable water stratification (fig. 4.1b) is more applicable for the latter, with major surface water salinity changes affecting the exchange of oxygen between the atmosphere and the bottom water mass, resulting in the development of anoxic bottom waters and enhanced preservation of OM. This is analogous to one explanation for the formation of the periodic Pleistocene Mediterranean sapropels (*e.g.* Rossignol-Strick *et al.*, 1982). Enhanced salinity stratification is a valid argument for the development of anoxic intermediate/deep waters in many areas during OAEs, but as the samples discussed in this chapter concern shale deposition in lower latitude areas where such factors are unlikely to play a large part, this model is generally not discussed. However, large river input into parts of the North Atlantic may have aided stratification to some degree (Ryan and Cita, 1977; see below), and orbitally-induced variations in climate is thought to have affected parts of the low-latitude Cretaceous Tethys (Barron *et al.*, 1985). Combinations of different models can also be applied, for instance during periods of high marine transgressions when the upper part of the midwater OMZ may have become raised onto such shelf areas, leading to the intensification of anoxia within the epicontinental sea basins (Schlanger and Jenkyns, 1976; Fischer and Arthur, 1977). So in different environments, the conditions giving rise to deposition of black shales may have interplayed in different ways but with the oceanic system held at generally low oxygen levels, periodically being tipped in favour of OM preservation (Arthur *et al.*, 1984) with local productivity factors (see above) during OAEs playing a more important role in ancient shale deposition (*e.g.* Waples, 1983).

#### **Cenomanian/Turonian anoxic event**

The Cen/Tur OAE is perhaps the most widely studied as black shales have been found in diverse geological settings, *i.e.* deposited in epicontinental seas, on continental slopes and shelves, on submarine plateaux and in deep, abyssal ocean basins. The strong positive  $\delta^{13}\text{C}$  spike in the biogenic carbonate and in  $\text{C}_{\text{org}}$  is found to correlate with the Cen/Tur boundary in both shelf and pelagic limestones in sections throughout the world (*e.g.* Arthur *et al.*, 1988) and, together with patterns of faunal and floral



change (*e.g.* Jarvis, 1988), is taken as good evidence for the existence of a short, defined period, during which organic carbon, mainly planktonic in origin (Dean *et al.*, 1981; Stein *et al.*, 1986), was substantially withdrawn from the oceanic reservoir (Schlanger *et al.*, 1987). Estimates for the span of peak burial of OM are typically at least 0.5 Myr (Schlanger *et al.*, 1987; Arthur *et al.*, 1987). The fact that sediments rich in OM are not found in every Cen/Tur section implies that the concept of a world ocean undergoing a single, continuous OAE is far from the truth (*e.g.* Waples, 1983). In fact, it is more likely (as discussed earlier) that a variety of depositional models were in place (albeit under conditions favouring oxygen depletion), with basin stagnation (*e.g.* Brumsack and Thürow, 1986; de Graciansky *et al.*, 1984; Stein *et al.*, 1986), expanded and intensified OMZs, possibly associated with upwelling (*e.g.* Arthur *et al.*, 1987), turbiditic redeposition of shelf sediments rich in OM (*e.g.* Degens *et al.*, 1986) and high organic supply resulting from terrestrial run-off (*e.g.* Habib, 1982) all being proposed as explanations for the formation of Cen/Tur black shales. Many authors have contended that during the event, a large eustatic rise in sea level was a major driving force behind the enhanced global deposition of OM-rich shales under differing patterns of oceanic and climatic circulation (Schlanger and Jenkyns, 1976; Fischer and Arthur, 1977; Jenkyns, 1980; Arthur *et al.*, 1987). However, it may also be argued that the ultimate driving force was the increased volcanicity and sea floor spreading which in turn would have resulted in eustasy and increased levels of CO<sub>2</sub> (Jenkyns, 1999). For reviews of the occurrences of Cen/Tur black shales see Salaj (1978), Jenkyns (1980, 1985), Arthur and Premoli-Silva (1982), Thürow *et al.* (1982), van Graas *et al.* (1983), Waples (1983), de Graciansky *et al.* (1984), Herbin *et al.* (1986), Kuhnt *et al.* (1986), Stein *et al.* (1986) and Schlanger *et al.* (1987).

#### *This study*

This chapter involves the analysis of porphyrin distributions in black shale samples deposited during the Cen/Tur OAE. These comprise a suite taken from a variety of outcrops from Central Italy (Umbria) and a section from Tunisia (Oued Bahloul), plus a range of DSDP core samples from the North Atlantic. Due to the large palaeoceanographical differences between these locations and the importance of local effects on the control of OM accumulation, each setting is first discussed in turn. Porphyrin distributions are then discussed and if possible used to shed further light on the chemistry of the marine waters in which the black shales were deposited; specifically, the presence of HMW CAPs (*c.f.* chapter 2) is sought which, together with

extended chain maleimides, would prove the existence of green sulphur bacteria within the palaeo water columns and hence whether or not PZA could have existed during the deposition of black shales in open marine settings.

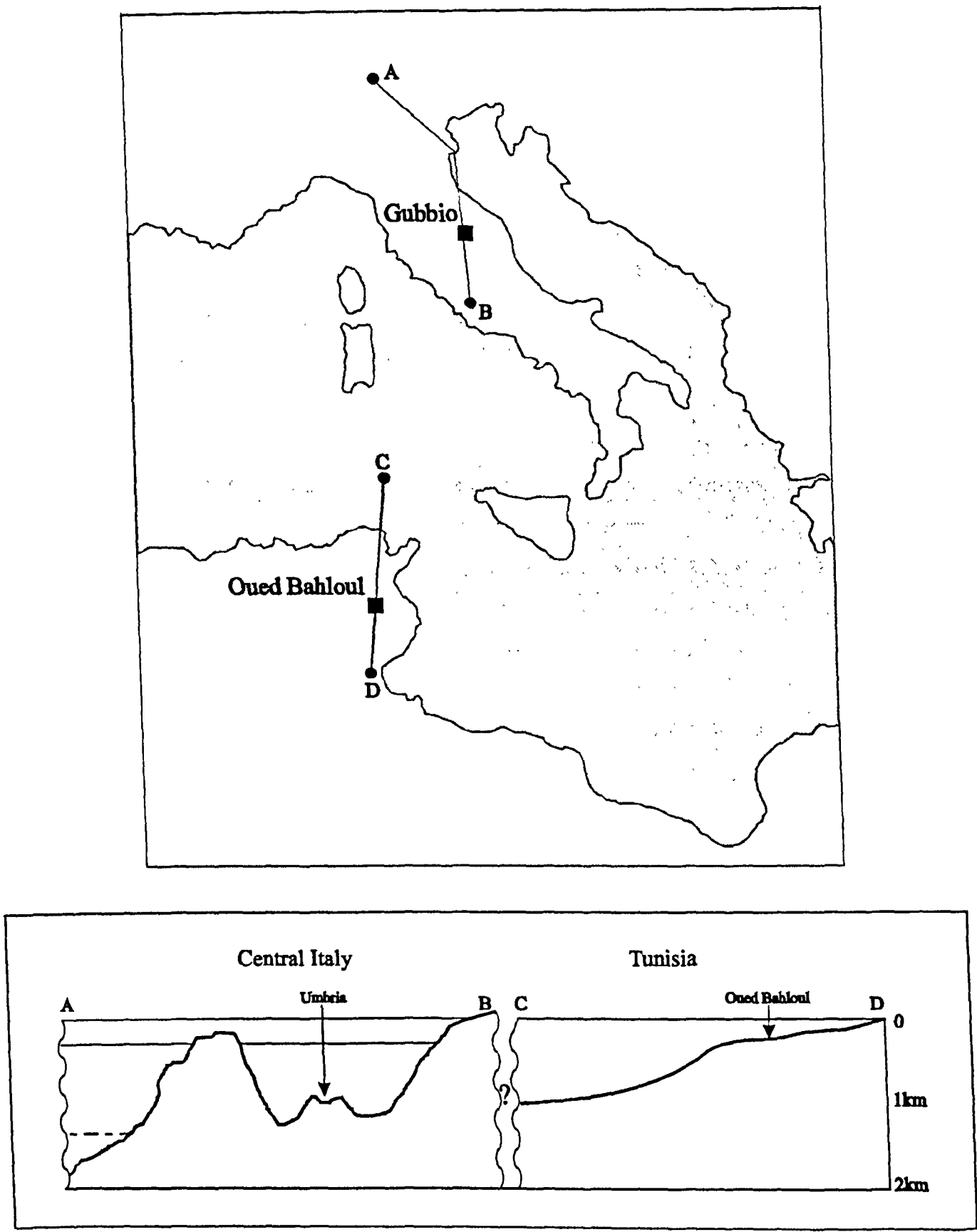
### **Tethyan Margin**

Samples from the Gubbio area of the Umbrian Appenines of Central Italy and from Oued Bahloul in the Tunisian Atlas represent organic-rich shales deposited on the margin of the Tethys Ocean. Fig. 4.2 shows the present day map of the area, together with a schematic cross-section for the two local areas showing approximate palaeo water depths (from Farrimond, 1987).

#### **Central Italy “Livello Bonarelli”**

In the Umbrian Appenines, the Livello Bonarelli divides the Scaglia Bianca Formation (Cenomanian) from the Scaglia Rossa Formation (Conacian-Santonian). These formations are cherty pelagic limestones which are almost totally devoid of OM (<0.2% TOC). The Bonarelli horizon, on the other hand, is a sharply contrasting, relatively thin (60-110 cm) level consisting of dark brown/black laminated shales and grey/brown radiolarian siltstones, highly enriched in OM (up to 31% TOC; Farrimond *et al.*, 1990), and is generally considered to span the Cen/Tur boundary (Arthur and Premoli Silva, 1982). A positive  $\delta^{13}\text{C}_{\text{carb}}$  excursion has been found in the pelagic limestones close to the Bonarelli horizon (Scholle and Arthur, 1980) and a  $\delta^{13}\text{C}_{\text{org}}$  positive excursion peak is noted as occurring entirely within the Bonarelli horizon (Arthur and Premoli-Silva, 1982). Most workers agree that the horizon spans a depositional time period of 350,000-700,000 years (Arthur and Premoli-Silva, 1982; de Boer, 1982). Palaeolatitudes, derived from palaeomagnetic studies in Umbria (Vandenberg *et al.*, 1978), suggest the location of Umbria (part of the Apulian block) to have been between 20° and 30° N during most of the Cretaceous, so the region was probably within a semi-arid subtropical zone with the more northerly parts of the region most sensitive towards astronomically-induced sedimentary cycles (see below; de Boer, 1991). The non-bioturbated, finely laminated black mudstone shales contain abundant OM in the form of thin wisps, which has been found to be largely of marine (algal/bacterial) type II origin with high hydrogen and low oxygen indices. Fish scales and vertebrae are common on the surfaces of the laminae, together with an abundance of pyrite, although the Bonarelli interval itself is almost completely devoid of carbonate (Jenkyns, 1985; Herbin *et al.*, 1986; Schlanger *et al.*, 1987; Farrimond *et al.*, 1990). It

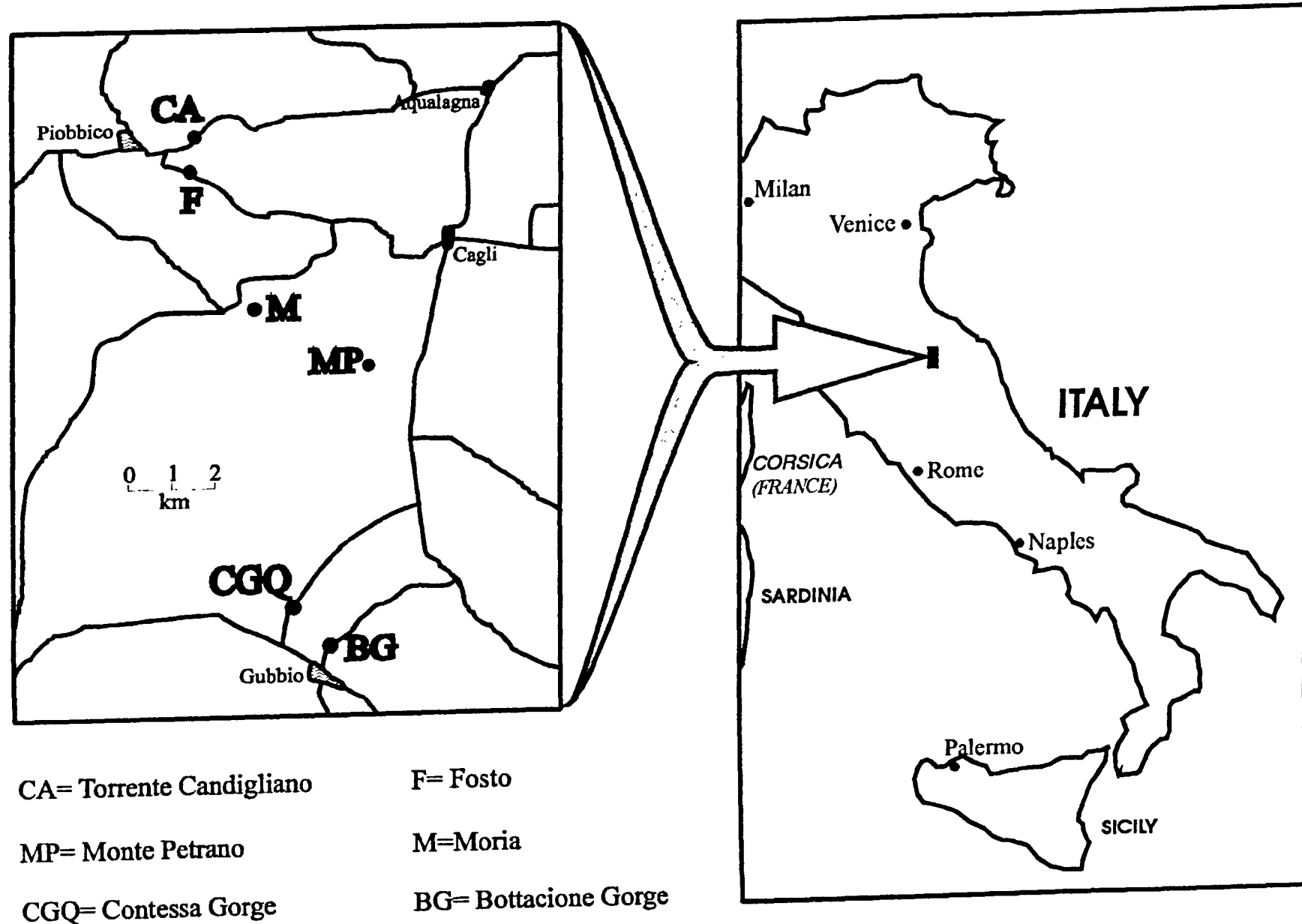
Fig. 4.2. Present day map showing Gubbio and Oued Bahloul localities together with highly schematic cross-sections for the Cen/Tur (Based on Farrimond, 1987)



is not, however, clear whether the carbonate was not produced in the surface waters or was produced and dissolved in caustic bottom waters (Arthur and Premoli-Silva, 1982). The horizon is exposed at different locations around the Gubbio area, north of Perugia (fig. 4.3), and is considered to be the “type section” of the Cen/Tur OAE (Schlanger and Jenkyns, 1976). The OM enrichment can also be traced further north where sediment beds, deposited over a range of palaeodepths, and identical in age and lithology, can be found within the Trento region and the Euganean Hills near Padova (Bosellini *et al.*, 1978; Arthur and Premoli-Silva, 1982).

The enhanced preservation of OM with fine laminations, lack of burrowing and absence of benthic organisms suggests that anoxic conditions existed at and/or above the sea bed. Iron, together with certain trace elements (*e.g.* Zn, V, Cu, Cr and Co), is also in relatively high abundance, being associated with OM or as sulphides, further indicating anoxic conditions (*e.g.* Price, 1976; Brumsack 1980, 1983). Similarities between the characteristics of the Bonarelli sediment and sediments deposited on continental slopes under OMZs in high productivity regions of modern oceans (*e.g.* Calvert, 1964; Berger and Soutar, 1970; Burnett, 1977; Arthur and Premoli-Silva, 1982), together with the widespread occurrence of similar layers throughout the margin of the Tethys, have led some authors to suggest that the Bonarelli represents deposition under anoxic conditions during a relatively brief period of expansion and intensification of a mid-water oxygen-minimum layer (Schlanger and Jenkyns, 1976; Arthur and Premoli-Silva, 1982; Jenkyns, 1985; Farrimond *et al.*, 1990). This is because most of the examples of Cen/Tur sediments with enriched OM come from either sequences exposed on land (such as the Bonarelli) which show evidence of deposition on slopes, or from DSDP sites in relatively shallow (<2500m) water (Schlanger and Jenkyns, 1976); furthermore, the Cen/Tur within deeper ocean sequences is characterised in the majority of locations by slowly deposited oxidised sediment (Arthur and Schlanger, 1979; Arthur and Natland, 1979) and there is a notable lack of black shales in more shallow (<200m) areas (Schlanger *et al.*, 1987). Organic-rich sedimentation of the Bonarelli is in fact thought to have occurred in a basinal environment (Bernoulli and Jenkyns, 1974; Jenkyns, 1980) at a palaeodepth of approximately 1km (fig. 4.2) or less (Arthur and Premoli-Silva, 1982). The high silica and phosphate content, also typical of sediments deposited off Peru and in the Gulf of California, together with the high abundance of radiolaria, suggests high productivity, possibly associated with an unstable, upwelling environment (Arthur and Premoli-Silva, 1982; Leckie, 1984;

Fig. 4.3. Map showing positions of Umbrian Cen/Tur sampling locations.



Farrimond *et al.*, 1990), rather than a stratified, restricted anoxic/dysaerobic basin regime. Abundant algal-derived biomarkers also substantiate this argument (van Graas *et al.*, 1983; Farrimond *et al.*, 1990), at least for the continental margin of the Tethys. However, the causes and conditions giving rise to an expansion of the OMZ are not fully understood. It has been postulated that the eustatic sea level rise at the Cen/Tur boundary would give rise to significant changes in circulation and result in an increased supply of OM (Haq *et al.*, 1987). Such a relatively rapid change in ocean circulation could result in a sudden overturn of intermediate to deep, nutrient-rich waters, stimulating surface productivity. The deep waters were probably old and already oxygen-deficient, rich in CO<sub>2</sub>, nutrients and dissolved silica (Arthur and Premoli-Silva, 1982). This low level of oxygenation during the Albian to Cenomanian resulted from the decreased solubility of oxygen in the warm, saline deep water due to the prevailing warm, equable Cretaceous climate (see earlier), and in other less equatorial regions (*e.g.* Northern epicontinental Tethyan seas) due to periods of intense precipitation and the resulting salinity contrasts between surface and deep waters (Barron *et al.*, 1985). With an intensified, expanded OMZ resulting in large areas of the Tethys in contact with oxygen-depleted water, it is possible that the extent of organic richness of sediments deposited within different areas was controlled by the local intensity of the upwelling (*e.g.* Farrimond *et al.*, 1990). This upwelling may have commenced well before deposition of the Cen/Tur black shales when the oceans were subjected to stirring (Jenkyns, 1985). The thin and meagre sedimentary record that exists prior to the Cen/Tur (and Toarcian) OAE (Wiedenmayer, 1980; Géczy, 1984), indicates that during these times major submarine erosion was taking place, probably due to intense bottom-current activity (Jenkyns, 1985), possibly resulting in an increased nutrient flux to the deep, already oxygen-deficient waters. This in turn may have been controlled, not only by climatic change, but also largely by plate tectonics and continental drift controlling gateways for bottom currents (Berggren and Hollister, 1977). In fact, North (1980) stated that such tectonic movements were important during the mid-Cretaceous in the western Tethys in that they were responsible for creating many local basins which in turn resulted in the local deposition of laminated, TOC-rich sediments. These may be analogous to the basins formed in the southern Californian borderland during the Tertiary (Ingle, 1980), which still result in local prevailing anoxia during the present day (fig 4.1e). It is also apparent that black shales and organic-poor lithologies within the Livello Bonarelli are rhythmically interbedded (de Boer, 1982; Arthur *et al.*, 1987),

suggesting that major cyclical changes took place in levels of oxygenation and/or productivity/upwelling. It has been suggested that these are in turn controlled by climatic signals (Milankovitch cycles) which are amplified responses to changes in the Earth's orbital parameters (Berger 1978, 1988; Fischer, 1981; Einsele and Seilacher, 1982). This fits with De Boer's (1982) estimate that such astronomical cycles could have influenced the global sedimentation at a mean value of approximately 25,000 years, with sedimentary rhythms in the 20 ka to 2 Ma range (de Boer, 1983). Such variations in the shifts of climatic zones are thought to give rise to changes within the ocean of global circulation, eustasy, bottom water formation (Fischer *et al.*, 1990), productivity and oxygen levels (de Boer, 1982; Herbert and Fischer, 1986), supply of terrigenous matter and carbonate dissolution, with an especially high sensitivity to such astronomically-induced processes at latitudes of about 30° (de Boer, 1991), *i.e.* in the areas in between the dry tropics and the moister, more northerly latitudes. In such areas, orbital-related variations in the seasonal amplitude of solar insolation and thus in seasonal climate, may have also produced variations in monsoonal winds and evaporation/precipitation patterns (as modelled by Barron and Washington, 1982b; Barron *et al.*, 1985) which would have consequently resulted in changes in the intensity and location of in shelf area production of WSBW (Thierstein, 1989), hence giving rise to the cyclic changes in the levels of bottom water anoxicity and its rate of formation (Herbert and Fischer, 1986), with palaeo-coastal geography effecting important periodic changes on regional and local intensities of upwelling and nutrient supply (Prell, 1984).

In general, variations in sea-level, oxygen levels and intensity of upwelling, both in time and space, may well have been responsible for the cyclical changes in the extent of the OMZ, thereby resulting also in the lateral changes seen within the Bonarelli deposits of the Umbrian basin (and elsewhere during the Tethyan Cen/Tur OAE). Reconstructions of palaeoenvironments are considerably aided by information regarding the intensity and duration of the oxygen depleted conditions. However, previous work has shown that it is difficult to distinguish between sediments that were deposited in dysaerobic, anoxic or euxinic (anoxic plus free H<sub>2</sub>S) environments. Levels of sulphur content compared with TOC can be informative in this respect (*e.g.* Leventhal, 1983; Raiswell and Berner, 1985), where plots of sulphur vs. TOC fall into the classification fields of "non-marine fresh water", "normal marine" and "euxinic". However, the sulphur content of the Bonarelli is generally low (<0.7%) with the

exception of samples very high (>15%) in TOC. As a result, the majority of the previously analysed samples with moderate to high TOC (3-15%) and low sulphur content (0-1%) have unusually high C/S ratios and fall into the classification field “non-marine fresh water” although they are obviously marine, as opposed to the “normal marine” trend where sulphur content is supposedly proportional to TOC. The samples high in TOC do have higher levels of sulphur, but do not, however, conform to Raiswell and Berners “euxinic” classification, as sulphur content is still too low (Farrimond *et al.*, 1990). This reduced sulphur content, possibly resulting from weathering or diagenetic mobilisation of pyrite, or from competition for sulphur uptake from iron (*e.g.* Gibson, 1985), thus results in little firm evidence regarding the extent of oxygen depletion during deposition of the Bonarelli sediments (Farrimond, 1987). The study of porphyrin distributions within the Bonarelli sediments could perhaps shed further light on the redox state of the palaeo water column.

#### **Tunisia “Oued Bahloul”**

The Bahloul formation (fig. 4.2) is a much larger section, comprising 30 m of cyclical, laminated dark grey/brown/black shales interbedded with bioturbated brown/grey shales (Schlanger *et al.*, 1987). The laminated units at Oued Bahloul contain abundant fish scales and skeletal debris together with a common occurrence of pyrite nodules and, unlike the Bonarelli, carbonate contents are high (60-80% CaCO<sub>3</sub>; Farrimond *et al.*, 1990). The sediments also have generally high TOC content (up to 7.1%) and largely marine-derived type II OM (Herbin *et al.*, 1986; Barrett *et al.*, 1997). These features are again characteristic of deposition under anoxic conditions, although the rhythmic, lithological variations suggest that intermittently, oxygenation took place, allowing the resurgence of benthic activity on the sea floor. Depositional conditions were similar in many respects to the Bonarelli, with an expanded and intensified OMZ being probably the best model to explain the preservation of black shales high in OM. In fact, significant upwelling was predicted for this region by the model of Barron (Arthur *et al.*, 1987), and a  $\delta^{13}\text{C}_{\text{org}}$  excursion of 3-4‰ occurs within the section (Schlanger and Jenkyns, 1976; Arthur *et al.*, 1988) further evidencing high organic burial as a result of increased levels of productivity. The sediments of the Tunisian shelf were deposited in a shallower region than the Bonarelli (fig. 4.2), so that with changes in upwelling intensity and variations in sea level causing cyclical changes in the vertical extent of the OMZ, oxygen-deficient conditions were more intermittent



during the Cen/Tur OAE than in the Umbrian region. Previous work by Farrimond *et al.* (1990) found evidence (hopanes and hopenes) for an important bacterial contribution to the OM, particularly in the lower part of the section, with the presence in some samples of 17 $\alpha$ (H),18 $\alpha$ (H),21 $\beta$ (H)-28,30-bisnorhopane, believed to be associated with highly reducing environments (Grantham *et al.*, 1980) and/or bacterial mats in shallow water in upwelling areas (Kats and Elrod, 1983).

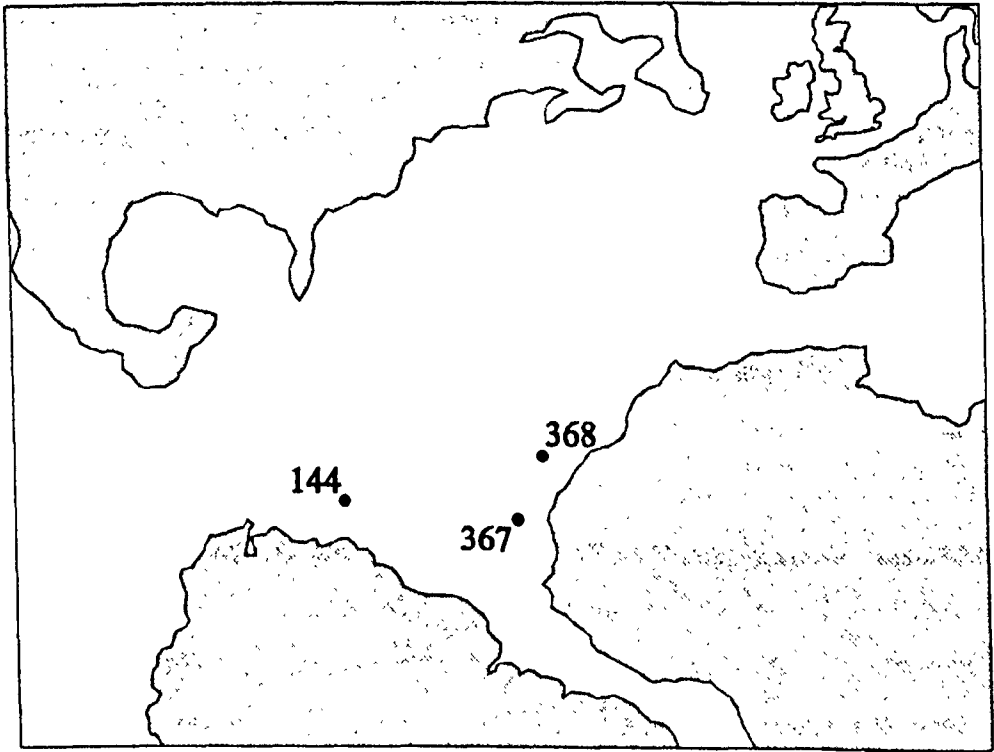
### North Atlantic

Fig. 4.4 shows a palaeoceanographical map of the North Atlantic Ocean during Cen/Tur times and indicates the locations of the three DSDP sites from which samples were taken. All three are in the southern North Atlantic basins with the Demerara Rise (site 144; leg 14; core 4) to the west of the mid-oceanic ridge and the Cape Verde Basin (sites 367; leg 41; core 18 and 368; leg 41; core 63) to the east. Furthermore, the sites are abyssal with sites 144 and 367/8 occurring at palaeo water depths of 3000 and 3700m respectively (Chénet and Francheteau, 1979). Although TOCs of Cen/Tur sediments are high, bulk accumulation rates were generally low throughout the Atlantic, due presumably to a shallow CCD (de Graciansky *et al.*, 1984; Arthur and Dean, 1986) and the widespread epicontinental seas acting as sediment traps for terrigenous OM (Ehrmann and Thiede, 1985). This resulted in low accumulation rates of organic carbon, although with highest rates occurring in low latitude regions, rates of OM were higher in the southern basins (Kuhnt *et al.*, 1990) and were also an order of magnitude higher at sites 367/368 in the east than at site 144 in the west (Stein *et al.*, 1986) and also considerably higher than those in the Livello Bonarelli.

A number of different models have been proposed for the formation of organic-rich shales in the Cretaceous North Atlantic. Extensive anoxicity of bottom waters has been put forward by some authors as enabling the enhanced preservation of OM throughout the Cretaceous (*e.g.* Arthur and Schlanger, 1979; Jenkyns, 1980; Tissot *et al.*, 1980; Summerhays and Masran, 1983; Bralower and Thierstein, 1984; Stein *et al.*, 1986), in particular in the southern North Atlantic; here the OAE seems to have begun earlier than in most other locations (Arthur *et al.*, 1987), especially at site 367 where there is almost continuous black shale deposition from Aptian to Cenomanian (Shipboard Scientific Party, 1977a). Indeed, the deposition of carbon-rich beds over longer time periods in the more equatorial regions (*e.g.* Tissot *et al.*, 1980), together with the observation that deposition of shales at 367/368 began before the  $\delta^{13}\text{C}$  excursion

**Fig. 4.4. Palaeogeography of North Atlantic Ocean during Cen/Tur times with circles indicating positions of investigated sites. Numbers refer to DSDP sites**

Taken from Sinninghe Damsté and Koster (1998)



(Arthur *et al.*, 1988; Herbin *et al.*, 1986), suggests that local mechanisms contributed significantly to the overall enrichment, especially as these organic-rich rocks accumulated slowly (see above). On the other hand, the occasional occurrence of burrowed, oxidised sediments above and below some other black shale intervals argues against the uninterrupted continuity of this high level of oxygen depletion over the entire basin (Waples, 1983), with repeated alterations of stagnant and oxic conditions being invoked by others to explain such occurrences (Stow and Dean, 1984). De Graciansky *et al.* (1986) suggests that during the Cenomanian, anoxia was permanent in the Cape Verde Basin (site 367), but episodic elsewhere. Although the black shales from these DSDP sites are extensively laminated, this is evidence only for anoxic bottom waters and not for an entirely anoxic deep water column. For instance, in parts of the modern ocean, degradation of OM at the sediment water interface results in the formation of bottom water anoxicity (see earlier model) allowing the preservation of laminae (Summerhays, 1983; Calvert, 1983, 1987). It is also possible for laminations to be preserved in sediments which have been redeposited as turbidites (see below). An intensified and expanded OMZ has also been proposed to have formed due to enhanced degradation of OM perhaps combined with sluggish circulation (*e.g.* Demaison and Moore, 1980; Waples, 1983), causing black shales to accumulate where this zone impinges upon continental shelves. Indeed, Parish and Curtis (1982) noted a general agreement between theoretically modelled palaeo upwelling areas and areas containing Cretaceous black shale deposits. The higher sediment accumulation rates in the eastern North Atlantic basins, at site 367 in particular (Stein *et al.*, 1986), seem to confirm this, although other authors still maintain that the overall productivity and rate of sediment accumulation of much of the North Atlantic was relatively low (Waples, 1983; Bralower and Thierstein, 1984), hence arguing that restriction of bottom water circulation was perhaps a more important factor than high input of OM to the water column (*e.g.* Lancelot *et al.*, 1972). Mid-water OMZs do not fully explain the deposition and preservation of black shales rich in OM in the abyssal regions of the North Atlantic such as the sites 144, 367 and 368 studied here, unless the productivity was so high that the OMZ intensified and expanded to such an extent that it reached the abyssal plain. It has been proposed that some of the OM may have reached the deep ocean sites within turbidity flows (Dean and Gardener, 1982; Degens *et al.*, 1986; Arthur and Dean, 1986), although the distal turbidites present have much lower TOC values and high carbonate contents (de Graciansky *et al.*, 1986). Rapid burial of

sediments results in better preservation of OM, so that black shales forming on continental slopes or shelves may be redeposited rapidly and preserved even in oxygenated deep basins. Such processes have been proposed for the formation of turbiditic black shales at sites 530 and 534 in the Angola (Dean *et al.*, 1984) and Blake-Bahama (Robertson and Bliefnick, 1983) basins respectively. However, given the extensive nature of the OM preservation in these abyssal sites (TOC 6-26%) it seems likely that various different circulatory factors may have combined and resulted in the intensification of oxygen depleted conditions at intermediate and deep water depths within the southern North Atlantic basins. This could then have given rise to severely oxygen depleted conditions within much of the southern part of the North Atlantic, with productivity signals resulting from upwelling, together with perhaps an increased input of terrestrially derived nutrients at times from extensive river inflow (Ryan and Cita, 1977; Jenkyns, 1980), resulting in OM-enriched abyssal black shales, without the need for turbiditic redeposition. So, although each black shale deposit is probably initiated by a group of global or ocean-wide conditions, the individual characteristics of shales at each site would be determined by local or regional factors (*e.g.* Meyers *et al.*, 1986). The extremes in depositional conditions at sites 367 and 368 are exemplified in particular by the anomalously high TOC (up to 50%) and  $\delta^{13}\text{C}_{\text{org}}$  excursion of 5.5-6‰ (2‰ higher than at any other Cen/Tur site) attributed to the upwelling-induced high productivities resulting in lower  $p\text{CO}_2$  (Arthur *et al.*, 1988).

The nature and characteristics of the oceanic circulation patterns that existed in the North Atlantic are therefore important when attempting to understand why the large majority of the southern North Atlantic may have been anoxic or at least extensively depleted in oxygen during much of the mid-Cretaceous and, in particular, during the Cen/Tur boundary event that gave rise to the deposition of abyssal black shales at DSDP sites 144, 367 and 368.

### **Circulation of the mid-Cretaceous Atlantic**

The development of black shales throughout the Cretaceous was determined by the existence of a young, but already deep Atlantic Ocean. By the mid-Cretaceous, the North Atlantic had reached about half its present width, and a central gyre had probably formed, similar to those in the north and south hemispheres of the Pacific, causing upwelling along the eastern margins (Roth, 1987). The ocean seems to have had a poor connection to other ocean basins, with the absence of any major connections to the

more northerly (boreal) seas making the contribution of high latitude, cold waters to the Atlantic small. Without the thermohaline circulation seen in the present day Atlantic, the vertical circulation was probably driven by the sinking of the WSBW (see earlier). Such water was produced in tropical/sub-tropical marginal evaporitic and reef-bordered basins in northern South America, the platform regions of the Gulf of Mexico, Florida and the Caribbean, the western borders of the Tethys and southern Europe (Roth, 1978), hence fuelling the oxygen-deficiency and increased salinity of the intermediate/deep waters layers (Brass *et al.*, 1982; Wilde and Berry, 1982; Saltzman and Barron, 1982). Another important factor concerns the extensive oxygen-minimum layer that existed at intermediate depths within the eastern borders of the Pacific Ocean. The open connection through the Caribbean and across the Central American Sill was several hundred metres deep, allowing interchange of surface waters between the two ocean basins. However, with the high eustatic sea level, estuarine circulation (Berger, 1970) may have existed in the North Atlantic with oxygen-depleted, nutrient-rich intermediate water from the Pacific flowing into the Atlantic, whilst surface water (possibly low salinity due to the high river input; Ryan and Cita, 1977; Jenkyns, 1980) flowed back out to the Pacific. Hence, in the absence of vigorous vertical circulation, this input of oxygen-deficient water from the Pacific would strengthen the already strong levels of nutrients and oxygen depletion within the North Atlantic (Thierstein and Berger, 1978; Summerhays and Masran, 1983; Summerhays, 1986). A reduction in this influx during low sea-level stands would help explain the lowered flux of WSBW and hence a return to more oxidising conditions during such time periods. It is thought that during the Cenomanian, with the separation of Africa from South America and the opening of the South Atlantic (Sclater *et al.*, 1977; Thiede, 1979; Koutsoukos, 1987; Koutsoukos and Merrick, 1986; Dias-Brito, 1987), a massive injection of highly saline, old nutrient-rich and oxygen-deficient water would have spread northwards from the northern South Atlantic (Thierstein and Berger, 1978; Thiede, 1979). Laminated, organic-rich (TOC up to 27%) sediments from the Cenomanian-Santonian Brazilian marginal basins have been found to contain high concentrations of metalloporphyrins (with vanadyl porphyrins dominating in samples with higher sulphur contents), low Pr/Ph, and an abundance of 28,30-bisnorhopane and 25,28,30-trisnorhopane (thought to be indicative of anoxic depositional conditions; *e.g.* Curiale *et al.*, 1985), thereby evidencing the existence of anoxic, nutrient-rich conditions in this part of the northern South Atlantic (Mello *et al.*, 1989). These deep waters would, in turn, displace surface-

ward the deep nutrient-rich oxygen-deficient water already present for much of the mid-Cretaceous in the North Atlantic. This would result not only in widespread oxygen-depletion throughout much of the deep and intermediate waters of the southern North Atlantic, but also in upwelling of old, nutrient-rich water into the surface waters, resulting in a huge productivity signal and consequent exceptional preservation of OM during the Cen/Tur (Thierstein and Berger, 1978; Tucholke and Vogt, 1979; Summerhays, 1981; Roth, 1987). Such an influx from the northern South Atlantic would presumably affect the eastern sub-basin of the southern North Atlantic more than the west, especially considering the possible affect the mid-oceanic ridge would have on deep water circulation between the east and west (Summerhays, 1986). Indeed, many authors have indeed postulated a restricted circulation, especially in these deep and intermediate water masses (*e.g.* Schlanger and Jenkyns, 1976; Berggren and Hollister, 1977; Thiede and van Andel, 1977; Arthur, 1979), a situation that led to the generation of specific local and regional supplies of terrigenous (*i.e.* detrital clay minerals) materials as evidenced by the characteristic mineralogical developments of each DSDP drill site (Chamley and Roberts, 1982). The highest productivity would thus more probably be expected in regions such as along continental margins or in open ocean divergences where upwelling took place, but with the signal being distributed basin-wide in turbidity currents and maintained under the wholesale conditions of preservation.

### **Supply of organic matter**

Rates of accumulation of OM, together with TOC values, have been shown to be higher in the east than the west, inferring perhaps that rates of upwelling were indeed higher off northwest Africa than off eastern North America, although models have predicted upwelling to have occurred in both regions (Parrish and Curtis, 1982). There may also have been a greater input of terrigenous supply in some areas (Parrish *et al.*, 1982; Summerhays, 1986), with some authors proposing that there was indeed an abundant supply of terrestrial plant material from the American continent to the western North Atlantic during the mid-Cretaceous as a whole (Jenkyns, 1980; Cool, 1982; Habib, 1982; Robertson and Bliefnick, 1983). Others, however, argue that the enrichment of OM is associated primarily with marine OM (Deroo *et al.*, 1977; Summerhays, 1981, 1986; Simoneit and Stuermer, 1982; Waples (1983). The Cen/Tur boundary black shale event is very pronounced indeed in the upper part of core 18 at site 367, with *ca.* 6 m of shales having an average TOC of 30% (Herbin *et al.*, 1986). OM preserved at site 367

has been shown to contain fatty acids and *n*-alkanes of terrigenous origin (Simoneit and Stuermer, 1982) although Deroo *et al.* (1977); Herbin and Deroo (1982), Rullkötter *et al.*, 1982 and Hebin *et al.* (1986) showed that the Cenomanian at the same site is dominated by type II OM assumed to be almost entirely marine, and indigenous (autochthonous), as also with site 144 (Simoneit, 1975, 1978, 1980, Simoneit and Stuermer, 1982).

Carbon-rich samples have high hydrogen (*ca.* 800) and low oxygen indices, hence corresponding to excellent potential oil source rocks, although 368-63, being close to a intrusive volcanic sill, corresponds to the beginning of the principal zone of oil formation (Deroo *et al.*, 1977). They are also enriched in the trace metals Ag, Cd, Cu, Mo, Ni, Sb, V and Zn (Brumsack, 1986), similar to the enrichments recorded in the Black Sea sediments, thought to be precipitated as metal sulphides (*e.g.* Brewer and Spencer, 1974) from euxinic deep waters (Brumsack, 1980, 1986). It is interesting to note that such special trace metal chemistry is different from other black shales such as those in recent upwelling sediments (Brumsack, 1986) from the Gulf of California or in the German Posidonia Shale (Chapter 5). The Pr/Ph ratio from the site 367 sample analysed in this study is 0.3, and sulphur values are also high (*ca.* 2-8% for the samples analysed from the three sites) further indicating strong anoxic conditions (Didyk *et al.*, 1978). Sediments drilled at site 144 from core 4 were found to contain noticeable amounts of H<sub>2</sub>S (Shipboard Scientific Party, 1972), and were interpreted at the time as being deposited in an environment that alternated throughout the Cretaceous between aerobic and anaerobic, though generally favourable for the preservation of OM. The majority of sediments from these sites generally show an absence of benthic organisms and burrows, with a lack of bioturbation resulting in 85% lamination at site 367 (Bralower and Thierstein, 1987). Thus, although anoxic bottom water conditions are apparent, analysis of the porphyrins present at all three southern North Atlantic DSDP sites, together with maleimides (both free and from oxidation of the tetrapyrrole pigments; Crawford personal communication) should indicate whether or not conditions of anoxia were prevalent enough in the rest of the water column to reach the photic zone at these deep ocean sites, thereby allowing the growth of the green sulphur bacteria within the Cen/Tur North Atlantic Ocean.

## **RESULTS – LIVELLO BONARELLI**

### **General**

Results presented in this section concern the porphyrin distributions obtained from a suite of 31 black shale samples, selected from six locations in Gubbio and the surrounding area of the Umbrian Appenines (Fig. 4.3) during June 1996 under the supervision of Dr. Hugh Jenkyns. Five of the sites had been sampled previously by Farrimond (1987), from which small amounts of sediment remained from four samples, allowing comparison. Samples were generally taken from as deep as possible within outcrops, so as to minimise the effects of weathering. Each was submitted for TOC and S analysis (table 4.1), with CaCO<sub>3</sub> analysis showing negligible carbonate in all Bonarelli samples (results not shown).

Location	Sample	TOC (%)	S (%)
Monte Petrano	MP0	11.2	0.6
	MP1	18.3	2.5
	MP2	21.9	3.1
	MP3	20.8	2.5
	MP4	10.9	1.2
	MP5	16.8	1.9
	MP6	17.2	1.7
Moria	MP7	2.3	1.2
	M15	2.9	0.2
	M3	15.1	1.1
	M5	17.6	2.4
	M7	16.4	1.6
	M14	3.2	0.4
	M16	0.3	2.1
Contessa Gorge	M11	3.2	0.5
	CGQ1	12.4	1.3
	CGQ2	4.4	0.5
	CGQ3	16.3	2.9
	CGQ4	5.7	1.0
	CGQ5	0.2	0.3
Bottacione Gorge	CG†	19.5	2.1
	BG1	13.4	0.9



	BG2	7.7	0.5
	BG3	9.0	0.5
	BG4	6.8	0.3
	GU1†	4.8	0.2
Fosto	FOS1	25.3	5.8
	FOS2	29.7	4.9
	FOS3	21.1	2.9
	FOS4	15.3	1.9
	FOS5	22.4	4.7
	F1†	31.2	4.0
Gorgo A Cerbara	GCLB	18.5	2.1
	CA†	16.1	1.5

Table 4.1 TOC and Sulphur data for Cen/Tur Livello Bonarelli samples

† = Collected by Farrimond (1987)

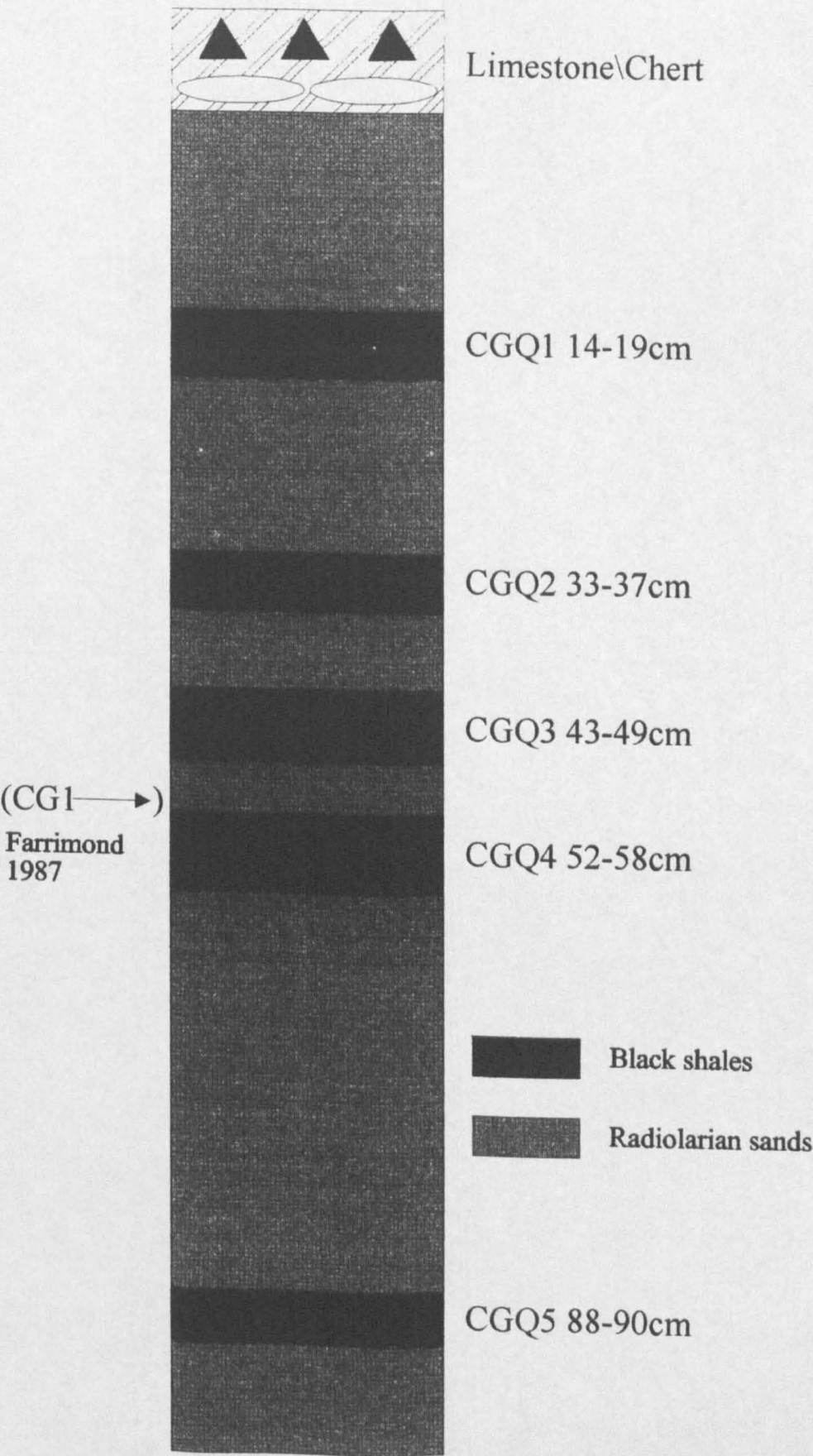
Results are presented first for samples from the Contessa Gorge quarry (CGQ) and subsequently for the other sites (fig. 4.3). The Farrimond (1987) samples obtained from radiolarian sand interbeds, showed very low levels of TOC, and the total organic extracts (TOEs) were typically light coloured and contained no traces of pigments, as evidenced by Uv/vis analysis. Hence, the later sampling concentrated exclusively on the layers of black shales. Modified porphyrin maturity parameters (MPMPs) were also calculated for each sample, being based on the parameters of Sundararaman (1992) and Huseby (1996). Here,  $MPMP = C_{28}A / (C_{28}A + C_{32}D)$ , where  $C_{28}A$  = sum of peak areas of all  $C_{28}$  Aetio components and  $C_{32}D$  = peak area of DPEP. These results are tabulated in Appendix A.

### **Contessa Gorge Quarry**

#### *Porphyrin distributions*

The Livello Bonarelli is exposed in the extensive Contessa Gorge quarry which runs parallel to the roadside, a few km outside Gubbio. It can be seen from some distance as a black “line”, ca. 1 metre thick, running through an otherwise cream-coloured limestone exposure. Samples were taken from the end of the quarry, where there is a good exposure close to ground level. Fig. 4.5 shows the lithological section and details the points at which the five samples (CGQ1-5; between 200 and 400g) were taken.

Fig. 4.5. Lithological section of the Cen/Tur Livello Bonarelli at the Contesa Gorge site showing the stratigraphic positions of the studied samples



Also shown is the approximate stratigraphic position of sample CG1, examined by Farrimond (1987) from a road-side exposure close-by. TOC ranges from 5.7 to 16.3%, with sulphur between 0.25 and 1.25% and negligible carbonate (table 4.1).

The demetallated vanadyl porphyrin fraction from CGQ1 was found to contain a range of components, mainly of the CAP type but also with a significant presence of aetios (fig 4.6). Significant peaks, identified from the spectra, include C<sub>29</sub>-C<sub>33</sub> CAPs (*m/z* 435, 449, 463, 477 and 491), with DPEP (1) being the most abundant, and aetio types within the range C<sub>28</sub>-C<sub>32</sub> (*m/z* 423, 437, 451, 465 and 479) eluting earlier than the CAPs.

MPMPs (Appendix A) from 0 to 0.3, confirming the low maturity assigned by Farrimond *et al.* (1990), although the values for the ex-nickel porphyrins are higher than for the ex-vanadyls.

### HMW CAPs

A range of HMW CAPs in the ex-vanadyls of CGQ1 elute in the expected HMW region (*c.f.* Chapter 2). The partial mass chromatograms (34 to 44 min) for the C<sub>32</sub> to C<sub>35</sub> CAPs and appropriate spectra are shown in fig 4.7a. Coinjection (figs 4.7b,c) with the two C<sub>34</sub> standards (33 and 34b respectively) derived from the bacteriochls *d*, clearly shows enhancement of peak *c* (*m/z* 505 chromatogram). However, the major C<sub>34</sub> CAP peak *b* coincides with the standard (46a,b) not derived from bacteriochls (fig 4.8a; *c.f.* chapter 2). The *m/z* 519 chromatograms before (4.7a) and after (4.8b) coinjection of the *i*-Bu, Et C<sub>35</sub> CAP show enhancement of the front shoulder of the main C<sub>35</sub> peak, indicating that although this component is present by retention time comparison, it is not the major C<sub>35</sub> CAP component (unlike Kupferschiefer, chapter 2). Coinjection of the Et, Et C<sub>33</sub> CAP (34a) also shows the presence of a C<sub>33</sub> CAP in CGQ1, comparable in retention time to this bacteriochl *d*-derived component (fig 4.8c). Hence, although there are notable differences in the distribution compared with the Kupferschiefer, there are, by retention time comparisons and coinjection studies, HMW CAPs present in the CGQ1 sample of the Livello Bonarelli that are derived from the bacteriochls *d* present in the green strains of the green sulphur bacteria. Furthermore, the free maleimides of the same sample revealed the presence of Me *i*-Bu maleimide, a specific biomarker of Chlorobiaceae (Crawford, personal communication), thereby confirming the existence of PZA during deposition of CGQ1. Interestingly, the same sample also contains a series of C<sub>14</sub>-C<sub>18</sub> monoaromatic 2,3,6-substituted isoprenoids (results not shown), possibly derived from the green strains of Chlorobiaceae, but no traces of diaryl isoprenoids derived from isorenieratene of the brown strains.

Fig 4.6. Partial HPLC-MS base peak chromatogram of demetallated vanadyl fraction with carbon numbers of major peaks labelled.

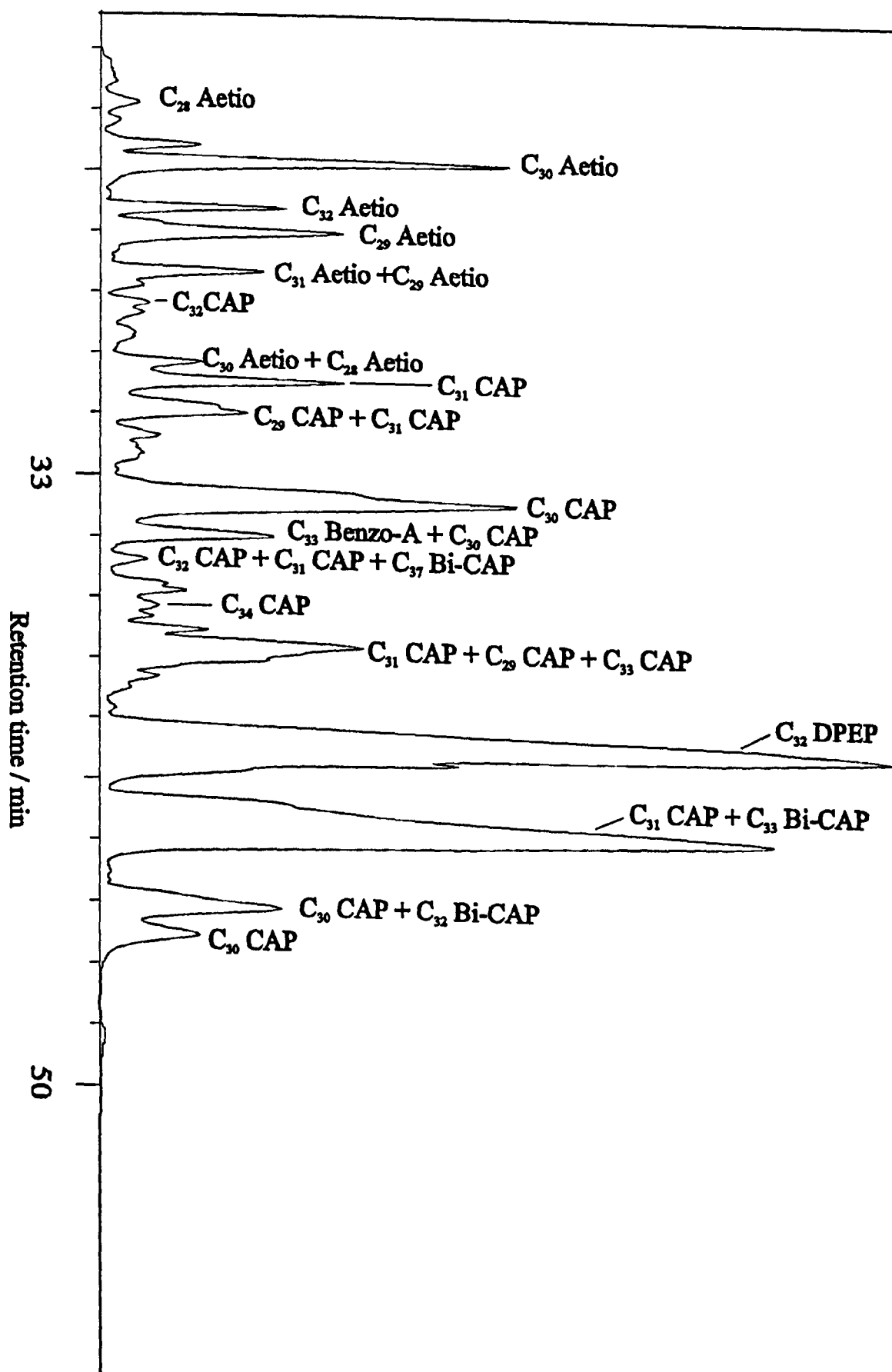


Figure 4.7 Partial mass chromatograms for HMW components of ex-vanadyl fraction

(a) before co-injection of standards (b) after co-injection of  $C_{34}$  *n*-Pr Et (34b) and (c) of  $C_{34}$  *i*-Bu Me (33) standards

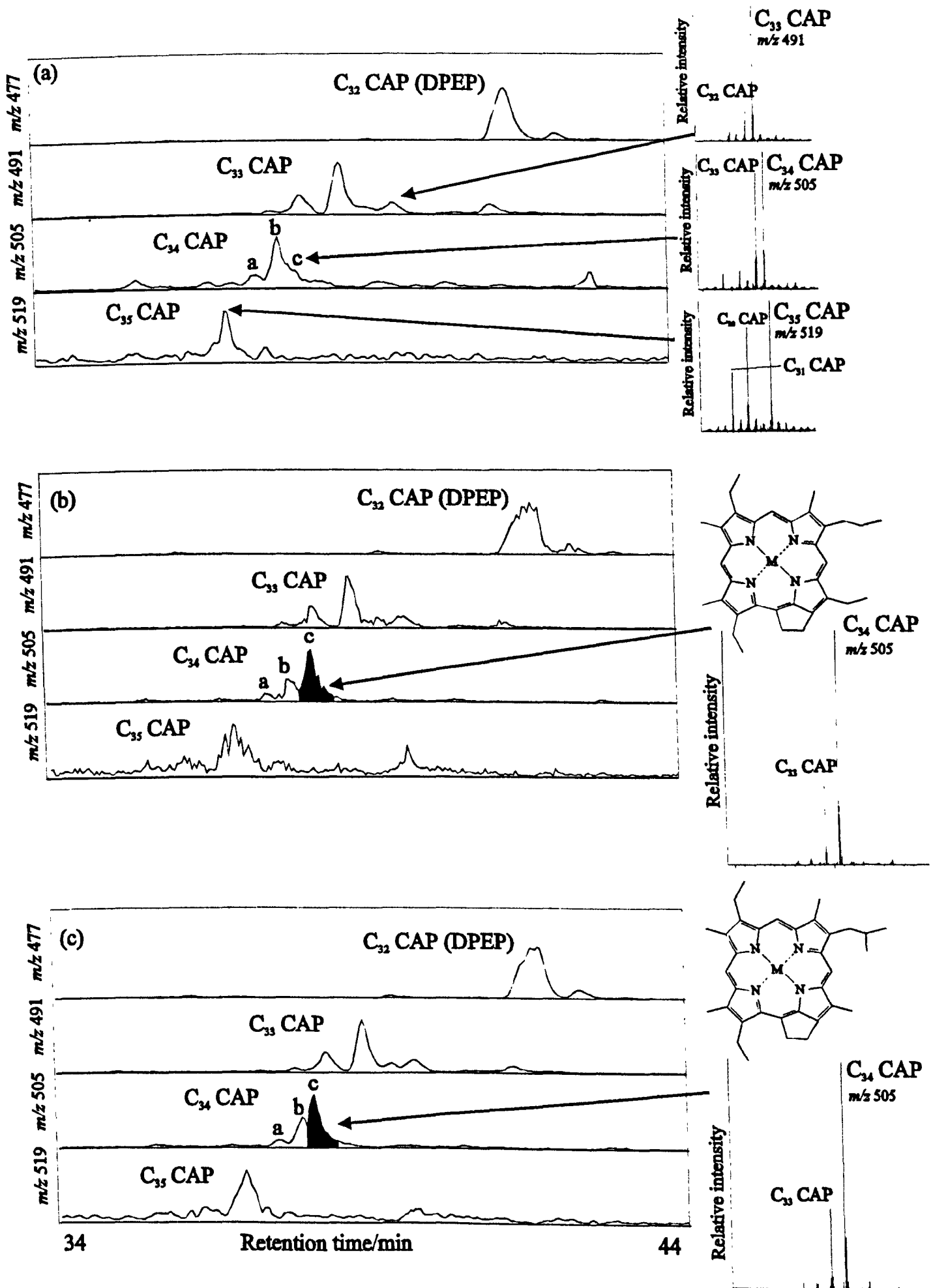


Figure 4.8 Partial mass chromatogram for HMW components of ex-vanadyl fraction after co-injection of

(a)  $C_{34}$  non-PZA (46a,b) standard (b)  $C_{35}$  *i*-Bu Et (34c) standard and (c)  $C_{33}$  Et Et (34a) standard

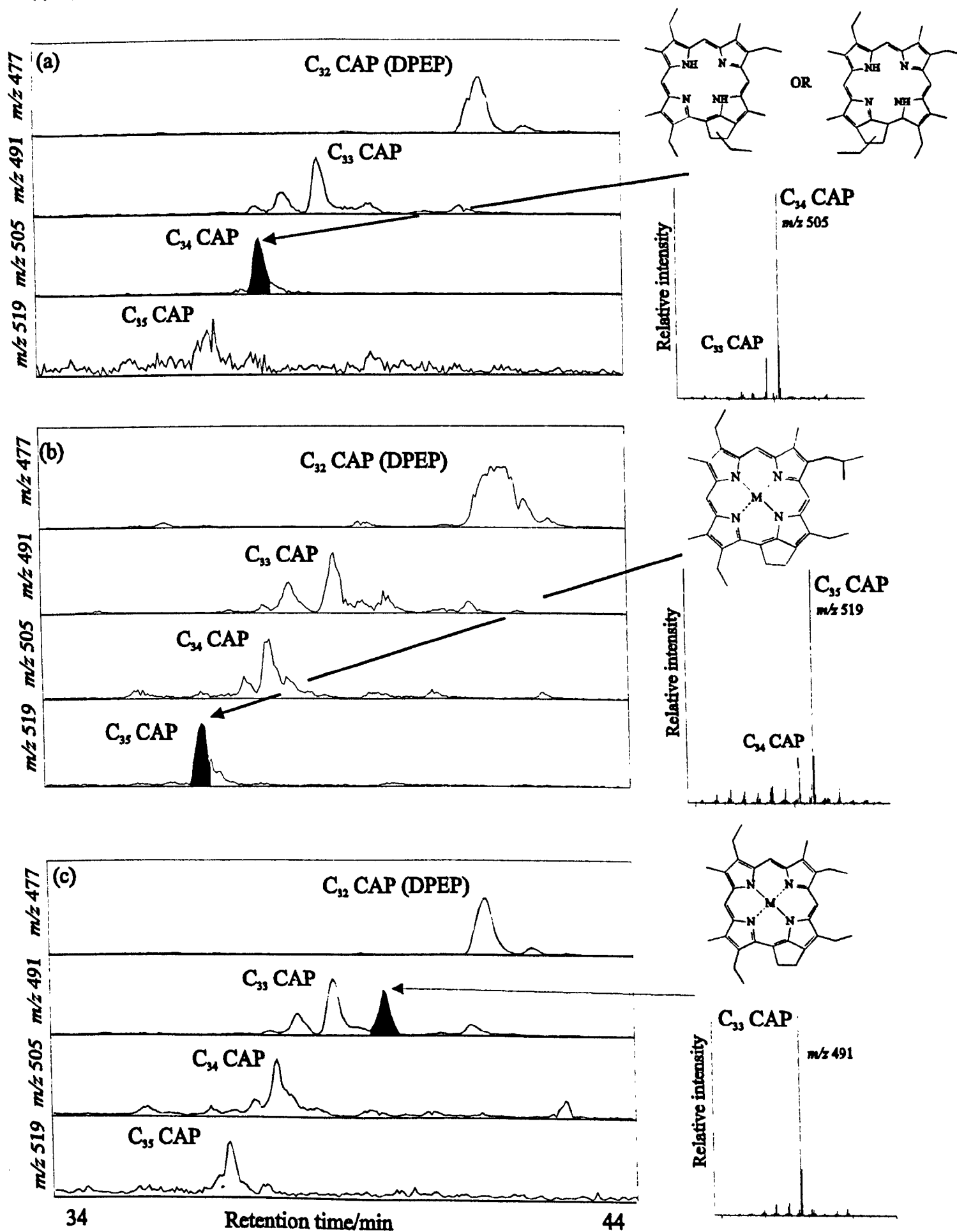


Fig 4.9 summarises the coinjection results, with shaded peaks indicating components in the porphyrin distribution with identical retention times. Due to the small amounts of standards available, all further analysis were immediately preceded by a run of the ex-iron fraction of the bulk Kupferschiefer sample (chapter 2), as this has a higher proportion of bacteriochl *d*-derived CAP components than CGQ1. Samples CGQ2, 3 and 4 were analysed in this way. CGQ2 is highly siliceous, with most of the OM trapped in the silica (Jenkyns, personal communication) and CGQ5 is mostly radiolarian sand; consequently no traces of metallo porphyrins were found. Distributions similar to CGQ1 were found in CGQ3 and 4 for the ex-vanadyl fraction. The appropriate mass chromatograms are shown in fig 4.10, with shaded peaks identifying components with the same retention times as the bacteriochl *d*-derived components. Such peaks are in fact only apparent in CGQ3 (fig 4.10b) at levels just above the imposed limit of detection (chapter 2), as evidenced by the mass spectra of the individual peaks (fig 4.10). It therefore seems that bacteriochl *d*-derived CAPs are present at very minor levels indeed in CGQ3, lower than CGQ1 and that no CAPs indicative of Chlorobiaceae are apparent in the lowermost sample, CGQ4 (fig 4.10c). In fact, no Me *i*-Bu maleimide was found in CGQ3 or CGQ4 (Crawford, personal communication). Other C<sub>34</sub> and C<sub>35</sub> CAPs are also apparent in CGQ1 and 3, eluting both before and after the bacteriochl *d*-derived components (fig 4.10a,b). It is possible that some of these components may be derived from the bacteriochls *c* of the green Chlorobiaceae (*c.f.* chapters 2 and 3).

Figs 4.11a and b show the respective mass chromatograms of the CAPs from the demetallated nickel and vanadyl porphyrins from the CG sample collected by Farrimond (1987). Although this sample was from a different exposure, albeit close to the quarry, the level is thought to correspond to that of CGQ4 (Jenkyns, personal communication). These results clearly show no C<sub>34</sub> or C<sub>35</sub> CAP components eluting with the retention times of the HMW CAP standards, further indicating that there is no evidence for Chlorobiaceae in the water column during deposition of shale deposited 50-60cm below the top of the section (fig 4.5).

The chromatograms for the demetallated nickel porphyrins of CGQ1 are also included (fig 4.11c), showing that, in this case, the CAP distributions are similar with peaks corresponding in retention time to the bacteriochl *d*-derived standards.

In summary, the lack of maleimide confirmation for CGQ3, together with the lack of porphyrin and maleimide data for CGQ2 and CGQ4, provides no evidence for the

Fig. 4.9 Partial mass chromatograms for CAPs of CGQ1, with shaded peaks showing components co-eluting with porphyrins derived from bacteriochl *d* series

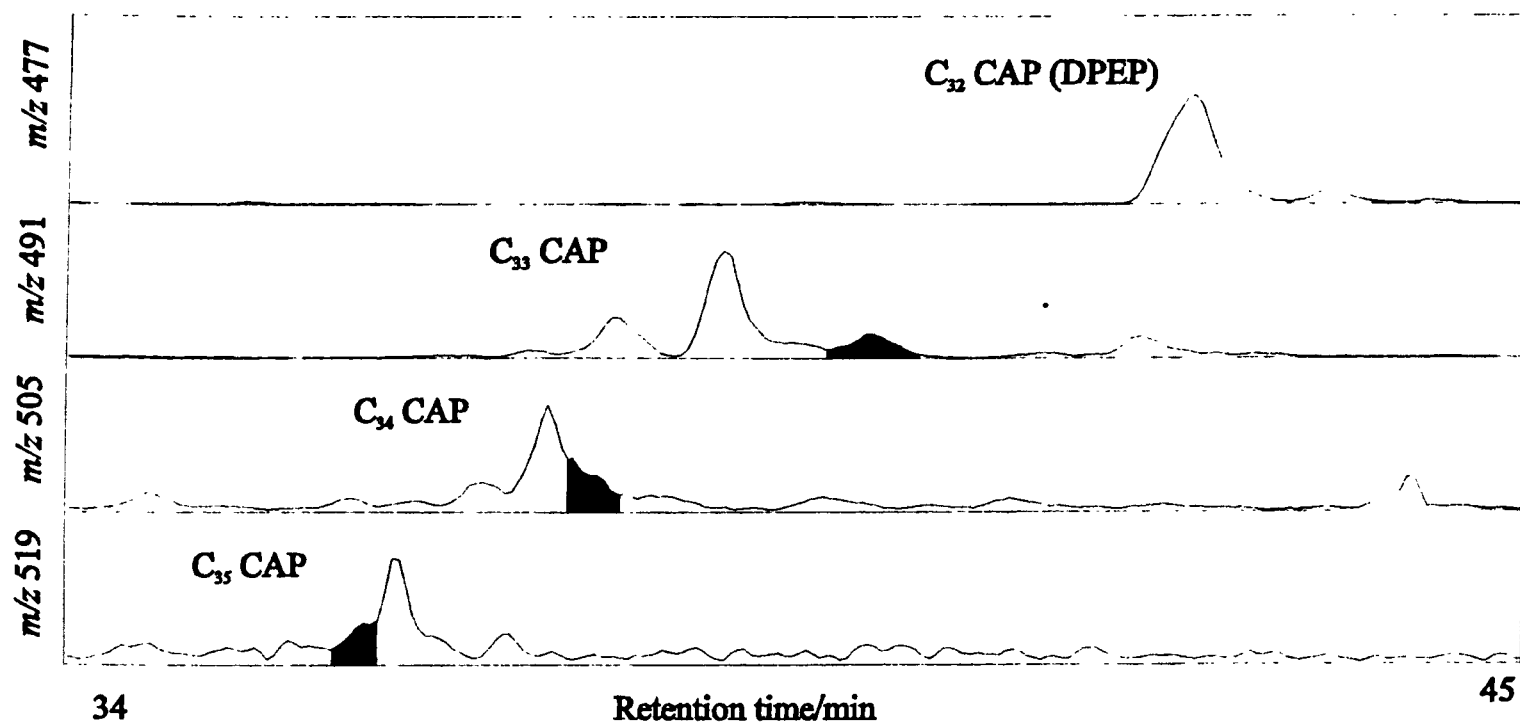




Fig. 4.10 Partial mass chromatograms for HMW CAPs in Livello Bonarelli samples from Contessa Gorge Quarry (CGQ)

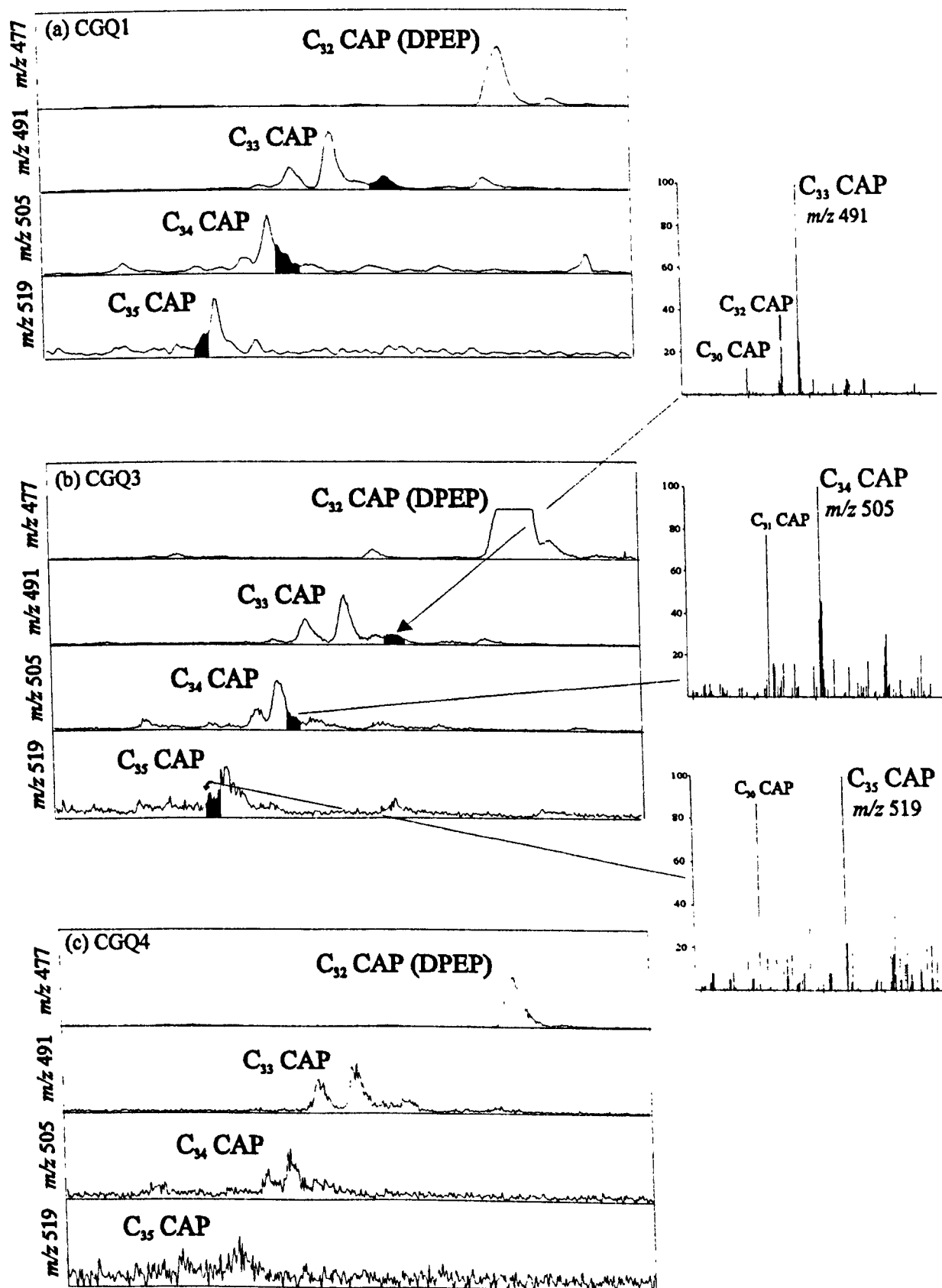


Fig 4.11. Partial mass chromatograms of CAPs in Contessa Gorge samples (a) "CG" ex nickel (b) "CG" ex vanadyl (collected by Farrimond, 1987) (c) CGQ1 ex nickel

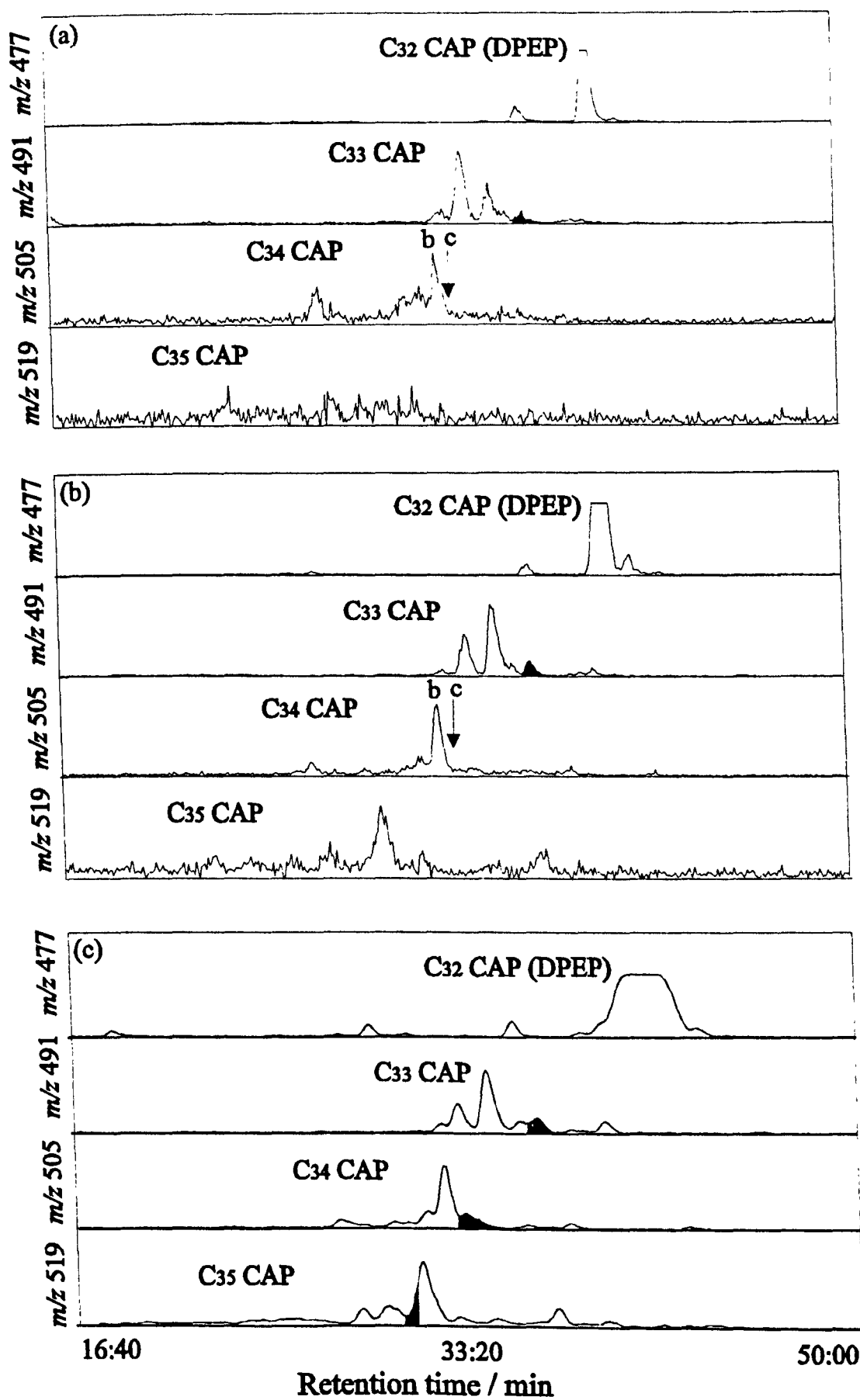
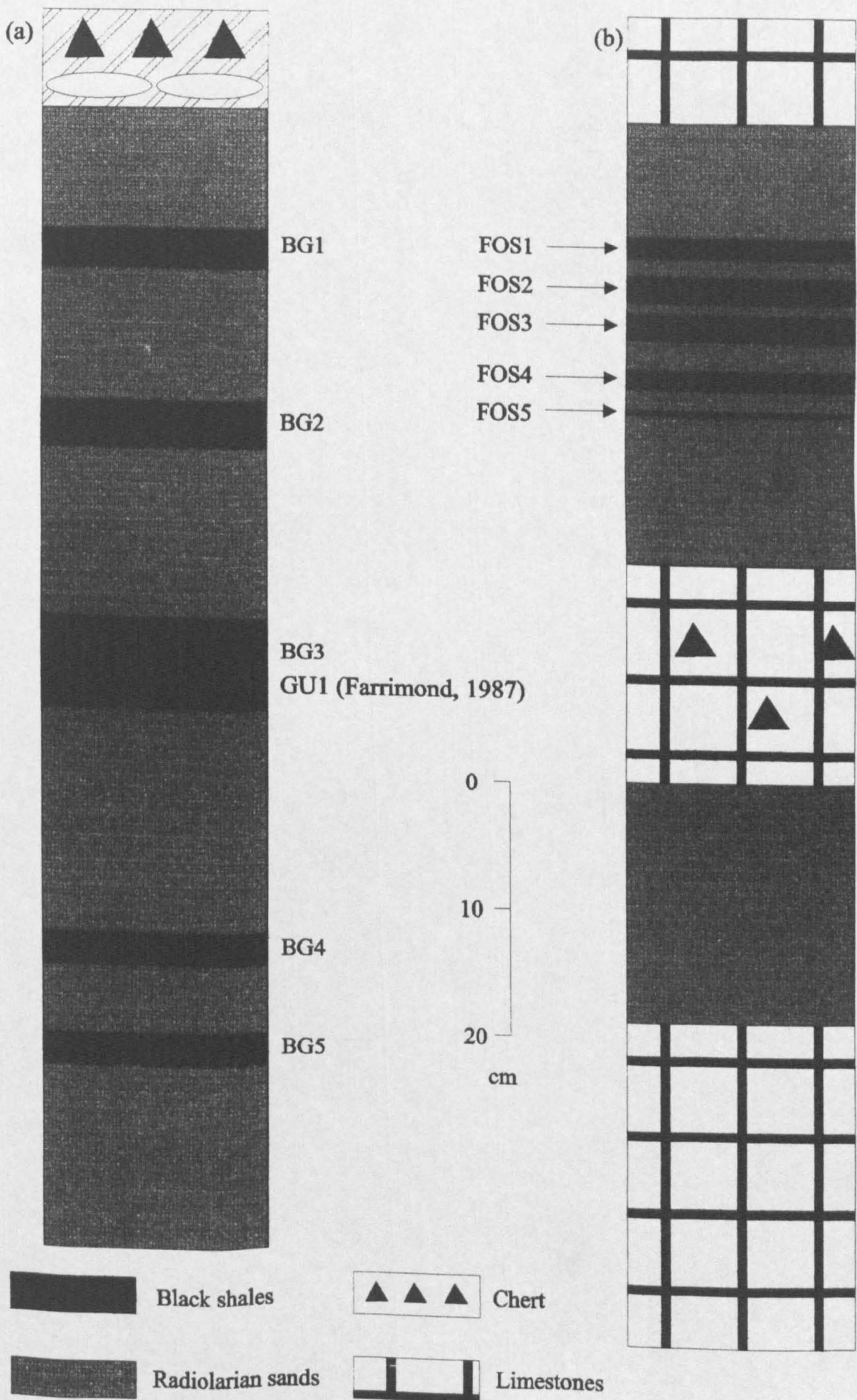


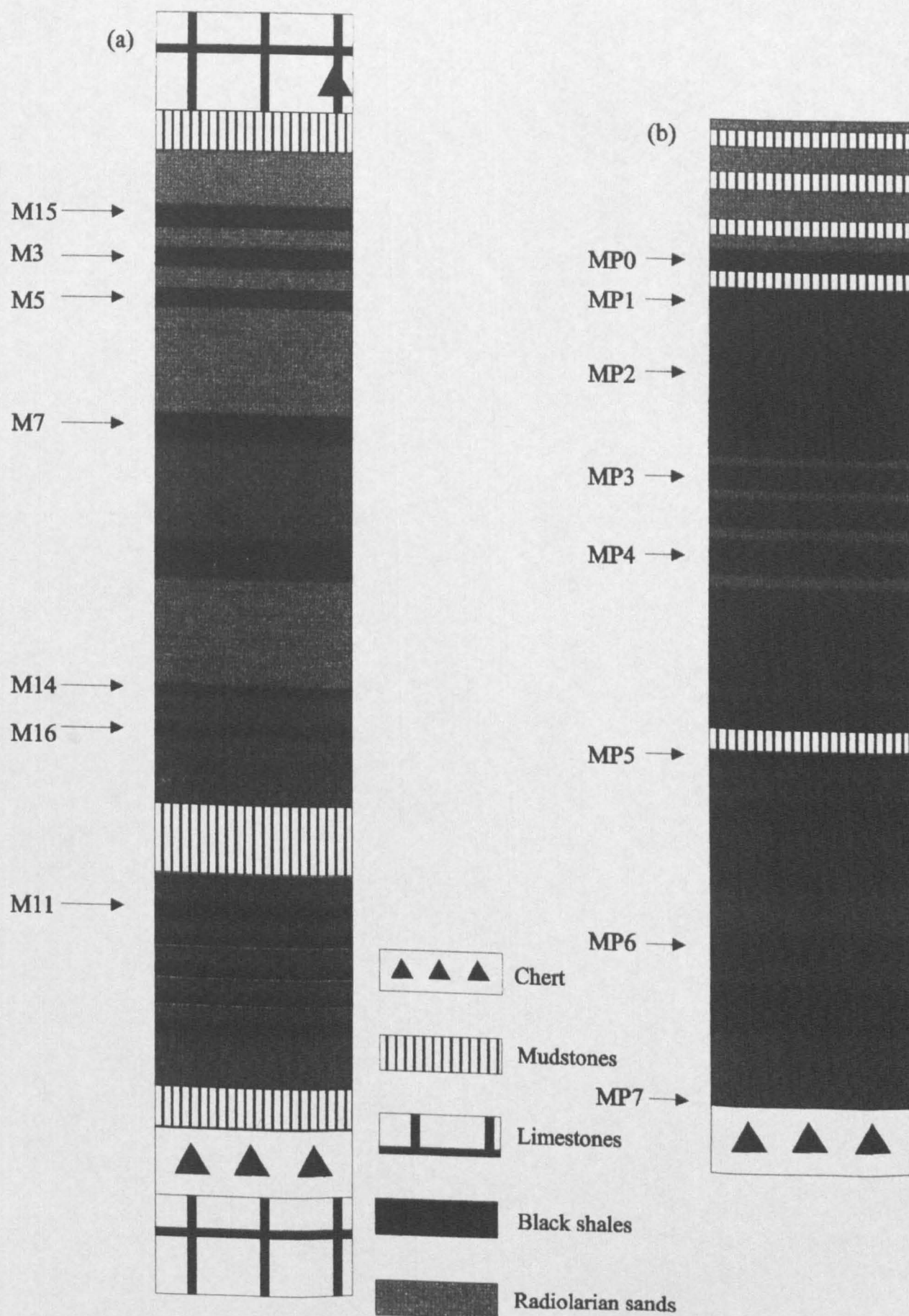
Fig. 4.12. Lithological sections of the Cen/Tur Livello Bonarelli at (a) Bottacione Gorge, Gubbio (b) Fosto (taken from field observations)



Page  
numbering as  
original

Fig. 4.13. Lithological sections of the Cen/Tur Livello Bonarelli at (a) Moria  
(b) Monte Petrano (Cagli area)

Taken from Arthur and Premoli-Silva (1982) and field observations



existence of PZA, although there is both porphyrin and maleimide evidence for CGQ1. This is the first time PZA has been recognised in a Livello Bonarelli sediment deposited during the Cen/Tur OAE in the Tethys Ocean, and importantly indicates that the levels of dissolved oxygen declined occasionally to such an extent in parts of the water column of the ocean, that free H<sub>2</sub>S was present and coincided with the zone of light penetration, allowing the growth of green sulphur bacteria.

### **Bottacione Gorge**

Just up from the walls of Gubbio, beside the road winding north east through the Bottacione Gorge (BG), is an exposure of the Bonarelli in the limestone cliffs. The base of the Bonarelli was found not to be exposed at this site, but the top 90cm was still visible up to the top of the section. The section (fig 4.12) consists of five major black shale horizons between interbeds of lighter siliceous rocks, mudstones and radiolarian sands. Five shale samples (BG1-5) were taken, one from each horizon. BG5 was, however, found not to contain any OM in the TOE and is not discussed further. Sample GU1, described by Farrimond *et al.* (1990), corresponds to sample BG3 taken from the horizon 40-47 cm below the top of the section. TOC values range from 6.7 to 13.4%, with sulphur between 0.3 and 0.9% and negligible carbonate (table 4.1). Sediments (between 90 and 220g) were extracted, fractionated and analysed by Uv/vis for metallo porphyrins, before demetallating and analysing the porphyrin distributions by HPLC-MS in the usual way.

### *Porphyrin distributions*

The ex-nickel (BG1-4) and ex-vanadyl (BG1-3) distributions of all four samples consist mainly of CAP and aetio types, with DPEP again the most abundant component (Appendix C). Maturities, as expressed by the MPMP (Appendix A) range from 0.1 to 0.36, again with higher values for the ex-nickel porphyrins (mean Ni-MPMP = 0.30) compared with the ex-vanadyls (mean VO-MPMP = 0.10), so the samples are immature (*c.f.* Farrimond *et al.*, 1990). HMW CAP distributions in the ex-nickel fractions are shown in fig 4.14, and shaded peaks indicate components that correspond to the CAPs derived from the bacteriochls *d*. The *m/z* 505 and *m/z* 519 chromatograms show that C<sub>34</sub> and C<sub>35</sub> HMW CAPs with the same retention as the C<sub>34</sub> (33 and 34b) and C<sub>35</sub> (34c) standards and appropriate spectra are present in the top three samples BG1, 2 and 3 (fig 4.14a-c). In contrast, BG4 contains no C<sub>34</sub> or C<sub>35</sub> components with the same retention times as these standards. Figs 4.15a-c show the corresponding mass chromatograms for the demetallated vanadyl porphyrins of BG1-3, and also reveal

Fig. 4.14. Partial mass chromatograms of CAPs in demetallated nickel porphyrins from Bottacione Gorge, Gubbio (BG1-4)

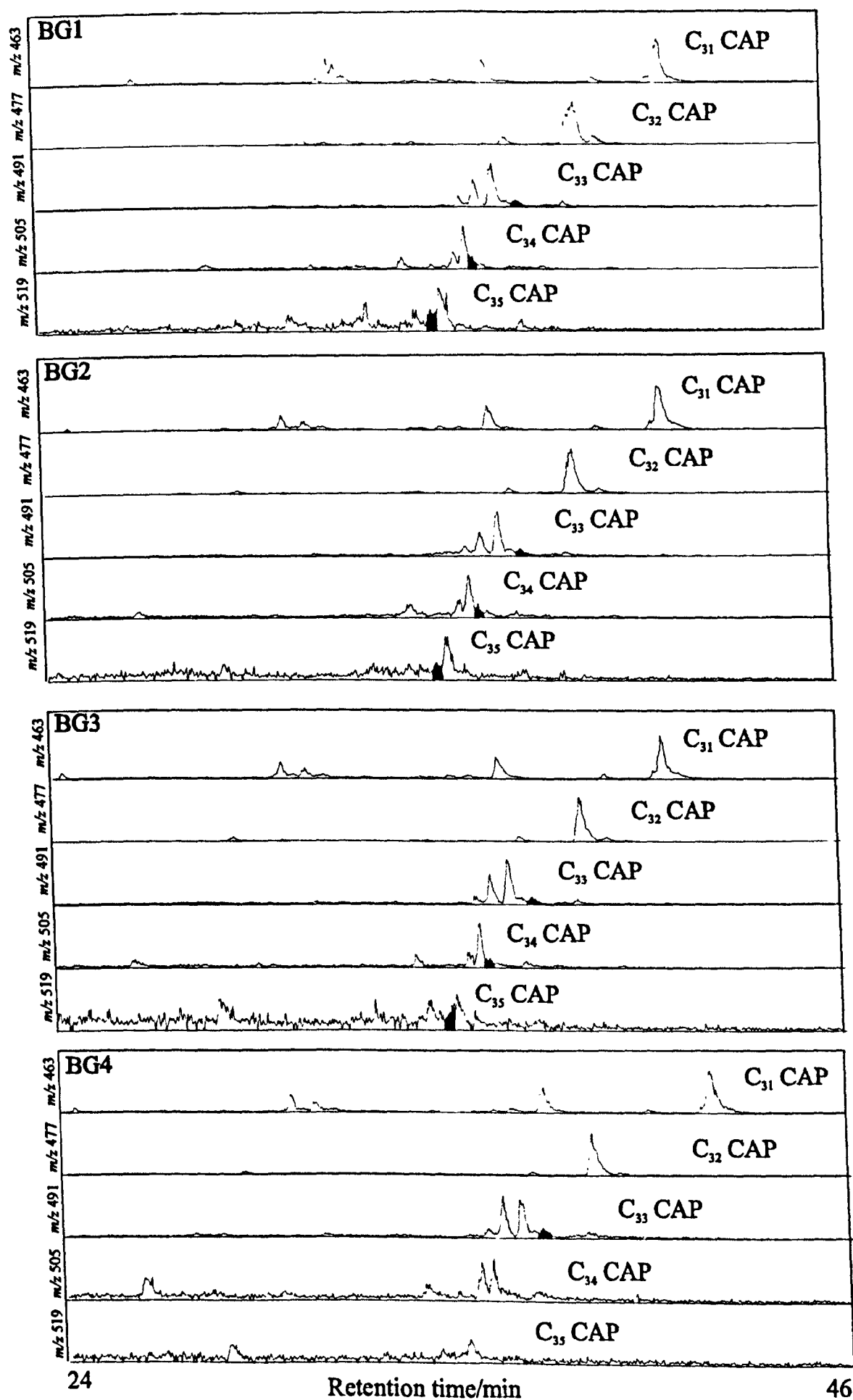
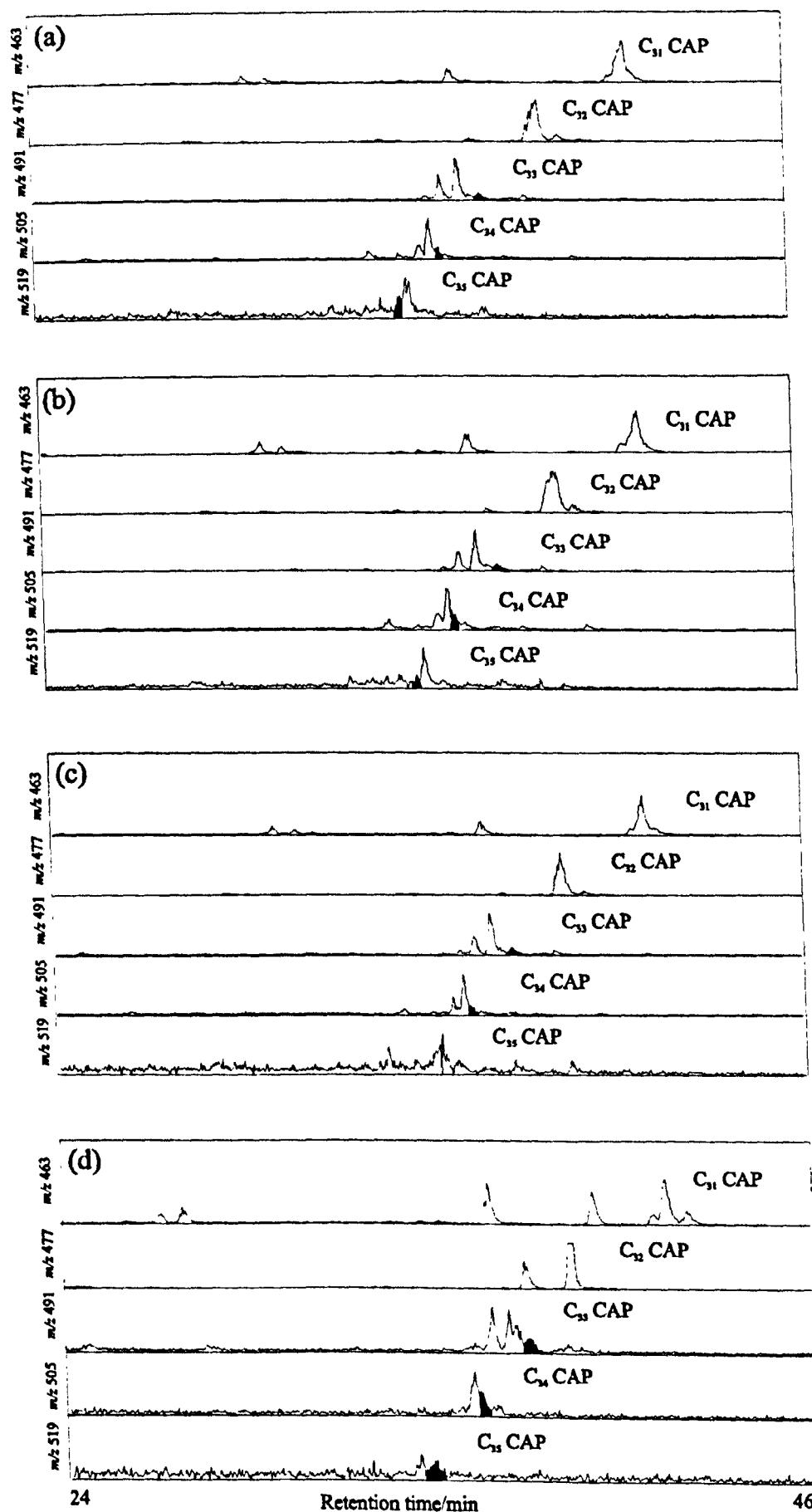


Fig. 4.15. Partial mass chromatograms of CAPs in demetallated vanadyl porphyrins from Bottaccione Gorge, Gubbio

(a-c) BG1-3, collected 1996 (d) GU1, Farrimond (1987)





HMW CAPs corresponding to the components derived from the bacteriochls *d*. The results from the Farrimond (1987) sample, GU1 (fig 4.15d), also clearly indicate the presence of these components. Maleimide distributions also show the presence of Me *i*-Bu maleimide in BG1-3, but not in BG4 (Crawford, personal communication), together with the possible presence of Me *i*-Bu maleimide in GU1. Hence, the porphyrin and maleimide data together suggest that PZA existed during deposition of the top three samples BG1 to 3 (9-12, 23-26 and 40-47cm from top respectively; fig 4.12a), but there is no evidence for such conditions during deposition of BG4 (65-67 cm from top). Again, there are also early and late eluting C<sub>34</sub> and C<sub>35</sub> CAPs in samples BG1-3 which may be derived from the bacteriochls *c* and/or *e*. However, some of these components are also present in BG4 (non-PZA), suggesting therefore that not all are derived from the bacteriochls (fig 4.14d).

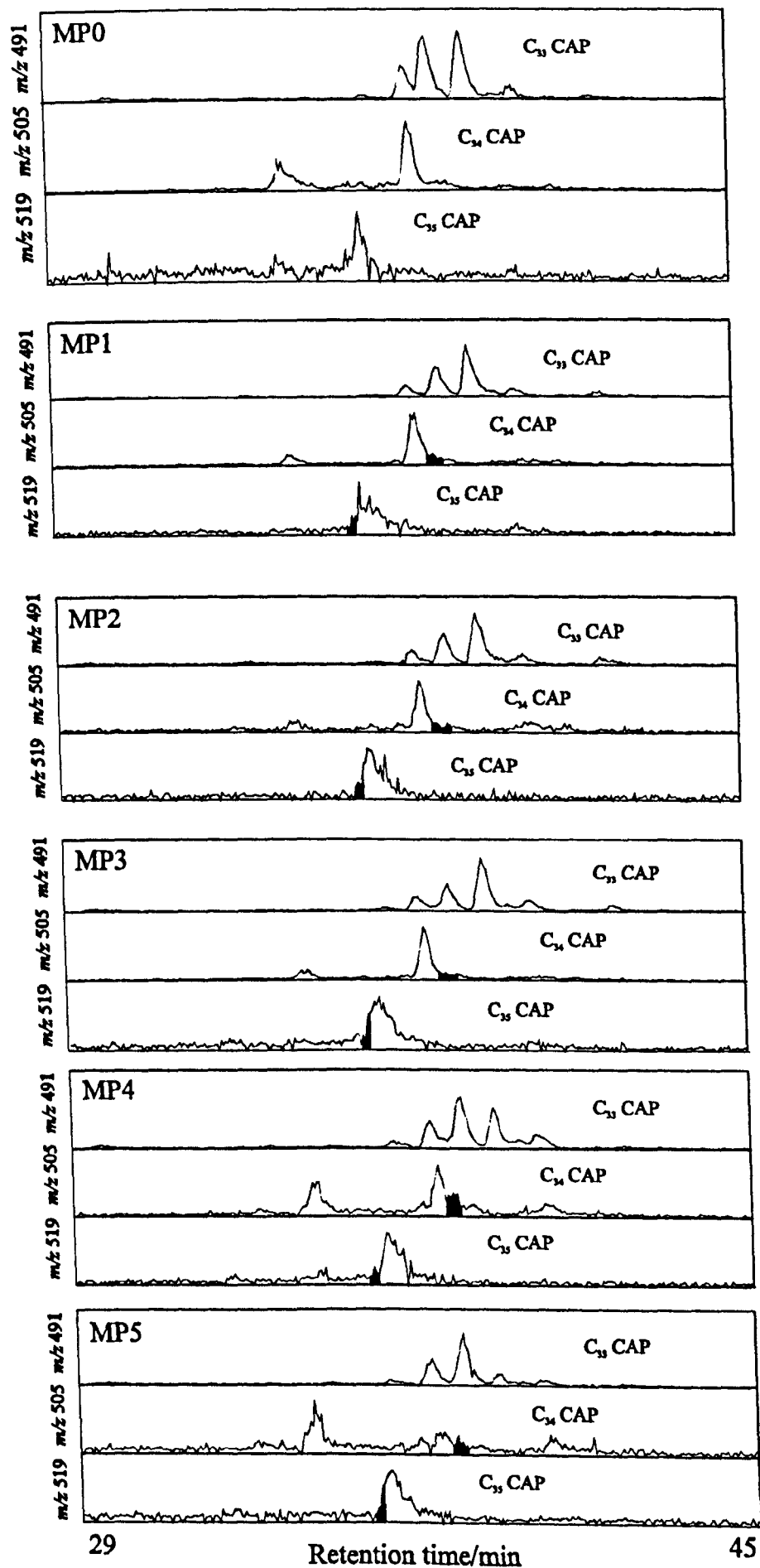
### **Monte Petrano, Cagli**

The Livello Bonarelli is also exposed in a road-cut section near the summit of Monte Petrano (MP), near Cagli (fig 4.3); 97 cm, covering the whole of the Bonarelli Cen/Tur event can be seen imbedded within cherts, limestones and radiolarian sandstones. The section (fig 4.13b) contains numerous intervals of black shales, which enabled eight samples (MP0-MP7) to be taken. MP7 was found to consist of mainly radiolarian-based material supporting a very thin wisp of black shale, whereas the other samples (MP0-MP6) consisted of more black shale, with less radiolarian material. The TOE of MP7 was a very light brown colour and contained only *ca.* 1µg of nickel porphyrin, not enough for demetallation and subsequent HPLC-MS analysis. Uv/vis analysis shows there to be higher levels of nickel porphyrins in samples MP0-MP4 (1.6-2.4 µg Ni porphyrin / g sediment), with much lower concentrations in MP5 and 6. Vanadyl porphyrins were also detected in significant quantities in samples MP0-4. MPMPs calculated (Appendix A) range from 0.08 to 0.37, with the mean Ni-MPMP = 0.27 and VO-MPMP = 0.10, *i.e.* similar to the other Bonarelli samples.

### ***Porphyrin distributions***

HPLC-MS analysis reveals similar distributions of CAPs and aetios as seen at the other Livello Bonarelli sites discussed above (Appendix C). The mass chromatograms of the HMW CAPs (C<sub>33</sub> to C<sub>35</sub>) in the demetallated nickel porphyrin fraction, eluting in the region between 30 and 45 min, are shown in fig 4.16. Results from MP6 are not shown, as the S/N ratio of the mass chromatograms of the HMW CAPs was especially low

Fig. 4.16. Partial mass chromatograms of HMW CAP's ( $C_{33}$  -  $C_{35}$ ) from demetallated nickel porphyrin fractions from Monte Petrano section (MP0 - MP5)



with so little free base porphyrin available (approximately 8µg) after demetallation. The shaded peaks, again indicating the components with the same retention position as the bacteriochl *d*-derived standards, are seen in most of the samples (MP1-MP5), but with especially clean mass spectra for these peaks in MP1, 2 and 4. This would indicate, that PZA occurred during deposition of much of the Bonarelli at Monte Petrano, but was more marked in MP1, 2 and MP4 than MP3 and 5, with no evidence during deposition of the final black shale interval, MP0, and also presumably at the beginning of the event (MP6).

The greater concentrations of bacteriochl *d*-derived components seen in MP1-4, do not necessarily coincide with the highest TOC values (table 4.1). Interestingly though, the ex-vanadyl distributions of the Monte Petrano samples are markedly different to those of the ex-nickels. The former contain a lower range of carbon numbers, with CAPs in the range C<sub>28</sub> to C<sub>33</sub> and fewer aetio types present. No HMW CAPs (C<sub>33</sub> to C<sub>35</sub>) are found with the retention times of the bacteriochl *d*-derived standards (fig 4.17a).

Maleimide distributions contain Me *i*-Bu maleimide in samples MP1 to MP5 inclusive, confirming that there were periods of PZA during deposition of much of the event at the Monte Petrano site (Crawford, personal communication).

Other HMW CAPs are observed eluting close to the HMW region, both before and after the bacteriochl *d*-derived components. Fig 4.17b also shows the CAP mass chromatograms in one Monte Petrano ex-nickel sample and reveals CAP components, eluting earlier than the region shown in fig 4.16, comparable to components observed in Kupferschiefer (chapter 2) and in VdG (chapter 3). Some of these may perhaps be derived from other bacteriochls, such as c and/or e, in the green and/or brown strains of Chlorobiaceae. Unfortunately, no aromatic hydrocarbon fractions from Monte Petrano have been analysed for the presence of diaryl isoprenoids derived from isorenieratene, so the existence of the brown strains of Chlorobiaceae is unknown at present.

It does seem, however, from the HMW CAP and maleimide distributions, that periods of PZA did exist during much of the deposition of the Livello Bonarelli black shales at the Monte Petrano site during the Cen/Tur event.

### **Moria**

Close to the village of Moria, the Livello Bonarelli is exposed by the roadside, and is still in favourable condition despite being sampled extensively over recent years (Jenkyns, personal communication). The section, just over 1 m thick, again consists of

Fig. 4.17a. Example of partial mass chromatograms of HMW CAPs ( $C_{33}$ - $C_{35}$ ) from demetallated vanadyl porphyrin fraction from Monte Petrano

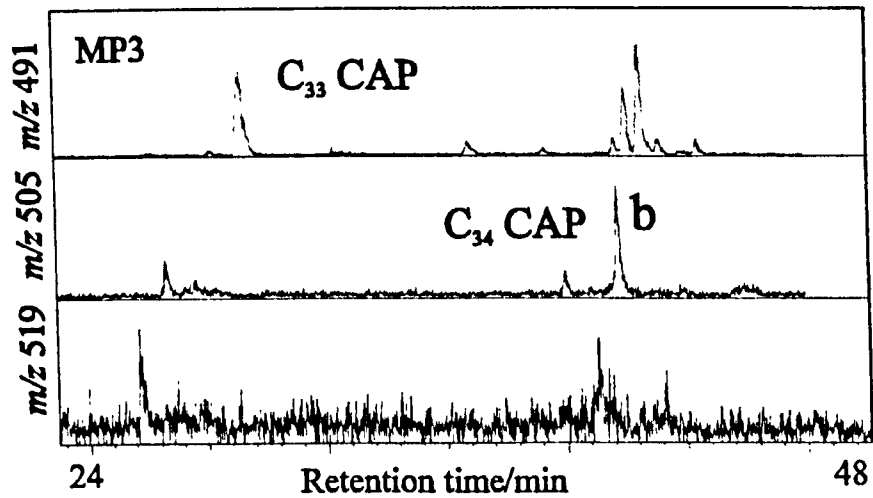
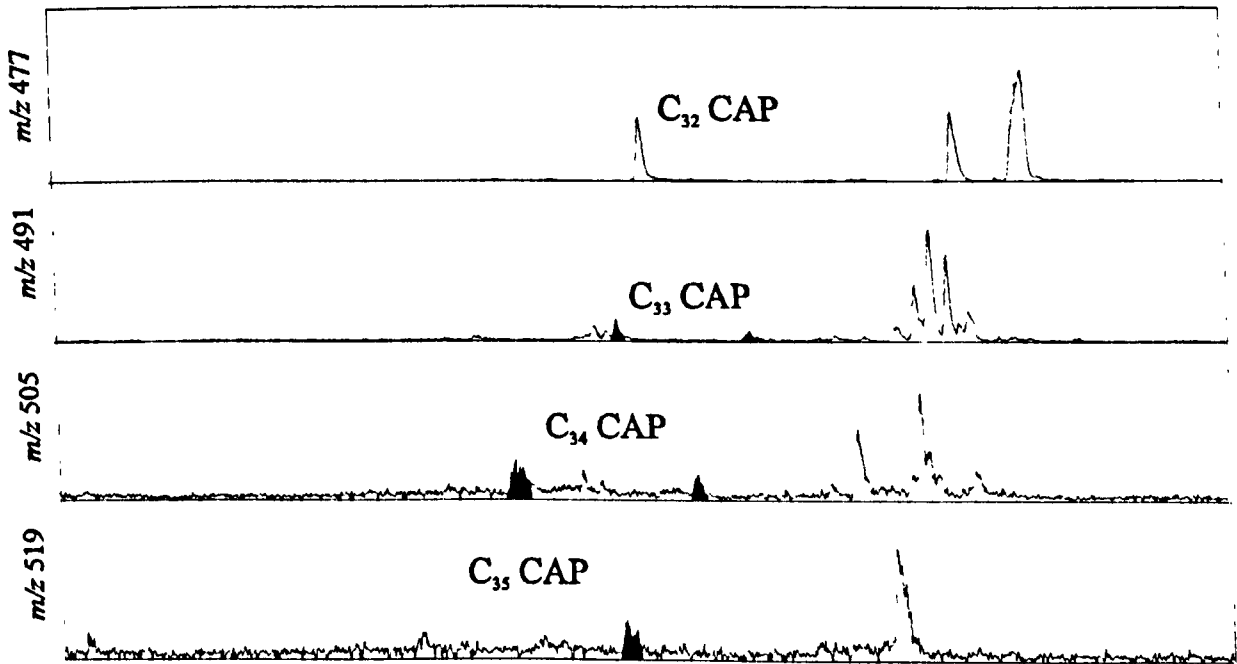


Fig. 4.17b. Mass chromatograms of HMW CAPs in demetallated nickel porphyrin fraction of MP4 with shaded peaks showing early eluting components



interbedded black shales, radiolarian sands and mudstones (fig 4.13a). Samples taken include some detailed previously (M3, M7 and M11) by Farrimond *et al.* (1990), together with some other shale horizons, not sampled previously (M14, M15 and M16). TOCs vary from 0.3 to 17.6%, sulphur from 0.3 to 2.4% (table 4.1) and  $\text{CaCO}_3$  is again negligible. Previous work on the Moria section by Farrimond *et al.* (1990) suggested that the general trend of increasing TOC and sulphur towards the top of the section indicated an increase in the levels of oxygen depletion during deposition of the later part of the Bonarelli, even though the presence of radiolarian sands in between each black shale horizon represents a periodic return to more oxidising environments. It would therefore be interesting to see whether the porphyrin distributions indicate the extension of such anoxicity into the photic zone, and if so, whether the extent of this PZA is comparable with sediments previously thought to be deposited under more anoxic conditions (see below).

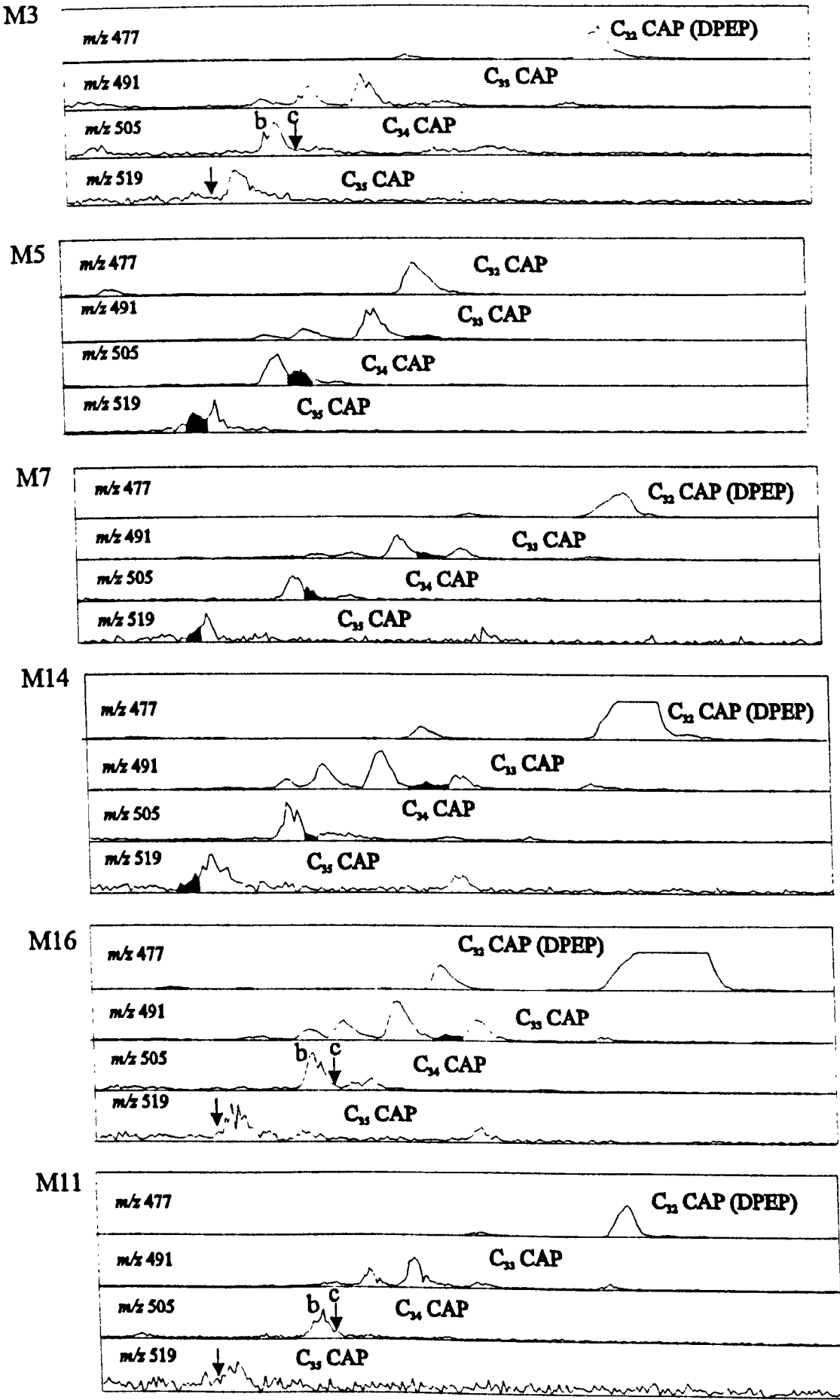
#### *Porphyrin distributions*

Porphyrin fractions were obtained in the usual way, with samples yielding a mixture of both nickel and vanadyl porphyrins to varying extents. HPLC-MS analysis of the demetallated fractions again revealed the usual mix of CAP and aetio types (Appendix C). A range of HMW CAPs are seen eluting in the HMW region as confirmed by the mass spectra. The appropriate partial mass chromatograms are shown in fig 4.18, with shaded peaks indicating components, confirmed by their spectra, with the same retention time as the bacteriochls *d* derived standards. Samples M5, M7 and M14 from horizons within the middle of the section show evidence for Chlorobiaceae, whereas samples M11 and M16 nearer the base and M3 near the top, do not. This therefore seems to show that PZA also occurred in the water column during deposition of parts of the Livello Bonarelli at the Moria site, although the results agree only in part with the inferences drawn from TOC and sulphur trends (see above). Furthermore, the porphyrins seem to also show that PZA was more prevalent in the middle of the event, rather than at the beginning and the end. Unfortunately, no maleimide data are available for any of the Moria samples, so no further confirmation of the presence of Chlorobiaceae is available at present.

#### **Fosto**

Along a mountain road close to the village of Fosto, near the town of Piobbico, the Livello Bonarelli is exposed within the limestone cliffs of a road cutting. The whole bed has rotated so that the section runs vertically. Deformation has also occurred, with

Fig. 4.18. Partial mass chromatograms of CAPs ( $C_{32}$ - $C_{35}$ ) in Moria section



the horizon having quite a varied thickness along its length. Consequently, the section (fig 4.12b) looks markedly different from the other Bonarelli sites, with five major thin black shale horizons close to each other in the top third of the section. A limestone pod is also highly visible within the Bonarelli itself. Five black shale samples were taken (FOS1-5), one from each of the distinct horizons (fig 4.12b); these were found to be high in organic carbon, with TOCs reaching 30% (table 4.1). One sample, F1, taken previously (Farrimond *et al.*, 1990), was also still available for analysis, coming also from one of these black shale horizons. Although much less sediment was collected from this location (between 35 and 75g per sample), the extracts contained enough metallo porphyrins for demetallation and HPLC-MS analysis to be carried out on samples FOS1-4.

### *Porphyrin distributions*

Fig 4.19 shows the demetallated vanadyl porphyrin distributions, and shaded peaks are again used to indicate the HMW CAP components with the same retention time as the bacteriochl *d*-derived standards. The overall distributions are again very similar to those seen in samples from other Bonarelli sites, with a dominance of CAPs and aetio type porphyrins in all four samples (Appendix C). Vanadyl MPMPs range from 0.08 to 0.12 (mean 0.10), inferring that, at least from vanadyl porphyrin distributions, the maturity of these samples, is low as indicated previously (Farrimond *et al.*, 1990). The major C<sub>34</sub> peak again corresponds to “peak b” and the major C<sub>35</sub> component elutes just after the bacteriochl *d*-derived CAP (34c) in all four samples. Such peaks are, as previously discussed, not representative of components derived from Chlorobiaceae. There are, however, much smaller peaks in FOS1 and 2, with the possible inclusion of FOS3, which correspond to the bacteriochl *d*-derived C<sub>34</sub> CAPs. These are confirmed by the mass spectra in FOS1 and 2, but not clearly enough in FOS3. Also, a C<sub>35</sub> component peak is visible, eluting at the same retention time as the bacteriochl *d*-derived CAP in FOS1, but no such peaks are detectable in FOS2-4. Hence, it seems that bacteriochl *d*-derived components may be present in FOS1 and FOS2, but the evidence is not strong enough for FOS3 and absent in FOS4. The Farrimond *et al.* (1990) sample, F1, was also analysed, and the results from the demetallated iron porphyrin fraction are shown in fig 4.20. C<sub>33</sub> and C<sub>34</sub> components are again present, confirmed by their spectra, with the same retention times as the bacteriochl *d*-derived standards. No acceptable mass spectrum was obtainable for the very small C<sub>35</sub> component present, so the component could not be completely assigned in this

Fig. 4.19. Partial mass chromatograms of CAPs ( $C_{32}$ - $C_{35}$ ) from demetallated vanadyl porphyrin fractions from Fosto section (FOS1-4)

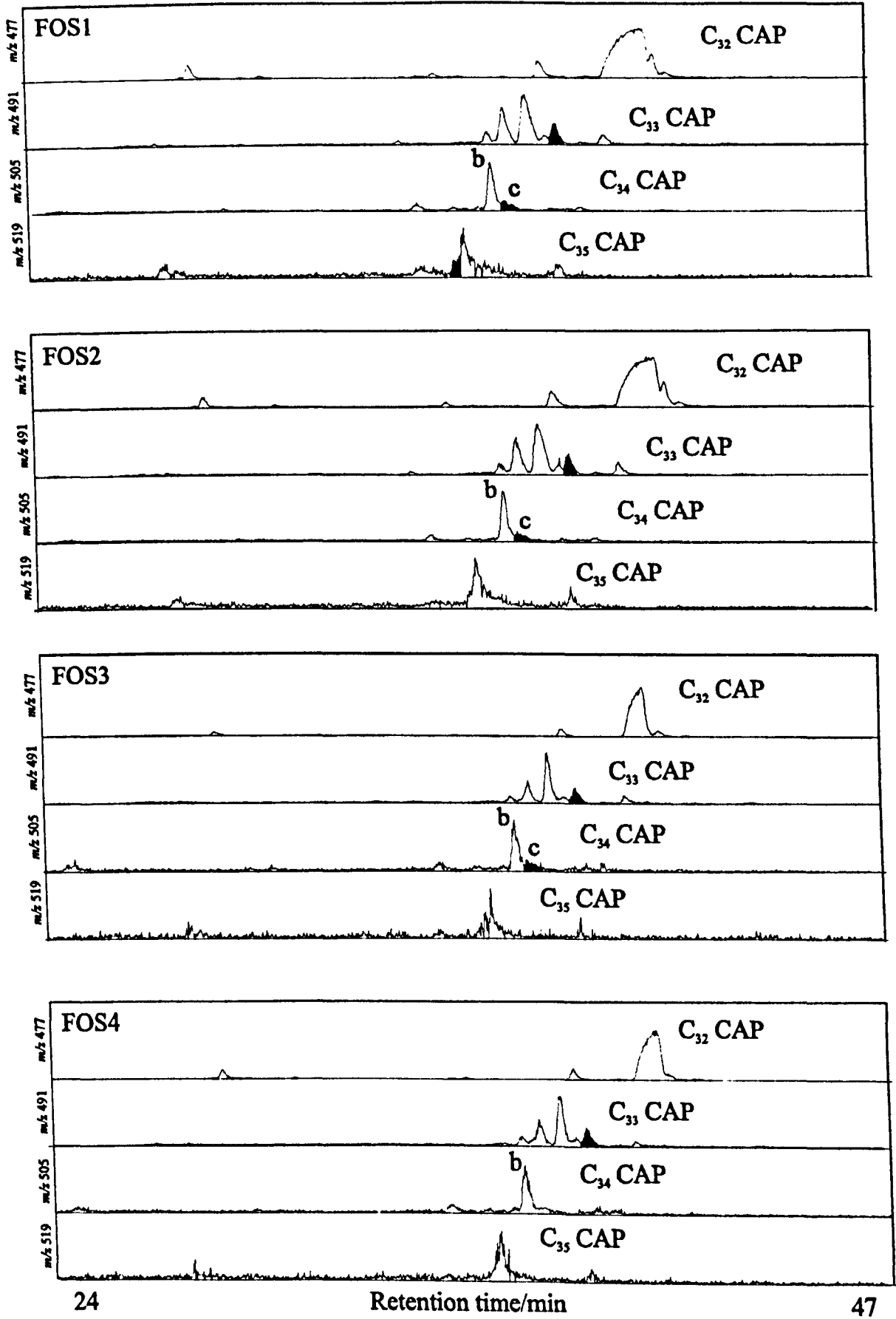
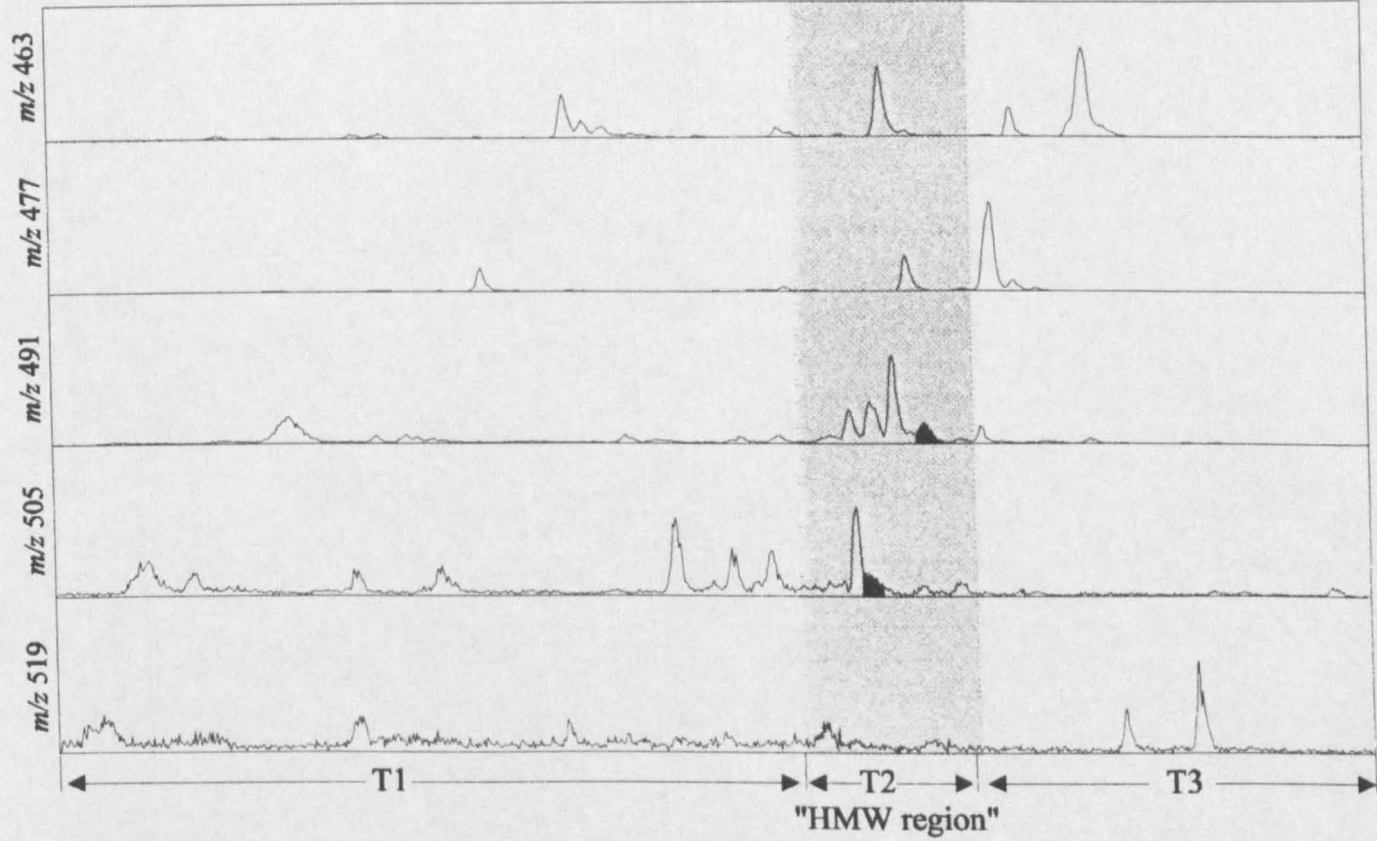




Fig. 4.20. Mass chromtaograms showing CAP components eluting in F1 demetallated iron porphyrin fraction  
Shaded peaks correspond to bacteriochl d-derived standards.  
Shaded area is T2- HMW region



instance. The ex-nickel and ex-vanadyl fractions were also analysed (results not shown) and found to contain comparable distributions.

In general, it therefore seems that HMW CAPs are present within some of the Fosto shales, in particular FOS1, as evidenced by the presence of both C<sub>34</sub> and C<sub>35</sub> CAP components, but at very low concentrations. However, analysis of the free maleimides did not reveal the presence of any Me *i*-Bu maleimide in any of the Fosto FOS1-4 samples (Crawford, personal communication), so does not back up the tentative porphyrin evidence of PZA in this case. Without further confirmation of the existence of pigments from green sulphur bacteria, it is therefore difficult to say with confidence from the above results whether or not PZA existed during deposition of the black shales at Fosto.

However, the Farrimond-collected Fosto sample, F1, contains the C<sub>34</sub> peak *c* component (fig 4.20) and was also found to contain Me *i*-Bu maleimide (Crawford, personal communication) in the free maleimide fraction. It appears therefore that this one Fosto sample, taken from an unknown position in the outcrop (Farrimond, 1987), does contain evidence for PZA. Fig 4.20 also clearly shows a number of CAP components in the demetallated iron fraction of F1, eluting before and after the HMW region, *i.e.* within the "T1" and "T3" regions. Some of these, confirmed by their mass spectra, elute with approximately the same retention times as the early eluting CAPs seen in Kupferschiefer and VdG (discussed in chapters 2 and 3 respectively). Normal phase semi-preparative HPLC was used to separate sub-fractions T1 and T3 from the rest of the ex-iron fraction. This procedure was repeated until over 500µg of porphyrin from the combined T1 and T3 fractions had been collected. This fraction was then oxidised under UV light by a colleague, who then analysed the resulting maleimides by GC-MS. The maleimides from the oxidation of sub-fractions T1 and T3 contained Me *n*-Pr and Me *i*-Bu maleimides (Crawford, personal communication), thereby giving evidence that these other HMW CAPs contained extended chains that were indicative of a derivation from the bacteriochls of Chlorobiaceae. It therefore seems possible that some of the observed components, either the early CAPs or the late CAPs, are derived from bacteriochls *e* and/or *c*, both of which contain a Me substitution at C-20. It is also interesting to note that the oxidised porphyrins contained relatively large concentrations of Me *i*-Pr maleimide (Crawford, personal communication), thus giving evidence for the presence of *i*-Pr-substituted porphyrins, eluting in fraction T1 and/or T3.

In summary, although it is difficult to confidently assign the presence of bacteriochl *d*-derived components, because of the negative results from the free maleimides, it does certainly appear that other bacteriochls of Chlorobiaceae were present in the water column, which through diagenesis gave rise to other CAPs indicative of either the green or brown strains of Chlorobiaceae. As yet, however, the aromatic hydrocarbon distributions have not been analysed, so the presence or otherwise of diaryl isoprenoids, derived from the isorenieratene of the brown strains of green sulphur bacteria, cannot be confirmed.

### **Gorgo A Cerbara – Torrente Candigliano**

The Livello Bonarelli is exposed 3km west of Piobbico in limestones along the Torrente Candigliano river valley, which runs parallel to the road from Piobbico to Acqualanga (fig 4.3). One large sample was taken from a thick black shale horizon close to the centre of the Bonarelli, the actual sample (GCLB) being then taken from the centre of the “chunk” to further minimise weathering effects. The laminated sample is high in organic carbon (TOC = 19.3%) with high sulphur (2.4%) and negligible carbonate (0.04%) and is from the same horizon as sample CA collected by Farrimond (1987). HPLC-MS analysis of both the demetallated nickel and vanadyl porphyrins in GCLB and CA revealed the presence of a range of CAP and aetio components, with a MPMP calculated for the ex-vandyl porphyrins of GCLB of 0.09 (Appendix A), again indicating a low maturity. Also observed, in both GCLB and CA, are C<sub>34</sub> and C<sub>35</sub> CAP components with the same retention time as the standards derived from the bacteriochls *d*. Furthermore, Me *i*-Bu and Me *n*-Pr maleimides were detected in both CA and GCLB (Crawford, personal communication) which, together with the porphyrin results, give good evidence for the existence of Chlorobiaceae in the palaeowater column during black shale deposition at this site.

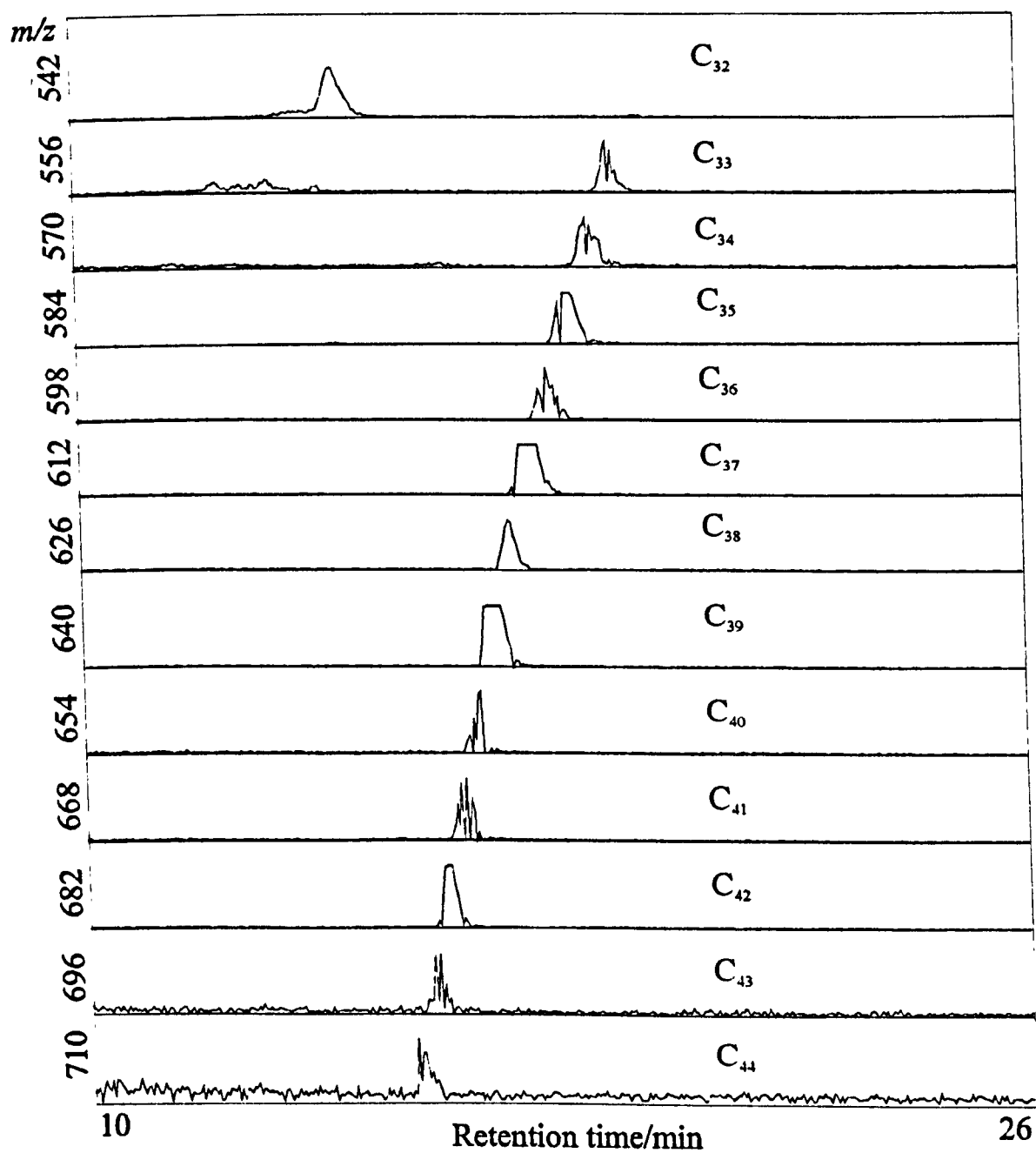
## **DISCUSSION – LIVELLO BONARELLI**

### **General**

As the mass chromatograms of many of the Bonarelli samples show, the HMW CAP peaks with the same HPLC retention times as the bacteriochl *d*-derived standards are relatively small or absent. The spectra in a number of cases have low S/N ratios, so that some (with S/N ratio >2) are taken to represent biomarkers of the bacteriochls *d*, whereas other slightly smaller peaks give poorer spectra (S/N ratio <2) and are hence not assigned as bacteriochl *d*-derived components. Similarly, the low S/N ratio seen in some mass spectra from the maleimide distributions results in some samples not being

assigned PZA. This may explain the few differences between the results from the porphyrin distributions and those from the extended chain maleimides, as the complementarity between HMW CAP and extended chain maleimide distributions has previously been shown to be close (chapter 2; fig 2.10, 2.11). In the examples where evidence for PZA is not clear from the distributions of both types of components such conditions may still have existed in the water column during deposition of the black shales. Each shale represents a long period of deposition during which frequent changes in the water column could have occurred. Hence, it is possible that changes in oxygen depletion or indeed presence or strength of PZA are not clearly recorded in the HMW CAP or maleimide distributions because of insufficient stratigraphic resolution. Indeed, given the high TOC values but low overall concentration of bacteriochl *d*-derived HMW CAP components, together with the low amounts of co-occurring extended chain maleimides seen in most of the Bonarelli samples, it is suggested that the occurrence of PZA was not a long term feature but only occurred periodically. There are also again notable CAP components present which are from unrecognised sources, in particular the prominent series of HMW CAPs whose C<sub>34</sub> component elutes with peak **b** of the Kupferschiefer distribution, which has the same retention time as the non-PZA standard isolated by Gibbison *et al.* (1996; 46a,b). This series can be seen in most of the Bonarelli demetallated porphyrin distributions together with some other samples, with distributions reaching high carbon numbers (>C<sub>37</sub> in some cases). For example, when the vanadyl porphyrin fraction of Fosto F1 was accidentally analysed as such by HPLC-MS, the mass chromatograms (C<sub>32</sub> vanadyl CAP = *m/z* 542), revealed (fig 4.21) an extended series of CAPs (confirmed by the spectra and on-line PDA analysis) stretching up to C<sub>44</sub> (*m/z* 710). The presence of such highly alkylated components in this immature shale is perplexing as components with such carbon numbers have traditionally been associated with samples of higher maturities where generation has occurred, such as the Boscan oil (Quirke *et al.*, 1980a; Barwise and Whitehead, 1980), although subsequent demetallation and HPLC-MS of the free bases showed the presence of CAPs up to just C<sub>37</sub>. Maleimides with very long chains have also been seen in maleimide distributions extracted from samples of Kupferschiefer taken from the Northern Permian Basin (Crawford, personal communication). Hence, alkyl chains up to C<sub>16</sub> were present, with the lower carbon number members having the same retention times as the *n*-alkyl maleimide standards (Et Me (44); *n*-Pr Me (49); *n*-Bu Me (50) maleimide). In light of this evidence, it may be the case that the HMW

Fig 4.21 HPLC-MS of vanadyl CAPs obtained from Fosto (F1)  
Bonarelli sample- (C<sub>32</sub> - C<sub>44</sub>)



CAP series with highly extended alkyl chains are in fact *n*-alkyl CAP components (e.g. 47a,b), and hence are not derived from any of the bacteriochls.

The results also show many other HMW CAPs eluting before and after the bacteriochl *d*-derived CAPs. Although these are present in highest abundance within the ex-iron porphyrin fraction of F1 (fig 4.20), many of the other Bonarelli samples contain similar components, although most do not contain the components eluting very early as in the VdG (chapter 3) and Kupferschiefer (chapter 2) samples. The oxidation products of the T1+T3 fractions of F1 revealed a high abundance of Me *i*-Pr maleimide, showing that *i*-Pr-substituted porphyrins were present. Some of the components may be derived from the bacteriochls *c* series of the green Chlorobiaceae or from the bacteriochls *e* series of the brown Chlorobiaceae. However, the presence of some of these components in samples which do not contain any maleimides indicative of PZA, implies that some of them are not derived from the bacteriochls of Chlorobiaceae. Further work involving the analysis of the aromatic hydrocarbons of these samples should reveal whether aryl isoprenoids derived from isorenieratene are present, and hence whether there was any contribution to the sedimentary record from the brown strains of Chlorobiaceae.

#### Variations in depositional conditions

Because the PZA components are present in some of the samples at concentrations around the limit of detection (see above), it is difficult in some instances to draw conclusions regarding the distribution of PZA throughout some of the individual Bonarelli sections. There are, however, samples where the presence of the C<sub>33</sub> and especially C<sub>34</sub> and C<sub>35</sub> CAPs is backed up by the presence of Me *i*-Bu maleimide (table 4.2).

Sample	C <sub>33</sub> CAP	C <sub>34</sub> CAP	C <sub>35</sub> CAP	Me <i>i</i> -Bu maleimide	PZA?
CGQ1	✓	✓	✓	✓	✓
CGQ2	-	-	-	-	-
CGQ3	✓	✓	✓	×	?
CGQ4	✓	×	×	×	×
CG†	✓	✓	✓	✓	✓
BG1	✓	✓	✓	✓	✓
BG2	✓	✓	✓	✓	✓
BG3	✓	✓	✓	✓	✓

BG4	✓	×	×	×	×
GU1†	✓	✓	✓	✓	✓
MP0	✓	×	×	×	×
MP1	✓	✓	✓	?	?
MP2	✓	✓	✓	-	✓*
MP3	✓	✓	✓	✓	✓
MP4	✓	✓	✓	✓	✓
MP5	✓	✓	✓	✓	✓
MP6	-	-	-	-	-
M15	-	-	-	-	-
M3	×	×	×	-	×
M5	✓	✓	✓	-	✓*
M7	✓	✓	✓	-	✓*
M14	✓	✓	✓	-	✓*
M16	✓	×	×	-	×
M11	×	×	×	-	×
FOS1	✓	✓	✓	×	?
FOS2	✓	✓	×	×	?
FOS3	✓	✓	×	×	?
FOS4	✓	×	×	×	×
F1†	✓	✓	✓	✓	✓
GCLB	✓	✓	✓	✓	✓
CA†	✓	✓	✓	✓	✓

Table 4.2. Identification of PZA in Livello Bonarelli sediments.

\* = Evidence from porphyrins

† = Collected by Farrimond (1987)

✓ = positive identification only

- = no results available

×

? = Evidence not clear

Hence, evidence from HMW CAP distributions for PZA has been obtained, to varying extents, at all six sites. However, back up from the maleimides was not obtained for the Fosto sediments, (except F1) where Me *i*-Bu maleimide was not detected, or for Moria, as no maleimide analysis was carried out for the samples from this section. Me *i*-Bu

maleimide was detected, however, in the oxidation products of the combined early and late eluting CAPs (fractions T1 + T3) from the demetallated iron porphyrin fraction of F1, suggesting the presence of pigments derived from bacteriochls other than bacteriochl *d*.

In summary, it is apparent that PZA occurred periodically during the deposition of the Livello Bonarelli black shales, such that the level of oxygen depletion in the water column was severe enough for H<sub>2</sub>S to exist, allowing the growth of green sulphur bacteria. On the other hand, in some cases there is no evidence for PZA from either the porphyrin or maleimide distributions.

### **Palaeoenvironment**

The present study and the maleimide study of Crawford (personal communication) have shown that oxygen-depleted conditions seem occasionally to have been more intense than previously envisaged. Previous work has shown evidence for bottom water anoxia as well as the possible presence of sulphide in the water column (Brumsack, 1986). With anoxia existing at the sediment-water interface at approximately 1km palaeodepth (Arthur and Premoli-Silva, 1982) and also in the photic zone, it is conceivable that anoxic conditions periodically extended, at least locally, from the photic zone to the sea floor. This model implies to a certain extent that extensive oxygen depletion would have been as a result of sluggish conditions (*e.g.* Degens and Stoffers, 1976), so that dissolved oxygen was not returned efficiently to the bottom and intermediate waters. Indeed, traditionally, PZA is thought to occur only in stagnant basins (fig 4.1). Although bottom water circulation may have been restricted within the Umbrian Basin, it is, however, difficult to apply this model to the entire water column in the Tethys Ocean, as water conditions were almost certainly not stagnant in this open ocean setting. The two other possibilities in light of the new evidence for PZA, are 1) that anoxic conditions existed only at certain intermittent levels (*i.e.* at the base of the photic zone and at the sediment water interface), or 2) the water column was completely anoxic as a result of factors other than just water stratification. It is difficult, however, to distinguish these two states, as the evidence to date points only to an anoxic sediment/water interface together with anoxia in the photic zone, so a model involving a continuously anoxic water column cannot be invoked. Whatever the cause of this oxygen depletion, the water column clearly returned to a more oxygenated state for significant periods of time during the Cen/Tur OAE, thought perhaps to be related to climatic changes induced by periodic changes in solar insolation (*e.g.* Barron *et al.*,



1985; Herbert *et al.*, 1986; de Boer, 1991). Such high frequency cycles are also seen in some sediments of Albian age from the Tethys (chapter 5) and in the North Atlantic, where black shale deposition in the latter is thought by some authors to be driven primarily by continental nutrient supply during wet periods (*e.g.* Hofmann *et al.*, 1997). The high frequency nature of these excursions in oxygenation/productivity in the Bonarelli argues against the notion of sluggishness on a larger time scale, and indeed that if such changes only reflect surface productivity, then relatively rapid changes in deep water upwelling rates must have occurred in brief periods of time.

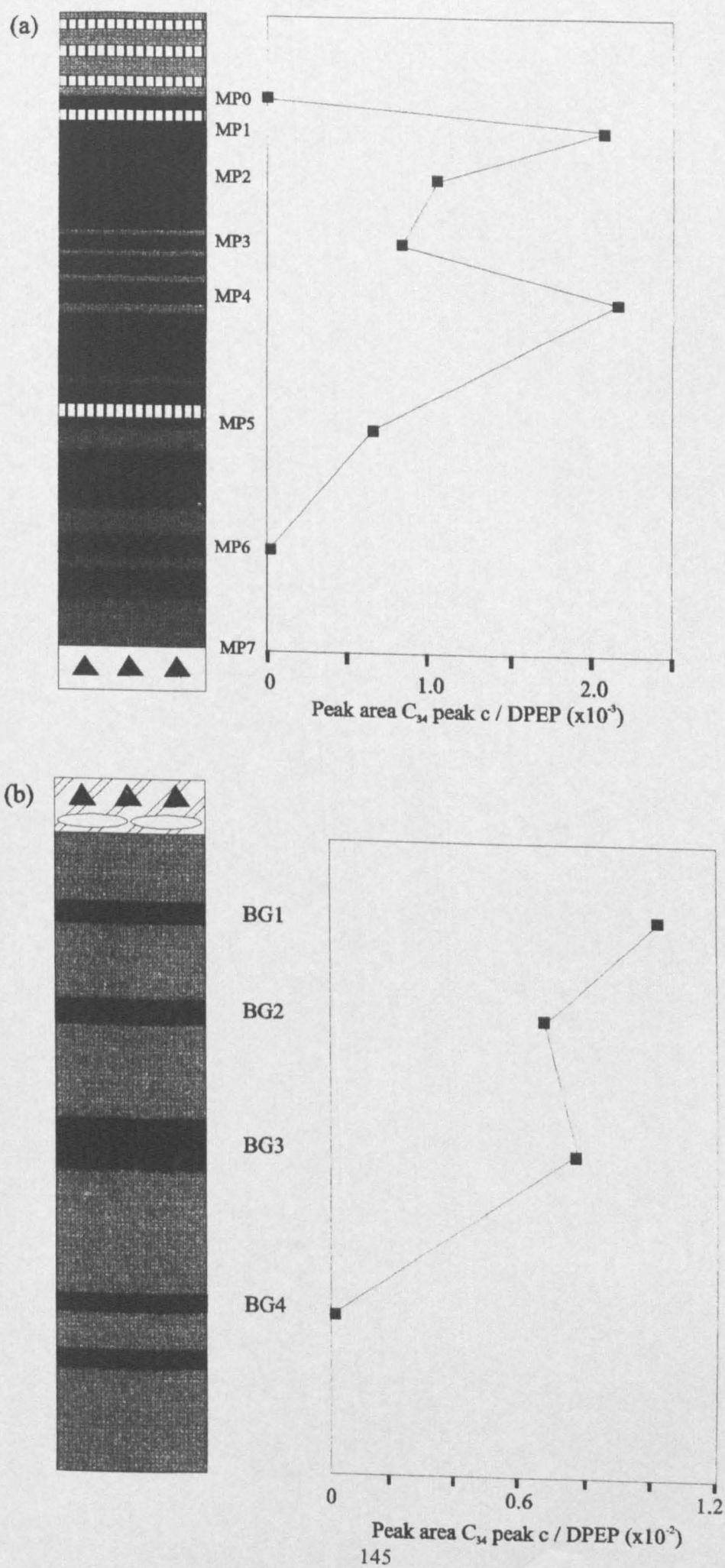
In the absence of stagnation, the joint effects of primary productivity and conditions resulting in high OM preservation must have been at times sufficient to develop the conditions necessary for the growth of anaerobic photosynthetic bacteria. An expanded and intensified OMZ model has often been postulated (see above) for large areas of the Tethys containing oxygen-depleted water. It seems possible that the intensity of such an expanded OMZ could at times reach a level where the water within the OMZ contained no traces of dissolved oxygen, leading to nitrate and sulphate reduction with the generation of  $H_2S$ . Such a model seems reasonable, considering the similarities between the characteristics of the sediments of the Livello Bonarelli and those deposited in the modern ocean on shelves under OMZs (see above). Even in today's well-mixed oxygenated oceans, the presence of free sulphide has been detected during certain conditions in the waters below the photic zone of the Peru upwelling region (Dugdale *et al.*, 1977) and in the Indian Ocean (Ivanenkov and Rozanov, 1961).

Although such conditions occur only rarely, it is possible to envisage them being maintained to a greater extent when overall conditions were favourable for the preservation of OM and the development and intensification of oxygen-depleted conditions. As discussed earlier, the prevailing warm, equable climate that may have existed during the Cretaceous (although more recently questioned; Sloan and Barron, 1990; Sellwood *et al.*, 1994) would have resulted in lower initial oxygen water solubilities, favouring oxygen-deficiency in many of the oceans during those times (*e.g.* Schlanger *et al.*, 1987). The bottom waters were oxygen deficient during the Cretaceous, prior to the Cen/Tur OAE, so were probably old and rich in  $CO_2$ , silica and nutrients (Arthur and Premoli-Silva, 1982). The nutrient flux to these deep waters may have increased further due to the erosional effects of intense bottom current activity (Jenkyns, 1985) and it has been speculated that such activity was related to the onset of intense upwelling, perhaps 500,000 years or more before the OAE (Jenkyns, 1985).

which in turn resulted in the onset of high productivity. Black shales deposited earlier than the Cen/Tur OAE, during the Aptian-Albian in the Gubbio area (chapter 5) and just prior to the Cen/Tur at Fosto (Arthur and Premoli-Silva, 1982; Farrimond *et al.*, 1990), as well as many other areas of the Tethys, North Atlantic and the Pacific, are thought to have formed when there was a combination of oxygen –depletion in deep water masses with episodic productivity (Schlanger and Jenkyns, 1976; Fischer and Arthur, 1977; Arthur and Premoli-Silva, 1982). Such episodes may have been enhanced and maintained by the increased benthic phosphorous release under conditions of sluggish bottom water anoxicity (Van Cappellen and Ingall, 1994) within the deep basinal setting. With the eustatic rise in sea level beginning during the Cenomanian, significant changes in circulation may have resulted in the periodic overturn of this deep, nutrient-rich water. This could have resulted in the introduction of the anoxic water into the surface layers, further stimulating primary productivity (Haq *et al.*, 1987), eventually resulting in the increased supply of OM to the already oxygen-depleted water column, and the subsequent periodic occurrence of PZA. The maximum high stand of sea-level during the Cen/Tur OAE is suggested by some authors to be the ultimate driving force behind the global nature of the deposition of organic-rich shales (Arthur *et al.*, 1987; Erbacher and Thurow, 1997). Such transgressions would have formed flooded, arid continental shelves along the continental Tethyan margin, resulting in the increased production of WSBW and the intensification of continental weathering (Weissert, 1990; Föllmi *et al.*, 1993), increased rates of nutrient-leaching, with upwelling generating higher productivity and an expansion and intensification of the OMZ.

The porphyrin results show that the distribution of PZA varied throughout the region, and it may be the case that the local intensity of upwelling, controlled perhaps by local climatic variations (Barber and Smith, 1981; Calvert, 1987), was a factor in determining the extent of oxygen depletion. Table 4.2 indicates that at the two sites close together in the centre of the region (Monte Petrano and Moria), PZA is apparent only during the middle of the event. This can be seen in fig. 4.22a for Monte Petrano, where the ratio of the C<sub>34</sub> peak c to DPEP is plotted, showing maxima in samples MP1 and MP4, with no PZA detectable in MP0 or MP6. This suggests that at the beginning of the event, the oxygen depletion was not high enough for the production of H<sub>2</sub>S and growth of the green sulphur bacteria. As the event progressed, the evidence suggests that the intensity of the OMZ increased in this area, perhaps as a result of upwelling-

Fig. 4.22 Depth plots of  $C_{34}$  peak c component vs DPEP through Livello Bonarelli sections  
(a) Monte Petrano (b) Bottaccione Gorge



induced increases in primary productivity, so that PZA could occur. It seems that similar processes would result in the changes in chemistry within the water column during deposition at the other sites (*e.g.* Bottacione Gorge; fig 4.22b) where the intensity of the signal from components derived from the bacteriochls is seen to increase during the event. The differences, however, in the amounts of bacteriochl *d*-derived CAPs present in each location suggests that the variable extent and/or frequency of the PZA was perhaps as a result of local factors. The presence of Me *i*-Bu maleimide in the oxidation products of the T1+T3 (see earlier) demetallated iron porphyrin fraction of F1 suggests that other bacteriochls of Chlorobiaceae were also present at times.

Recent work by Sinninghe Damsté and Köster (1998) reported a lack of isorenieratene-derived di-aryl isoprenoids in a Bonarelli sample (location/position not disclosed); however, only one example was analysed and some of the samples in this study do not show evidence for PZA, so therefore their negative result is not deemed significant.

### RESULTS – OUED BAHLOUL

Extracts of the Tunisian black shales were obtained from Paul Barrett, Newcastle Research Group, who collected the samples from outcrops at Oued Bahloul (fig 4.2). Eighty four samples were used (OB 0-83), many of which had TOCs < 2%, but with a few above 5%. These were taken at selected depths from the thirty metre Cen/Tur section, shown in fig 4.23. The majority were found not to contain any pigments, with only a few containing just enough metallo porphyrin for demetallation and HPLC-MS analysis. Bulk geochemical data (Barrett, personal communication) are shown in table 4.3 for the five samples (OB6, 17, 28, 68, 71/72).

Sample	Section depth (m)	TOC (%)	S (%)	CO <sub>3</sub> (%)
OB71/72	23.9	3.9	0.2	72
OB68	22.9	3.6	0.3	75
OB28	10.6	8.2	0.3	62
OB17	5.8	6.7	0.3	67
OB6	1.3	7.0	0.3	72

Table 4.3. Bulk geochemistry for Oued Bahloul samples (Barrett, personal communication)

(Stratigraphy from Schlanger et al., 1987 and Salaj, 1976)



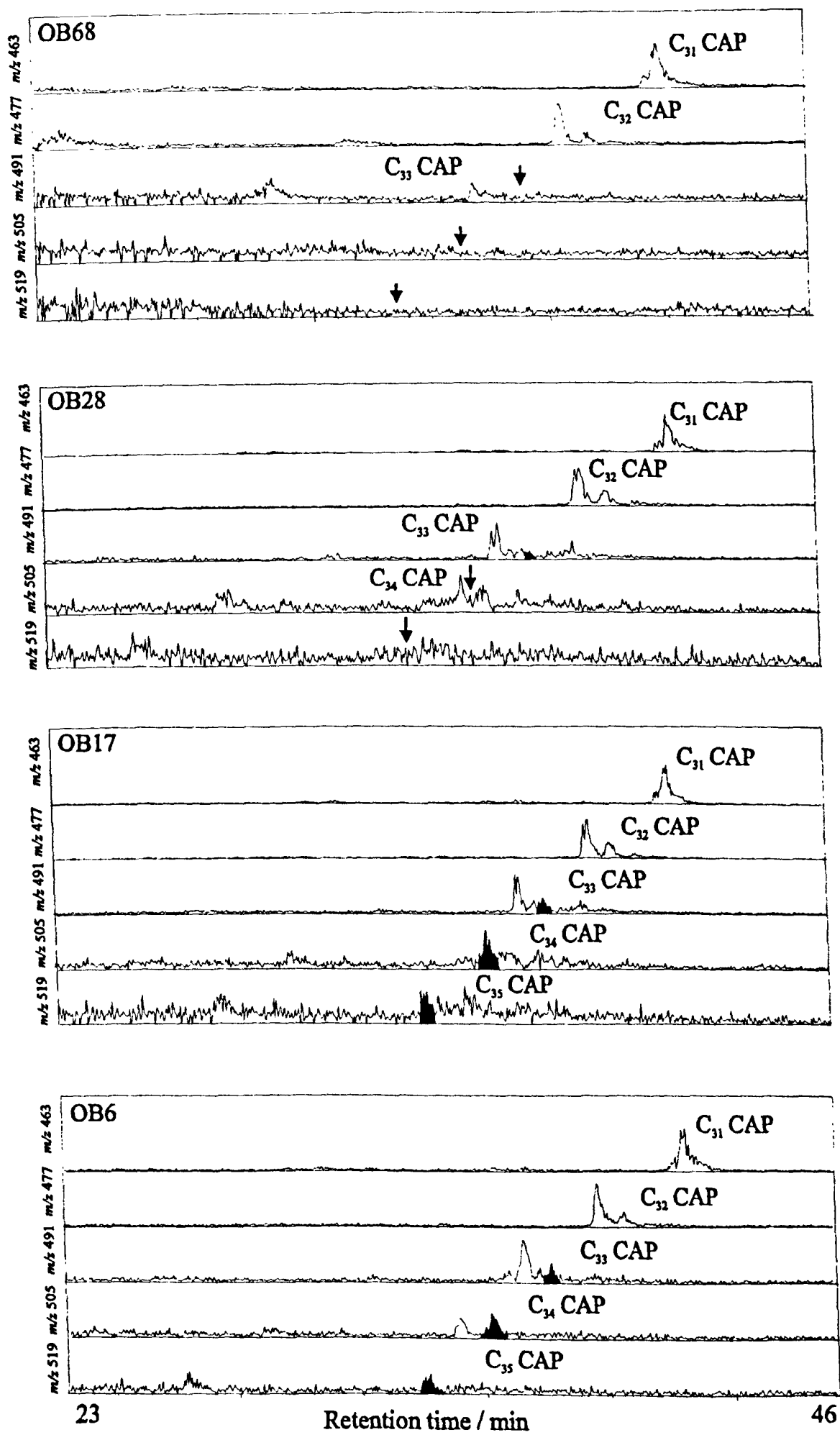
Vanadyl porphyrins were present in OB6, 17, 28 and 68 and nickel porphyrins in all five samples. The distributions show a range of CAP and aetio-type components (Appendix C), but with significantly more of the latter than in most of the Livello Bonarelli sediments (see above). MPMPs for the demetallated nickel porphyrins range from 0.22 to 0.76, which is significantly higher than the Bonarelli samples, and confirms that the samples from Oued Bahloul are of higher maturity as noted previously by other workers (*e.g.* Kuhnt *et al.*, 1990; Farrimond *et al.*, 1990).

Fig 4.24 shows results for the ex-nickel species, with shaded peaks again indicating the presence of peaks corresponding to bacteriochl *d*-derived standards, confirmed by their mass spectra, and arrows showing the same retention position if no components are present. Evidence for the presence of these components is seen in samples OB6 and OB17, with C<sub>33</sub>, C<sub>34</sub> and C<sub>35</sub> peaks present at the correct retention times. PZA evidence in OB28 is less clear as the distribution contains C<sub>33</sub> and C<sub>34</sub> component peaks, but the mass spectrum of the C<sub>34</sub> CAP is not clear enough for confirmation and no C<sub>35</sub> CAP peak is evident. OB68 contains no HMW CAP species in the correct retention region, and the results for OB71/72 are not shown as they were also found to contain no HMW CAPs, with very low levels of porphyrin resulting in very noisy chromatograms.

Hence, the porphyrin results suggest that PZA was present during deposition of samples OB6 and OB17, but with little or no evidence in OB28, OB68 and OB71/72. Me *i*-Bu maleimide was also detected in samples OB6 and OB17 but not in the others (Crawford, personal communication), providing further evidence that PZA occurred at times. These two samples were deposited early during the OAE (1.28 and 5.80 m, fig 4.23) inferring that the intensity of the oxygen-depletion was strongest at an early stage. With no evidence for PZA throughout most of the section, it therefore seems that the oxygen depletion was sufficient for periodic pulses of productivity (perhaps associated with changes in sea level and upwelling; Farrimond *et al.*, 1990) to be recorded in the black shale intervals, but was generally not intense enough for the development of PZA. With an intensified OMZ model best explaining the deposition of these shales (Farrimond *et al.*, 1990), the porphyrin and maleimide evidence suggests that the OMZ intensity was at its greatest early during the Cen/Tur event. This would coincide with the early stages of the high sea level stand, which may have resulted in a greater flux of nutrients to the water column eroded from the submerged African continental shelf, with subsequent upwelling resulting in higher levels of productivity and an intensified



Fig 4.24 Partial mass chromatograms of CAPs in demetallated nickel porphyrins from Oued Bahloul (Tunisia)



OMZ. The transgression may also have resulted in the overturn and upwelling of older, more nutrient-rich waters which were present in a deep depression on the continental shelf (Kuhnt *et al.*, 1990) and in the deeper regions of the Tethys earlier during the Cretaceous (see earlier).

In summary, porphyrin and maleimide data, suggests that PZA occurred only relatively briefly when older, deeper water was initially brought onto the Tunisian shelf; after this the OMZ seems to have become less intense, with black shale deposition being maintained only by more conventional upwelling, as predicted by the model of Barron (Arthur *et al.*, 1987), without the additional input of nutrients from the deeper regions and from transgression-related erosional processes.

### RESULTS – SOUTHERN NORTH ATLANTIC

DSDP core samples were analysed from three locations; sites 367 and 368 (leg 41) from the eastern North Atlantic off the African margin, and site 144 (leg 14) from the west (table 4.4; fig 4.4).

Sample Name	Leg	Hole	Core	Section	Interval (cm)	Depth (m)	Sediment wt. (g)
367-02	41	367	18	02	91-95	638.41	50
367-03	41	367	18	03	50-60	639.50	75
368-60	41	368	60	03	15-22		78
368-63	41	368	63	03	120-125	979.20	45
144-02	14	144	4	02	50-60	215.00	48
144-03	14	144	4	03	50-60	216.50	45

Table 4.4. Details of North Atlantic DSDP samples

Uv/vis analysis showed all samples (except 368-60) to contain chlorins and four to contain metalloporphyrins. Bulk geochemical data from these four are shown in table 4.5.

Sample	TOC (%)	S (%)	CaCO <sub>3</sub> (%)	Ni-P (µg)	VO-P (µg)
367-02	29.5	8.14	0.08	70	145
368-63	9.59	2.04	0.83	1650	7100
144-02	5.76	0.3	6.6	95	110
144-03	8.95	0.86	3.79	135	195

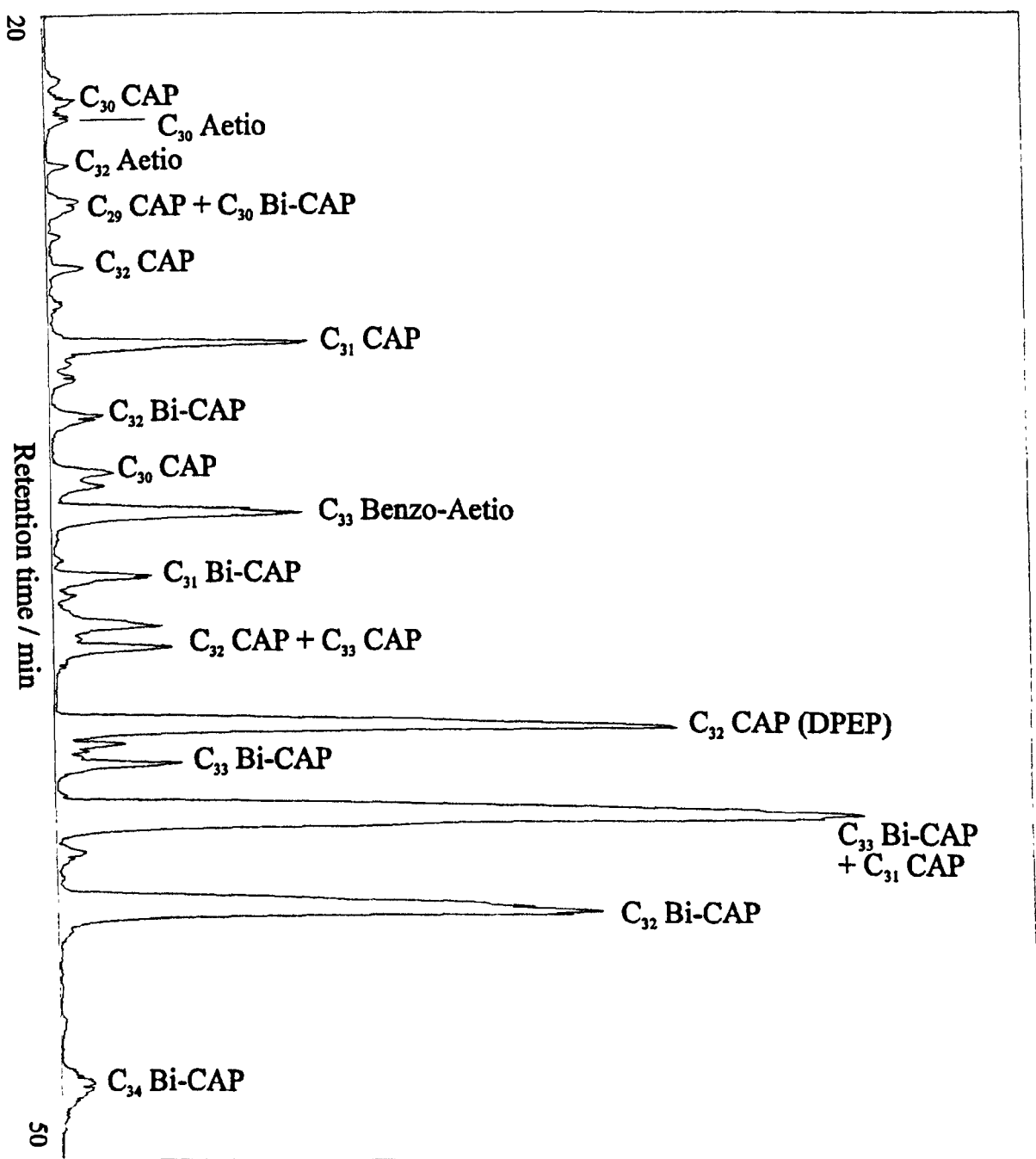


Table 4.5. Bulk geochemical data for DSDP North Atlantic samples containing porphyrins

*Porphyrin distributions*

The overall HPLC-MS distribution of the demetallated vanadyl porphyrins from 367-02 is shown in fig 4.25. Bi-CAPs within the C<sub>30</sub>-C<sub>34</sub> range are present in relatively high abundance. These components have been observed as minor components in many samples (Chicarelli and Maxwell, 1986; Verne-Mismer *et al.*, 1987; Prowse *et al.*, 1987; Boreham *et al.*, 1990; Keely *et al.*, 1994); these include samples discussed within this thesis, especially the Vena del Gesso samples (chapter 3), and the components have been postulated as originating mainly from chl *a* (chapter 1). Although DPEP is also an abundant peak, the other CAPs are in low abundance. Also, compared with most other porphyrin distributions seen so far, 367-02 contains only very low abundances of aetio-type components, suggesting a low contribution from the haeme groups present in bacterial cytochromes and/or a low extent of conversion of the chlorophyll contribution to aetioporphyrins *via* defunctionalisation (chapter 1). The base peak chromatograms of the ex nickel porphyrins are similar, as are the ex nickel and ex vanadyl porphyrins of samples 144-02 and 144-03 (Appendix C), although there seems to be a higher aetio contribution in the 144 samples. The distribution in sample 368-63 is, however, different (Appendix C), showing a great similarity with the distributions of the Livello Bonarelli porphyrins (see above); with a greater contribution of both CAPs and aetio types, with DPEP the most abundant porphyrin and the Bi-CAPs present as more minor components. A higher contribution of aetio-types might perhaps be expected in this case, possibly reflecting a higher maturity for the 368-63 sample, due to the local heating effects of the intrusion of basaltic sills (Lancelot *et al.*, 1977; Deroo *et al.*, 1977; Baker *et al.*, 1977; Herbin *et al.*, 1986; Huseby, 1996) and leading to an increased release of aetio porphyrins from the kerogen (*e.g.* Barwise, 1987). However, MPMPs (Appendix A) show lower values for both the eastern samples as compared with the western samples (ex-Ni-MPMP = 0.16, 0.15, 0.48, 0.54 for 367-02, 368-63 and 144-02 and -03 respectively). On the other hand, a higher maturity at site 368 might relate to the much larger amounts of metalloporphyrins in 368-63 as compared with 367-02 (table 4.5), which may have been generated from the kerogen, as found in laboratory thermal heating experiments (Van Berkel and Filby, 1987).

Fig 4.25 Partial HPLC-MS base peak chromatogram of demetallated vanadyl fraction of 367-02 with carbon numbers of major peaks labelled



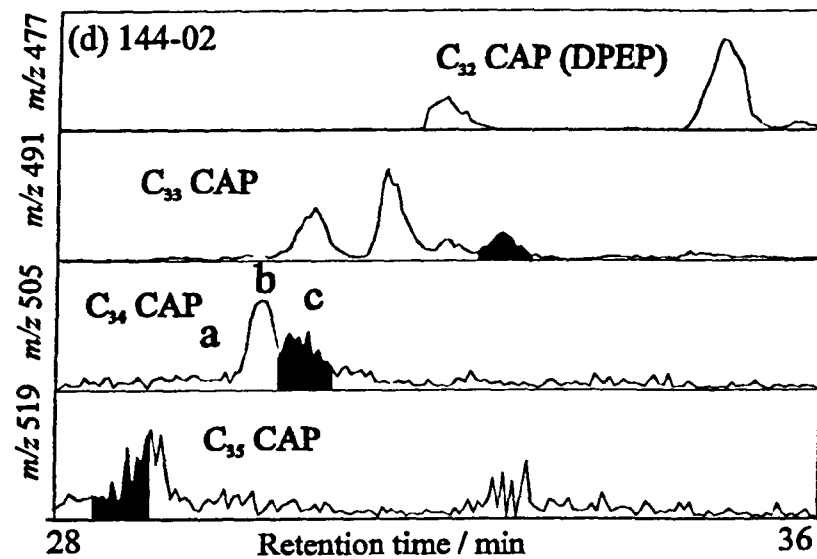
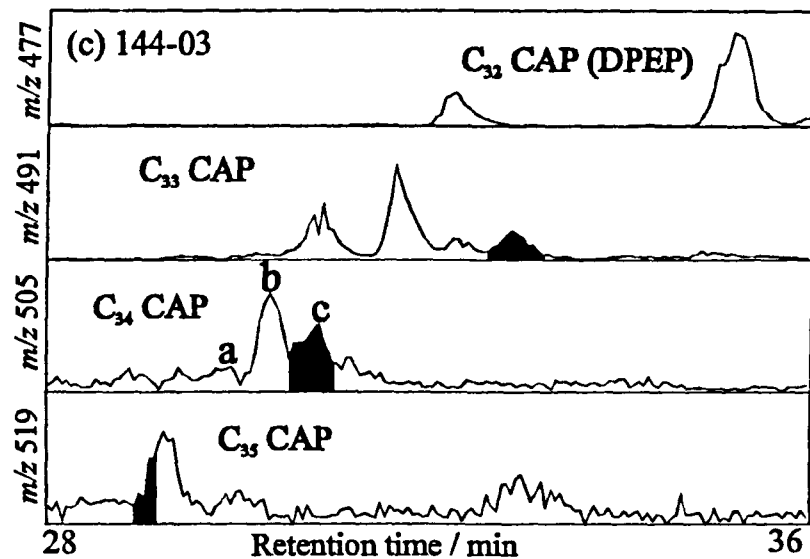
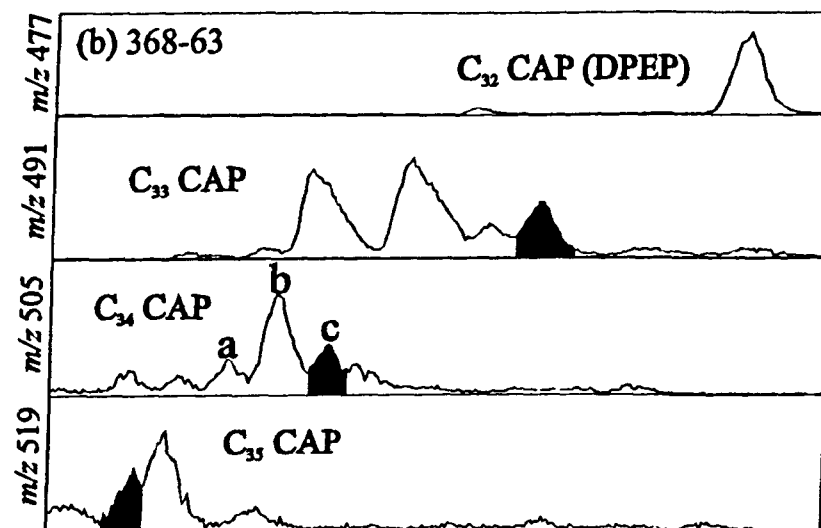
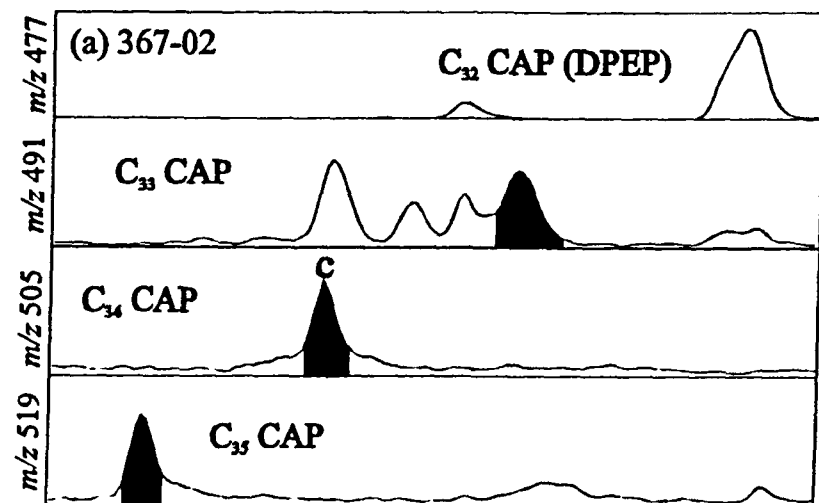
### HMW CAP distributions

A range of HMW CAP components elutes in the expected region (fig 4.26). The demetallated vanadyl porphyrins of the four samples clearly show the presence of (C<sub>33</sub>-C<sub>35</sub>) CAP components with the same retention times as the bacteriochl *d*-derived standards (peaks shaded). The distribution in 367-02 (fig 4.26a) differs from the others, as the bacteriochl *d*-derived components are the only C<sub>34</sub> and C<sub>35</sub> CAP peaks observed in the respective mass chromatograms. So, although there are fewer CAP components in 367-02, there is clear evidence for the presence of porphyrins derived from the bacteriochls *d*-derived from Chlorobiaceae.

The chromatograms of 368-63 and the two 144 samples, show greater similarities with the HMW CAP distribution of the Kupferschiefer bulk sample (chapter 2), with a greater multiplicity of peaks, especially in the *m/z* 505 (C<sub>34</sub>) chromatogram (fig 4.26 b-d). Fig 4.26 b shows that 368-63 contains at least five C<sub>34</sub> CAPs, although the origin of the components which do not correspond to the standards remains unknown. These components are also seen in 144-02 and 144-03. Peak **b**, having the same retention time as the non-bacteriochl standard (46a,b) is the most abundant, as is the case with the Bonarelli CAP distributions (e.g. fig 4.7a), but the abundance of peak **c** relative to peak **b** is much higher in all the Atlantic samples than in any of the other Cen/Tur samples analysed. The high relative abundance of the bacteriochl *d*-derived porphyrins at site 367 indicates the clearest imprint of PZA in all the Cen/Tur samples.

Me *i*-Bu maleimide occurs in the eastern samples (Crawford, personal communication). Sample 367-02, in particular, contains a very high abundance, further showing that the bacteriochl:chl *a* ratio was indeed higher at this site than at the others. The  $\delta^{13}\text{C}$  value of this component was also found to be significantly enriched compared with Me Et maleimide of mainly phytoplanktonic origin (Crawford, personal communication), thereby confirming an origin from Chlorobiaceae (chapter 1). Interestingly, no Me *n*-Bu maleimide was detected in 367-02, a component which was present in all the Livello Bonarelli samples (Crawford, personal communication). This would seem to provide further evidence for the previous notion (see above) that the C<sub>34</sub> peak **b** CAP, present as the major C<sub>34</sub> CAP in all the Livello Bonarelli samples, and the major Bonarelli non-PZA C<sub>35</sub> CAP, both absent from the 367-02 porphyrin chromatograms, correspond to the C<sub>34</sub> and C<sub>35</sub> CAPs (47a,b) with an *n*-Bu substituent at C-12.

Fig 4.26 Partial mass chromatograms of CAPs ( $C_{32}$ - $C_{35}$ ) in ex-vanadyl porphyrins from Southern North Atlantic  
(a) 367-02 (b) 368-63 (c) 144-03 (d) 144-02



Me *i*-Bu maleimide was also detected in significant quantities in 368-63. Furthermore, an aliquot of the demetallated vanadyl porphyrin fraction of 368-63 was oxidised to maleimides containing significant quantities of Me *i*-Bu maleimide (Crawford, personal communication). Unfortunately, due to the high concentration of chlorins present in the maleimide fractions of the 144 samples, it was impractical to inject sufficient amounts of the fraction to detect by GC-MS the presence of extended chain maleimides in both 144-02 and 144-03 (Crawford, personal communication).

Recent work (Sinninghe Damsté and Koster, 1998) has shown that Cen/Tur black shale samples from sites 144 and 367 contain abundant isoprenoid derivatives (38,52-54) from isorenieratene along with sulphide-bound isorenieratane (35). Furthermore, such components were enriched in  $^{13}\text{C}$  by 10-15‰ compared with phytoplanktonic-derived components. Hence, the tentative evidence of PZA in 144-02 and 144-03 from the porphyrin distributions confirms the evidence from the same site obtained from the aryl isoprenoids.

It is also noted that the porphyrin distribution shows no presence of any HMW CAPs eluting before the bacteriochl *d*-derived components. The only other HMW components observed elute after this region, with one series eluting closely after the bacteriochl *d* C<sub>34</sub> and C<sub>35</sub> CAPs (fig 4.26a), and two more series eluting *ca.* 2-3 mins later (not shown). It is possible that, with the large concentrations of isorenieratene derivatives detected (Sinninghe Damsté and Koster, 1998), one of these later eluting series may be derived from the bacteriochls *e* series.

## DISCUSSION – SOUTHERN NORTH ATLANTIC

These organic-rich samples were deposited at abyssal sites (3000-3700m palaeowater depth), which infers that the shales either represent pelagic sedimentation and were deposited either in a continuously anoxic water column or with a high productivity and sedimentation rate in a partly oxygenated water column, or that they were deposited on the continental slope and were redeposited later *via* turbidity currents. Regarding the latter, turbidites have been found in some of the site 368 cores, but these, as mentioned earlier, are characterised by lower TOC and high CaCO<sub>3</sub> values (de Graciansky, 1986) and contain significant levels of oxidised OM, as seen in turbiditic material further north from the Madeira abyssal plain (Cowie *et al.*, 1995); sample 367-02 comes from a core (core 18) which contains no turbidites (Shipboard Scientific Party, 1977a). Furthermore, the presence in the studied samples of extensive preservation of laminations with no evidence of benthic burrowing, and high concentrations of trace

metals, gives strong evidence for bottom water anoxicity (see earlier). Even so, our results showing the presence of anoxic conditions in the photic zone, cannot be used to prove that the entire water column was anoxic. The expanded and intensified OMZ model could explain the occurrence of anoxic conditions in the photic zone, but it is unlikely that such a zone, overlying a mainly oxic water column above the abyssal plain, could result in the preservation of shales highly enriched in OM. However, the presence of organic-rich deposits along the west-east trend from site 367 in the west (TOC up to 50%) 330 km to the Casamance area in the east ("Banc du Large" and "Brikama" formations; TOC up to 10%) does seem to imply that, over a wide range of palaeo depths, a large part of the water column was anoxic in much of this large southeastern North Atlantic Basin (Herbin *et al.*, 1986; Kuhnt *et al.*, 1990). It is difficult to envisage how anoxic bottom waters, which were present through much of the Cretaceous at site 367 could form, purely as a result of high productivity and the resulting expansion of the OMZ, unless the OMZ expanded outwards and downwards to such a large extent that it reached the abyssal floor at sites 367 and 368. It has been estimated that the productivity in the water column overlying the abyssal site 367 (*i.e.*  $50 \text{ g C m}^{-2} \text{ y}^{-1}$ ; Bralower and Thierstein, 1984) was substantially lower than those calculated for present-day productivity (Waples, 1983; Bralower and Thierstein, 1984; Bralower and Thierstein, 1987) in regions of upwelling ( $200\text{--}3600 \text{ g C m}^{-2} \text{ y}^{-1}$ ; Millero, 1996), where the intensity of oxygen-depletion is only rarely intense enough for the massive denitrification which needs to occur before water column sulphate reduction can begin, leading to the generation of free  $\text{H}_2\text{S}$ . Planktonic productivity is thought to have been lower still at site 144 (Shipboard Scientific Party, 1972).

Estimations of moderate productivity, together with evidence of bottom water anoxicity and black shales high in TOC over much of the basin, together with the data presented here, seems to back up the previous suggestions that an expanded OMZ existed, being maintained by upwelling-induced productivity (as predicted by models of Parish and Curtis, 1982) over the related shelf environments, but was superimposed on a water column with sluggish circulation (Kendrick, 1979; Tucholke and Vogt, 1979) which was already extensively depleted in oxygen (*e.g.* de Graciansky, 1986), especially in the eastern basins. The warm, equable climate (Frakes, 1979; Barron, 1983; Jenkyns *et al.*, 1994) and the slower WSBW-driven circulation (see earlier) would have resulted in lower initial oxygen solubilities, lower oxygen concentrations and increased residence times (sluggishness) of intermediate/deep water and hence bottom water renewal,

throughout this low latitude region. Dugdale *et al.* (1977) have shown that even in today's well-mixed oxygenated ocean, a return to upwelling areas of oxygen-depleted waters can result briefly in denitrification and sulphate reduction. According to Waples (1983) most of the southern North Atlantic laminated, TOC-rich sediments were deposited in deep basins below the CCD, with limited circulation. This may also have been the case at site 144, where sediment deposition during the Cenomanian is thought to have occurred in a deep trough narrower than today (Shipboard Scientific Party, 1972), with the relatively young sea floor in the area maybe increasing the average temperature (Sclater and Francheteau, 1970), hence further fuelling the potential for oxygen deficiency, however the exact relationship of the site to the spreading Mid-Atlantic Ridge is not known (Berger and von Rad, 1972).

So, although the North Atlantic as a whole can hardly be described as a stagnant basin, various physical factors such as the presence of the mid-oceanic submarine ridges and sills (Ryan and Cita, 1977; Tissot *et al.*, 1979) and tectonically controlled basins (Arthur and Schlanger, 1979), although difficult to reconstruct precisely (Barron, 1987), may have combined with other circulatory effects, perhaps together with increases in nutrient fluxes and higher localised productivity, resulting in restricted circulation and thus longer residence times of deep/intermediate waters and a greatly reduced flux of oxygen to the deep water layers. According to the calculations of Thierstein (1989), bottom water renewal would certainly have to decrease markedly in order for the deep waters to become euxinic, whilst maintaining a "normal" productivity (Brumsack, 1980). So although the stagnant basin model is not applicable to this area, there may have been times when the entire water column of the southern North Atlantic was anoxic (*e.g.* Arthur and Schlanger, 1979). As also previously discussed, the high eustatic sea level that existed during the Cenomanian-Turonian, may have allowed the influx of intermediate level oxygen depleted water from the Pacific across the Caribbean, resulting in an increased intensification of the oxygen depletion throughout most of the water column. Similarly, an injection of old, nutrient-rich, anoxic water during the opening of the South Atlantic would have strengthened the anoxicity and nutrient availability in the southern North Atlantic, presumably to a greater extent in the eastern sub basin, a pattern which is seemingly reflected in the data regarding the relative amounts of PZA biomarkers presented here (see above) and in recently published work (Sinninghe Damsté and Koster, 1998).

Other work has shown that there were increased ocean floor spreading rates during the Cen/Tur, together with increased submarine volcanism and hydrothermal activity, as evidenced by the seawater strontium isotope record (Ingram *et al.*, 1994). This may have resulted in an increased sulphidic flux (von Damm *et al.*, 1985), resulting from contact of hot basalts at the mid-oceanic ridge with the ocean water (Walker, 1986), independent from that formed as a result of primary production, in turn strengthening the conditions of anoxia/euxinia in the bottom/intermediate waters.

In summary, it seems likely that a combination of factors resulted in an extensively anoxic water column during the Cen/Tur in the southern North Atlantic Ocean. The data show that Chlorobiaceae proliferated in the palaeowater column at DSDP sites 367 and 368 in the east and were present, to a lesser extent, at DSDP site 144 in the west.

## DISCUSSION - CAPs

### *Organic richness and sulphur content*

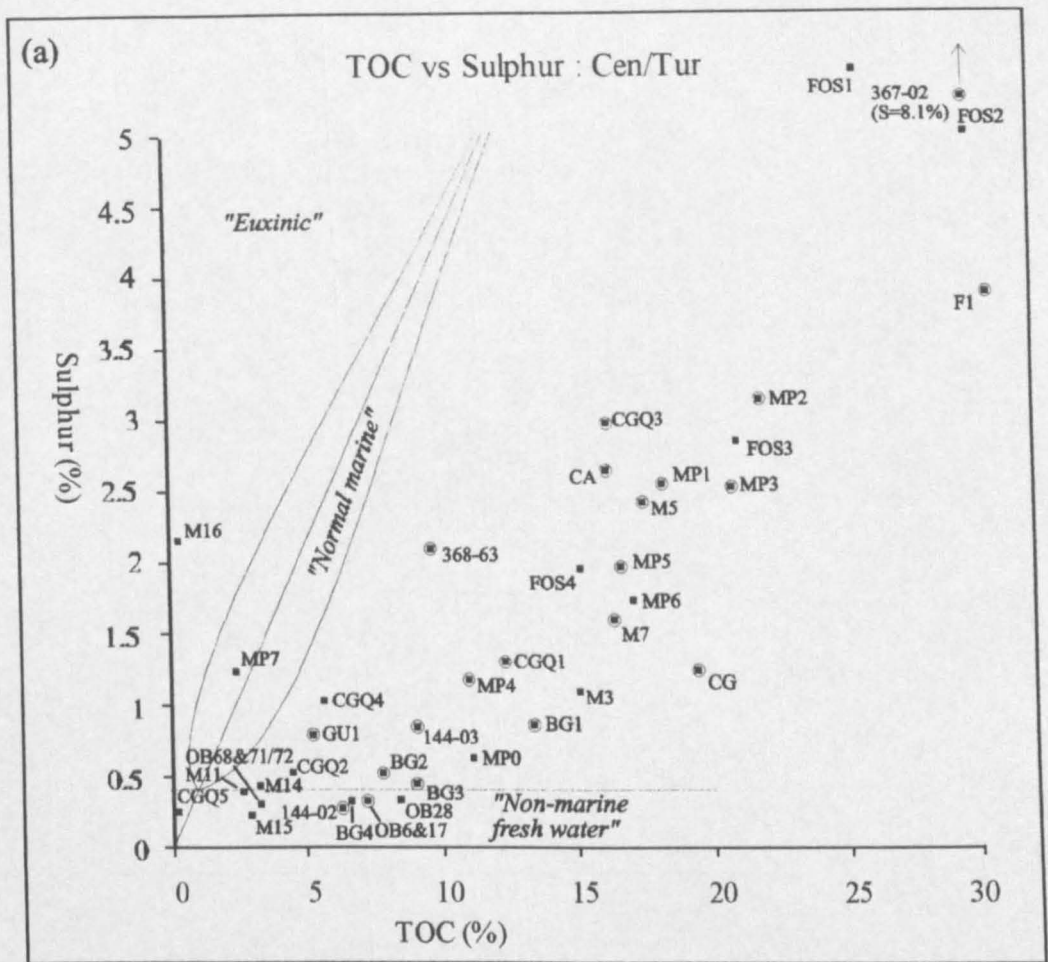
Fig 4.27a shows a plot of TOC against sulphur for all of the Cen/Tur samples analysed in this chapter and extends that of Farrimond *et al.*, (1990); samples shown to contain biomarkers of PZA are circled. It can be seen that most of the samples fall into a broad range where TOC values are approximately proportional to sulphur values, although, as noted by Farrimond *et al.* (1990), this range falls outside the regions classified by Berner and Raiswell (1983) as being either “euxinic” or “normal marine”, with some of the low sulphur samples even falling into the “fresh water” trend. Also, the trend in fig 4.27a is not parallel to the “normal marine” trend, and even sample 367 does not fall into the “euxinic” category. Furthermore, no particular patterns or trends are observable concerning those samples associated with a PZA regime or not. For instance, some PZA samples are present in the “fresh water” field, and it is apparent that some PZA and non-PZA samples are clustered together very closely in some areas of the plot. Therefore, there seems to be no particular relationship evident between TOC, sulphur and the occurrence or not of PZA in these Cen/Tur black shales.

### *Porphyrim metallation*

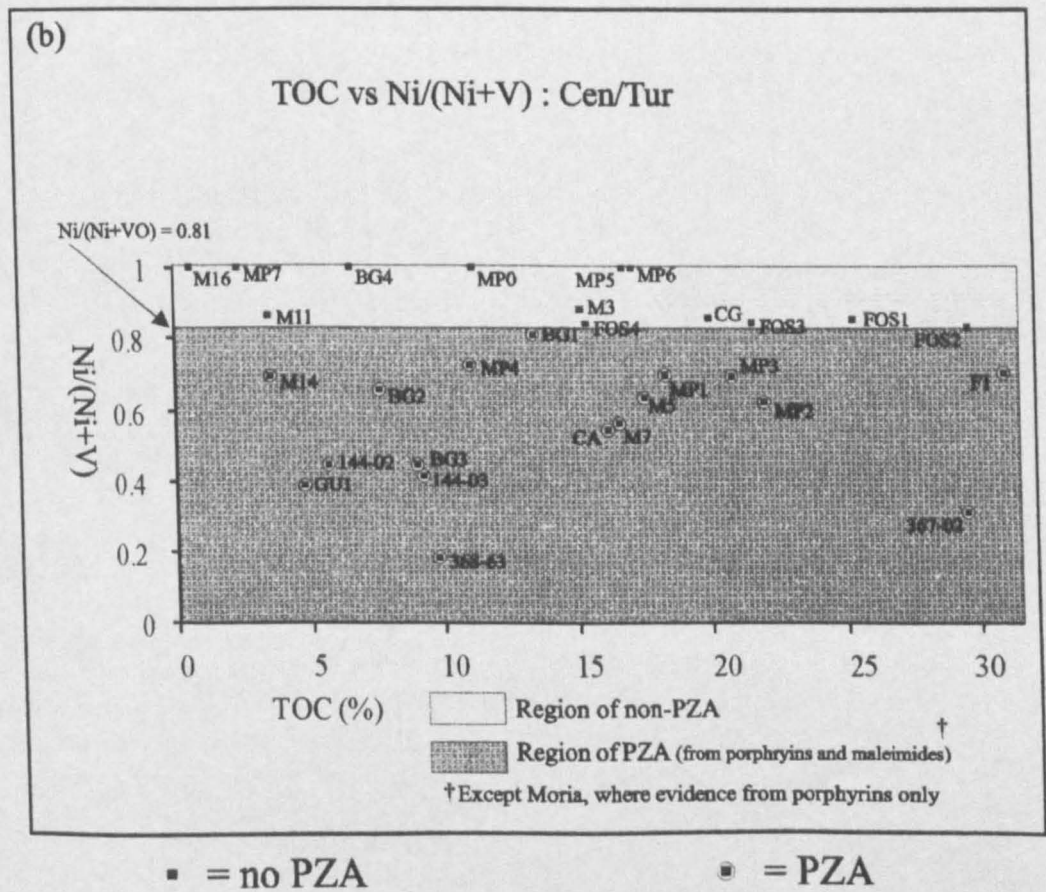
Changes in Ni:VO porphyrin ratio are thought to be dependent on both the redox state of the water column (Peters and Moldowan, 1993) and/or possible maturation effects (Huseby *et al.*, 1996) in samples which have generated organic matter. Lewan (1984) proposed that the ratio is a reflection of the level of oxygen depletion, as Ni (II) is more stable than VO (II) over a wider range of Eh-pH, so that VO porphyrins are generally thought to form only under anoxic conditions. The Ni:VO ratio may be lowered further



Fig 4.27 Relationship between PZA, TOC (%) and (a) Sulphur (b) Ni/(Ni+VO) porphyrin ratio



Fields of "normal marine", "non-marine fresh water" and "euxinic" from Berner and Raiswell (1985)

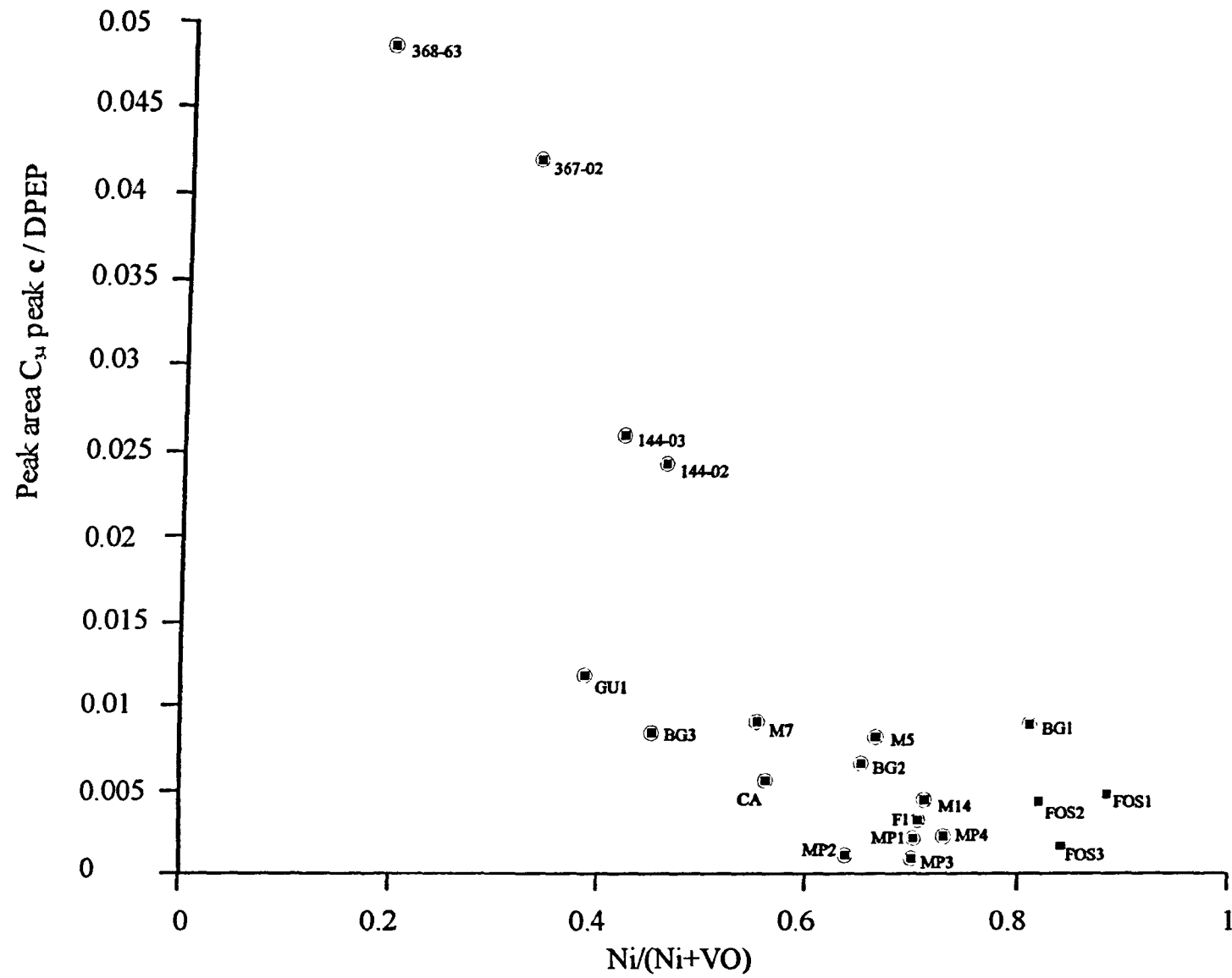


if sulphide is present in the water column, scavenging Ni(II) ions to form NiS. Hence, it was proposed that a very low Ni:VO ratio was associated with anoxicity/euxinia in the palaeo marine setting. This theory was backed up by determinations of such ratios in Toarcian (Moldowan *et al.*, 1986; Sundararaman *et al.*, 1993), and other Jurassic shales (Huseby *et al.*, 1996), and also in Cretaceous Brazilian continental margin sediments (Mello *et al.*, 1989) where the low Ni:VO ratios were correlated with samples deposited in more reducing environments. However, other authors report the occurrence of higher Ni:VO ratios in other Toarcian samples which, from probe-MS studies, were suspected to contain biomarkers of Chlorobiaceae (Eckardt *et al.*, 1991). As mentioned above, the ratio may also become altered if the sediments are subjected to high degrees of thermal stress, but these Cen/Tur samples are of low to moderate maturity.

Fig 4.27b is a plot of TOC against the porphyrin Ni/Ni+VO ratio, with samples again circled which are indicative of PZA. The figure shows that the sample set can be divided into two and without exception samples with Ni/Ni+VO  $\leq 0.81$  contain biomarkers indicative of PZA, whereas samples with Ni/Ni+VO  $\geq 0.81$  do not.

Therefore, it appears from these results that this criterion can be applied to help discern whether Cen/Tur black shale samples are deposited in a water column indicative of PZA or not (but see chapter 5). It is also interesting to note that samples close to the line on either side seem to be ones which are more difficult to interpret. The Fosto samples (Fos1-4), for example contain very small abundances of the peak c C<sub>34</sub> CAP components (fig 4.19), but were assigned as not showing the presence of PZA, as the presence of Me *i*-Bu maleimide was not sufficiently clear (Crawford, personal communication). Similarly, samples from sites 368 and 367 significantly have the lowest Ni:VO ratios and these samples contain a more intense bacteriochl signal than any of the other samples analysed. It is also noted that the Oued Bahloul samples are not included, as, due to the low amounts of porphyrins present, the metallo porphyrin fractions were not quantified. However, vanadyl components were present in both the samples revealing PZA, whereas OB71/72 did not contain vanadyl species or any HMW CAPs with the same retention times as the bacteriochl *d*-derived standards. Fig 4.28 plots the ratio of the peak area of C<sub>34</sub> peak c to DPEP (of ex-nickel distributions) against the Ni/(Ni+VO) ratio, and suggests an inverse trend, so that the samples with the highest Ni/(Ni+VO) ratios also contain the lowest relative amounts of bacteriochl *d*-derived C<sub>34</sub> CAPs.

Fig 4.28 Ni/(Ni+VO) ratio vs. peak area ratio of C<sub>34</sub> peak c CAP to DPEP in PZA samples



This relationship does, therefore, imply that the Ni/Ni+VO ratio can give some indication of the redox conditions of the water column during deposition of the Cen/Tur sediments, although ideally more samples need to be analysed to confirm this trend.

## CONCLUSIONS

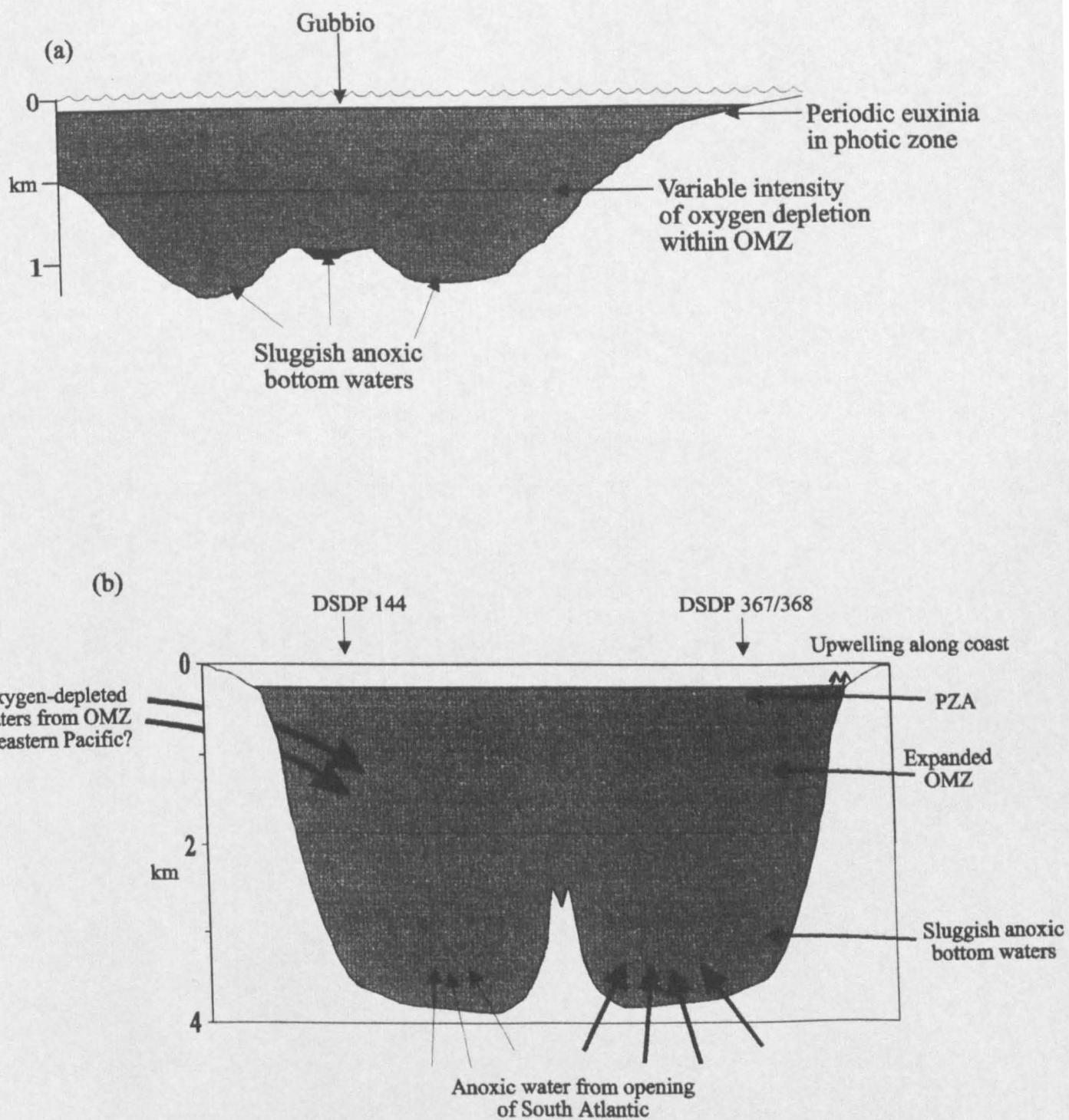
Porphyrin distributions, in particular, the presence of HMW CAPs with the same HPLC retention times as standards derived from the bacteriochls *d* of Chlorobiaceae, have been used to show that PZA was a characteristic of the water column during deposition of Cen/Tur black shales in a variety of palaeogeographical and oceanographical settings. Confirmation of PZA has, however, only been assigned when backed up with maleimide data (from Crawford, personal communication). It is noted though, that the good agreement between the results from these two types of biomarkers has shown further the value of the HMW CAP retention time method for assigning occurrences of PZA. Furthermore, results have shown that Cen/Tur samples containing metalloporphyrins with a Ni/(Ni+VO) ratio  $\leq 0.81$  were deposited under conditions of PZA, with low values corresponding to samples with higher relative amounts of bacteriochl *d*-derived components.

It has been shown for the first time that PZA existed periodically at six Livello Bonarelli sites in the Umbrian Appenines, at Oued Bahloul in Tunisia and the recent work of Sinningh  Damste and K ster (1998) showing the existence of PZA in the southern North Atlantic during Cen/Tur black shale deposition has been confirmed, particularly in the eastern sub-basin. The same authors also analysed one sample from the Bonarelli and found no evidence for PZA. The more detailed examination of a number of Bonarelli samples has however shown that temporal and spatial variations existed in the palaeo water column, and highlights the potential problems that may arise in the interpretation of the complex regional and local depositional processes of ancient black shales when analysing a restricted sample set.

The Livello Bonarelli and Oued Bahloul samples in general contained relatively low amounts of porphyrins derived from the bacteriochls of Chlorobiaceae compared with the algal-derived chls, a pattern also seen in the maleimide results. Inter and intra-bed variations in the ratios of the abundance of the C<sub>34</sub> peak *c* component compared with DPEP, as seen in the partial mass chromatograms and displayed graphically for two locations in fig 4.22, together with the similar variations in the amounts of Me *i*-Bu maleimide (Crawford, personal communication), infer that the frequency of PZA varied

considerably during deposition of the Cen/Tur shales along the continental margin of the Tethyan Ocean. The results indicate that local factors played a prominent role in the development of anoxic depositional conditions, and show further that a simple model of a continuous, uniform OMZ impinging on the Tethyan continental margin is simplistic. It seems likely that during the Cen/Tur along the continental margin of the Tethys, periodic pulses of productivity arose as a result of the varying degrees of regionalised and localised nutrient supply and upwelling. These conditions were superimposed on a water column that varied, both spatially and temporally, but was at times prone to oxygen deficiency. Hence, the idealised model shown in fig 4.29a best depicts the state of the water column during deposition of the black shales in the Umbrian Basin. With the Livello Bonarelli samples showing the existence of PZA at certain times during black shale deposition of during the Cen/Tur OAE, it is perhaps not surprising that PZA was more prevalent in the southern North Atlantic, considering the more severe conditions of oxygen depletion which many authors propose to have existed during this time (see earlier). Although this period was seemingly characterised by high equable temperatures, reduced bottom water circulation and an overall tendency towards oxygen deficiency and preservation of OM, differences between the ratios of PZA biomarkers from the Atlantic sites, implies further that localised factors played a role in the production/preservation of OM. The ratio of the C<sub>34</sub> and C<sub>35</sub> bacteriochl *d*-derived CAPs to DPEP is, in all the Atlantic samples, much higher than the corresponding ratio in all of the Livello Bonarelli or Oued Bahloul samples, a pattern which is also seen in the maleimide distributions. This shows that the contribution of bacteriochl *d*-containing organisms in both the western and eastern regions of the southern North Atlantic was higher than in the margins of the Tethys ocean during the Cen/Tur boundary event. This would in turn seem to suggest that the extent of the oxygen depletion was more intense in the former. With such an extensive contribution of Chlorobiaceae recorded in a sample (367-02) of very high TOC content but which seems to represent a moderate productivity (*e.g.* Bralower and Thierstein, 1984), it appears likely that anoxic conditions existed within the photic zone for a significant period of time at site 367 during the Cen/Tur. Taken with other evidence for anoxic abyssal bottom waters at sites 367 and 368, as well as other regions of the West African margin, it seems likely that the anoxic conditions were strengthened during the Cen/Tur event at these sites with a high influx of nutrients and oxygen-depleted waters from the adjacent continental basins and from the South Atlantic and Pacific during the large

Fig 4.29 Schematic model of deposition of Cenomanian/Turonian black shales  
 (a) Livello Bonarelli (b) Southern N. Atlantic DSDP sites



marine transgression, so that anoxic conditions may even have existed at times throughout the entire water column.

**CHAPTER 5**  
**LC-MS STUDIES OF PORPHYRINS FROM**  
**BLACK SHALES DEPOSITED DURING THE**  
**APTIAN AND TOARCIAN**  
**OCEANIC ANOXIC EVENTS**



## INTRODUCTION

### General

This chapter concerns black shales deposited during two other major OAEs, the Aptian 1a (Mid-Cretaceous) and the Toarcian (Jurassic). Here, widespread deposition of organic-rich sediments occurred during both of these time periods under a variety of depositional regimes. The Aptian “Livello Selli” samples are taken from the Umbria region, being deposited on the continental margin of the western Tethys. Toarcian samples include a suite also from Umbria (Valdorbia) plus a sample from further north in Italy (Belluno), also both deposited on the continental margin of the Tethys. Other samples come from two epicontinental basinal sites; the Paris Basin (Semécourt and Colombotte) and from Holzmaden in the S.W German Basin. It should be noted that much of the discussion in chapter 4, in particular concerning the general effects of Jurassic/Cretaceous warm equable temperatures, WSBW, sluggish ocean circulation, marine transgressions and local productivity/preservational factors also apply to the samples discussed in this chapter.

### Aptian OAE:- “Livello Selli”

Organic-rich shales and marls occur throughout the Aptian and Albian in many parts of the world, being deposited in a wide range of oceanic settings. A review of the occurrences of these deposits can be found in Jenkyns (1980). Many of these locations are thought to be characterised by a brief period in the Lower Aptian (<1Myr) of high productivity and peak levels of anoxia/dysoxia, within the midst of longer periods of periodic oxygen depletion (*e.g.* Arthur *et al.*, 1990; Bralower *et al.*, 1994). However, the duration of these events has been found to vary between different settings (Bralower *et al.*, 1994).

In the Italian Apennines, the Scisti a Fucoidi covers the large rhythmic series of pelagic limestones, marlstones and black shales deposited between early Aptian and late Albian, and is related to the Aptian OAEs (Arthur *et al.*, 1990), being described in detail by Pratt and King (1986) and Coccioni *et al.* (1987, 1989, 1992). A number of thin, discrete black shale intervals are found at regular intervals, representing an extensive interval of periodic oxygen deficiency coupled to Milankovitch-type climatic cycles similar to those of the Cen/Tur shales described in chapter 4 (Herbert and Fischer, 1986; Fischer *et al.*, 1990). One of the most prominent intervals is the Livello Selli, deposited during the earliest Aptian (*ca.* 118 Myr) OAE (OAE1a; Arthur *et al.*, 1990), corresponding to the early stages of deposition of the Scisti A Fucoidi (Coccioni

*et al.*, 1992). The Gorgo A Cerbara section, 3km west of Piobbico (fig 4.3), contains a prominent exposure of the Livello Selli a few hundred yards upstream from the Livello Bonarelli exposure (sample GCLB, chapter 4) beside the Torrente Candigliano. This 190cm section, devoid of planktonic and benthic foraminifera (Coccioni *et al.*, 1992) consists of a series of laminated black shales interbedded with bioturbated limestones, mudstones and radiolarian sands. Such low carbonate content may have been as a result of a higher CCD (see below) in the early Aptian (Thierstein, 1979), and/or low coccolithophore/high dinoflagellate production in high fertility surface waters (Bralower *et al.*, 1994 and refs. therein). Coccioni *et al.* (1987, 1989) describe the section as being separated into two intervals of equal thickness; a lower “green” interval and an upper “black” interval, with pyrite deposition seen at the base of the upper “black” section which also contains fish remains. As with the Livello Bonarelli sediments (chapter 4), the Livello Selli is of low thermal maturity (Pratt and King, 1986) and contains no turbiditic structures, representing pelagic sedimentation in the deep Umbrian Basin along the continental margin of the western Tethys. The OM is primarily marine derived (Pratt and King, 1986), with TOCs reaching 9% (Coccioni *et al.*, 1986) although the highest value measured in the shales examined here and by Pratt and King (1986) is <6% (see below; table 5.1). Although most of the black shales deposited within the Scisti a Fucoidi represent periods of low to moderate productivity, the Livello Selli with higher TOC, and a positive  $\delta^{13}\text{C}_{\text{org}}$  excursion of *ca.* 2‰ (Schlanger *et al.*, 1987; Weissert, 1989) is thought to represent a period of enhanced productivity similar to that seen during deposition of the Livello Bonarelli (Coccioni *et al.*, 1992). Indeed, similarities between the two events have been noted, with Aptian-Albian transgressions, resulting from tectonic plate motion and consequent expansion of mid-oceanic ridges (Hays and Pitman, 1973; Hay *et al.*, 1988; Erbacher and Thürow, 1997), thought to be responsible for the development of anoxic conditions and increases in the global production of organic carbon (Jenkyns, 1980).

An ocean-wide nannoconid extinction occurred 40-100 kyr before the Selli (at the beginning of the “early critical interval”), correlating with the onset of the C-isotope excursion (Weissert *et al.*, 1998). During the “early critical interval”, prior to the Livello Selli, the nannofossils decrease in overall size and diversity, consisting primarily of small hedbergellids (Coccioni *et al.*, 1992). These smaller species are found under oxygen depleted conditions, as they have a higher surface to volume ratio

and lower oxygen consumption (Berhhard, 1986; Phleger and Soutar, 1973). Further evidence for an expanded OMZ, as opposed to the stable expansion of anoxic bottom waters, comes from the benthic forams, which remain during this critical interval until the beginning of the Livello Selli (Coccioni *et al.*, 1992). Pre-Livello Selli radiolaria fluctuation events are also thought to result from the OMZ expansion due to the increased nutrient-enhanced productivity (Erbacher *et al.*, 1996). However, it is also noted that most Aptian-Albian black shale deposits are found in the more restricted small ocean basins, inferring that limited deep water circulation was still an important control (Schalnger and Jenkyns, 1976; Ryan and Cita, 1977; Jenkyns, 1980; Görür, 1994). Lateral equivalents of the Livello Selli in France and Switzerland also contain positive carbon isotope excursions (Brown *et al.*, 1997), although significant differences in the isotope curves suggest that local factors imposed a significant imprint onto the wider pattern of carbon burial during this time period. Furthermore, Aptian-Albian black shales cored from the Atlantic and deposited over a wide range of palaeo depths, contain a significant terrestrial input (*e.g.* Jenkyns, 1980), with the high frequency rhythmic shale deposition interpreted as being initiated by productivity increases and OMZ expansion as a result of the increased influx of nutrients from land during more humid climatic periods (Hofmann *et al.*, 1997). Cyclical black shales are also deposited further north along the margins of the Tethys and are interpreted as relating to changes in water circulation with shale deposition occurring during periods of stagnation in the deep Lombardy and Belluno basins (Weissert *et al.*, 1979). However, the Umbrian Livello Selli is generally thought to have been deposited as a result of a relatively brief productivity event (Coccioni *et al.*, 1992; Bralower *et al.*, 1994) due to increased nutrient levels from weathering and run-off (Weissert *et al.*, 1998) in association with a large marine transgression (Jenkyns, 1980). This occurred in combination with the effects of oxygen depleted bottom water conditions in the deep Umbrian Basin, the latter being periodically present throughout much of the Cretaceous as a result of increased temperatures, WSBW supply and reduced circulation (Weissert, 1989; Arthur and Premoli-Silva, 1982; Pratt and King, 1986; Coccioni *et al.*, 1992; Bralower *et al.*, 1994; Görür, 1994). Furthermore, the correlation between the OAE and an abrupt increase in spreading rates and mid-plate volcanism (Larson, 1991; Bralower *et al.*, 1993, 1994), would have led to increased levels of CO<sub>2</sub> (and a subsequent rise in the CCD), sea level (Schlanger *et al.*, 1981), temperature and oxygen deficiency (Erbacher and Thürow, 1997). This may have resulted in an overturn of the water

column promoting a large productivity event *via* the mixing of nutrient-rich oxygen depleted bottom waters with surface waters (e.g. Vogt, 1989).

Analysis of porphyrin and maleimide distributions should therefore shed further light on the redox state of the upper water column during this early Cretaceous OAE.

### Toarcian OAE

This OAE (early Toarcian, *ca.* 192 Myr, early *falciferum* Zone) is represented by large benthic and planktonic faunal changes (Hallam, 1987b) and the widespread, deposition of black shales (e.g. Baudin *et al.*, 1990), particularly throughout Europe, lasting *ca.* 0.5 Myr (Jenkyns, 1988), in a range of pelagic sections and in epicontinental seas (Hallam, 1981; Jenkyns, 1988; Farrimond *et al.*, 1988, 1989; Katz, 1995). Most Toarcian pelagic sediments occur together with a positive carbon isotopic excursion,  $\delta^{13}\text{C}_{\text{carb}}$ , (Jenkyns and Clayton, 1986, 1997; Jenkyns, 1988) within the *falciferum* zone of the same magnitude as that at the Cen/Tur (Schlanger *et al.*, 1987); this together with the OM-enrichment and type II kerogen, again suggests a global factor behind the wide ranging deposition of organic-rich shales (Arthur *et al.*, 1988; Jenkyns *et al.*, 1994; Jenkyns and Clayton, 1997). An upwelling-induced productivity event, inferred from a negative  $\delta^{13}\text{C}_{\text{carb}}$  excursion seen in Italian, Swiss and Hungarian sections (*spinatum* and *tenuicostatum* zones) prior to the *falciferum* zone, is interpreted as reflecting the upwelling of isotopically-light  $\text{CO}_2$ , derived from bacterial decomposition of OM, prior to the depositional event (Jenkyns and Clayton, 1986). Although samples examined here are exclusively from European sections, sediments of the similar age from other areas (e.g. Australia, Japan, Alaska, Argentina) display similar sedimentological and isotopic characteristics, implying further the concept of a global OAE (e.g. Jenkyns, 1988; Baudin *et al.*, 1990). However, in SW German and Paris Basin sections, a negative isotope excursion is seen within the *falciferum* zone (Küspert, 1982; Moldowan *et al.*, 1986; Hollander *et al.*, 1991), which contradicts the pattern of large global carbon burial, unless outweighed by the effects of recycling of isotopically light  $\text{CO}_2$  from within shallow anoxic layers (Küspert, 1982; McKenzie, 1982; van Kaam Peters, 1997), or with significant changes in the planktonic community (*i.e.* as a result of calcareous nannoflora being replaced, during deposition, by non-carbonate secreting plankton which showed greater discrimination against  $^{13}\text{C}$ ; Jenkyns and Clayton, 1986). However, Jenkyns and Clayton (1997) have subsequently shown that the negative  $\delta^{13}\text{C}$  excursion pre-dates the positive excursion. Strontium isotope curves show a rapid drop

in the seawater  $^{87}\text{Sr}/^{86}\text{Sr}$  ratio during the Early Jurassic, as seen in Aptian and Cen/Tur times (see earlier) and is here also thought to represent an increase in volcanism and/or hydrothermal and tectonic activity, with the latter possibly associated with the rifting of the Central Atlantic (Jones *et al.*, 1994).

### *Southern European sections*

Toarcian black shales occur throughout this region which stretches from Austria/Hungary in the north, to Tunisia/Sicily/Greece in the south (Jenkyns, 1988). They were deposited on the continental margins of the Tethys Ocean over a variety of palaeo depths and are generally lower in TOC than samples deposited further north in Europe (Jenkyns, 1985, 1988; Baudin *et al.*, 1990). Previous authors generally describe the expansion of an OMZ (Jenkyns, 1985, 1988), maintained and intensified by transgression-related (Hallam, 1981, Haq *et al.*, 1987) upwelling over the continental margin (Parrish and Curtis, 1982), and poor deep ocean circulation (see above), with black shale deposition occurring where this OMZ impinges on the continental slope (Jenkyns, 1985, 1988; Farrimond *et al.*, 1988; Baudin *et al.*, 1990). The two Italian locations from which samples were taken are shown in fig 5.1. A palaeogeographical cross-section (from Farrimond *et al.*, 1988) of the northern Italian region is shown in fig 5.2.

### **Belluno**

Toarcian black shales are exposed at Longarone, near Belluno, north of Venice and east of the Trento Plateau, in a trough with a palaeo depth of approximately 1km and width of *ca.* 30km (fig 5.2). Black shales have been described from most of the major locations depicted in fig 5.2. Those from the Belluno Trough are laminated, dark brown-coloured, and contain fish remains, being interbedded with radiolarians and limestones (Jenkyns, 1988). It is thought that anoxic conditions developed gradually during the Toarcian in this area (Farrimond *et al.*, 1994). One sample from near the bottom of the 6m section (collected by Farrimond, 1987), has TOC and S = 3.3% and 0.42% respectively, and contains abundant OM of low maturity with minimal terrestrial contribution (Farrimond *et al.*, 1988, 1994).

However, synchronous deposits in the deeper Generoso Trough, in the Lombardian Basin west of Val Varea (fig 5.2), contain red limestones and do not include black shales, further strengthening the argument for the expanded OMZ model of organic-rich shale deposition along this continental margin during this OAE (Jenkyns, 1988).

As postulated by Jenkyns (1988), a lateral expansion of the OMZ may have occurred as

Fig 5.1 Map of Italy showing locations of Toarcian samples

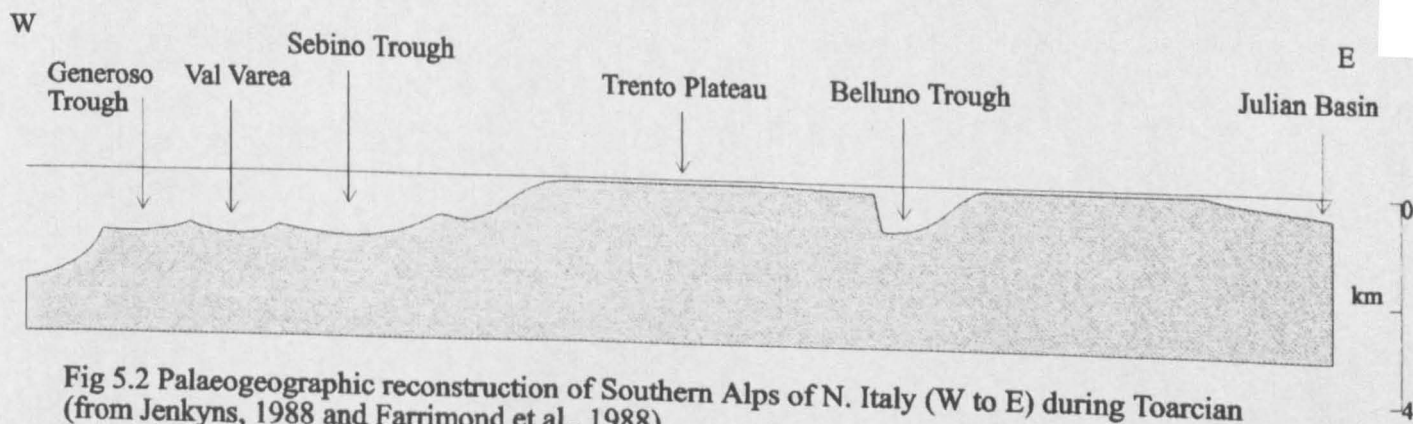


Fig 5.2 Palaeogeographic reconstruction of Southern Alps of N. Italy (W to E) during Toarcian (from Jenkyns, 1988 and Farrimond et al., 1988)

a result of the increased nutrient supply, subsequent upwelling, as predicted by Parrish and Curtis (1982), and increased productivity over the North European continental shelf further north, during marine transgressions. Although there is strong evidence, therefore, for the presence of a substantial OMZ over much of this region (*c.f.* chapter 4), it is difficult to determine to what extent this reached, and indeed whether this region of the water column was ever completely devoid of oxygen. For instance, the lower TOC values in the Tethyan margins compared with samples deposited on the shelf further north, together with the low degree of steroid preservation seen in the Belluno sediment, and in sediments from other basins, was taken by Jenkyns (1988) and Farrimond *et al.* (1988) as resulting from the degradation of OM in a partly oxygenated water column. This implies that part of the water column was oxygenated so that the OMZ did not expand throughout the entire water column in this region and the development of anoxic conditions was not quite as widespread as originally proposed (Baudin *et al.*, 1990). Also, a lack of correlation between TOC and S is seen in a selection of north Italian Toarcian sediments (Jenkyns, 1988), as seen previously in the Cen/Tur sediments (Farrimond *et al.*, 1990 and chapter 4). Thus, further investigation is required into the redox state of the water column, from an investigation of bacteriochl-derived porphyrins and maleimides.

#### Valdorbia

A large exposure of *ca.* 15m of *falciferum* shales and limestones is seen in a cliff exposure at Valdorbia (fig 5.1) near Gubbio, although the base of the zone is not visible. Seven samples were collected from levels 2m apart in June 1996 under the supervision of Dr. Hugh Jenkyns, and contain TOC values between 2.5 and 6.5%. This section also exhibits a pronounced  $\delta^{13}\text{C}$  positive shift of *ca.* 2‰ within the early *falciferum* zone which peaks at the base of the exposed section (Jenkyns and Clayton, 1986). With Valdorbia located in the Umbrian Basin, the palaeogeography of the setting is similar to that of the Cen/Tur Livello Bonarelli shales, although the depth of the basin during the Jurassic is still debated, with palaeobathymetrical interpretations ranging from “deep” to no more than 200m (Palliani *et al.*, 1998 and refs. therein). The sea-level rise is thought to have led to increased primary productivity resulting in an expanded OMZ maintained by the general stability of the water column and a decrease in bottom water oxygenation (Farrimond *et al.*, 1988; Palliani *et al.*, 1998). Climatic-eustatic fluctuations are also thought to be important controls on the production and

preservation of OM (*e.g.* Mattioli, 1997) with sediments of greatest TOC corresponding to deposition during the maximum level of Toarcian transgression (Hallam, 1988; Palliani *et al.*, 1998). Recent work on early Toarcian sediments from elsewhere within Umbria concludes, from interpretation of nannofossils, that the chemocline existed near the sediment-water interface and that fully anoxic conditions were not generally present within the water column of the Umbrian Basin during this time period (Palliani *et al.*, 1998). So again, analysis of porphyrin and maleimide distributions might therefore shed further light on the nature of the water column during this OAE.

### **North European sections**

Early Toarcian shales in the more northerly shelf regions of Europe are situated at slightly higher latitudes than the northerly limit of Tethys and were deposited in epicontinental basins which formed due to widespread flooding (*e.g.* Hallam, 1975; Loh *et al.*, 1986). They therefore represent depositional environments different from those of the sediments deposited on the continental margins of the Tethys, *i.e.* more closely related to the modern Black Sea (fig 4.1). The two basins discussed (Paris Basin and South German Basin) were restricted (silled), but had open connections to each other and to the northern Tethyan margin (Riegraf *et al.*, 1984; Katz, 1995). Authors generally propose that Toarcian deposition occurred in shallow, stratified, productive anoxic basins (*e.g.* Kaufmann, 1981; Küspert, 1982; Jenkyns and Clayton, 1986; Prauss and Riegel, 1989; Hollander *et al.*, 1991), with stagnation of the warm, nutrient-rich waters arising from reduced water column circulation due to the seas deepening during marine transgressions which began earlier during the Liassic (Hallam, 1981), and due to the general low solubility of oxygen in the higher sea temperatures of the Jurassic. The transgression is also thought to have resulted in an increased nutrient flux from flooded land areas into the epicontinental seas, resulting in higher productivity (Hallam, 1981; Jenkyns, 1985). Stratification may also have been influenced to some extent by salinity stratification during more humid periods, suspected by some authors to have affected the north of the Tethys (*e.g.* Farrimond *et al.*, 1989), with large volumes of river run-off further facilitating such development as well as increasing the flux of nutrients and detrital clays to the seas (Jenkyns, 1988; Littke *et al.*, 1991b; Prauss *et al.*, 1991). Trace metal concentrations, similar to those of Black Sea sediments, support the idea of deposition under anoxic water (Brumsack, 1988, 1991), with high Co, Mn and Pb concentrations interpreted as arising from a major fluvial source (Brumsack, 1991). Black shales are thought therefore to have been deposited during times of higher



productivity, but in combination with conditions, described above, favourable to enhanced preservation of OM (e.g. Disnar *et al.*, 1996). The coincidence between the transgressions and deposition of organic rich shales (Hallam, 1981) could be explained further by the onset of upwelling along the Tethys margin further south (Jenkyns, 1988), although it is debatable whether such upwelling directly affected black shale deposition in Northern Europe (Tyson, 1987). The time span of black shale deposition in these epicontinental seas is longer than the time period in the continental margins of the Tethys Ocean (see above), and is generally thought to be between one (Hallam, 1975) to three million years (Littke *et al.*, 1991a). Hence, increased nutrient supply is thought to have resulted more from increased surface run-off (Littke *et al.*, 1991b) rather than from the inflow of nutrient rich waters from the Tethys (Fleet *et al.*, 1987).

#### *Paris Basin (Semécourt and Colombotte)*

“Schistes Cartons” were deposited up to a maximum thickness of 30m in parts of the Paris Basin (Tissot *et al.*, 1971). Shales of the *falciferum* zone have characteristics similar to those deposited elsewhere (Jenkyns, 1988), being dark-coloured and generally laminated (Hollander *et al.*, 1991). Semécourt is positioned in the north east of the Paris Basin, with Colombotte lying in the south east (MacKenzie *et al.*, 1980a). The positions of the samples within the sections is unknown (MacKenzie *et al.*, 1980a; Farrimond *et al.*, 1989). The Semécourt sample (SM; TOC = 6.8%) and the more southern Colombotte sample (CL; TOC = 7.9%) are of low maturity (MacKenzie *et al.*, 1980a,b; Farrimond *et al.*, 1989), both being buried at relatively shallow depths (ca. 700m; MacKenzie *et al.*, 1980a). Laminations, with complete preservation of calcareous nannoplankton and pyrite indicates the presence of anoxic bottom waters, with the occurrence of sulphate reduction within the sediment (Hollander *et al.*, 1991). Other previous data suggest most of the OM is of marine origin, with a relatively minor terrestrial component (Alpern and Cheymol, 1978; Farrimond *et al.*, 1989; Hollander *et al.*, 1991). There is also tentative biomarker evidence for bottom waters of higher salinity in the northern region of the basin (Huc, 1976; MacKenzie *et al.*, 1980a; Farrimond *et al.*, 1988; ten Haven *et al.*, 1986), which may have originated from the shallower regions of the basin, and led to increased stratification (Farrimond *et al.*, 1988).

#### *SW German Basin (Holzmaden)*

The Posidonia shale (Posidonienschiefer), deposited throughout the southern German Basin in the Posidonia Sea, is found at Holzmaden, near Stuttgart. Early classification

described the deposition and excellent preservation of the shales in the extensive shallow sea under stagnant, anoxic conditions, similar to that of the present Black Sea (Seilacher, 1970), with evidence for anoxic bottom waters from the lack of bioturbation with preserved laminations, fossils and pyrite. However, observations from fossils of current activity (Kauffman, 1981) and periodic benthic colonisation infers that the redox boundary fluctuated throughout deposition of the shales (Kauffman, 1978) with periods of stagnation occasionally interrupted by less anoxic and more circulatory periods (Brenner and Seilacher, 1978).

Two samples (HL10 and HL12) of dark grey, laminated shales were provided by Dr. C.B. Eckardt, both coming from outcrops at Holzmaden from the Middle Lias  $\epsilon$  (Unterer Schiefer, horizon II/4) of the Lower Toarcian (Eckardt *et al.*, 1991; Waring, 1991). They had a maximum burial depth of *ca.* 800m (Moldowan *et al.*, 1986) resulting in marginally maturity of the hydrogen-rich OM ( $R_o$  *ca.* 0.51%; Kuspert, 1983). The TOC values are 11.5% and 11.9% respectively, with sulphur 1.8% for both samples. Although there are variations in porphyrin concentrations and Ni:VO ratios over the entire Toarcian section, with very low Ni/(Ni+VO) porphyrin ratios in some sections supporting an anoxic depositional environment (Moldowan *et al.*, 1986), the sample studied contains high amounts of porphyrins with a significant presence of vanadyls ( $Ni/(Ni+VO) = 0.72$ ).

Recent work by van Kaam Peters (1997) on Toarcian samples from two sites in the SW German Basin found the presence of isorenieratane (35) in all samples, but with markedly higher concentrations in samples from the *falciferum* zone of the Middle Lias  $\epsilon$ . One from the Unterer Schiefer (correlating with the Holzmaden samples) contained significant, but lower concentrations of isorenieratane. Probe mass spectra of the total porphyrins obtained previously from one of the Holzmaden samples, showed the presence of CAP and aetio components in the  $C_{26}$  to  $C_{33}$  range in the nickels and a similar range reaching  $C_{34}$  in the vanadyl CAPs (Eckardt *et al.*, 1991; Waring, 1991). Demetallated fractions more clearly showed the presence of HMW CAPs (up to  $C_{35}$ ) with molecular ions corresponding to Bi-CAP and Benzo-types also identified.

## RESULTS AND DISCUSSION – APTIAN


The lithological section of the Livello Selli exposure at Gorgo A Cerbara is shown in fig 5.3. Six samples (GAC1-6) were selected (160-330g sediment) for analysis (table 5.1).

Sample	TOC (%)	S (%)	Ni Porph (µg)
GAC1	3.87	1.00	650
GAC2	2.64	1.07	450
GAC3	0.97	0.36	45
GAC4	0.87	0.61	35
GAC5	5.16	1.04	2600
GAC6	3.54	0.9	1690

Table 5.1 TOC and S and porphyrin data for Livello Selli samples (GAC1-6)

Nickel porphyrins were present in all 6 samples, but no vanadyls were detected. The demetallated Ni porphyrins were found to contain a range of CAP and aetio-type porphyrins with overall distributions very similar to the distributions seen in the Cen/Tur Livello Bonarelli samples (chapter 4). The base peak chromatograms (*e.g.* GAC1; fig 5.4) show a range of components, mainly of the CAP type but also with a significant presence of aetios. Significant peaks, identified from the spectra, include C<sub>29</sub>-C<sub>33</sub> CAPs (*m/z* 435, 449, 463, 477 and 491), with DPEP (1) the most abundant, and aetio types within the range C<sub>28</sub>-C<sub>32</sub> (*m/z* 423, 437, 451, 465 and 479). MPMPs calculated for these samples range from 0.18 to 0.57 (Appendix A) showing a low to moderate maturity. The results show a range of CAPs eluting in the expected HMW region (*c.f.* chapter 2) with patterns similar to the Bonarelli CAPs, with the bacteriochl *d*-derived CAPs (confirmed by the mass spectra), present in three of the six samples (GAC1, 5 and 6; fig 5.5). These components (shaded) are again present in low abundance with, for example, the C<sub>34</sub> peak *c* present in all three samples in a much lower abundance than the non-PZA peak *b*. Porphyrin results therefore show evidence for PZA in GAC1, deposited early during the Selli event, and in GAC5 and 6, the last black shales to be deposited in the section.

The free maleimides in samples GAC1, 5 and 6 contain Me *i*-Bu maleimide (Crawford, personal communication), confirming the presence of a bacteriochl-derived component in the same samples.



Green/grey shales

Fig 5.4 Base peak chromatogram of ex-nickel porphyrins in Livello Selli sample GAC1

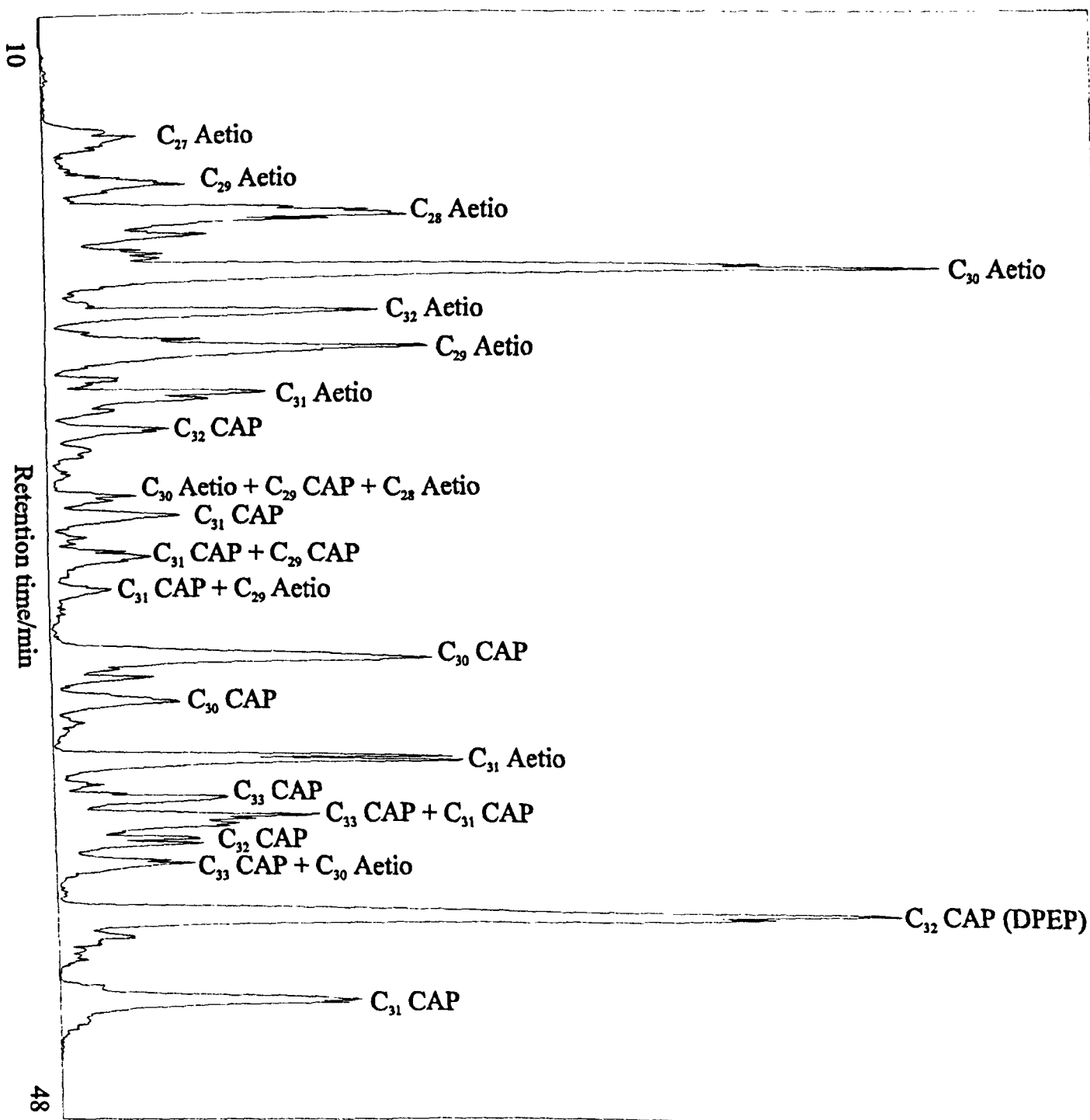
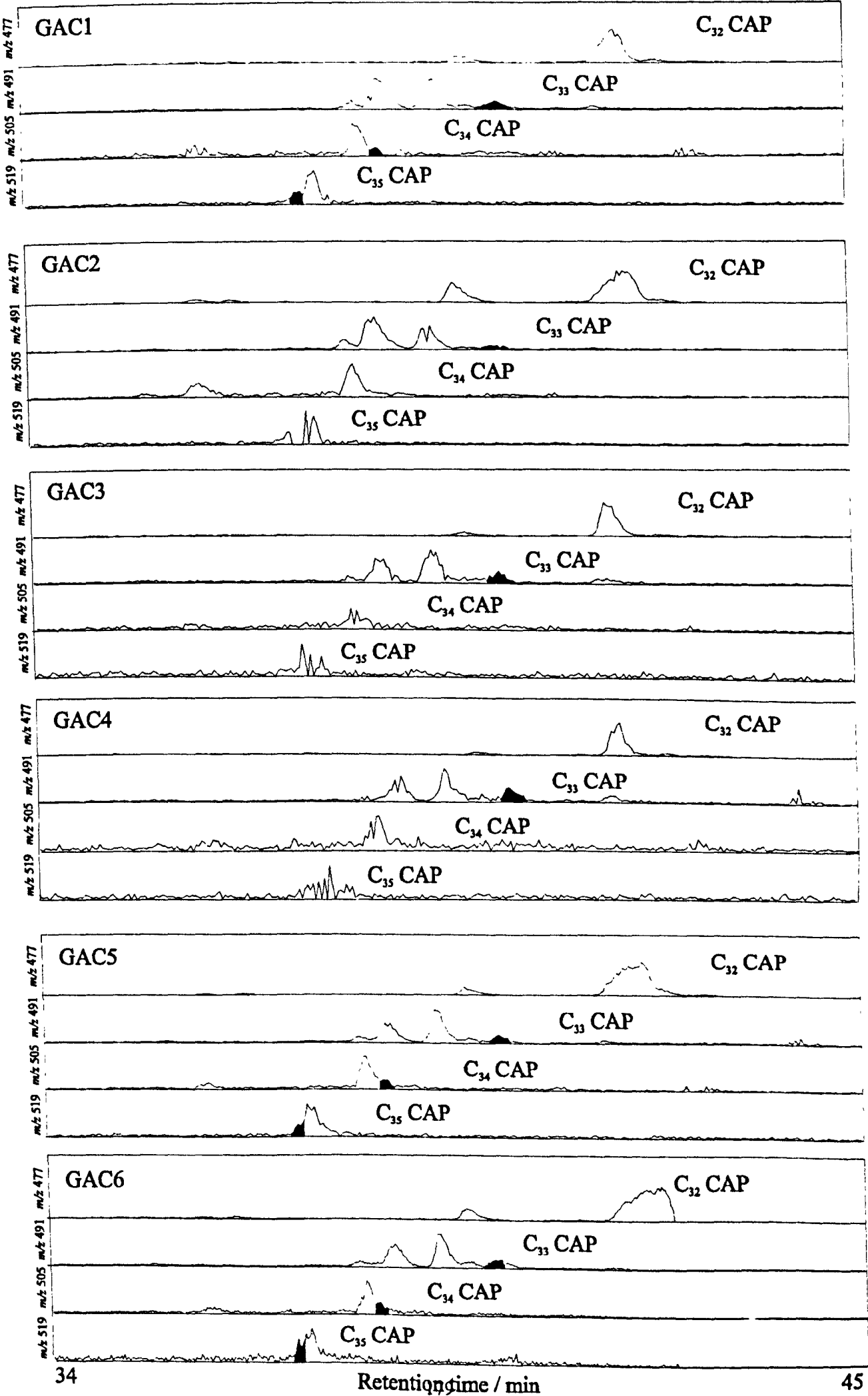


Fig 5.5 Partial mass chromatograms of CAPs (C<sub>32</sub>-C<sub>35</sub>) in Livello Selli samples from Gorgo A Cerbara

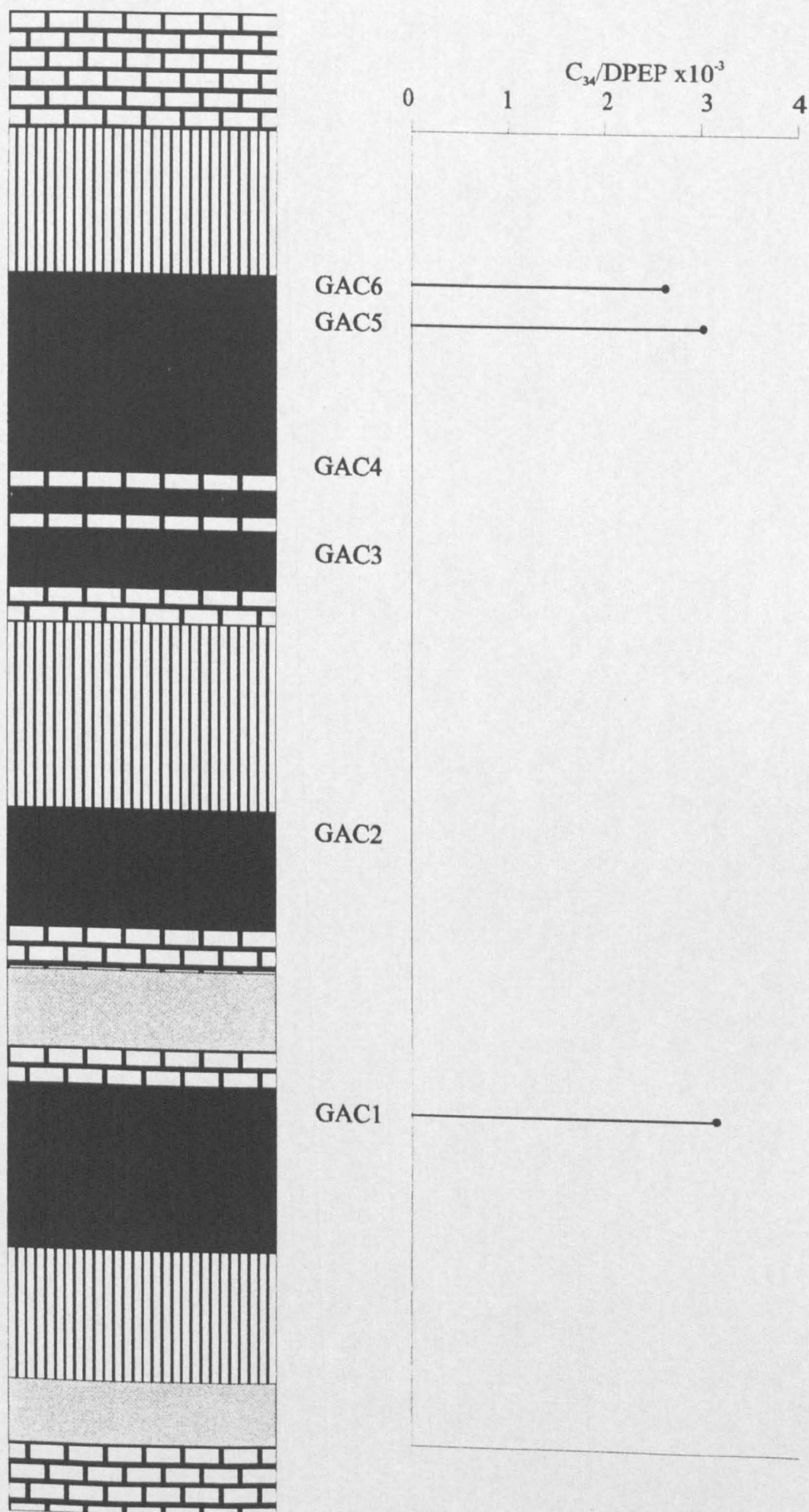


Hence PZA existed at the time of deposition of the Livello Selli during the Aptian OAE1a, indicating that the level of oxygen depletion, associated with black shale deposition, was periodically sufficiently intense over this part of the Tethyan continental margin (*ca.* 27 Myr prior to the Cen/Tur event) for anoxic conditions within the photic zone.

Lower  $^{87}\text{Sr}/^{86}\text{Sr}$  ratios measured in the Livello Selli sediments, as with the Livello Bonarelli (chapter 4), have been attributed to increased submarine volcanism, hydrothermal activity and sea-floor spreading during this time (Ingram *et al.*, 1994 and refs. therein). In turn, this may well have increased the flux of sulphide to the water column (Walker, 1986), decreasing the overall oxygen concentration.

This evidence from porphyrins and maleimides, together with evidence for the transgression-related stepwise extinctions of radiolaria and foraminifera and deposition of type II black shales containing indicators of a productivity-induced event (see above), thereby seems to strengthen the idea of the model of an intensified and expanded OMZ which reached from the sluggish bottom waters of the Umbrian Basin. This occurred periodically as no evidence for PZA was found in GAC2-4. Hence, with the generally low levels of dissolved oxygen in the sluggish waters during the Aptian, it seems that localised increases in productivity at the beginning and end of the Livello Selli, were sufficient to have resulted in the temporary expansion of anoxic waters into the photic zone. Fig 5.6 shows a plot of the ratio of peak areas of the  $\text{C}_{34}$  peak *c* relative to DPEP in the samples. The three samples containing evidence of PZA (GAC1, 5 and 6) have  $\text{C}_{34}/\text{DPEP}$  ratios of approximately 0.003, *i.e.* less than seen in the Bottacione Gorge samples, but similar to the Monte Petrano Livello Bonarelli samples (fig 4.28; chapter 4). Therefore, it seems that the relative contribution of green sulphur bacteria, and hence the intensity/frequency of anoxic water within the photic zone of the water column, were not significantly different during deposition of parts of the Livello Selli, as compared with the Livello Bonarelli, even though the TOCs are lower in the former. It is also noted that these samples contain no vanadyl porphyrins, so they are the first samples to be analysed in the present study which reveal PZA but have a  $\text{Ni}/(\text{Ni}+\text{VO})$  porphyrin ratio  $< 0.81$ , so therefore the relationship seen for the Cen/Tur samples in chapter 4 does not hold for these samples, for reasons unknown.

Fig 5.6 Plot of ratio of  $C_{34}$  peak c to DPEP in samples from Livello Selli section at Gorgo A Cerbara





## RESULTS – TOARCIAN

### Tethyan Continental Margin

#### *Valdorbia*

The seven samples (VAL1-7) revealed the presence of nickel porphyrins, but no vanadyls. Amounts of nickel porphyrin, plus TOC and S values are shown in table 5.2, although, unfortunately, bulk data were only obtained for three of the samples.

Sample	Depth below top of section (m)	TOC (%)	S (%)	Ni-porph. (µg)
VAL1	0.5	2.7	0.12	3
VAL2	2.5	-	-	5
VAL3	4.5	-	-	49
VAL4	6.5	6.5	0.43	34
VAL5	8.5	-	-	18
VAL6	10.5	-	-	19
VAL7	12.5	3.9	0.55	72

Table 5.2 TOC, S and Ni-porphyrin data for *Valdorbia* sediments

Samples VAL1 and 2 contained only minor amounts of porphyrins (table 5.2), so could not be analysed further, whereas the VAL3-7 fractions were demetallated. Fig 5.7 shows the base peak chromatogram of VAL4, with mass spectra of major peaks showing the presence of a range of CAP (C<sub>28</sub>-C<sub>33</sub>) and aetio-type (C<sub>26</sub>-C<sub>32</sub>) components. MPMPs for the samples range from 0.07 to 0.2 for VAL3-6, inferring a low thermal maturity, although the deepest sample VAL7 seems to have a more moderate maturity, with a higher value of 0.52 (Appendix A). A range of HMW CAPs elutes in the “expected” HMW region, with most samples showing distributions similar to the Umbrian samples deposited during the Cen/Tur (chapter 4) and in the Aptian (see earlier). The mass chromatograms again indicate those corresponding to the bacteriochl *d*-derived CAPs (fig 5.8). C<sub>33</sub>-C<sub>35</sub> components are present in samples VAL3, 4, and 7. The free maleimides (Crawford, personal communication) showed the presence of Me *i*-Bu maleimide in VAL1 to VAL7, excluding VAL5 and 6, confirming the porphyrin results. Only the C<sub>33</sub> peak is present in VAL6 which, on its own, is not taken as evidence for PZA (see above), and no Me *i*-Bu maleimide was found. VAL5 showed peaks corresponding to the C<sub>33</sub> and C<sub>34</sub>, but not C<sub>35</sub> components, and again no Me *i*-Bu maleimide was found.

Fig 5.7 Base peak chromatogram of ex-nickel porphyrins in Toarcian sample VAL4 from Valdorbia

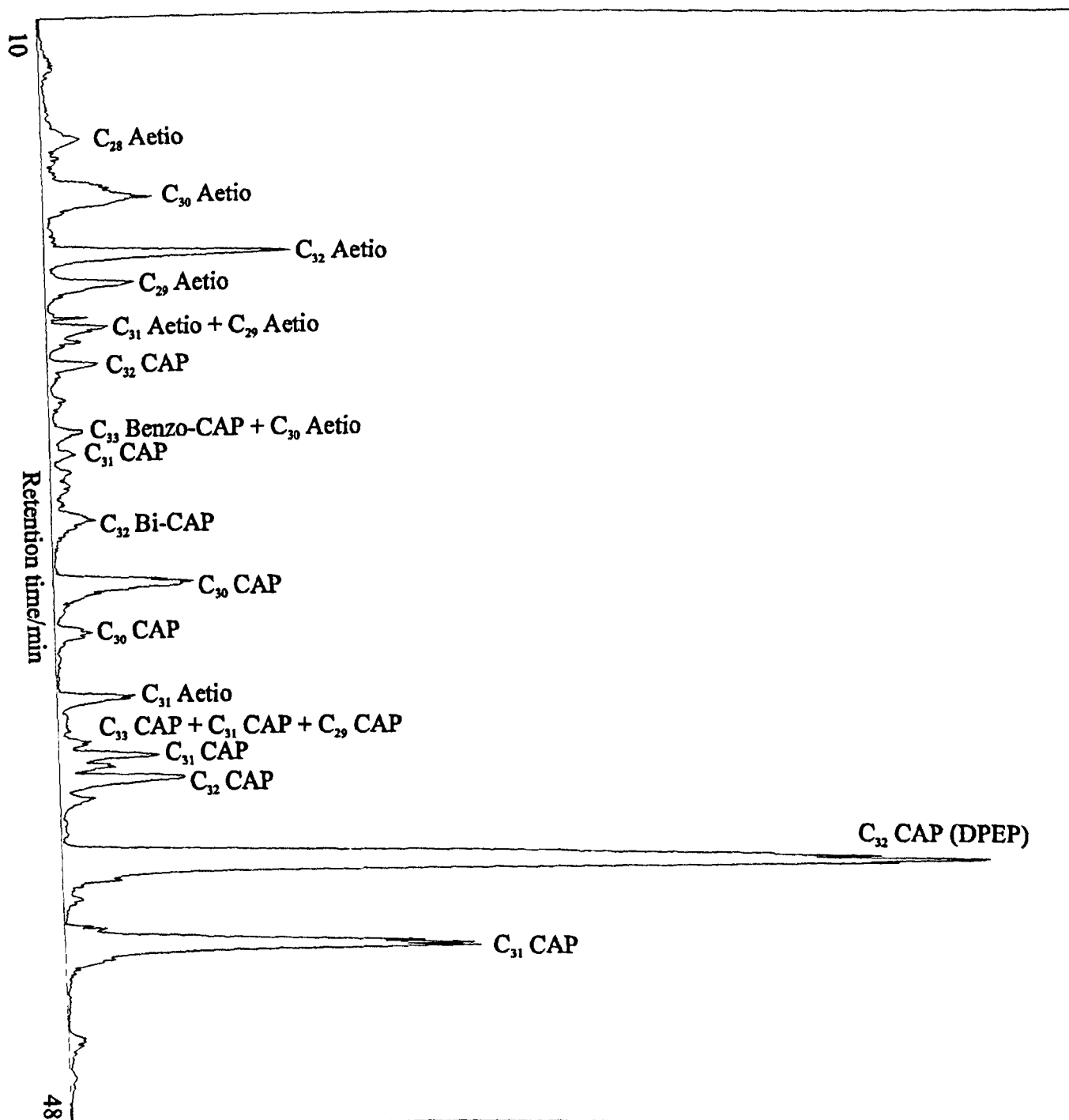
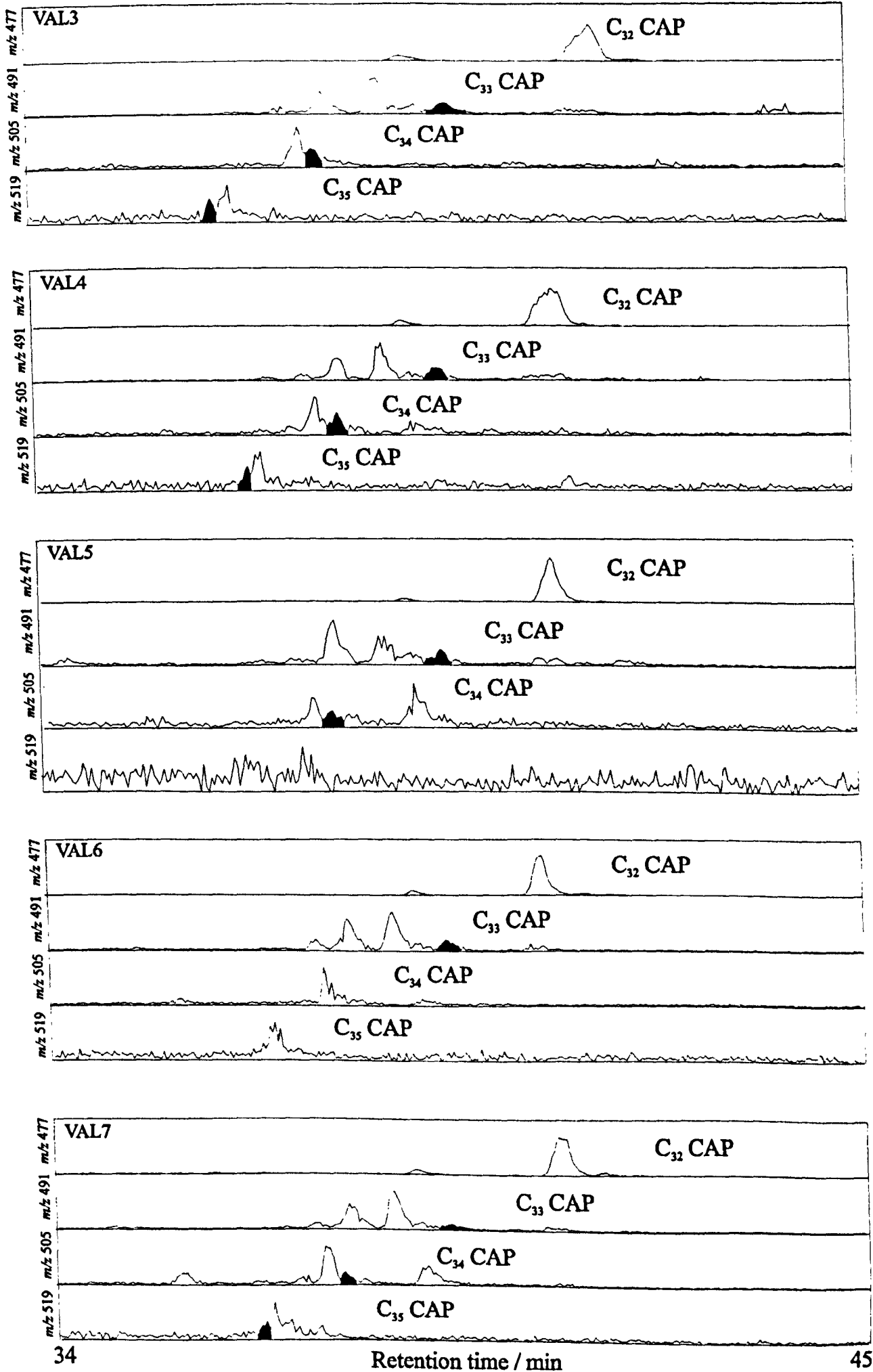


Fig 5.8 Partial HPLC-MS chromatograms of CAPs ( $C_{32}$ - $C_{35}$ ) in ex-nickel Toarcian samples from Valdorbia



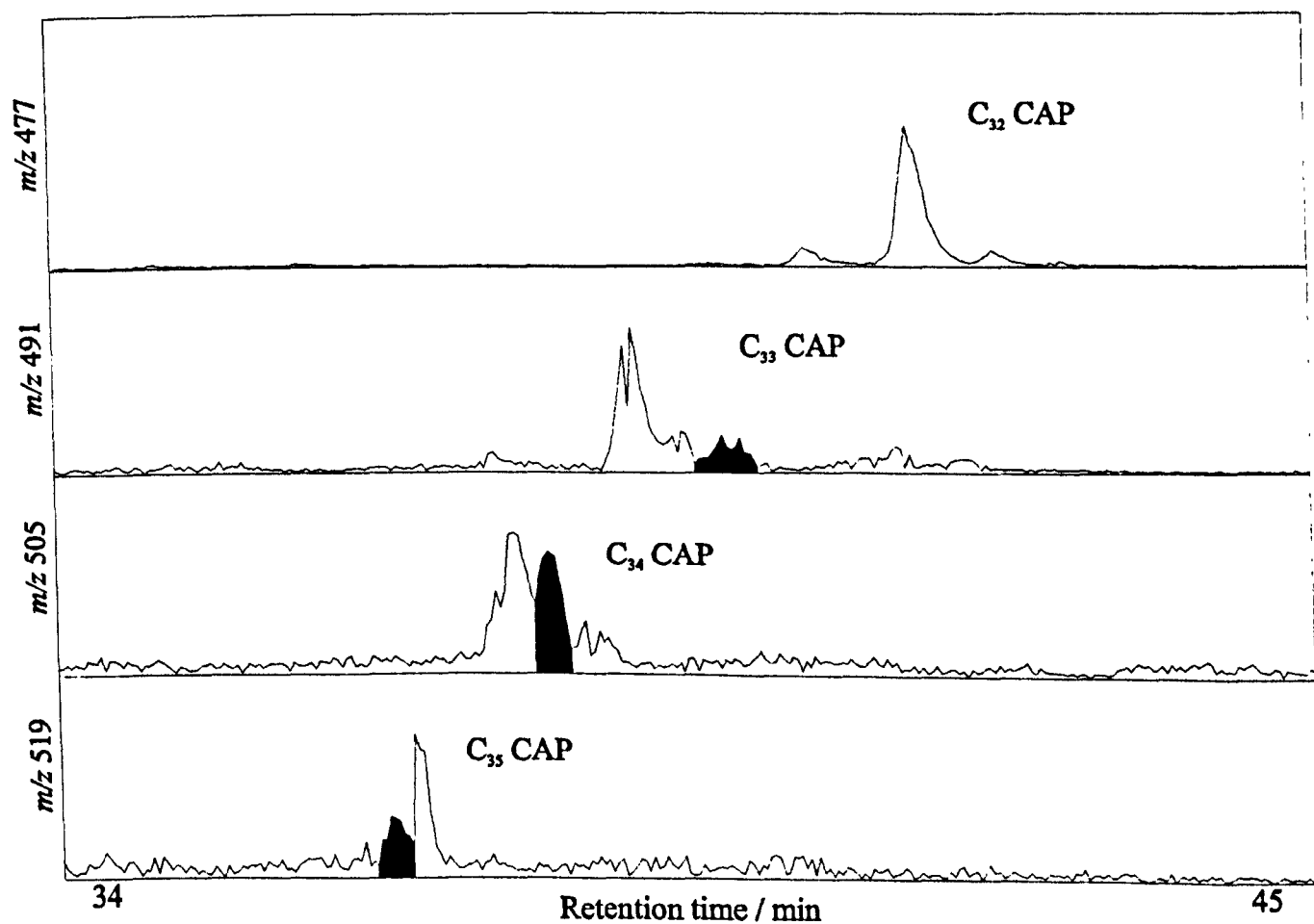
Hence there is good evidence for the existence of PZA during deposition of certain of the Valdorbis shales during the Early Toarcian OAE, showing that the chemocline did at times extend beyond the sediment/water interface and into the photic zone (*c.f.* Palliani *et al.*, 1998), but was not a feature throughout black shale deposition. Although these shales are significantly lower in OM content than the Bonarelli sediments, the ratio of the bacteriochl-derived C<sub>34</sub> peak c to DPEP is similar in VAL3 and 7, although the ratio in VAL4 is *ca.* 0.04, which is higher than in any of the Bonarelli samples, and closer to the ratio seen in the site 367 and 368 black shale samples from the Southern North Atlantic (fig 4.28; chapter 4; see also below). Furthermore, the ratio of Me *i*-Bu to Me Et maleimide follows the same pattern, with a maximum value in VAL4, and lower values again for VAL3 and 7; the ratio is also significantly greater in these samples than in the Cen/Tur Bonarelli or Aptian Selli samples (Crawford, personal communication). Therefore, for samples VAL3 to 7, the results show that PZA was most prevalent during deposition of VAL4, although high amounts of Me *i*-Bu maleimide were also found in VAL1 and 2 (Crawford, personal communication), from which, unfortunately, very low amounts of porphyrins were extracted (table 5.2). With both the porphyrin and maleimide ratios significantly higher in VAL4 than in any of the Livello Bonarelli or Livello Selli samples, this infers that during periods of Toarcian black shale deposition, anoxia occurred within the photic zone for longer periods or occurred more frequently. It is again interesting to note again that no vanadyl porphyrins were present, so, like the Livello Selli samples, the samples fall outside the pattern seen in the Cen/Tur samples (fig 4.27; chapter 4) where evidence for PZA was found in all samples where  $\text{Ni}/(\text{Ni}+\text{VO}) \leq 0.81$ .

Fig 5.8 also shows the presence of a C<sub>34</sub> CAP eluting *ca.* 1min after the bacteriochl *d*-derived C<sub>34</sub> CAP in samples VAL4 to VAL7. With no evidence for PZA from maleimides in VAL5 and 6, it seems unlikely for this component to be derived from the bacteriochls, and hence seems to be a component of unknown origin.

### *Belluno*

The demetallated vanadyl porphyrin fraction was provided by Dr. A. Rosell-Melé. HPLC-MS analysis showed a similar distribution to the Valdorbis samples, with series of CAP and aetio types the most abundant components in the base peak chromatogram (Appendix C). The mass chromatograms for the C<sub>34</sub> CAPs (fig 5.9) reveal the three peak multiplicity seen in Kupferschiefer (chapter 2), including peak c. The C<sub>35</sub> CAP

Fig 5.9 Partial mass chromatograms of ex-vanadyl HMW CAPs from Toarcian sample from Belluno (BL)



chromatogram also reveals the presence of a peak corresponding to the bacteriochl *d*-derived C<sub>35</sub> CAP, so there is evidence for the presence of the green sulphur bacteria in the Toarcian water column of the Belluno Trough.

The ratio of the C<sub>34</sub> CAP peak *c* component to DPEP is 0.04 and approximately the same as the highest ratio in the Valdorbia samples (VAL4). Although no maleimide studies were carried out on this sample, the porphyrin results therefore infer that PZA was as prevalent in the Belluno area of the north of Italy, at the beginning of the Toarcian OAE, as at times in the Umbrian Basin further south. Although this area is represented by only the one sample, it does appear that these oxygen-deficient conditions may have extended over a large area of the Tethyan continental shelf during the early Toarcian, and that the intensity of the anoxicity was severe enough so that deposition of many of the black shales was at times characterised by episodes of PZA.

### **North European Epicontinental Seas**

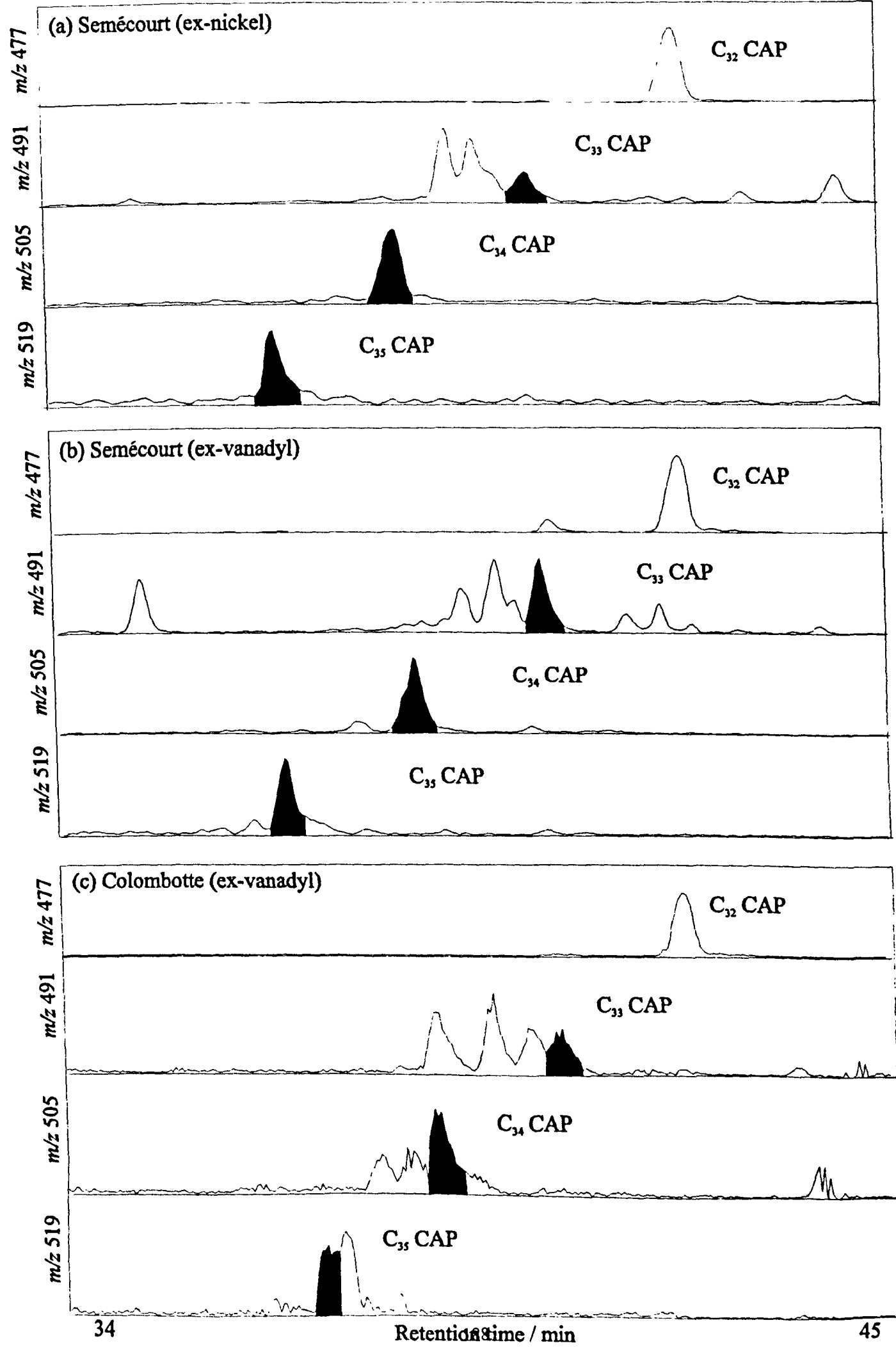
#### *Paris Basin*

Demetallated porphyrin fractions were provided by Dr. A. Rosell-Melé. The mass chromatograms of the CAPs of the Semécourt and Colombotte samples from the Paris Basin are shown in figs 5.10a-c. The base peak chromatograms (not shown) contain the usual range of CAPs and aetios with minor contributions from Bi-CAPs (Appendix C). The ex-nickel and ex-vanadyl porphyrins of Semécourt, both clearly show the presence of peaks (shaded) with the same retention time as the bacteriochl *d*-derived CAP standards (fig 5.10a and b). The C<sub>34</sub> and C<sub>35</sub> peaks are here, however, the major peaks in each chromatogram, with, for example, the C<sub>34</sub> peak *c* significantly larger than the non-PZA peak *b* CAP. The *m/z* 491 chromatogram also shows the presence of an early and some later eluting C<sub>33</sub> CAP components in the ex-vanadyl fraction (fig 5.10b).

The distribution of the HMW CAPs in the ex-vanadyls of the Colombotte sample also contains peaks corresponding to C<sub>34</sub> and C<sub>35</sub> bacteriochl *d*-derived standards, although the peak multiplicity is greater than in the Semécourt distributions (fig 5.10c).

The C<sub>34</sub> peak *c* to DPEP ratios are 0.04 for Colombotte, and 0.06 and 0.05 for the ex-nickel and ex-vanadyl porphyrins of Semécourt, so again, as with the Bonarelli samples, there are no significant differences between each metallo porphyrin fraction. These ratios are significantly higher than those seen in the continental margin samples of Cen/Tur (chapter 4) and Aptian age, although not much higher than the ratio seen in VAL4 and in Belluno (see below).

Fig 5.10 Partial HPLC-MS chromatograms of demetallated porphyrins from Paris Basin



GPC (chapter 7) was used to further clean-up the metallo porphyrin fractions of the two samples (HL10 and HL12) before demetallation. Better yields were obtained after demetallation of the vanadyls, so although both ex-nickel and ex-vanadyl porphyrins were analysed by HPLC-MS, “cleaner” chromatograms and spectra were obtained for the ex-vanadyl porphyrins. The base peak chromatograms (not shown) were found to be almost identical to each other, both containing a range of CAPs (major peaks: C<sub>27</sub>-C<sub>33</sub>) and aetios (C<sub>27</sub>-C<sub>32</sub>) (Appendix C). The partial mass chromatograms of the CAPs (C<sub>32</sub>-C<sub>35</sub>) eluting in the HMW region are shown in fig 5.11, and the shaded peaks indicate the presence of C<sub>33</sub>-C<sub>35</sub> CAPs, with the same retention times and spectra, as the bacteriochl d-derived standards. Hence, there is evidence for PZA during deposition of these two samples at Holzmaden. This confirms the work of van Kaam Peters (1997) who detected the presence of isorenieratane in equivalent samples within the basin. The peak area ratios of the C<sub>34</sub> peak c component vs. DPEP are 0.02 and 0.03 for HL10 and HL12 respectively, both of which are lower values than those seen in the CAP distributions of the two samples from the Paris Basin.

### DISCUSSION – TOARCIAN

Fig 5.12 displays the ratios of the peak areas of C<sub>34</sub> peak c to DPEP for all the Toarcian samples. It can be seen that the ratios for all the epicontinental sea samples are significantly higher than most of the ratios seen in the Tethyan samples, with the exception of VAL4 and BL. This presumably reflects the overall greater length of time of extensive oxygen depletion that was present in the restricted epicontinental basins during the early Toarcian transgression, as compared with the situation in the more open continental margins of the Tethys (*c.f.* Farrimond *et al.*, 1988; 1994).

The relatively high ratio in the BL sample indicates that growth of green sulphur bacteria was extensive within the restricted Belluno trough, and means that a large part of the water column, including parts of the photic zone, was probably anoxic. This infers that the expanded and intensified OMZ (Jenkyns, 1985), led to significant periods and/or a higher frequency of PZA during deposition of this sample. The model of Farrimond *et al.*, (1988, 1989) suggested, however, from observations of the partial degradation of marine OM, that at times a considerable thickness of the water column was oxygenated above anoxic bottom waters (fig 5.13b). The present results show that an anoxic photic zone also existed, which fits more with the scenario depicted by Jenkyns (1985) in fig 5.13a. It therefore seems most likely that during this OAE, the



Fig 5.11 Mass chromatograms of ex-vanadyl CAPs ( $C_{32}$ - $C_{35}$ ) from Toarcian Holzmaden samples

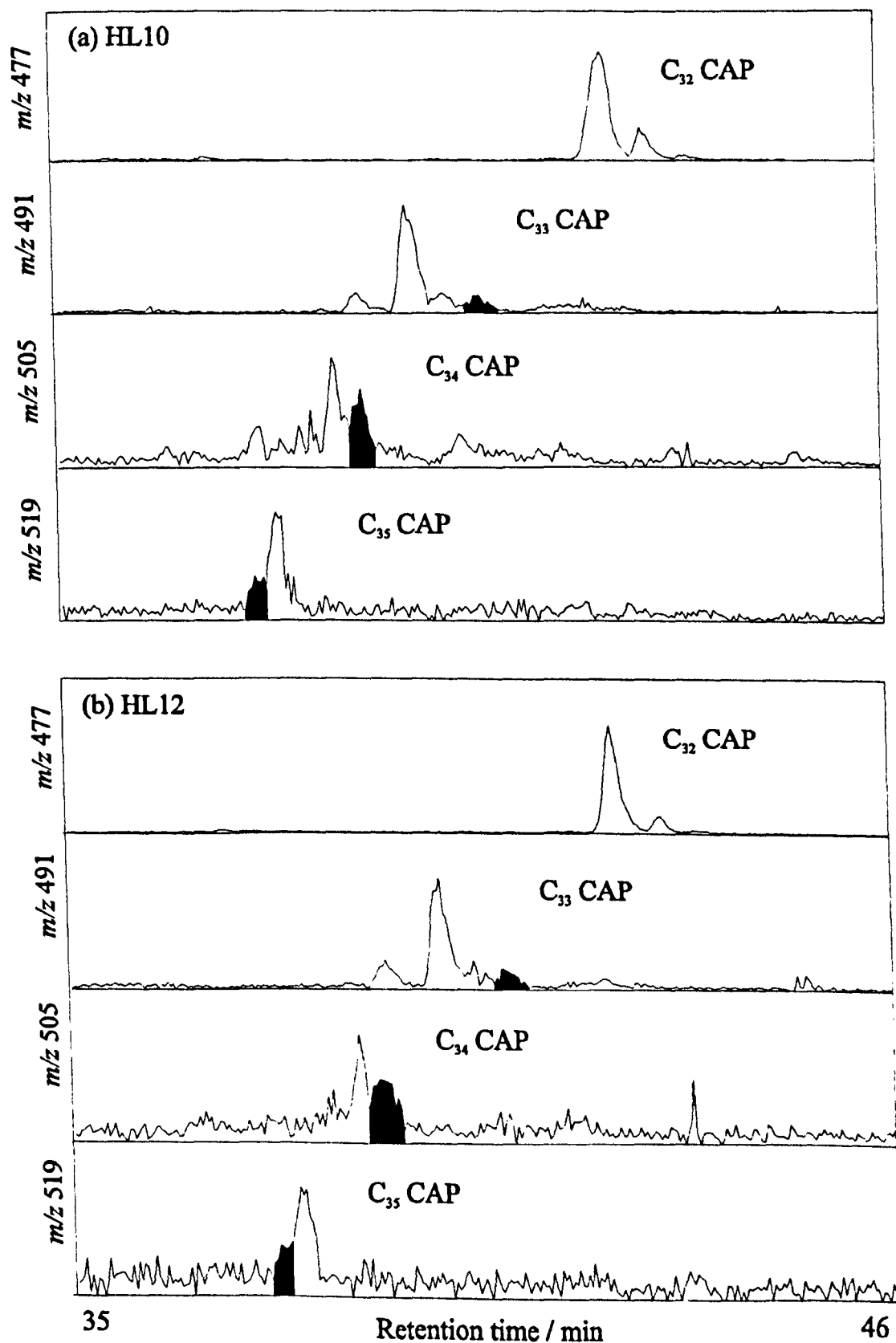


Fig 5.12 Peak area  $C_{34}$  peak c / DPEP for Toarcian samples (a) Valdorbia (b) Belluno (c) epicontinental sea samples

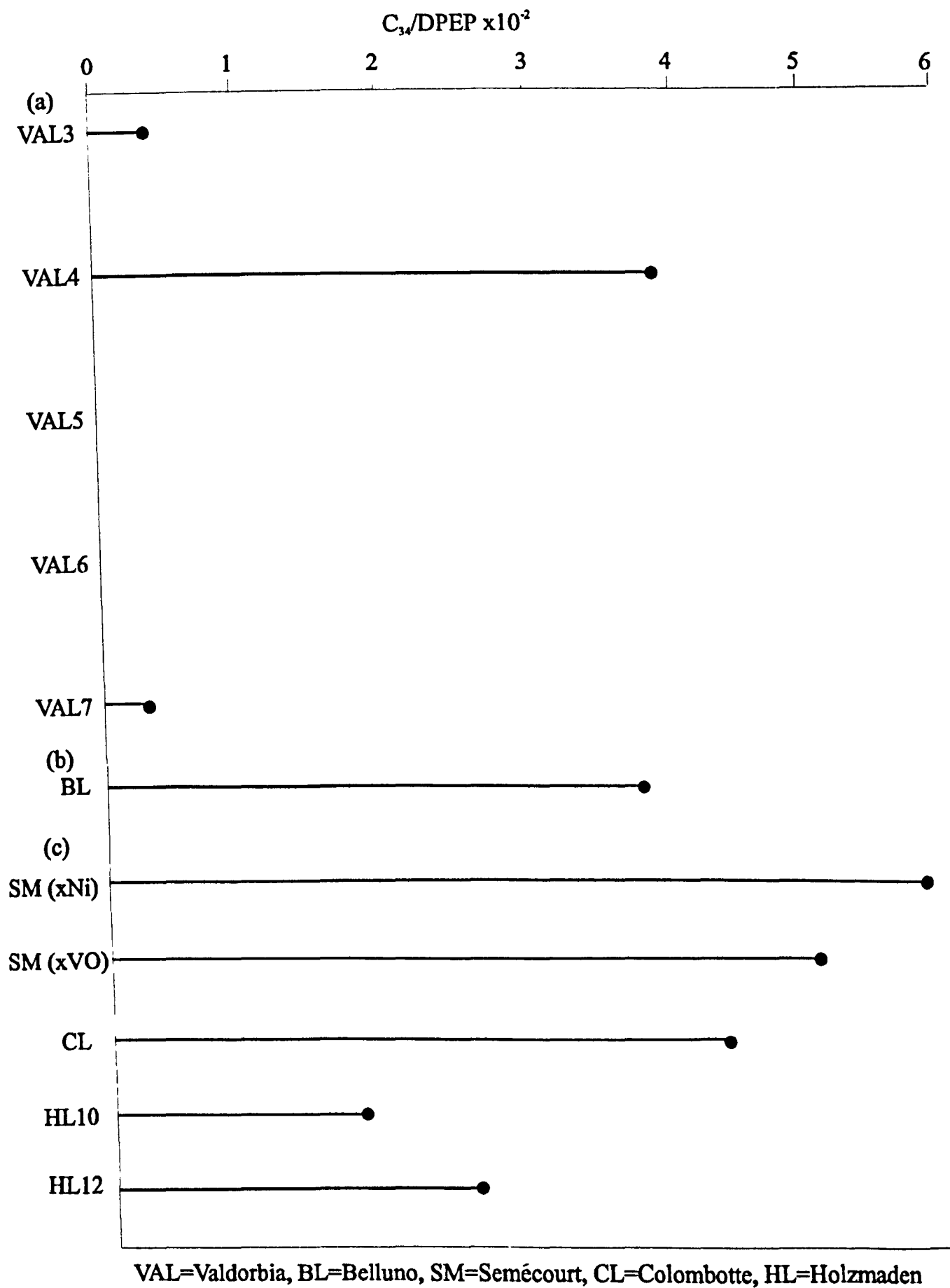
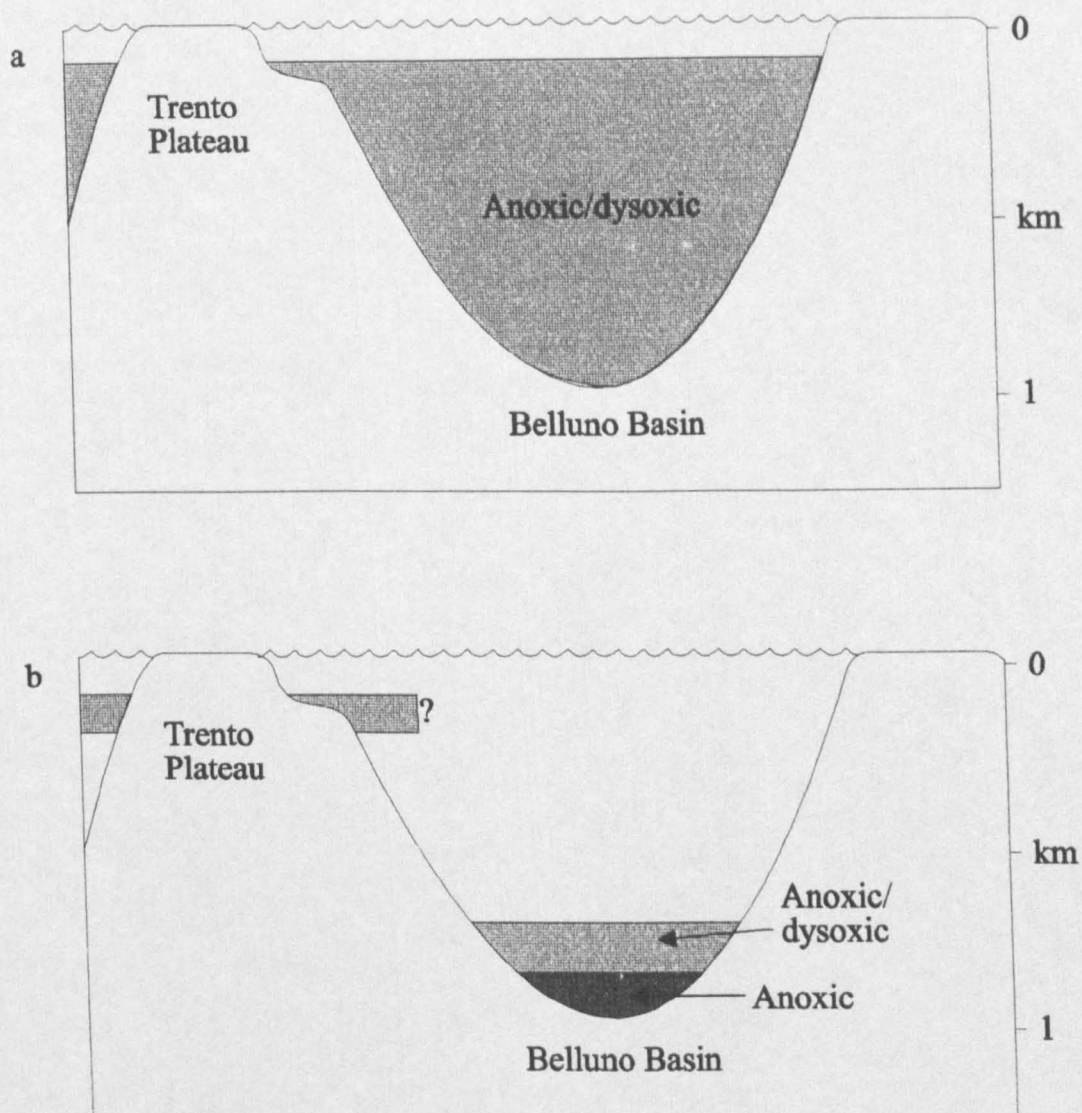


Fig 5.13 Sketches of depositional models within the Belluno Basin during the Toarcian (modified from Farrimond *et al.*, 1988)



(A) Expanded OMZ from high productivity resulting in anoxic basin (Jenkyns, 1985)

(B) Bottom water anoxia + oxic/dysoxic water column (Farrimond *et al.*, 1988)

redox state of the water column fluctuated between times when some degree of oxygenation existed, and others when the water column was mostly anoxic.

The same scenario also seems to be applicable to the deposition of the shales at Valdorbia, as present results have also shown the periodic presence of PZA in the water column during deposition of three samples, with particularly high amounts of bacteriochl *d*-derived components present in VAL4 (fig 5.12). Combining the evidence for PZA, together with previous evidence for anoxic bottom waters and a productivity event (from the pronounced  $\delta^{13}\text{C}$  positive shift; see earlier), it seems that at times, most of the water column of the Umbrian Basin was extensively oxygen depleted as a result of the intensification of an OMZ and generally sluggish circulation. The increased hydrothermal activity (see earlier) may also have increased the flux of sulphide to the water column in these areas, further decreasing the overall oxygen concentration.

Fig 5.12 shows that the  $\text{C}_{34}$  CAP/DPEP ratio is consistently high for all the epicontinental sea samples. Higher values are perhaps not surprising in warm, restricted stratified epicontinental sea environments, as the high productivity in combination with more restricted basinal circulation (Kaufmann, 1981; Küspert, 1982; Jenkyns and Clayton, 1986; Hollander *et al.*, 1991) would be expected to lead to greater periods of anoxicity overall compared with a more open marine environment.

As noted earlier, the ratio is similar in both the samples from the Paris Basin, although the ratios in both the Holzmaden samples are significantly lower. This may fit with the conclusions of previous workers who have stated that the water column of the Paris Basin was anoxic for greater lengths of time than in the German Basin, so that the chemocline existed within the photic zone for greater lengths of time (Hollander, *et al.*, 1991). The more extensive development of an anoxic water column in the Paris Basin may also have been as a result in part of high salinity bottom waters (Farrimond *et al.*, 1988 and refs. therein), furthering the tendency toward salinity stratification, a feature which has not been proved one way or another within the SW German Basin (Farrimond *et al.*, 1988). However, bearing in mind the low number of samples studied, together with the lack of a stratigraphic correlation between the samples from the two basins, it is impossible to describe how the extent of PZA varied throughout deposition of the Toarcian shales in each basin.

Van Kaam Peters (1997) used the differences in  $\delta^{13}\text{C}$  excursions between different locations to argue against the true global nature of carbon burial during the Toarcian

OAE. Results presented here also show that significant variations in the length and/or frequency of PZA occurred in both time and space. Again, there seems to be little relationship between extent of PZA and TOC, and furthermore, samples containing no vanadyl porphyrins have been shown to preserve a high PZA signal. There seems little doubt, therefore, that there were indeed substantial differences between the depositional regimes in place during the early Toarcian OAE. However, this study has shown that PZA was a common feature of the water column in both continental margin marine settings and in epicontinental seas, and it therefore seems that the deposition of OM-enriched shales characterised by PZA, was prompted in a variety of different palaeogeographical scenarios by local changes in productivity and preservation potential, but ultimately relating to the effects of global increases in temperature, hydrothermal flux, oxygen-depletion and sea-level.

**CHAPTER 6**  
**OVERVIEW AND FUTURE**  
**RECOMMENDATIONS**

## OVERVIEW

Porphyrin distributions have been used to assess the redox conditions in the photic zone of a variety of depositional environments by comparing HPLC-MS distributions and retention times of certain high molecular weight cycloalkanoporphyrin (HMW CAP) components with those of standards. A related study (Crawford, personal communication) details complementary structural and isotopic analysis of maleimides (1*H*-pyrrole-2,5-diones) from the same samples. Identification of the diagenetic products of green sulphur bacteria in sedimentary samples from both studies is taken as good evidence for recognition of photic zone anoxia (PZA) in the palaeo water column. Previous studies showed the presence of a series of minor C<sub>33</sub>-C<sub>35</sub> HMW CAPs in the demetallated iron porphyrin fraction of a bulk Kupferschiefer sample (Gibbison, 1996). These were shown to possess an Et substituent at C-12 and Et, *n*-Pr and *i*-Bu at C-8, with structures (34a,b,c) consistent with an origin from member of the bacteriochl *d* series present in the green strains of Chlorobiaceae. These bacteria, requiring light and H<sub>2</sub>S for photosynthesis, cannot live in the presence of oxygen, so are indicators of the presence of anoxic conditions and free H<sub>2</sub>S within the photic zone of a marine water column. Detection of such bacteriochl *d*-derived porphyrins in sediments therefore allows recognition of the occurrence of photic zone anoxia (PZA). Further evidence for the presence of Chlorobiaceae comes from the detection of Me *i*-Bu maleimide, a structurally specific marker of the bacteriochls *c*, *d* and *e* (Grice *et al.*, 1996a and Crawford, personal communication).

The HPLC gradient elution solvent programme for the separation of free base porphyrins was modified so that separation was achieved between C<sub>34</sub> CAPs derived from the bacteriochl *d* (34b and 33, which were not separated from each other) and the non-bacteriochl derived C<sub>34</sub> CAP standard (46a,b). Improved separation was also obtained between the C<sub>35</sub> bacteriochl *d*-derived CAP (34c) and another unknown C<sub>35</sub> HMW CAP component(s). Coinjection of the standards with the ex-iron fraction of the bulk Kupferschiefer sample allowed the determination of the exact retention positions of bacteriochl *d*-derived CAPs within the multiple peak mass chromatograms. In the three peak C<sub>34</sub> CAP distributions, the two C<sub>34</sub> standards derived from bacteriochl *d* (33, 34b), eluted as "peak c", whereas the non-PZA standard (46a,b), eluted as "peak b". The C<sub>35</sub> PZA standard (34c) eluted in the first, and more abundant peak, and the C<sub>33</sub> standard (34a) with one of the later eluting, major C<sub>33</sub> mass chromatogram peaks. Thus,

CAPs with the same retention times and mass spectra as these standards were assigned as indicators of the presence of bacteriochl *d*-derived porphyrins.

The demetallated nickel porphyrins in a number of samples from a Kupferschiefer core from the Lower Rhine Basin contained components (C<sub>33</sub>-C<sub>35</sub>) corresponding to the bacteriochl *d*-derived standards. This extends the work of Grice *et al.* (1996b) who found Me *i*-Bu maleimide throughout the core, suggesting that the entire deposition of Kupferschiefer in this region was characterised by periods of PZA. Ratios of the abundances of the three bacteriochl-derived HMW CAP components vs. DPEP were compared with the ratio of Me *i*-Bu maleimide to Me Et maleimide (from Grice *et al.*, 1996b). The ratio of the C<sub>34</sub> peak c component in particular compared favourably with the Me *i*-Bu/Me Et maleimide ratio. This suggested that this particular CAP peak is a reliable indicator, and that this approach could be tentatively used for the investigation of the occurrence of PZA, but with back up from structural and isotopic maleimide data. Results throughout showed the presence of the C<sub>33</sub> peak in most distributions, including those in samples with no C<sub>34</sub> or C<sub>35</sub> CAP components and with no evidence from the maleimides. It was therefore evident that other C<sub>33</sub> CAPs can elute with the same retention time as the bacteriochl *d*-derived C<sub>33</sub> standard (34a), so that this peak could not be used as a reliable indicator.

HPLC-MS analysis of the ex-vanadyl porphyrins of Serpiano oil shale showed the presence of peaks corresponding to standards derived from the bacteriochl *d* series, which together with previous maleimide evidence (Grice *et al.*, 1996a) strengthen the confirmation of the existence PZA during deposition of this oil shale.

Sediments from two Tertiary evaporitic settings, the Mulhouse and Vena del Gesso (VdG) basins, deposited in highly saline environments where restricted circulation led to the development of anoxic conditions were examined. Previous studies of the Mulhouse Basin revealed no diaromatic isoprenoids derived from the isorenaratene (30) of the brown strains of Chlorobiaceae (Sinninghe-Damsté *et al.*, 1993b), although probe MS analysis had detected the presence of HMW CAPs, which together with co-injection of a C<sub>34</sub> CAP (33) derived from a bacteriochl *d* with one sample, suggested the presence of anoxic conditions within the photic zone at the time of marl deposition (Keely and Maxwell, 1993). The HPLC-MS approach was thus used to determine whether bacteriochl *d*-derived components were present in any samples from this basin. The study confirmed the presence of HMW CAPs in the marls, especially in unit T, and provided further evidence for the presence of green strains of Chlorobiaceae during



deposition of the type A marls, thought to be deposited during periods of an increased contribution of marine waters and higher algal productivity. Several more abundant series of HMW CAPs, eluting both before and after the “expected HMW region” were also present. Although mass spectra confirmed they are indeed HMW CAPs, their structures and origin are unknown. Whilst they may derive from other bacteriochls of green sulphur bacteria, the absence of aryl isoprenoids derived from the aromatic carotenoids of Chlorobiaceae infers that they are derived from other sources. As previously suggested by Keely and Maxwell (1993), these might be the multicellular filamentous green bacteria (*Chloroflexus*), which contain the bacteriochls *c* as their principal chlorophylls but do not contain isorenieratene or chlorobactene. Probe mass spectra previously provided no convincing evidence for the presence of HMW CAP species in samples from VdG, although previous LC-PDA-MS analysis of three sub-samples of IV (*e.g.* IV-1-4) did reveal a minor C<sub>34</sub> CAP component (Keely *et al.*, 1995). Structural and isotopic analysis of the aromatic hydrocarbons in many of the marls, however, revealed the presence of isorenieratene (30) together with a range of <sup>13</sup>C-enriched isorenieratene-derived diaryl isoprenoids with 2,3,6-trimethyl substitution (Keely *et al.*, 1995; Schaeffer *et al.*, 1995; Kenig *et al.*, 1995). HPLC-MS analysis revealed no peaks corresponding to the bacteriochl *d*-derived standards, hence giving no evidence for the presence of the green strains of Chlorobiaceae. Hence the minor C<sub>34</sub> CAP observed by Keely *et al.*, 1995, does not appear to be derived from the bacteriochls *d* of the green strains. The distributions also revealed other early and late eluting HMW CAPs of unknown origin (see below).

The porphyrin distributions from a suite of Livello Bonarelli Cen/Tur black shale samples from six locations in Umbria, plus samples from one in Tunisia revealed the presence, in some of them, of C<sub>34</sub> and C<sub>35</sub> HMW CAPs corresponding to the bacteriochl *d*-derived standards. With few exceptions, maleimide data confirm the porphyrin results. Other HMW CAP series present in higher abundance than the bacteriochl-derived CAPs, were inferred to be *n*-alkyl CAP components (*e.g.* 47a,b) not derived from any of the bacteriochls. Oxidation of the (T1+T3) fractions of F1 revealed Me *i*-Bu maleimide (see below), and also a high abundance of Me *i*-Pr maleimide (55), showing the presence of *i*-Pr-substituted porphyrins.

The bacteriochl-derived components were present at all the locations within some samples, but not in others, inferring that PZA was not a consistent feature, but existed only periodically during deposition of the Cen/Tur black shales.

Ratios of the C<sub>34</sub> peak c component to DPEP plotted for some of the Livello Bonarelli sections showed that the intensity/frequency of PZA varied considerably throughout the event. Furthermore, lateral differences in the ratio from section to section inferred that within the same regional setting, local factors played an important role in the establishment of anoxic conditions. It was also noted that there was seemingly no relationship between TOC and occurrence of PZA, with some very organic-rich shales (e.g. Fosto) showing no conclusive evidence for PZA, whilst other less organic-rich samples (e.g. Bottacione Gorge), showed good evidence. The model of an intensified, expanded OMZ continuously impinging upon the continental margins, therefore appeared simplistic, as results have shown further that differences were present throughout the region in the relative amounts of green sulphur bacterial input, so that local changes also imparted significant effects on the nature of the water column. Therefore, whilst an expanded OMZ impinging on the continental margins resulted in black shale deposition, anoxic conditions did not continuously extend into the photic zone.

Cen/Tur black shales from three abyssal DSDP sites in the southern North Atlantic also contained HMW CAPs corresponding to the bacteriochl *d*-derived standards.

Bacteriochl-derived Me *i*-Bu maleimide was also detected in sites 367 and 368 in the eastern basin, although no conclusive evidence could be obtained for samples from site 144 in the west;  $\delta^{13}\text{C}$  data also showed this maleimide to be enriched relative to phytoplanktonic Me Et maleimide (Crawford, personal communication). Furthermore, the oxidation products of the porphyrins from sample 368-63 contained Me *i*-Bu maleimide. Taken together, these results confirm the recent work of Sinninghe Damsté and Köster (1998) who reported the presence of abundant,  $^{13}\text{C}$ -enriched aromatic hydrocarbons derived from the brown strains of Chlorobiaceae in similar samples from the same sites. Hence, the tentative evidence of PZA in 144-02 and 144-03 from the porphyrin distributions, although not backed up by maleimide data, confirms the presence for PZA in the west of the southern North Atlantic. Contributions of C<sub>34</sub> peak c, and Me *i*-Bu maleimide were higher in the DSDP samples than in those deposited along the continental margins of the Tethys, suggesting that the extent of the oxygen depletion was more prevalent in the former. These samples were deposited in abyssal sites (3000-3700m), much deeper than the proposed palaeo depth (ca. 1km) of the Livello Bonarelli samples. It is thought, therefore, that with the greater concentrations

of bacteriochl-derived components in the DSDP sites, an expanded OMZ in the equatorial Atlantic was superimposed on a water column already extensively depleted in oxygen. Whilst there is now evidence from these samples for an anoxic photic zone, and previous evidence for anoxic bottom waters from laminations and high trace metal content, it is not entirely clear whether the water column was continuously anoxic or not, although a combination of an expanded OMZ and existing anoxic bottom waters may have led to such conditions.

The study was extended to a range of samples deposited in the Tethyan realm during the Aptian and Toarcian OAEs and a number of Toarcian samples from Northern European epicontinental seas. Three out of six Livello Selli Aptian samples from Gorgo a Cerbara were found to contain evidence for PZA from both porphyrins and maleimides. This agreement confirms further the validity of the porphyrin approach and showed that PZA was also a periodic characteristic of the water column *ca.* 27 Myr prior to the Cen/Tur event. Many previous studies have noted similarities in the Aptian OAE1a and Cen/Tur OAEs, as they are both thought to record distinct productivity events resulting in the expansion of an OMZ, combined with a tendency towards extensive oxygen depletion. Indeed the bacteriochl to phytoplanktonic ratio as given by the porphyrin distributions showed similar values in both cases, with the C<sub>34</sub>/DPEP ratio of the Livello Selli samples similar to that found in the Livello Bonarelli samples from Monte Petrano. Therefore, it seems that the relative contribution of green sulphur bacteria, and hence the intensity/frequency of PZA, was not significantly different during periods of the Livello Selli deposition, as compared with Livello Bonarelli deposition, even though samples from the former are less organic-rich.

Evidence for the periodic existence of PZA in the Umbrian Basin during the Toarcian OAE was also apparent in the presence of bacteriochl *d*-derived HMW CAPs. Once more, the porphyrin and maleimide results correlated well, with PZA apparent from some samples and not others. The bacteriochl to phytoplanktonic ratio in sample VAL4 was substantially higher than in any of the Livello Selli or Livello Bonarelli samples. Indeed, the C<sub>34</sub> peak *c* to DPEP porphyrin ratio followed the same pattern as that in the Me *i*-Bu to Me Et maleimide ratio throughout the same samples in the Toarcian section. Evidence for PZA was also found from porphyrins in one sample deposited further north in the Tethys within the Belluno Trough. Although no maleimide studies were carried out on this sample, the ratio of the C<sub>34</sub> CAP to DPEP was approximately the same as that of VAL4, implying that PZA was as prevalent in this region at the

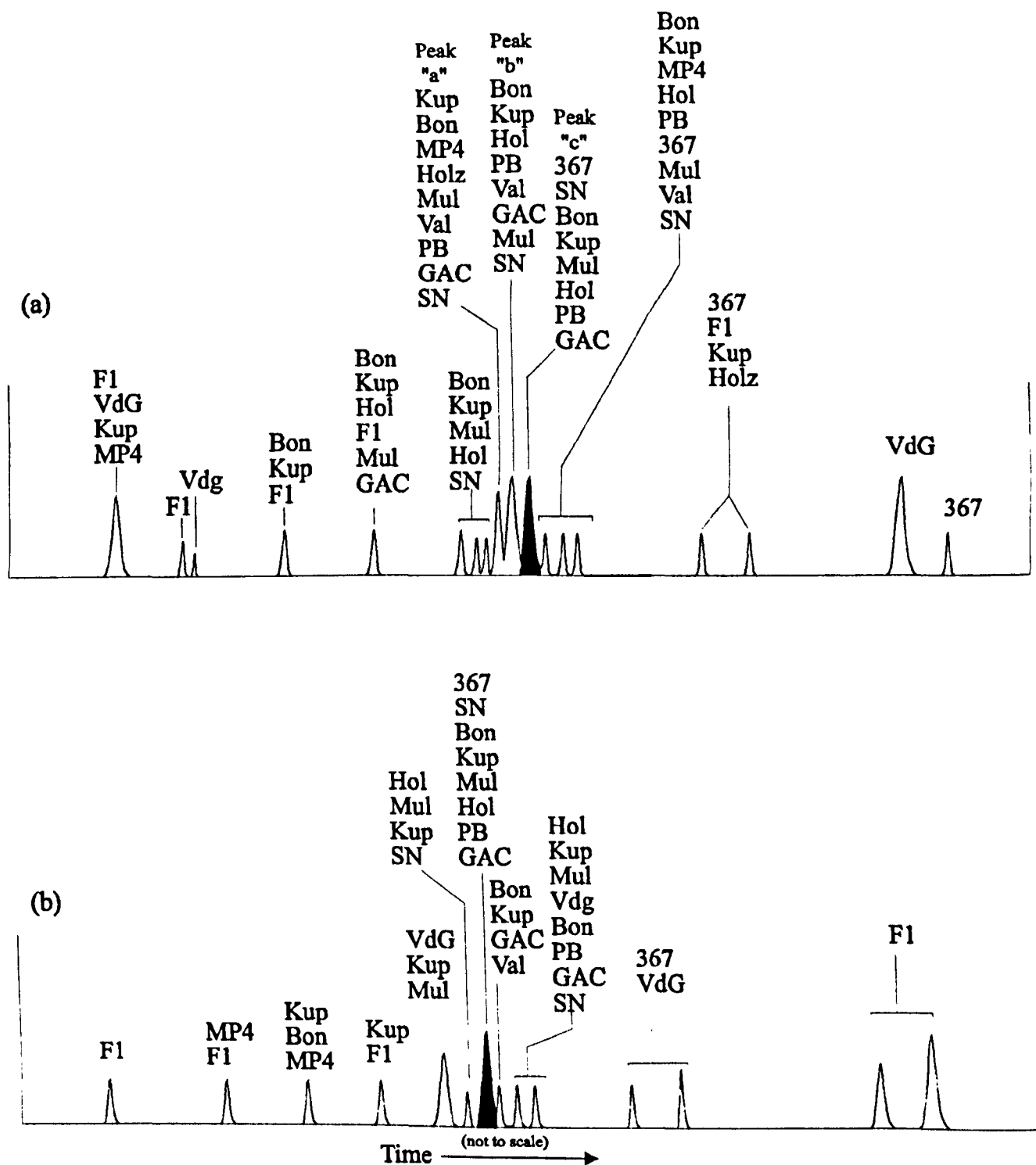
beginning of the Toarcian OAE, as at times in the Umbrian Basin further south. Therefore, although the water column may have fluctuated between times of oxygenation and times of oxygen depletion (Farrimond *et al.*, 1988), it seems that many of the early Toarcian Tethyan black shales analysed were characterised by periods of PZA, so that oxygen-deficient conditions may have periodically extended over a large area of the Tethyan continental shelf during the Toarcian OAE.

Porphyrin distributions in samples from the epicontinental seas of the Paris Basin and the SW German Basin also showed a significant presence of bacteriochl *d*-derived CAPs. The C<sub>34</sub> CAP/DPEP ratio was found to be high, suggesting that the deposition of each sample was characterised by long periods of PZA. This, it was argued, is perhaps expected when considering that deposition occurred in restricted and stratified environments, so that the moderate/high productivity would result overall in longer periods of anoxicity as compared with the degree of oxygen depletion experienced in a more open marine setting (*e.g.* Jenkyns, 1980). The higher C<sub>34</sub>/DPEP ratio in Semécourt and Colombotte as compared with Holzmaden may reflect a greater extent of oxygen depletion present in the Paris Basin (*c.f.* Hollander *et al.*, 1991).

A low Ni/(Ni+VO) porphyrin ratio has been used in the past as an indicator of euxinic conditions in the depositional setting of organic-rich sediments. Results from chapter 4 showed that, without exception, all Cen/Tur black shales with Ni/(Ni+VO) < 0.81 contained evidence for PZA from both porphyrins and maleimides, whereas those above this value did not. Furthermore, there seemed to be an inverse relationship between the relative amounts of bacteriochl to phytoplanktonic components present (from ratio of C<sub>34</sub> peak *c* to DPEP) and the Ni/(Ni+VO) ratio. However, in chapter 5, samples deposited during the Aptian and Toarcian OAEs were found to contain clear evidence for PZA, but with considerably lower TOCs and no vanadyl porphyrins. This study has therefore shown that whilst a low Ni/(Ni+VO) ratio can be an indicator of the presence of PZA, the opposite is not necessarily true, as sediments containing only nickel porphyrins may still exhibit strong molecular evidence for PZA.

Throughout this study, HPLC-MS has shown the presence of HMW CAPs other than the components derived from the bacteriochls *d* series. A schematic representation of the distribution of the C<sub>34</sub> and C<sub>35</sub> peaks is shown in fig 6.1. Considering these distributions and those of the other components, it is apparent that the distributions are among the most complex seen in any sedimentary biomarker distribution. The C<sub>34</sub> and C<sub>35</sub> distributions show that a number of peaks elute close to (both before and after) the

Fig 6.1 Schematic representation of (a)  $C_{34}$  and (b)  $C_{35}$  CAP components eluting in porphyrin fractions analysed during this study



Bon Livello Bonarelli  
 MP4 MP4 ex-nickel  
 F1 Fosto F1 ex-iron  
 Kup Kupferchiefer (bulk and/or core)  
 367 DSDP 367-02  
 SN Other N.Atlantic DSDP sites  
 GAC Livello Selli

Val Valdorbia  
 Hol Holzamden  
 PB Paris Basin  
 Mul Mulhouse Basin  
 Vdg Vena del Gesso

Shaded peaks indicate bacteriochl *d*-derived CAP components - see text for other details

bacteriochl *d* region within the respective chromatograms. Such peaks are present in many of the samples (fig 6.1), including Kupferschiefer, Mulhouse Basin, the Cen/Tur Livello Bonarelli, the Aptian Livello Selli and the Toarcian samples. Other peaks are also present in a smaller selection of samples which elute even earlier or even later (fig 6.1). The ex-iron fraction of Fosto F1, which contained early and late peaks, some of which were also present in Kupferschiefer, VdG, 367-02 and a few Bonarelli samples, was separated (normal phase prep-HPLC) into “early” (T1) and “late” (T3) fractions, which were combined and oxidised to maleimides. These contained Me *i*-Bu maleimide (Crawford, personal communication), giving evidence that some of these early and/or late eluting HMW CAPs also derive from Chlorobiaceae. An input of brown Chlorobiaceae in the southeastern North Atlantic was recognised recently from the detection of isorenieratene-derived aryl isoprenoids in samples from DSDP sites 367 and 368 (Sinninghe Damsté and Köster, 1998). Hence, it might be expected to see the presence of bacteriochl *e*-derived CAPs in the porphyrin distributions, although only minor late-eluting HMW components were observed in sample 367 (fig 6.1). Furthermore, none of the late C<sub>34</sub> components were observed in any of the VdG samples, which also contain evidence of PZA from the presence of isorenieratene (Keely *et al.*, 1995) and from the bacteriochl-derived Me *i*-Bu maleimide (Magnus, personal communication). It should be noted, however, that the bacteriochl to carotenoid ratio is much lower in the brown strains than in the green strains, which may result in low, and hence undetectable, concentrations of bacteriochl *e*-derived components.

With the notable exception of VdG, many of the samples contain evidence for the presence of the green Chlorobiaceae, from the presence of bacteriochl *d*-derived CAPs. These species, however, also typically contain the bacteriochls *c*, which together with the bacteriochls *e* of the brown Chlorobiaceae, have a C-20 methyl substitution. Indeed, as the structures of these bacteriochl-derived CAPs show (Appendix B), bacteriochl *e*-derived porphyrins containing the basic carbon skeleton would be identical to some of those derived from the *c* series. Therefore, even if some of the peaks shown in fig 6.1 could be positively identified as being derived from the bacteriochls *e*, it would be impossible to distinguish them from bacteriochl *c*-derived CAPs, *i.e.* to deduce whether they were derived from green or brown strains. Positive evidence for the presence of brown Chlorobiaceae can therefore only come from identification of <sup>13</sup>C-enriched isorenieratene-derived aryl isoprenoids.

In general, however, given the presence in many of the samples of C<sub>34</sub> and C<sub>35</sub> CAPs eluting close to the bacteriochl *d*-derived components, it is tempting to suggest that these are indeed bacteriochl *e* and/or *c* components. These components are also present, in much higher abundance, in the Mulhouse Basin marls, previously suspected to contain the bacteriochl *c*-containing *Chloroflexus* species (Keely and Maxwell, 1993). If these components have such an origin, then it would appear that the presence of a C-20 substituent has a relatively minor effect on the retention time. If this is the case, the origin of the species eluting earlier and later remains perplexing. Non-PZA HMW CAPs can also be present, such as the component identified by Gibbison, 1996 (46a, b), together with the presence of *i*-propyl and possibly *n*-alkyl substituted porphyrins (see above). There is also the possibility of a *n*-Pr C-17 substitution, *via* reduction of the propionic C-17 side chain, as evidenced by identification of such a component (56) in Boscan Crude Oil (Verne-Mismar *et al.*, 1986); this could result in another series of bacteriochl-derived CAPs (Appendix B). Furthermore, the identification of a C<sub>31</sub> component (14) in the Serpiano oil shale with an unsubstituted C-7 position, has shown that the functional group of chl *b* (Chicarelli and Maxwell, 1984) and/or chl *c*<sub>3</sub> (Verne-Mismar *et al.*, 1990), may be removed during diagenesis. Similarly, a DPEP-related component with an unsubstituted C-3 position (57) was identified in the Julia Creek and Messel oil shales (Chicarelli *et al.*, 1987). By analogy, the same could occur for bacteriochl-derived porphyrins, so that the functional groups at C-3 in the bacteriochls *c* (26), *d* (6) and *e* (27) and at C-7 in the bacteriochl *e* series could be removed, leading to one or even two β-H substitutions in the resulting CAPs. With the possibility of bacteriochl-derived CAPs extending to C<sub>38</sub> (Appendix B), the existence of unsubstituted β-positions could still give rise to CAPs > C<sub>33</sub>. This would also be expected to significantly alter the retention behaviour, as previous work has shown that for porphyrins of a given carbon number, the β-H substituted porphyrin elutes *ca.* 2 min earlier than the fully alkylated counterpart (Chicarelli *et al.*, 1986). Therefore, although the origin of many of the HMW components remains unclear, it is still possible that a number of them could result from diagenesis of the bacteriochls *c*, *d* or *e*. Nevertheless, identification of components corresponding to bacteriochl *d*-derived CAPs means that the HPLC-MS approach used in the present study is a valuable tool, especially in combination with maleimide studies, in the identification of PZA from ancient sediments.

## FURTHER WORK

1. The present study has revealed the complexity of the porphyrin distributions found in many ancient sediments. The work has been based largely on comparison of the HPLC-MS characteristics of such distributions with those of the known bacteriochl *d*-derived standards of Chlorobiaceae. Up to this point, however, only a small number of HMW CAP standards are available. There is a need for the synthesis of HMW CAP standards containing a Me substitution at C-20 position, *i.e.* components with the same carbon skeletons as the bacteriochls *c* and *e*. With three bacteriochl *e*-derived standards (C<sub>34</sub>-C<sub>36</sub>), HPLC analysis should reveal the true effects of C-20 Me substitution, and appropriate co-injection studies could be performed. Similarly, the synthesis of a C-8 *neo*-Pent substituted C<sub>36</sub> CAP would provide another bacteriochl *d*-derived standard for co-injection studies.
2. Even if bacteriochl *c* and *e*-derived HMW CAPs were identified, it is still clear that many other HMW CAPs are present, possessing a wide range of retention characteristics. This infers that there are still many other HMW components present in ancient samples of an unknown origin. The oxidation products of some of these fractions have shown unusually high concentrations of Me *i*-Pr maleimide, inferring that *i*-Pr substituted porphyrins are present. It was also proposed that series of *n*-alkyl substituted HMW CAPs were present in many of the samples. Preparative HPLC should therefore be used to isolate some of these early and late eluting components, to identify them by NMR. Whilst this is a lengthy and tedious procedure for minor components which co-elute with many other components, such as the bacteriochl *d*-derived CAPs (Gibbison, 1996), some of the early and/or late CAPs have been shown in some samples to be present in relatively high abundance.
3. Other techniques could also be used to determine the nature of the alkyl substituents in individual porphyrin components. HPLC-MS-MS investigations should be furthered, in order to determine whether precise and reliable fragmentation patterns of CAPs can be achieved. Development of a reproducible procedure could provide a further valuable tool in identification of extended alkylation within individual porphyrin components.
4. As shown in Appendix B, the HMW CAPs expected to be derived from the bacteriochls *e* are not structurally specific, in the sense that they would have the same structures as some of the components derived from the bacteriochls *c*. Hence, identification of C-20 Me-substituted components would not appear on its own to allow



conclusions concerning the presence of either the green or brown strains of Chlorobiaceae. This study has shown the presence of green Chlorobiaceae in many ancient sediments, but it would be interesting to determine whether aryl isoprenoid markers for brown Chlorobiaceae were also present in the same samples. Whilst green and brown sulphur bacteria do not generally co-exist (de Wit, personal communication), any single sample, usually representing deposition of several thousand years, could apparently record the simultaneous presence of both (*e.g.* DSDP site 367) during deposition. Further work should therefore be undertaken to examine the aromatic hydrocarbon distributions present in the other samples analysed during this study. As the brown strains are adapted to deeper environments than the green strains (Pfennig, 1989), detection of isorenieratene-derived components and bacteriochl-*d*-derived porphyrins in the same sample would perhaps record a fluctuating expanded OMZ model for PZA occurrence in open ocean settings.

5. As each black shale represents a considerable period of OM deposition, it would be interesting to see the changes in biomarker concentrations that occurred over short time intervals. If very fine sampling were possible, then large diameter samples would have to be taken to provide sufficient material so that bacteriochl-derived components could be detected. This study has shown, however, that such components are present at relatively low concentrations in the Tethyan OAE samples. Studies on thin shale sections would therefore be more sensibly performed on samples containing a more intense PZA signal, such as those deposited in restricted basinal environments.

6. There is also a need for the further analysis of black shale samples deposited during OAEs. Whilst this study included a suite of Cen/Tur samples, there are other regions where marine sediments of this age were deposited (Jenkyns, 1980). Furthermore, a limited number of Aptian and Toarcian OAE samples were analysed. Further work should also be directed at the analysis of more OAE samples from these three major events from other global sites. Results would then provide information about the occurrence or not of PZA in intensified OMZs during these time periods, or reveal whether PZA was specific to locations such as the western Tethys and southern North Atlantic. Studies of samples deposited in the Pacific during the Cretaceous OAEs should also be analysed, where black shale deposition is thought to have occurred in anoxic environments (*e.g.* Bralower *et al.*, 1994).

7. The porphyrin distributions in some of the samples analysed, *e.g.* Moria and Mulhouse samples, have not been backed up by maleimide studies. Analysis of the

Toarcian samples from the German and Paris Basins, in particular, needs to be extended to include not only maleimides, but also a larger suite of samples. Aryl isoprenoids have already been analysed from a suite of Toarcian samples from the SW German Basin (van Kaam Peters, 1997), so detection of bacteriochl *d*-derived HMW CAPs and maleimides would shed further light on the distribution of PZA in these epicontinental sea samples.

# **CHAPTER 7**

## **EXPERIMENTAL**

## GENERAL

### Solvents and Glassware

Rathburns distilled HPLC-grade solvents were used throughout all experimental and instrumental procedures. Water used in porphyrin demetallation procedures was double-distilled prior to use.

All glassware was cleaned thoroughly with a solution of "Micro" by being left to soak overnight. After rinsing with distilled water, the glassware was oven-dried and rinsed with acetone and dichloromethane.

### Extraction

Sedimentary rock samples were ground to a fine powder after removing potentially contaminated surface layers. The powder was homogenised before weighing an aliquot (50-450g) into solvent-cleaned 250ml Teflon centrifuge tubes ( $\leq 100\text{g}$  per tube). A solvent mixture of dichloromethane/methanol (3:1) was added and the sample extracted ultrasonically (15 min). After centrifugation (2500 rpm, 15 min) the supernatant was decanted off and the solvent evaporated using rotary evaporation. This procedure was repeated 3 times or until the solvent extract was colourless. Dry extracts were stored in a fridge or freezer until they were fractionated. DSDP samples (30-70g) were received as powders and in each case the entire sample was extracted as above.

### Fractionation

#### *Column chromatography*

Extracts were separated into their major crude fractions by flash column chromatography based on the procedure of Still *et al.*, 1978. Column size was chosen depending upon the sample size. The clean, dry column was typically packed with dichloromethane-extracted, dry, activated silica (150°C, 24h; approx. 200g per g extract) and pre-eluted with hexane. Extracts, usually ( $>0.5\text{g}$ ) pre-adsorbed on to the minimum volume of silica, were applied to the top of the column. Crude fractions were first obtained by applying solvent mixtures of increasing polarity. Four crude fractions were initially obtained, containing aliphatic and aromatic hydrocarbons (9:1 hexane/dichloromethane), nickel porphyrins (1:1 hexane/dichloromethane), vanadyl porphyrins (dichloromethane) and a polar fraction containing iron porphyrins and/or maleimides where present (methanol), respectively. In the case of the Holzmaden samples, the extract was initially chromatographed on a packed column packed with

alumina (grade II, neutral). Crude fractions were obtained containing aliphatic and aromatic hydrocarbons (toluene), nickel porphyrins (9:1 hexane/di-ethyl ether), vanadyl porphyrins (ethyl acetate) and a polar fraction (methanol).

Smaller silica-packed columns were then used for further purification of Ni and V=O porphyrin fractions from all samples, using the solvent scheme detailed above. In the case of some Cen/Tur samples a third column was employed to further purify any metalloporphyrins present, with nickel porphyrin and vanadyl porphyrin fractions being obtained using a 1:1 hexane/toluene mixture and toluene respectively.

A second larger silica flash column was employed to further separate the polar fraction. Fractions were obtained containing any vanadyl porphyrins (dichloromethane), maleimides (95:5 dichloromethane/acetone), an acetone fraction, iron porphyrins if present (propan-1-ol) and polars (methanol).

#### *Gel Permeation Chromatography (GPC)*

GPC was employed, using the method described by Rosell-Melé and Maxwell, 1996, for the further clean-up of some metallo porphyrin fractions (*i.e.* where porphyrin uv/vis absorption maxima were masked by other material), this technique having previously been shown to be useful as a purification step by removing macromolecular material from total extracts (Quirke, 1987). Fractionation was performed using a Polymer Laboratories (Shropshire, UK) PL-GEL, 10  $\mu$ l, 50 Å column (600x7.5 mm) column, with a Phenomenex (Cheshire, UK) Phenogel (10  $\mu$ l, 50x7.8 mm) guard column and a Rheodyne 7125 injection valve with either a 20  $\mu$ l or 100  $\mu$ l injection loop. Modified HPLC gradient elution (dichloromethane (40%) and methanol (60%) moving to 80% and 20% respectively at 40 min) was passed through the columns at a flow rate of 3 ml min<sup>-1</sup> and into a Waters 991 photodiode array (PDA) detector, monitoring the wavelengths corresponding to Ni (390, 510 and 550 nm) and VO porphyrins (410, 530 and 570 nm). VO porphyrins were obtained by collecting the eluant from 11 to 20 min and Ni porphyrins from 20 to 35 min. After solvent evaporation, the clean-up procedure was repeated using an isocratic solvent program with dichloromethane (51%) and methanol (49%) at a flow rate of 3 ml min<sup>-1</sup>.

## INSTRUMENTATION

### Ultraviolet/visible (Uv/vis) Spectrophotometry

UV/vis absorbance spectra were obtained in dichloromethane in a quartz cell (1 cm path length) using a Unicam UV2 spectrophotometer (slit width 2 nm; scan speed 120 nm min<sup>-1</sup>; absorbance range generally 450-700 nm). Ni, VO and free base porphyrin concentrations were calculated using the Beer-Lambert formula:

$$A = \epsilon \cdot c \cdot l$$

Where A = absorbance;  $\epsilon$  = extinction coefficient (mol<sup>-1</sup> cm<sup>-1</sup> l); c = concentration (mol l<sup>-1</sup>) and l = path length (cm). The extinction coefficients  $\epsilon$  = 22000, 17600 and 15600 were used for Ni, VO and free base porphyrins respectively (Chicarelli, 1985).

### High Performance Liquid Chromatography (HPLC)

In some cases (*i.e.* where >C<sub>32</sub> CAPs eluted in an “unexpected” region as determined by HPLC-MS) semi-preparative normal phase HPLC was utilized in order to concentrate a fraction containing such components. Analysis was performed using a Rheodyne 7125 injector valve with a 100  $\mu$ l injection loop, a Spherisorb S5W normal phase column (250x10 mm i.d.) with a solvent flow rate of 5 ml min<sup>-1</sup> giving a back pressure between 800 and 850 psi, with eluant monitoring performed with a Waters 991 PDA. Table 7.1 shows the solvent program (program 1) used for gradient elution, with the HMW fraction being collected between 12 and 18 minutes.

Time (min)	20% acetone/DCM	1% acetic acid/ hexane	1% pyridine/ hexane
0	15	70	15
14	15	70	15
20	25	50	25
25	25	50	25
30	15	70	15
35	15	70	15

Table 7.1. Solvent composition for gradient elution program 1 during normal-phase semi-preparative isolation of HMW CAP-containing fraction.

### Liquid Chromatography-Atmospheric Pressure Ionisation-Mass Spectrometry (LC-APCI-MS)

LC-APCI-MS analysis was performed using a method similar to that described by Rosell-Melé *et al.* (1996). A Waters 600-MS HPLC system was coupled to a Finnigan-MAT TSQ 700 triple quadrupole mass spectrometer via a Finnigan-MAT API interface. The interface was operated in APCI mode, with a vaporiser temperature of

500°C, capillary temperature of 250-300°C and a corona discharge current of 7µA. Nitrogen was used as the sheath gas (50 psi) and the auxiliary gas (10 ml min<sup>-1</sup>). On-line separation of free base porphyrins was achieved using normal phase analytical-scale HPLC. Columns used were three Spherisorb S3W columns (each 150x4.6 mm i.d.) connected in series, with a gradient solvent program employed (table 7.2: according to Barwise et al., 1986 (program 2) or the modified version shown as program 3). Analysis were performed using a solvent flow rate of 1 ml min<sup>-1</sup>, resulting in back pressures between 1800 and 2100 psi, with monitoring at 400 nm using a Waters PDA 991 system. Data were acquired on an Icis system.

Program	Time (min)	20% acetone/ DCM	1% acetic acid/ hexane	1% pyridine/ hexane
Program 2	0	5	90	5
	5	5	90	5
	20	15	77.5	7.5
	35	30	40	30
	45	30	40	30
	50	5	90	5
	70	5	90	5
Program 3	0	5	90	5
	15	14	78	8
	30	28	40	32
	40	30	40	30
	45	5	90	5

Table 7.2. Details of normal phase HPLC solvent programs utilised during LC-APCI-MS of free base porphyrins.

### Demetallation of metallo porphyrins

After dissolving the dry metallo porphyrin in a minimum volume of methane sulphonic acid (MSA; added under a stream of nitrogen), the nitrogen flow was continued (ca. 1 min) prior to heating in a sealed vial at 80°C for 2 h (Ni porphyrins), 100°C for 4 h (VO porphyrins) or 80°C for 4 h (Fe porphyrins). The mixture was allowed to cool to room temperature in the dark and was then diluted with 25% aqueous MSA before filtering through wet glass wool. Porphyrin dications were extracted with DCM five times or until the aqueous layer became colourless, and the extract was then added to fresh water and neutralised with saturated NaHCO<sub>3</sub>. The solution was then washed further with water (5x10 ml) to remove excess NaHCO<sub>3</sub> and the solvent was removed by rotary evaporation. Excess water was removed by azeotropeing with either toluene or acetone. UV/vis spectrophotometry of the dry product confirmed the completion of the

demetallation before the final clean-up, which involved adding the product in DCM to a small silica column and eluting the free base porphyrin with 5% acetone/DCM. Typical yields were 70 to >90%.



## **APPENDICES**

# APPENDIX A

Table showing modified porphyrin maturity parameters (MPMP) given by the ratio of peak areas:  $C_{28}/(C_{28}+C_{32}$  DPEP)

SAMPLE	C28 A	C32 D	C28/C28+C32
Kup ex Fe	134544244	354000000	0.275398279
Serpiano	10879956	66678504	0.140280712
OB68	10476698	3392103	0.755414834
OB28	2057536	3053780	0.402545254
OB17	2252555	4789903	0.319853523
OB6	382567	1350415	0.220756476
BG3xVO	25236379	247000000	0.092700245
BG2xVO	60028380	512000000	0.104939514
BG1xVO	31899125	266000000	0.107080291
BG4xNi	25178246	48665532	0.340966384
BG3xNi	93508178	163000000	0.364542677
BG2xNi	57210434	244000000	0.1899351
GU1xVO	5000201	272000000	0.018051254
BG1xNi	140922430	400000000	0.260522438
M5b xNi	0	69114272	0
M3 xNi	35829841	146000000	0.197051489
M3 xVO	62431924	173000000	0.265180367
M14 xNi	153000000	607000000	0.201315789
M14 xVO	10528542	91913328	0.102775769
M16 xNi	307852408	1020000000	0.231842339
M16 xVO	102532204	680000000	0.131026178
M7xNi	11329548	245000000	0.044199149
M7xVO	5678995	299000000	0.018639273
M11xNi	155202667	101000000	0.605780841
M11xVO	98662387	256000000	0.278186779
CGQ1bxNi	416723048	1280000000	0.245604637
CGQ1bxVO	161753951	1470000000	0.099128886
CGQ2	-	-	-
CGQ3	1043081	749000000	0.001390695
CGQ4	0	40147816	0
CG xNi	124000000	284000000	0.303921569
CG xVO	60817452	517000000	0.105253747
CG xFe	30035198	56247304	0.348103002
CA xNi	37819328	233000000	0.139647817
CA xVO	107000000	588000000	0.153956835
CA xFe	322138648	677000000	0.322416362
GCLB xNi	-	-	-
GCLB xVO	15222190	158000000	0.087876674
GCLB xFe	120000000	425000000	0.220183486
MP0 xNi	260136388	446000000	0.368393971
MP1 xNi	47817349	244000000	0.163860542
MP2 xNi	17332295	79486752	0.17901741
MP3 xNi	108705288	481000000	0.18433833
MP4 xNi	138885509	295000000	0.320097137
MP5 xNi	44781185	67102196	0.400248764
MP0 xVO	9898951	86039208	0.103180539
MP1 xVO	1138376	11919172	0.087181452
MP2 xVO	2660332	27748466	0.087485602
MP3 xVO	7751151	73944952	0.094877855
MP4 xVO	4658990	26186186	0.151044364

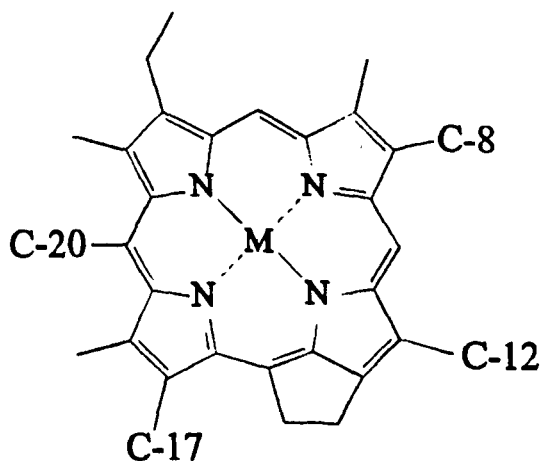
SAMPLE	C28 A	C32 D	C28/C28+C32
F1 xVO	27415586	2.06E+08	1.17E-01
F1 xNi	2.69E+08	1.50E+09	1.52E-01
F1 xFe	8547623	1.66E+08	4.90E-02
F1 fb	10942498	5.74E+08	1.87E-02
FOS1 xVO	61007696	4.69E+08	1.15E-01
FOS2 xVO	40421590	4.47E+08	8.29E-02
FOS3 xVO	16715078	1.58E+08	9.57E-02
FOS4 xVO	23146509	1.85E+08	1.11E-01
367 xNi	21806246	1.11E+08	1.64E-01
367 xVO	8043602	2.40E+08	3.24E-02
368 xNi	46076130	2.56E+08	1.53E-01
368 xVO	9075261	3.84E+08	2.31E-02
368 xFe	62059872	1.60E+08	2.79E-01
144-02 xNi	3.67E+08	3.93E+08	4.83E-01
144-02 xVO	1084110	1.57E+08	6.86E-03
144-03 xNi	1.79E+08	1.52E+08	5.41E-01
144-03 xVO	18152822	75077624	1.95E-01
GAC1 xNi	2.38E+08	2.82E+08	4.58E-01
GAC2 xNi	198184530	3.67E+08	3.51E-01
GAC3 xNi	92140608	69682912	5.69E-01
GAC4 xNi	91985744	78096824	5.41E-01
GAC5 xNi	1.26E+08	4.80E+08	2.08E-01
GAC6 xNi	76440712	3.38E+08	1.84E-01
HL10xNi	-	-	-
HL10xVO	15176919	1.42E+08	9.66E-02
HL12xNi	9226736	4995090	6.49E-01
HL12xVO	15176919	1.42E+08	9.66E-02
VAL3	38651836	2.01E+08	1.61E-01
VAL4	22818838	2.75E+08	7.66E-02
VAL5	13248900	77349496	1.46E-01
VAL6	26167023	80392640	2.46E-01
VAL7	136912723	1.27E+08	5.19E-01
Semct xNi	69207202	2.74E+08	2.02E-01
Semct xVO	1683681	2.63E+08	6.36E-03
Belluno xVO	61138494	79193152	4.36E-01
Colomb xVO	22634807	3.91E+08	5.47E-02

SAMPLE		C28 A	C32 D	C28/C28+C32
VDG				
II		28281240	40442088	0.4115231
III		539398	1.40E+08	0.0038381
VI		1845299	31307598	0.0556603
VII		0	88961272	0
VIII-1a		0	56457845	0
IX		547754	32179742	0.0167368
IV-4		2862207	1.49E+08	0.0188474
IV-6		6051834	1.59E+08	0.0366663
IV-7		438269	1.59E+08	0.0027488
IV-9		19518863	1.68E+08	0.1040901
IV-10		7879762	1.51E+08	0.0495958
Mulhouse				
Section	Depth(m)			
T	0.745	1062855	19233918	0.0523657
T	0.9	195319	1976137	0.0899484
T	1.62	0		0
T	2.3	0		0
T	2.69	0		0
Ti	6.215	68244	8854354	0.0076484
Ti	6.765	314937	5047385	0.0587315
Ti	6.985	0		0
Ti	8.515	344987	7267499	0.0453186
Ti	9.385	829113	5918406	0.1228767
Ti	10.735	41318	9108084	0.0045159
Ci	12.18	0		0
Ci	13.33	184836	1897074	0.0887819
Ci	14.565	71125	2088533	0.0329335
S	23.14	0		0
S	23.65	0		0
S	24.07	109116	2185663	0.0475497
S	26.275	87314	934198	0.0854753

# APPENDIX B

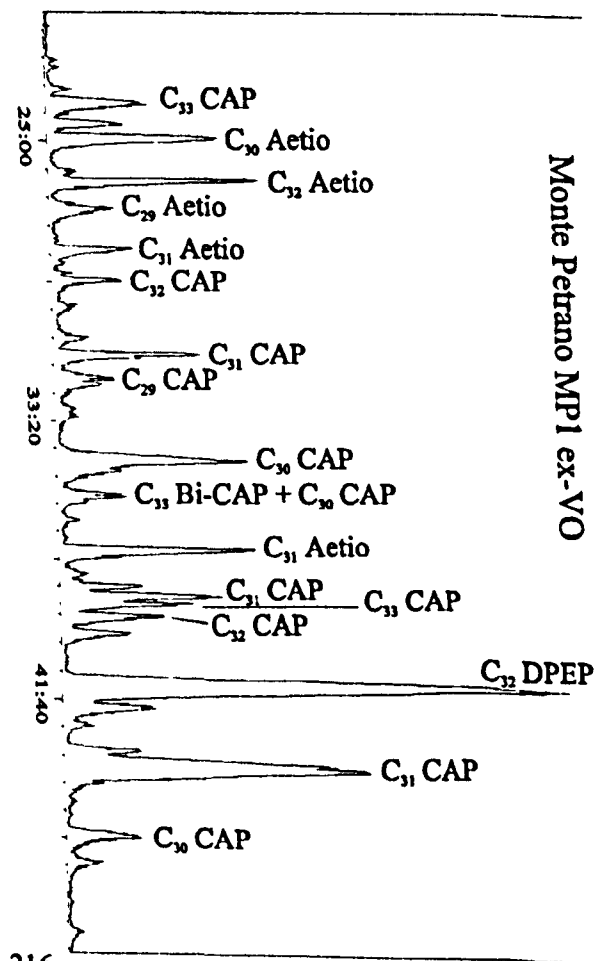
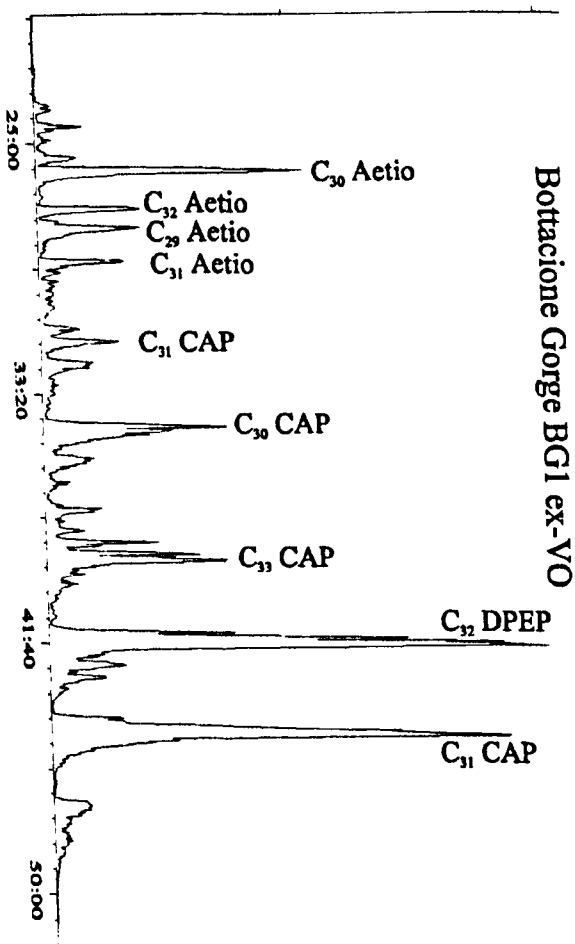
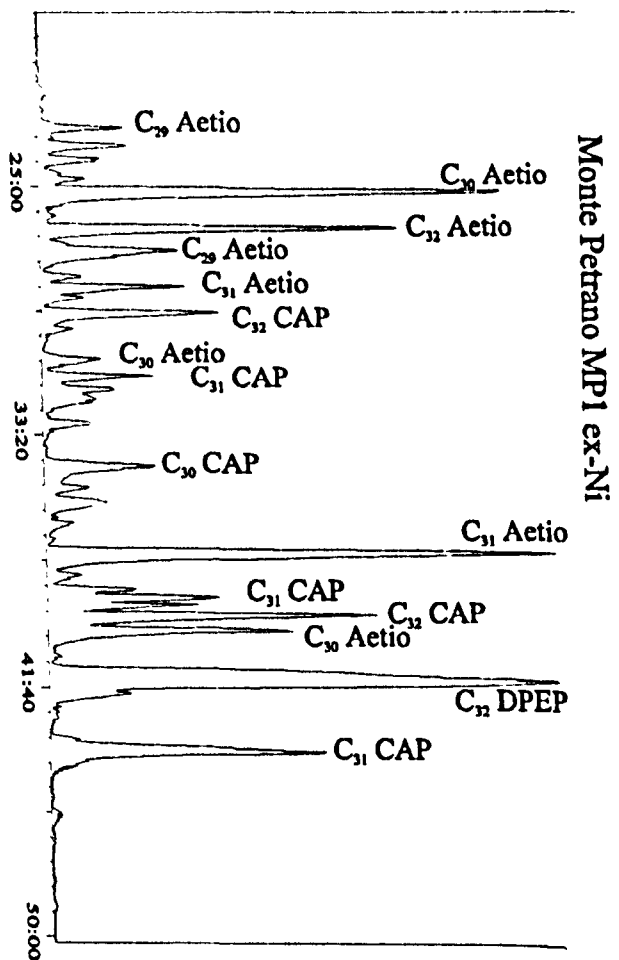
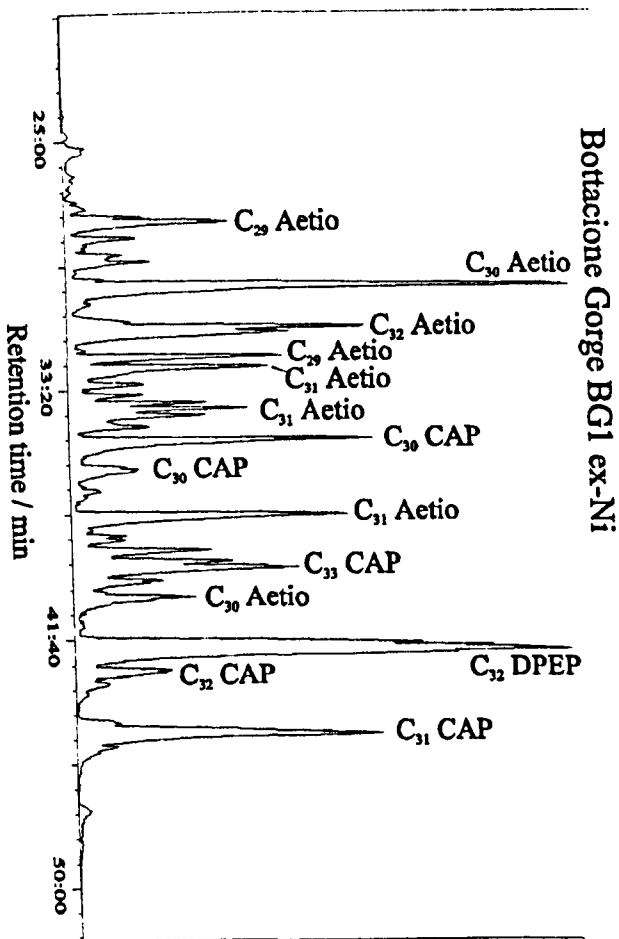
Substitution patterns and carbon no. for bacteriochls *c*, *d* and *e* of Chlorobiaceae

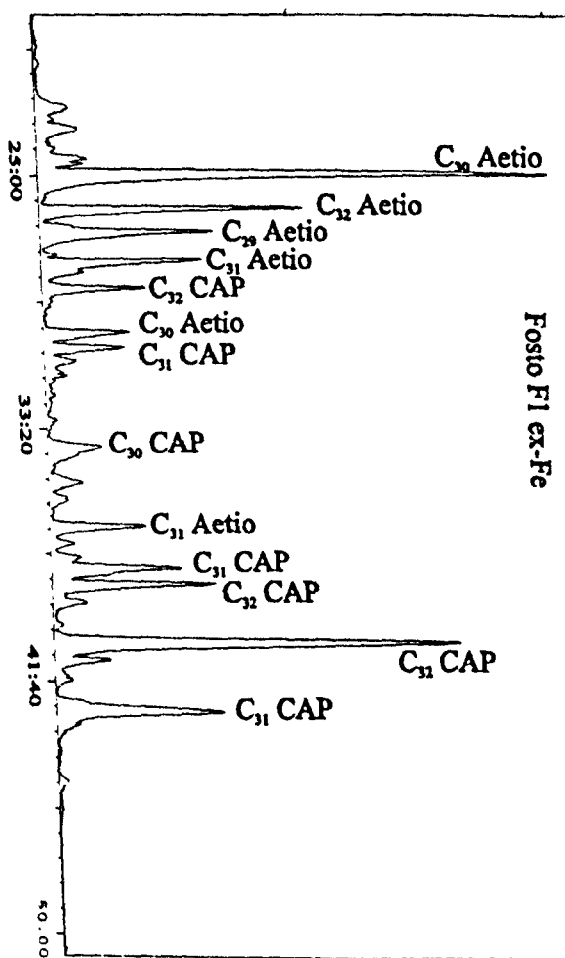
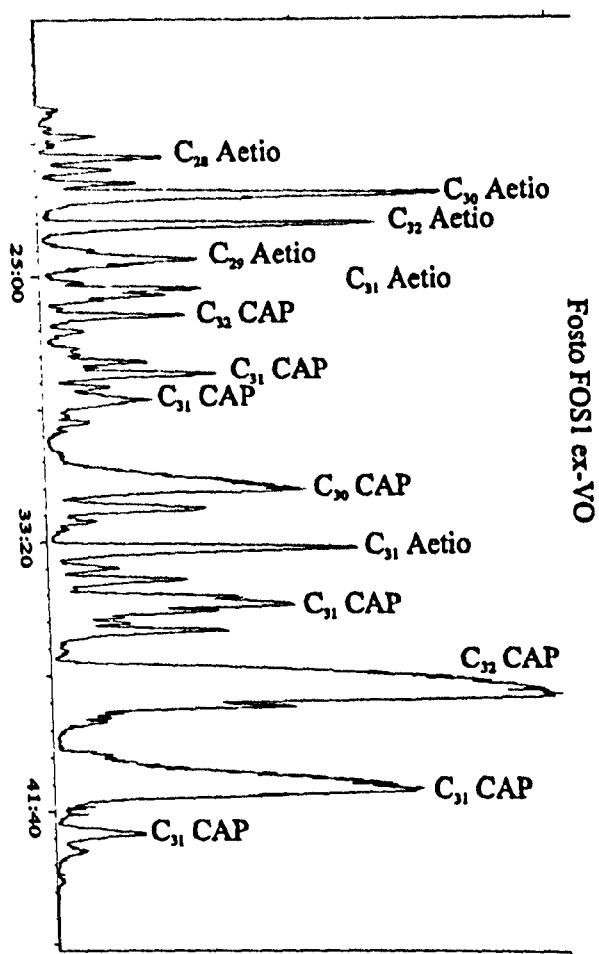
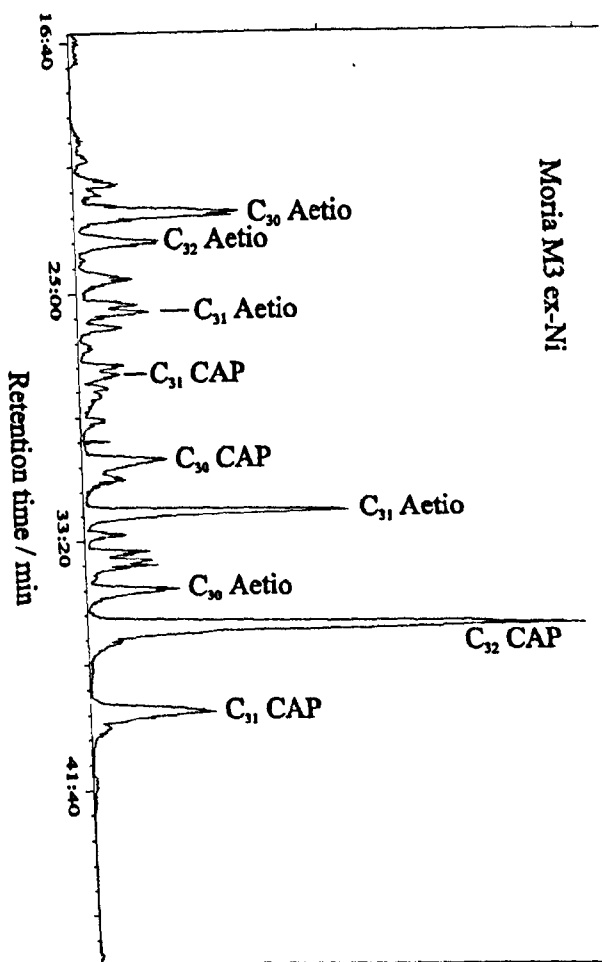
Bacteriochl	No. carbon atoms	Alkyl substitution			
		C-8	C-12	C-17	C-20
<i>d</i>	32	Et	Me	Et	H
<i>d</i>	33	<i>n</i> -Pr	Me	Et	H
<i>d</i>	34	<i>i</i> -Bu	Me	Et	H
<i>d</i>	35	<i>neo</i> -Pent	Me	Et	H
<i>d</i>	33	Et	Et	Et	H
<i>d</i>	34	<i>n</i> -Pr	Et	Et	H
<i>d</i>	35	<i>i</i> -Bu	Et	Et	H
<i>d</i>	36	<i>neo</i> -Pent	Et	Et	H
<i>c</i>	33	Et	Me	Et	Me
<i>c</i>	34	<i>n</i> -Pr	Me	Et	Me
<i>c</i>	35	<i>i</i> -Bu	Me	Et	Me
<i>c</i>	36	<i>neo</i> -Pent	Me	Et	Me
<i>c, e</i>	34	Et	Et	Et	Me
<i>c, e</i>	35	<i>n</i> -Pr	Et	Et	Me
<i>c, e</i>	36	<i>i</i> -Bu	Et	Et	Me
<i>c</i>	37	<i>neo</i> -Pent	Et	Et	Me
<i>d</i>	33	Et	Me	Pr	H
<i>d</i>	34	<i>n</i> -Pr	Me	Pr	H
<i>d</i>	35	<i>i</i> -Bu	Me	Pr	H
<i>d</i>	36	<i>neo</i> -Pent	Me	Pr	H
<i>d</i>	34	Et	Et	Pr	H
<i>d</i>	35	<i>n</i> -Pr	Et	Pr	H
<i>d</i>	36	<i>i</i> -Bu	Et	Pr	H
<i>d</i>	34	<i>neo</i> -Pent	Et	Pr	H
<i>c</i>	34	Et	Me	Pr	Me
<i>c</i>	35	<i>n</i> -Pr	Me	Pr	Me
<i>c</i>	36	<i>i</i> -Bu	Me	Pr	Me
<i>c</i>	37	<i>neo</i> -Pent	Me	Pr	Me
<i>c, e</i>	35	Et	Et	Pr	Me
<i>c, e</i>	36	<i>n</i> -Pr	Et	Pr	Me
<i>c, e</i>	37	<i>i</i> -Bu	Et	Pr	Me
<i>c</i>	38	<i>neo</i> -Pent	Et	Pr	Me

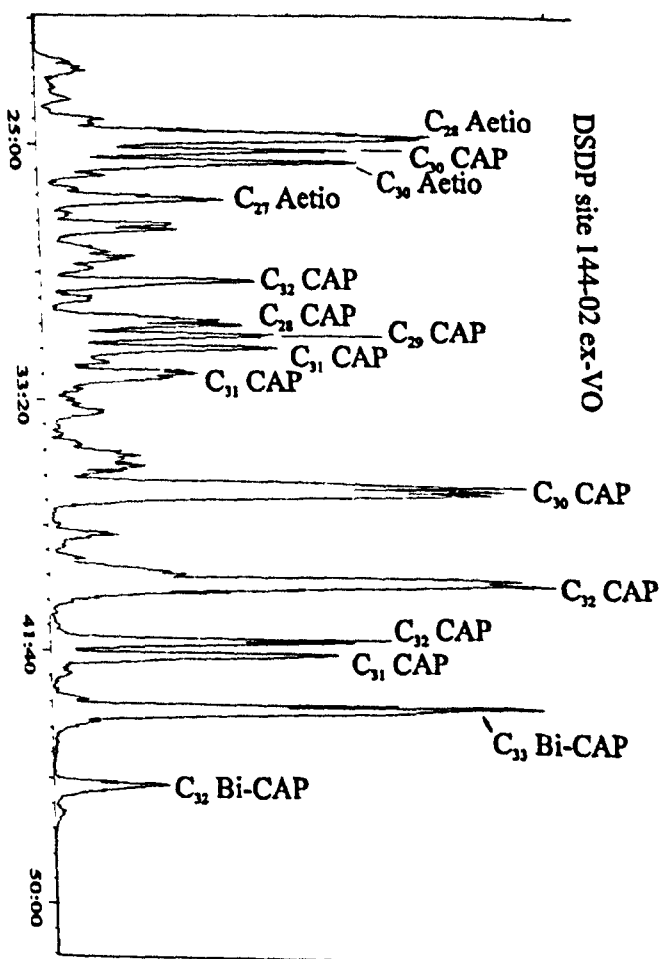
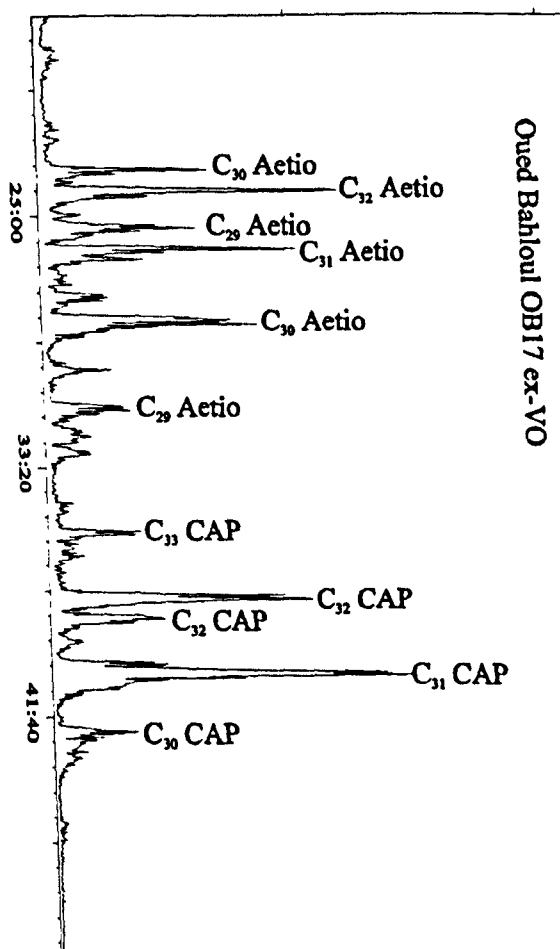
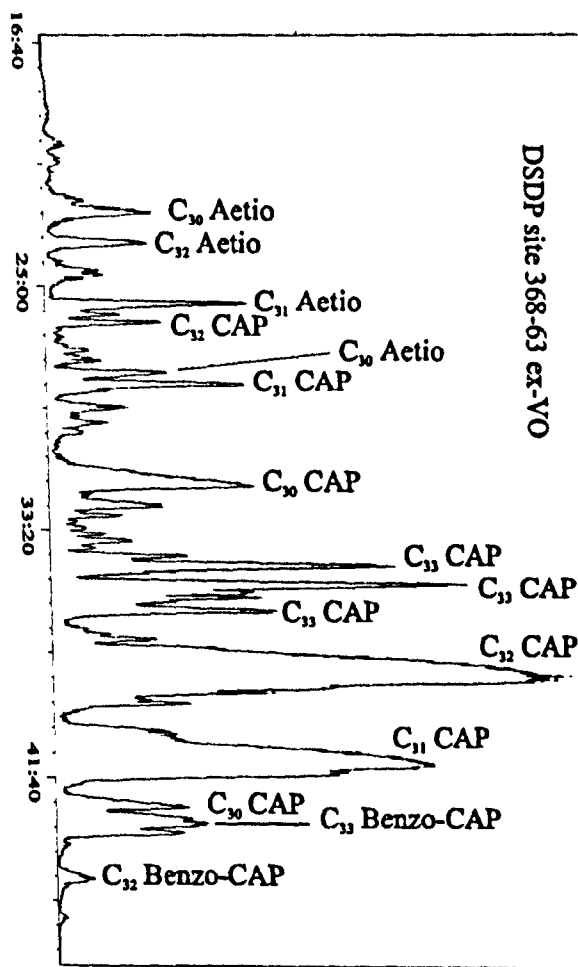
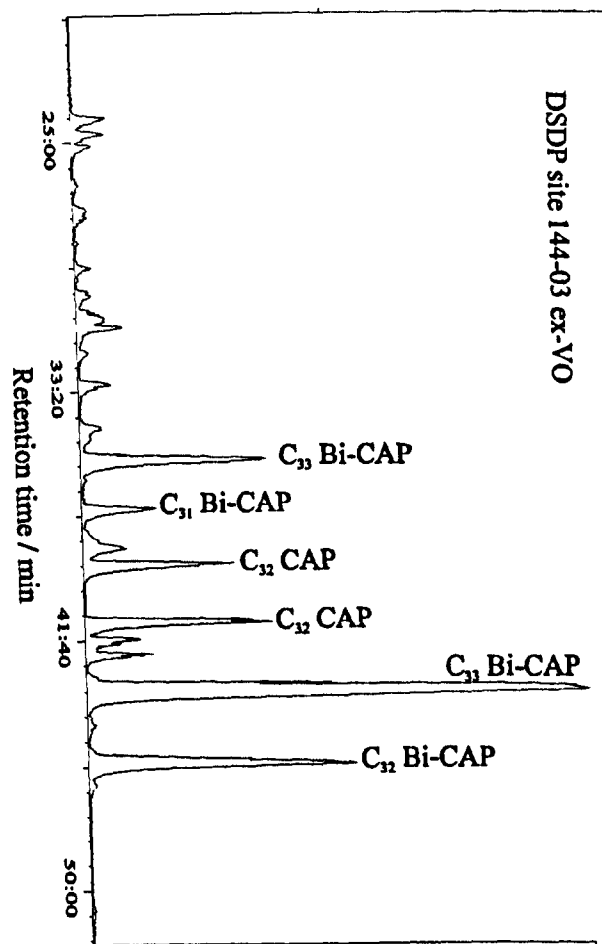


# APPENDIX C

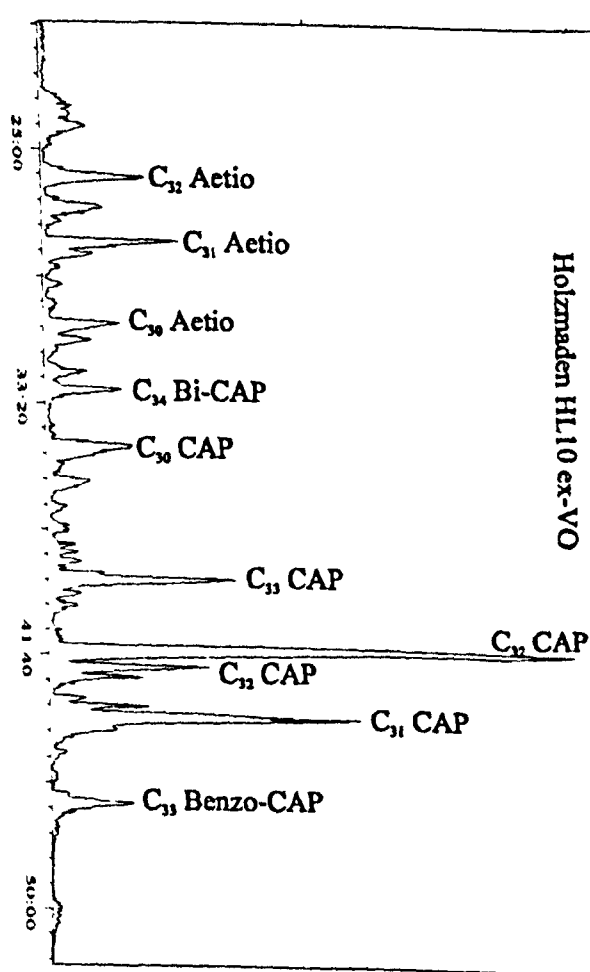
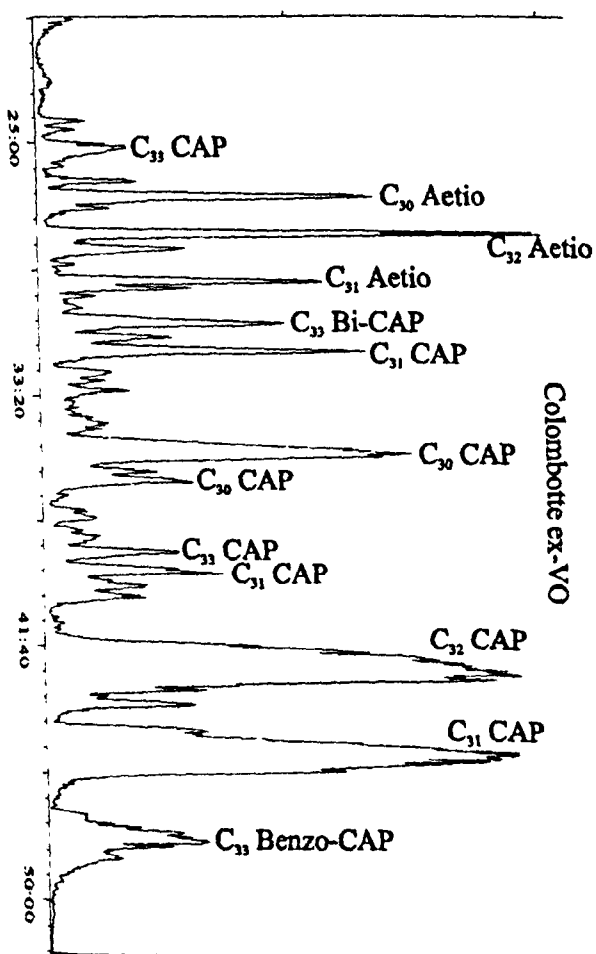
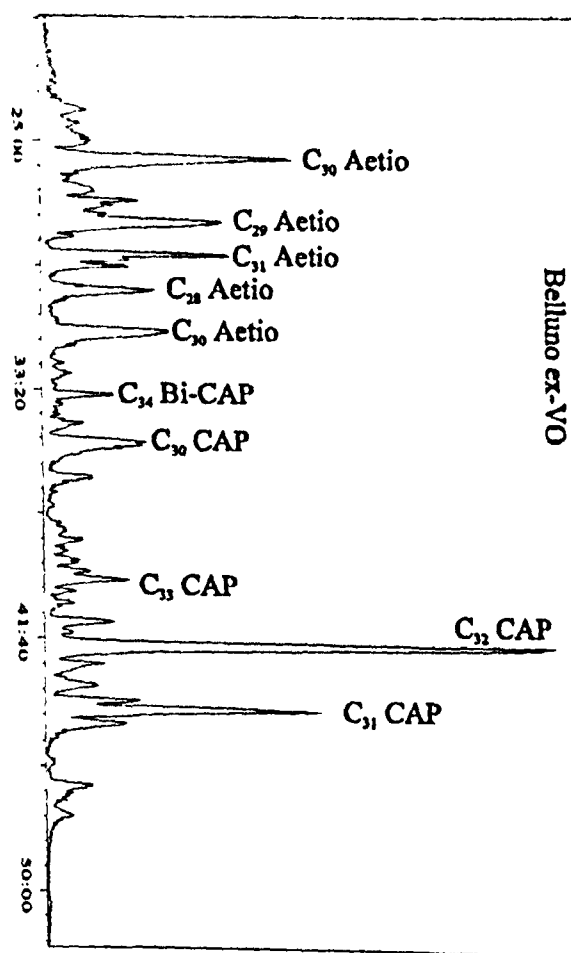
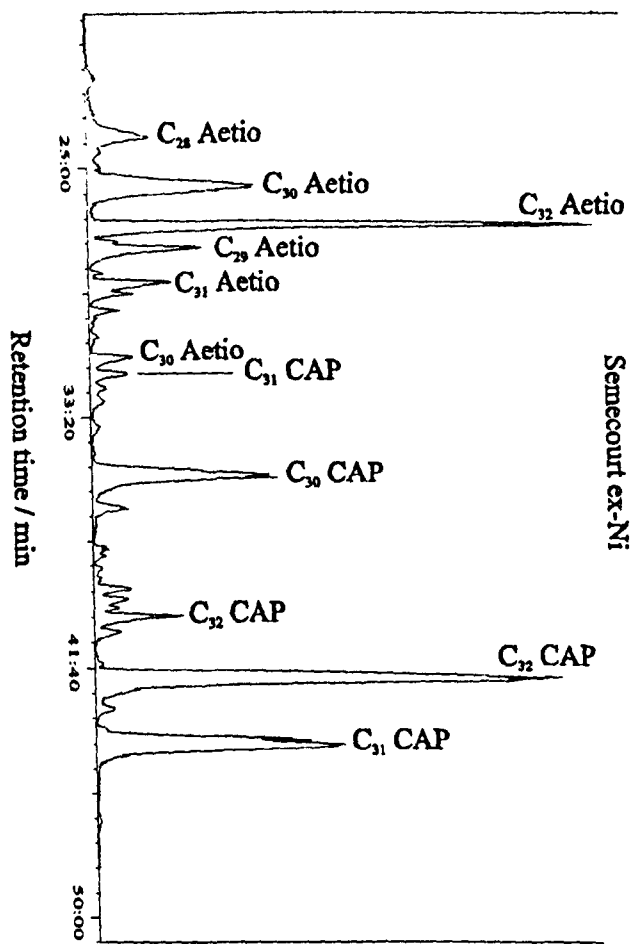
Base peak chromatograms of selected samples showing major components as identified by mass spectra



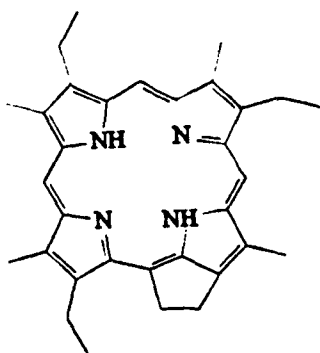




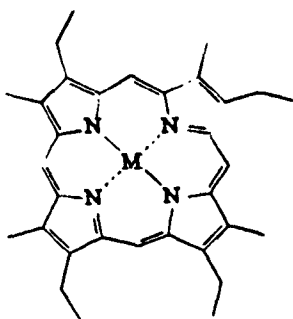




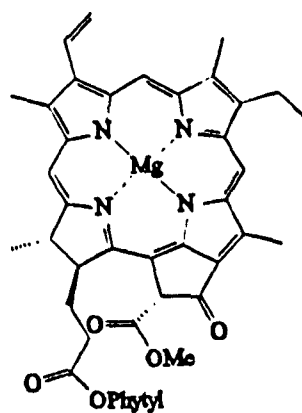
# STRUCTURES



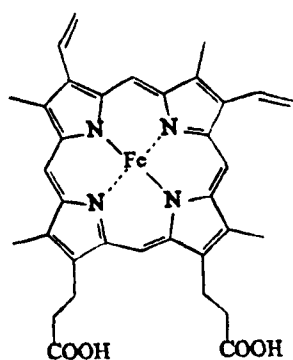
1



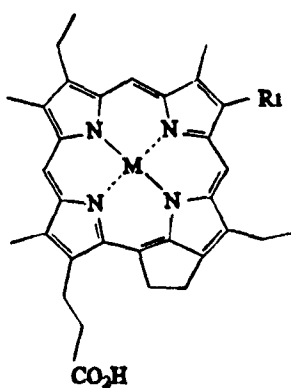
2



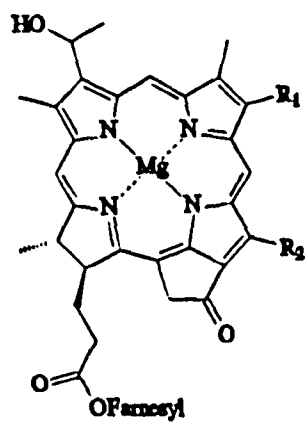
3



4

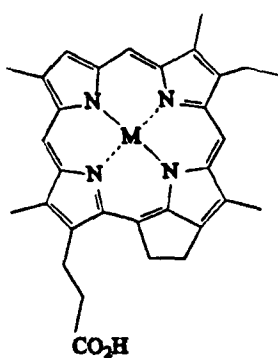


5  $R_1 = \text{Et}, n\text{-Pr}, i\text{-Bu}$

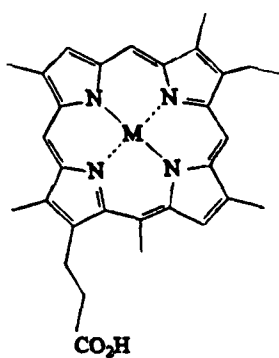


6  $R_1 = \text{Et}, n\text{-Pr}, i\text{-Bu}$

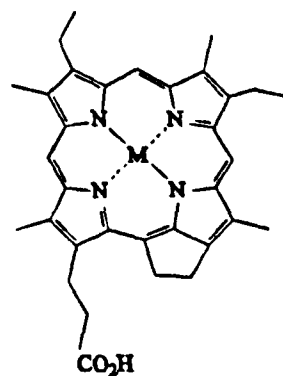
$R_2 = \text{Me}, \text{Et}$



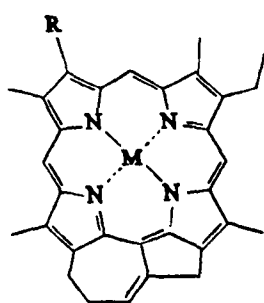
7



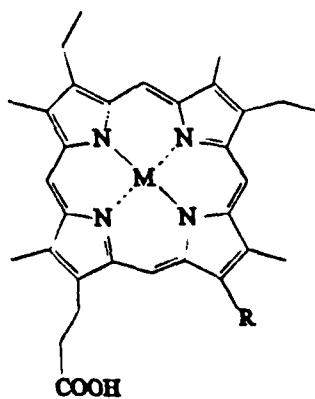
8



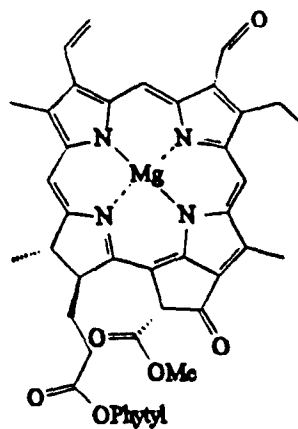
9



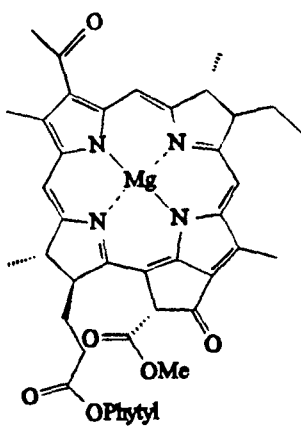
10a  $R = \text{Me}$   
b  $R = \text{Et}$



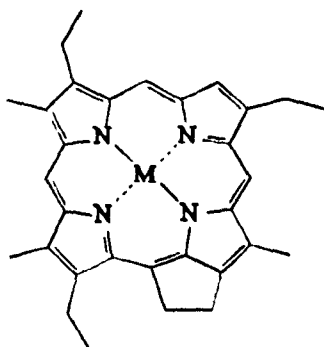
11a  $R = \text{H}$   
b  $R = (\text{CH}_2)_2\text{CO}_2\text{H}$



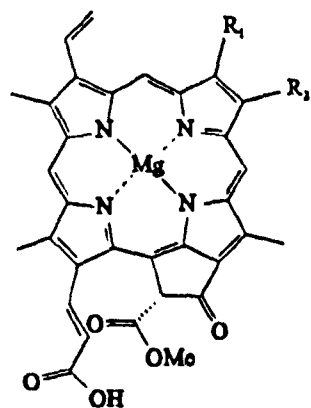
12



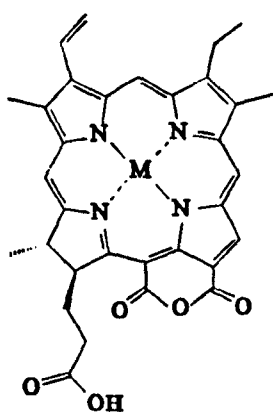
13



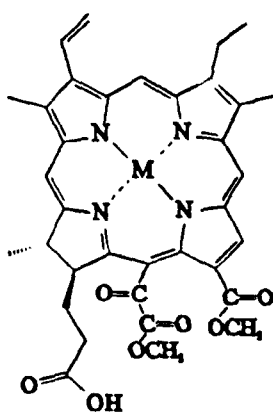
14



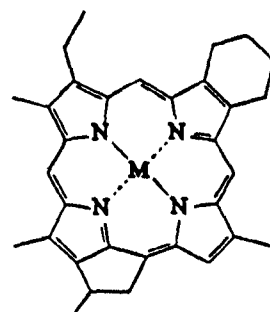
15 3a  $R_1 = \text{Me}$  ;  $R_2 = \text{Et}$   
 3b  $R_1 = \text{Me}$  ,  $R_2 = \text{Vinyl}$   
 3c  $R_1 = \text{CO}_2\text{Me}$  ,  $R_2 = \text{Vinyl}$



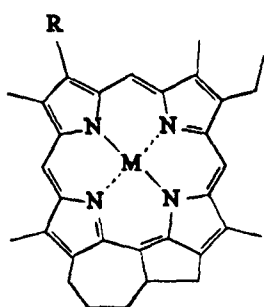
16



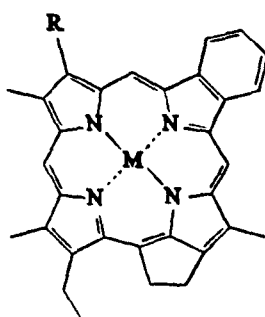
17



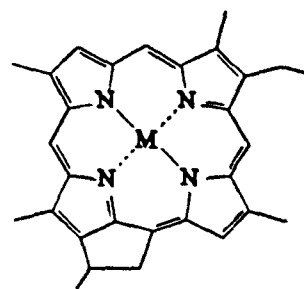
18



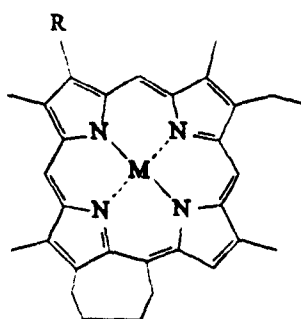
19a  $R = \text{Me}$   
 b  $R = \text{Et}$



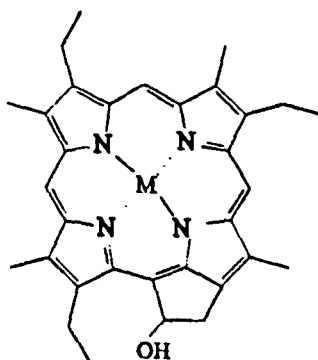
20a  $R = \text{Et}$   
 b  $R = \text{Me}$



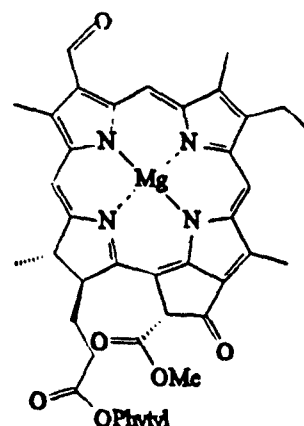
21



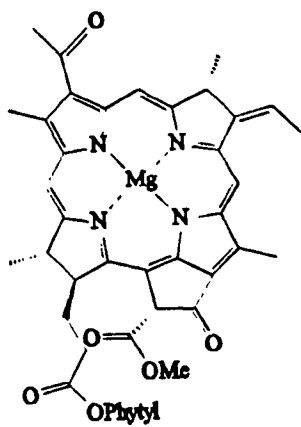
22a  $R = \text{Et}$   
 b  $R = \text{Me}$



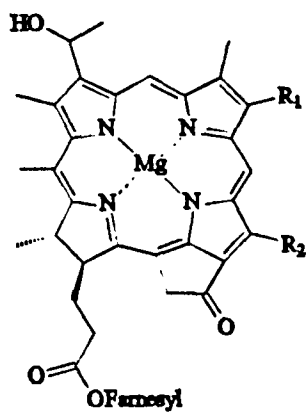
23



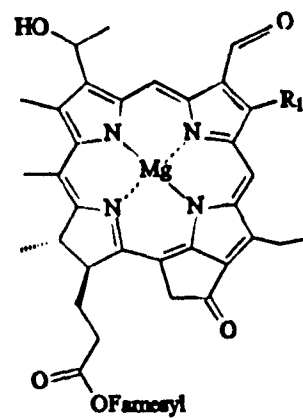
24



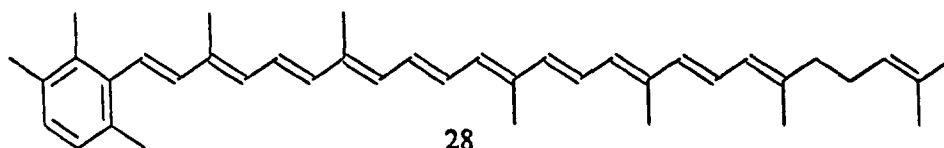
25



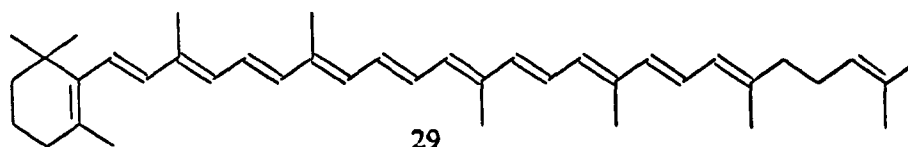
26  $R_1 = \text{Et}, n\text{-Pr}, i\text{-Bu}, \text{neo-Pent}$   
 $R_2 = \text{Me}, \text{Et}$



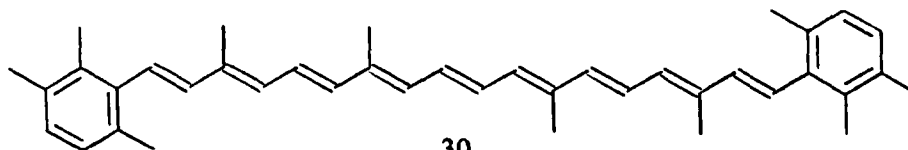
27  $R_1 = \text{Et}, n\text{-Pr}, i\text{-Bu}$



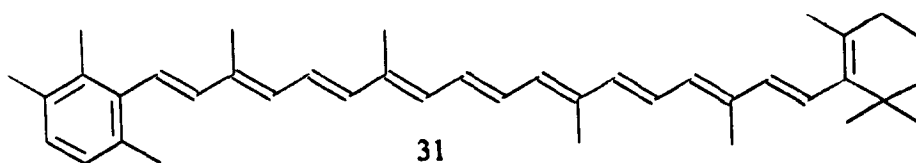
28



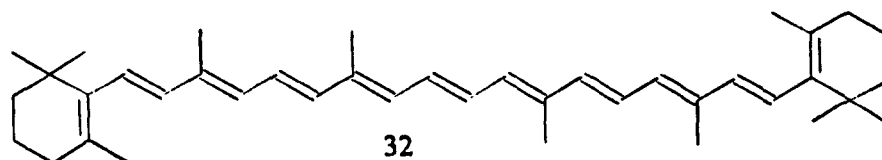
29



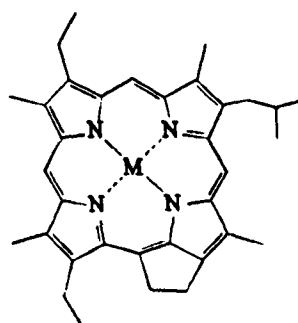
30



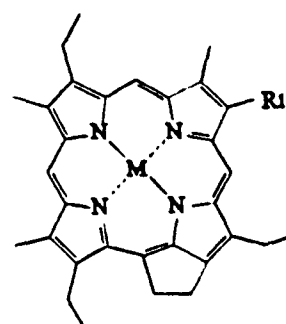
31



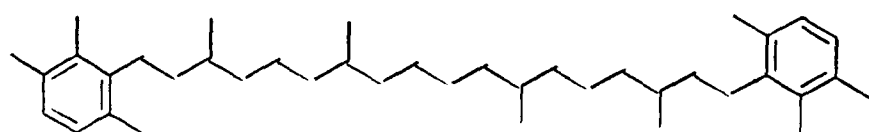
32



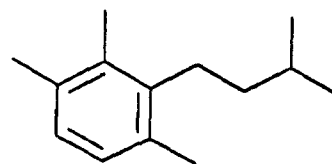
33



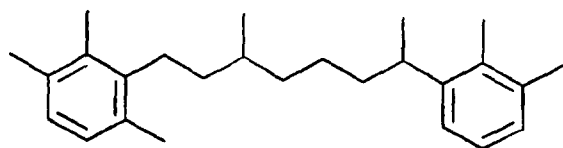
34 a  $R_1 = \text{Et}$   
 b  $R_1 = n\text{-Pr}$   
 c  $R_1 = i\text{-Bu}$



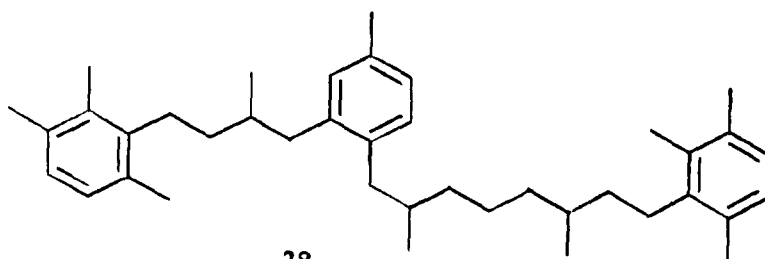
35



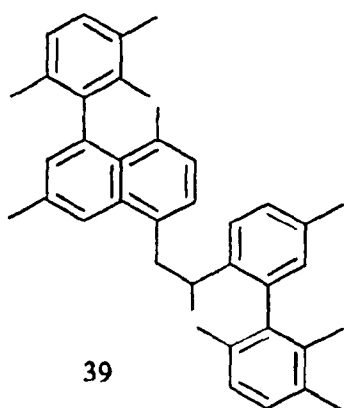
36



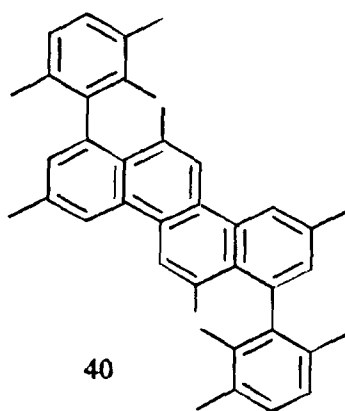
37



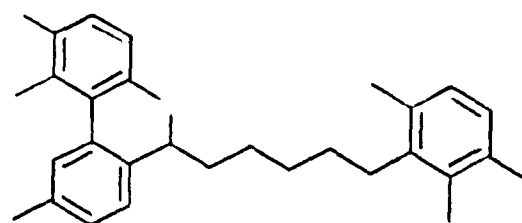
38



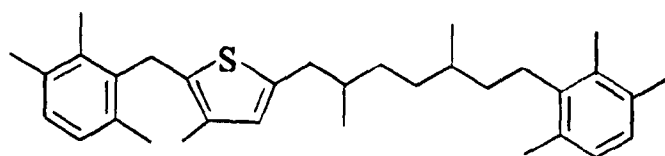
39



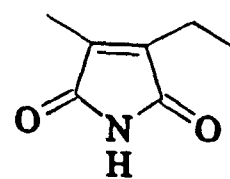
40



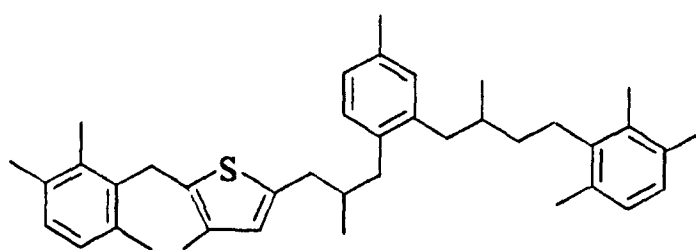
41



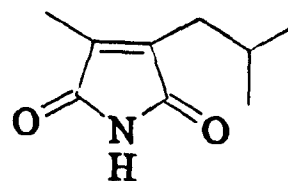
42



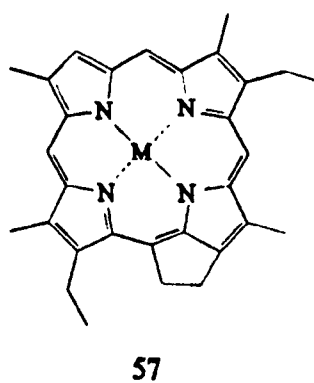
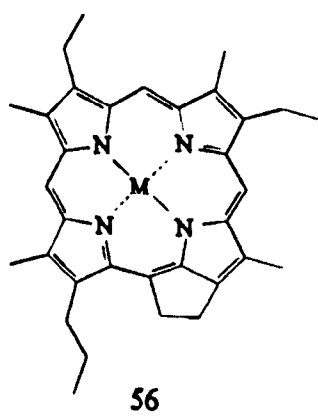
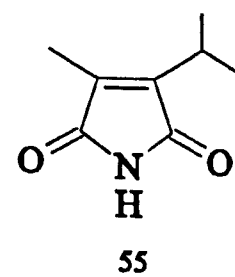
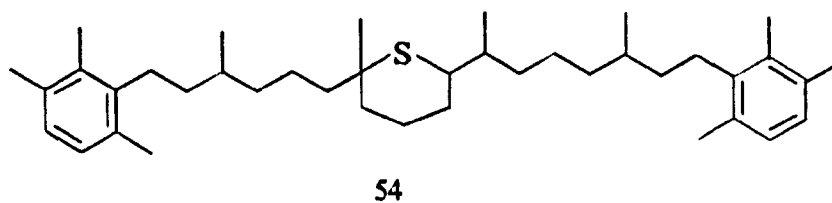
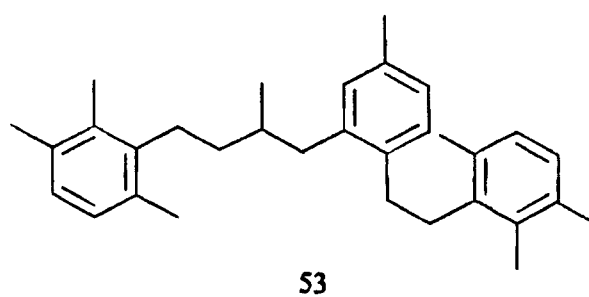
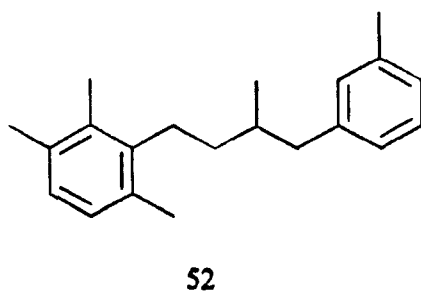
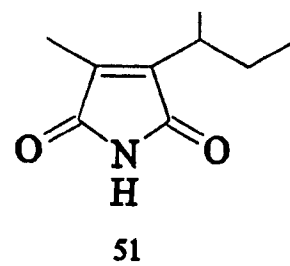
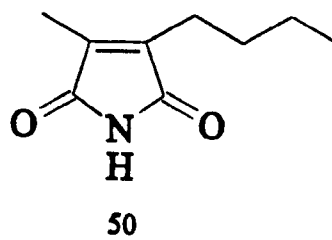
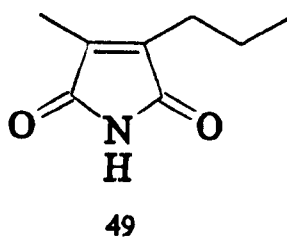
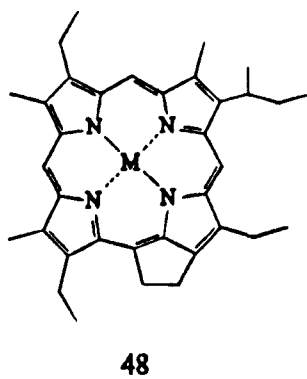
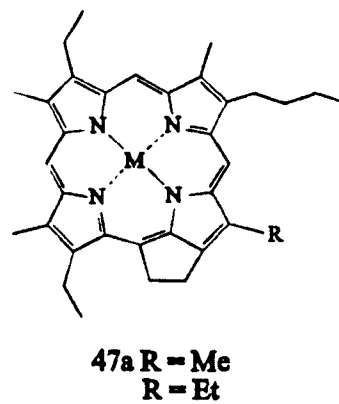
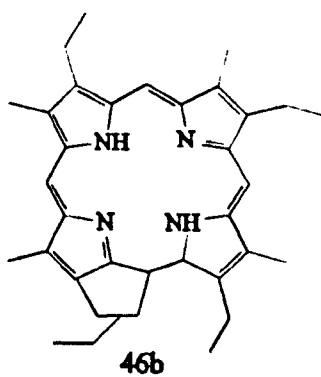
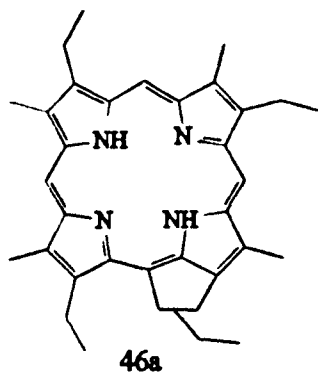
44



43



45



- Adam P., Schmid J.C., Mycke B., Strazielle C., Connan J., Huc A., Riva A. and Albrecht P. (1993) Structural investigation of nonpolar sulphur cross-linked macromolecules in petroleum. *Geochim. Cosmochim. Acta*, **57**, 3395-3419
- Altabet M.A., Francois R., Murray D.W. and Prell W.L. (1995) Climate-related variations in denitrification in the Arabian Sea from sediment  $^{15}\text{N}/^{14}\text{N}$  ratios. *Nature*, **373**, 506-509
- Alturki Y.L.A., Eglinton G. and Pillinger C.T. (1972) in *Advances in Organic Geochemistry 1971*, (Eds: von Gaertner H.R. and Wehner H.), Pergamon Press, Oxford, 1972, p.135
- Anderson R.Y. and Dean W.E. (1988) Lacustrine varve formation through time. *Palaeogeogr. Palaeoclimatol. Palaeoecol.*, **62**, 215-235
- Alpern B. and Cheymol D. (1978) Reflectance et fluorescence des organoclastes du Toarcien du Bassin de Paris en fonction de la profondeur et de la température. *Rev. Inst. Franc. Petrol.*, **33**, 515-535
- Arthur M.A. (1979) Palaeoceanographical events- recognition, resolution and reconsideration. *Rev. Geophys. Space Phys.*, **17**, 1474-1494
- Arthur M.A., Dean W.E. and Stow D.A.V. (1984a) Models for the deposition of Mesozoic-Cenozoic fine grained organic-carbon rich sediments in the deep sea. In *Fine Grained Sediments: Processes and Products*, (Eds: Stow D.A.V and Piper D), pp. 527-562. *Geol. Soc. London. Spec. Publ.*
- Arthur *et al.*, (1984b) Rhythmic bedding in Mesozoic-Cenozoic pelagic carbonate sequences: the primary and diagenetic origin of Melankovitch-like cycles. In: *Milankovitch and Climate* (Eds. Berger A., Imbrie J., Hays J., Kukla G. and Saltzman B.), Riedel Publ. Co., Holland, 191-222
- Arthur M.A. and Dean W.E. (1986) Cretaceous palaeoceanography of the western North Atlantic Ocean. In: *The western North Atlantic region* (eds. Vogt P.R. *et al.*) in the collection The geology of North America. Pp. 617-630 (Geol. Soc. Amer., 1986)
- Arthur M.A., Schlanger S.O., Jenkyns H.C. (1987) The Cenomanian-Turonian oceanic anoxic event, II. Palaeoceanographic controls on organic matter production and preservation. See Brooks and Fleet 1987, pp. 401-420
- Arthur M.A. and Natland J.H. (1979) Carbonaceous sediments in the North and South Atlantic: the role of salinity in stable stratification of early Cretaceous basins. In: *Deep drilling results in the Atlantic Ocean: Continental margins and palaeoenvironment*. Washington, American Geophysical Union, M. Ewing Series., **3**, 297-344
- Arthur M.A., Dean W.E. and Pratt L.M. (1988) Geochemical and climatic effects of increased marine organic carbon burial at the Cenomanian/Turonian boundary. *Nature*, **335**, 714-717
- Arthur M.A. and Premoli-Silva L. (1982) Development of widespread organic-rich strata in the Mediterranean Tethys, see Schlanger and Cita, 1982., pp. 7-54
- Arthur M.A. and Schlanger S.O. (1979) Cretaceous "oceanic anoxic events" as casual factors in development of reef-reservoired giant oil fields. *Bull. Am. Assoc. Petrol. Geol.*, **63**, 870-875
- Arthur M.A., Jenkyns H.C., Brumsack H.J. and Schlanger S.O. (1990) Stratigraphy, geochemistry and palaeoceanography of organic carbon-rich Cretaceous sequences. In: *Cretaceous resources, events and rhythms* (Eds: Ginsburg R.N. and Beaudoin B.), pp. 75-119 (Kluwer Academic Press, Dordrecht)
- Arthur M.A. and Sageman B.B. (1994) Marine black shales: Depositional mechanisms and environments of ancient deposits. *Annu. Rev. Earth Planet. Sci.*, **22**, 499-551
- Back T.G., Yang K. and Krouse H.R. (1992) Desulphurisation of benzo- and dibenzothiopenes with nickel boride. *J. Org. Chem.*, **57**, 1986-1990
- Baker E.W. (1966) Mass spectrometric characterisation of porphyrins., *J. Am. Chem. Soc.*, **88**, 2311
- Baker E.W., Yen T.F., Dickie J.P., Rhodes R.E. and Clark L.F. (1967) Mass spectrometry of porphyrins. II. Characterisation of petroporphyrins. *J. Am. Chem. Soc.*, **89**, 3631-3639
- Baker E.W., Palmer S.E. and Huang W.Y. (1977) Intermediate and late diagenetic terapyrrole pigments, leg 41; Cape Verde Rise and Basin. In: *Init. Rept. DSDP*, **41**, p. 825-837
- Baker E.W. and Palmer S. (1978) Geochemistry of porphyrins. In *The Porphyrins* (Ed: Dolphin D.) Vol. I, Part A, pp. 486-551. Academic Press, New York, San Francisco, London
- Baker E.W. and Louda J.W. (1983) Thermal aspects in chlorophyll geochemistry. In: *Advances in organic geochemistry 1981*. (Eds. Bjoroy M. *et al.*), pp.401-421. Wiley, Chichester
- Barber R.T. and Smith R.L. (1981) Coastal Upwelling Systems. In: *Analysis of Marine Ecosystems* (Ed: Longhurst A.A.) Acad. Press., pp. 31-68
- Barrett P., Tyson R.V., Farrimond P. and Jones D.M. (1997) *Absts. 18<sup>th</sup> Meeting Org. Geochem.*, 293-294
- Barron E.J. (1987) *Palaeogeog. Palaeoclimat. Palaeoecol.*, **59**, 3
- Barron E.J. and Peterson W.H. (1989) Model simulation of the Cretaceous ocean circulation. *Science*, **244**, 684-686



- Barron E.J. and Washington W.M. (1982a)** Atmospheric circulation during warm geologic periods: is the equator-to-pole surface-temperature gradient the controlling factor? *Geology*, **10**, 633-636
- Barron E.J. and Washington W.M. (1982b)** Cretaceous climate: a comparison of atmospheric simulations with the geological record. *Palaeogeog. Palaeoclim. Palaeoecol.*, **40**, 103-133
- Barron E.J. (1983)** A warm, equable Cretaceous: The nature of the problem. *Earth Sci. Rev.*, **18**, 305-338
- Barron E.J., Arthur M.A. and Kauffman E.G. (1985)** Cretaceous rhythmic bedding sequences: a plausible link between orbital variations and climate. *Earth Plant. Sci. Letts.*, **72**, 327-340
- Barwise A.J.G. and Whitehead E.V. (1980)** Separation and structure of petroporphyrins, in *Advances in Organic Geochemistry 1979*, Eds. Douglas A.G. and Maxwell J.R., Pergamon Press, Oxford, 1980 p. 181
- Barwise A.J.G., Evershed R.P., Wolff G.A., Eglinton G. and Maxwell J.R. (1986)** High performance liquid chromatography analysis of free-base porphyrins. I. An improved method. *J. Chromatog.*, **368**, 1-9
- Barwise A.J.G. (1987)** Mechanisms involved in altering DPEP-etio porphyrin ratios in sediments and oils. In: *Metal Complexes in Fossil Fuels*. (Eds:- Filby R.H. and Brathaver J.F.), ACS Symposium Series, **344**, 110
- Bauder C., Ocampo R. and Callot H.J. (1992)** Total synthesis of cyclopentenoporphyrins of sedimentary origin: desoxophylloerythroetioporphyrin, chlorophyll *c* fossils and related compounds. *Tetrahedron.*, **48**, 1535-1550
- Baudin F., Herbin J. and Vandenbroucke M. (1990)** Mapping and geochemical characterisation of the Toarcian organic matter in the Mediterranean Tethys and Middle East. *Adv. Org. Geochem. 1989.*, **16**(4-6), 677-687
- Beiersdorf H. and Knitter H. (1986)** Diagenetic layering and lamination. *Mitt. Geol. Paläontol. Inst. Hamburg.*, **60**, 267-273
- Bergaya F. and Van Damme H. (1982)** Stability of metalloporphyrins adsorbed on clays: A comparative study. *Geochim. Cosmochim. Acta.*, **46**, 349-360
- Berger W.H. (1970)** Biogenous deep-sea sediments: Fractionation by deep-sea circulation. *Bull. Geol. Soc. Am.*, **81**, 1385-1402
- Berger W.H. and von Rad U. (1972)** Cretaceous and Cenozoic sediments from the Atlantic Ocean. *Init. Repts. DSDP.*, **14**, (Eds: Hayes D.E., Pimm A.C., et al., 1972) Washington (U.S. Govt. Printing Office). Pp. 787-885
- Berger W.H. (1978)** Long-term variations of caloric insolation resulting from the earth's orbital elements. *Quat. Res.*, **9**, 139-167
- Berger W.H. (1979)** Impact of deep sea drilling on paleoceanography. In: *Deep drilling results in the Atlantic ocean*, **3**, (Eds. Talwani M., Hay W.W. and Ryan W.B.F.) Second Maurice Ewing symposium, *Amer. Geophys. Union*, pp. 297-314
- Berger W.H., Smetacek V.S. and Wefer G. (1989)** Productivity of the oceans: Present and past. New York: Wiley Interscience. 471
- Berger W.H. and Soutar A. (1970)** Preservation of plankton shells in an anaerobic basin off California. *Geol. Soc. Amer. Bull.*, **81**, 275-282
- Berger A.L. (1988)** Milankovitch theory and climate. *Rev. Geophys.*, **26**, 624-657
- Berggren W.A. and Hollister C.D. (1977)** Plate tectonics and palaeocirculation – commotion in the ocean. *Tectonophys.*, **38**, 11-48
- Berner R.A. and Raiswell R. (1983)** Burial of organic carbon and pyrite sulphur in sediments over Phanerozoic time: a new theory. *Geochim. Cosmochim. Acta.*, **47**, 855-862
- Berner R.A. (1992)** *Nature*, **358**, 114
- Bernhard J.M. (1986)** Characteristic assemblages and morphologies of benthic foraminifera from anoxic organic-rich deposits: Jurassic through Holocene. *J. Foram. Res.*, **16**, 207-215
- Betts J.N. and Holland H.D. (1991)** The oxygen content of ocean bottom waters, the burial efficiency of organic carbon, and the regulation of atmospheric oxygen. *Global Planet. Change* **5**, 5-18
- Blanc-Valleron M.M. (1986)** Enseignements géologiques tirés de l'étude systématique de la matière organique d'un bassin salifère. Le bassin potassique de Mulhouse (Alsace, France). *C. R. Acad. Sc. Paris.*, **302**, Série II, 825-830
- Blanc-Valleron M.M., Gely J.P., Schuler M., Dany F. and Ansart M. (1991)** La matière organique associée aux évaporites de la base du Sel IV (Oligocène inférieur) du bassin de Mulhouse (Alsace, France). *Bull. Soc. Géol. France.*, **162**, 113-122
- Blasco D. (1971)** Composicion y distribucion del fitoplancton en la region del afloramiento de las costas peruanas; *Investigacion pesq.*, **35**, 61-112

- Blum W., Richter W.J. and Eglinton G. (1988) Glass capillary gas chromatography-mass spectrometry at high temperatures. Direct analysis of free base porphyrins and metal porphyrin complexes extracted from the Serpiano oil shale. *J. High Res. Chrom. & Chrom. Commun.*, **11**, 148-156
- Blum W. and Eglinton G. (1989) Preparation of high temperature stable glass capillary columns coated with PS-090 (20% diphenyl substituted CH<sub>3</sub>O-terminated polysiloxane) a selective stationary phase for the direct analysis of metal-porphyrin complexes. *J. High Res. Chrom.*, **12**, 290-293
- Blum W. and Eglinton G. (1989) Glass capillary gas chromatography alkali flame ionisation detection at high temperatures. Direct analysis of free base petroporphyrins. *J. High Res. Chrom.*, **12**, 621-623
- Blum W., Ramstein P. and Eglinton G. (1990) Coupling of high temperature glass capillary columns to a mass spectrometer. GC-MS analysis of metallo porphyrins from Julia Creek oil shale samples. *J. High Res. Chrom.*, **13**, 85-93
- Blumer M. (1950) Porphyrinfarbstoffe und Porphrin-Metallkomplexe in schweizerischen Bitumina. *Helv. Chim. Acta.*, **33**, 1627-1637
- Blumer M. and Snyder W.D. (1967) Porphyrins of high molecular weight in a Triassic oil shale: evidence by gel permeation chromatography. *Chem. Geol.*, **2**, 35-45
- Bonnett R., Brewer P., Noro K. and Noro T. (1978) Chemistry of vanadyl porphyrins. *Tetrahedron.*, **34**, 379-385
- Bonnett R. and Czechowski F. (1980) Gallium porphyrins in bituminous coal. *Nature*, **283**, 465-466
- Bonnett R. and Czechowski F. (1981) Metals and metal complexes in coal. *Phil. Trans. R. Soc. Lond. A*, **300**, 51-63
- Bonnett R., Burke P.J. and Reszka A. (1983) Iron porphyrins in coal. *J. Chem. Soc., Chem. Commun.*, 1085-1087
- Bonnett R., Czechowski F. and Latos-Grazyski L. (1990) The direct characterisation of iron porphyrins from coal using paramagnetic shift effects on proton NMR spectra. *J. Chem. Soc., Chem. Commun.*, 849-851
- Boon J.J., Rijpstra W.L.C., de Lange F., de Leeuw J.W. Yoshika M. and Shimizu V. (1979) Black Sea sterol- a molecular fossil for dinoflagellate blooms. *Nature*, **277**, 125-127
- Boreham C.J., Fookes J.R., Popp B.N. and Hayes J.M. (1989) Origins of etioporphyrins in sediments: evidence from stable carbon isotopes. *Geochim. Cosmochim. Acta.*, **53**, 2451-2455
- Boreham C.J., Fookes J.R., Popp B.N. and Hayes J.M. (1990) Origin of petroporphyrins. 2. Evidence from stable carbon isotopes. *Energy and Fuels*, **4**, 658-661
- Bosellini A., Broglio Loriga C. and e Busetto C. (1978) I bacini cretacei del Trentino. *Riv. Ital. Paleont.*, **84**(4), 897-946
- Boylan D.B., Alturki Y.I and Eglinton G. (1969) Application of gas chromatography and mass spectrometry to porphyrin microanalysis. In *Advances in Organic Geochemistry 1968* (Eds: Schenck P.A. and Havenaar I.), pp. 227-240. Pergamon Press, Oxford.
- Bralower T.J. and Thierstein H.R. (1984) Low productivity and slow deep-water circulation in mid-Cretaceous oceans. *Geology* **12**, 614-618
- Bralower T.J. and Thierstein H.R. (1987) Organic carbon and metal accumulation rates in Holocene and mid-Cretaceous marine sediments: palaeoceanographical significance. See Brooks and Fleet 1987, pp. 345-369
- Bralower T.J., Sliter W.V., Arthur M.A., Leckie M.R., Allard D.J. and Schlanger S.O. (1993) Dysoxic/anoxic episodes in the Aptian/Albian (Early Cretaceous). *Am. Geophys. Union. Schlanger Memorial Vol., Monograph 73.*, pp. 5-37
- Bralower T.J., Arthur M.A., Leckie M.R., Sliter W.V., Allard D.J. and Schlanger S.O. (1994) Timing and palaeoceanography of oceanic dysoxia/anoxia in the Late Barremian to Early Aptian (Early Cretaceous). *Palaios.*, **9**, 335-369
- Brass G.W., Southam J.R. and Peterson W.H. (1982) Warm saline bottom water in the ancient ocean. *Nature* **296**, 620-623
- Brassell S.C., Comet P.A., Eglinton G., McEvoy J., Maxwell J.R., Quirke J.M.E and Volkman J.K. (1980) Preliminary lipid analysis of cores 14, 18 and 28 from Hole 416A. In *Initial Reports of the Deep Sea Drilling Project*, Vol. L. U.S. Govt. Printing office
- Brassel S.C., Wardroper A.M.K., Thomson I.D., Maxwell J.R. and Eglinton G. (1981) Specific acyclic isoprenoids as biological markers of methanogenic bacteria in marine sediments. *Nature.*, **290**, 693-696
- Brassel S.C., Eglinton G. and Maxwell J.R. (1983) The geochemistry of terpenoids and steroids. *Biochem. Soc. Trans.*, **11**, 575-586

- Brenner K. and Seilacher A. (1978)** New aspects about the origin of the Toarcian Posidonia shales. *N. Jb. Paläont., Abh.*, **157**, 11-18
- Brewer P.G. and Spencer D.W. (1974)** Distribution of some trace elements in the Black Sea and their flux between dissolved and particulate phases. In: *The Black Sea- Geology, Chemistry and Biology* (Eds: Degens, E.T. and Ross D.A.) *Am. Assoc. Pet. Geol. Mem.*, **20**, 137-143
- Brooks J. and Fleet A., Eds. 1987.** *Marine Petroleum Source Rocks*. London: Geol. Soc.
- Brown R., Tyson R.V. and Farrimond P. (1997)** Organic carbon isotope records of the Aptian Oceanic Anoxic Event (OAE1a) – Can the squiggles be correlated? *Absts. 9<sup>th</sup> Meeting British Org. Geochem. Soc.*
- Brumsack H.J. (1980)** Geochemistry of Cretaceous black shales from the Atlantic Ocean (DSDP Legs 11, 14, 36 and 41). *Chem. Geol.*, **31**, 1-25
- Brumsack H.J. (1986)** The inorganic geochemistry of Cretaceous black shales (DSDP Leg 41) in comparison to modern upwelling sediments from the Gulf of California. See Summerhays and Shackleton, pp.447-462
- Brumsack H.J. and Thurow J. (1986)** The geochemical facies of black shales from the Cenomanian/Turonian Boundary Event (CTBE). In: *Biogeochemistry of Black Shales* (Eds: Degens E.T., et al.) SCOPE/UNEP Sonderband, Mitteilungen des Geologisch-Paläontologischen Instituts der Universität Hamburg, **60**, 247-265
- Brumsack H.J. (1991)** Inorganic geochemistry of the German Posidonia Shale: palaeoenvironmental consequences. See Tyson and Pearson, 1991. Pp. 353-362
- Budyko M.I. and Ronov A.B. (1979)** Chemical evolution of the atmosphere in the Phanerozoic. *Geochem. Int.*:1-9 (*Geokhimiya* **5**, 643-654)
- Burnett W.C. (1977)** Geochemistry and origin of phosphorite deposits from Peru and Chile. *Geol. Soc. Am. Bull.*, **88**, 813-823
- Callot H.J. (1991)** Geochemistry of chlorophylls. In *Chlorophylls* (Edited by Scheer, H.) pp. 339-364. CRC Press, Boca Raton.
- Calvert S.E. (1964)** Factors affecting distribution of laminated diatomaceous sediments in the Gulf of California. In: *Marine Geology of the Gulf of California*. (Eds. van Andel T.H. and Schor J.J. Jr.) *Am. Ass. Palaeontol. Geol. Mem.*, **3**, 311-330
- Calvert S.E. (1983)** Geochemistry of Pleistocene sapropels and associated sediments from the eastern Mediterranean. *Oceanolog. Acta.*, **6**(3), 255-267
- Calvert S.E. (1987)** Oceanographic controls on the accumulation of organic matter in marine sediments. See Brooks and Fleet, 1987., pp. 137-152
- Calvert S.E. and Pederson T.F. (1992)** Organic carbon accumulation and preservation in marine sediments.: How important is anoxia? In: *Organic Matter* (Eds: Whelan J. and Farrington J.W.) Univ. Press. NY., pp. 231-263
- Calvert S.E., Nielsen B. and Fontugne M.R. (1992)** Evidence from nitrogen isotope ratios for enhanced productivity during formation of eastern Mediterranean sapropels. *Nature.*, **359**, 223-225
- Calvert S.E., Bustin R.M. and Ingall E.D. (1996)** Influence of water column anoxia and sediment supply on the burial and preservation of organic carbon in marine shales. *Geochim. Cosmochim. Acta.*, **60**(9), 1577-1593
- Canfield D.E. (1989)** Sulphate reduction and oxic respiration in marine sediments: Implications for organic carbon preservation in euxinic environments. *Deep Sea Res.*, **36**, 121-138
- Cardoso J.N., Wardroper A.M.K., Watts, C.D., Barnes P.J., Maxwell J.R., Eglinton G., Mound D.G. and Speers G.C. (1978)** Preliminary organic geochemical analyses: Site 391, leg 44 of the Deep Sea Drilling Project. In *Init. Rpt. Deep Sea Drilling Proj. Leg 44* (Eds: Benson W.E. et al.), pp. 617-624. US Govt. Printing Office.
- Carpentier B., Gely J.P., Blanc-Valleron M.M., Huc A.Y. and Ansart M. (1992)** Simulation de la sédimentation dans un bassin évaporitique à niveau d'eau sous influence eustatique: application au bassin paléogène de Mulhouse (Alsace, France). *Rev. Inst. Fr. Pét.*, **47-45**, 559-585
- Caulet J.P., Vénec-Peyré M., Vergnaud-Grazzini C. and Nigrini C. (1992)** Variation of South somalian upwelling during the last 160 ka: radiolarian and foraminifera records in core MD 85674. See Summerhays et al., 1992., pp. 379-389
- Chamley H. and Robert C. (1982).** Palaeoenvironmental significance of clay deposits in Atlantic black shales. See Schlanger and Cita, 1982 pp. 101-112
- Chénet P.Y. and Francheteau J. (1979)** Bathymetric reconstruction method: Application to the Central Atlantic Basin between 10°N and 40°N. In: Initial Reports of the Deep Sea Drilling Project, **51, 52, 53**, Part 2 (Donnelly T., Francheteau J., Bryan W., Robinson P., Flower M. and Salisbury M). Washington D.C., (US Government Printing Office), pp. 1501-1514

- Chicarelli M.L. and Maxwell J.R. (1984) A naturally occurring chlorophyll *b* related porphyrin. *Tet. Lett.*, **25**, 4701-4704
- Chicarelli M.L., Wolff G.A. and Maxwell J.R. (1984) Porphyrins with a novel exocyclic ring system in an oil shale. *Tetrahedron.*, **40**, 4033-4039
- Chicarelli M.L. (1985) The porphyrins of Serpiano oil shale: structures and significance. Ph.D. Thesis, University of Bristol
- Chicarelli M.L. and Maxwell J.R. (1986) A novel fossil porphyrin with a fused ring system: Evidence for water column transformation of chlorophyll? *Tet. Lett.*, **27**, 4653-4654
- Chicarelli M.L., Wolff G.A. and Maxwell J.R. (1986) High performance liquid chromatography analysis of free base porphyrins. II. Structure effects and retention behaviour. *J. Chrom.*, **368**, 11-19
- Chicarelli M.L., Kaur S. and Maxwell J.R. (1987) Sedimentary porphyrins: Unexpected structures, occurrence and possible origins. In: *Metal Complexes in Fossil Fuels: Characterisation and Processing* (Eds: Filby R.H. and Brathaver J.F.); *ACS Symposium Series 344*, pp. 40-67
- Chicarelli M.L., Hayes J.M., Popp B.N., Eckardt C.B. and Maxwell J.R. (1993) Carbon and nitrogen isotopic compositions of alkyl porphyrins from the Triassic Serpiano oil shale. *Geochim. Cosmochim. Acta.*, **57**, 1307-1311
- Clark J.P. and Philp R.P. (1989) Geochemical characterisation of evaporite and carbonate depositional environments and correlation of associated crude oils in the Black Creek Basin, Alberta. *Bull. Can. Petr. Geol.*, **37**, 401-416
- Claypool G.E., Holser W.T., Kaplan I.R., Sakai H. and Zach L. (1980) The age curves of sulphur and oxygen isotopes in marine sulphate and their mutual interpretation. *Chem. Geol.*, **28**, 199-260
- Clayton J.L., Warden A., Daws T.A., Lillis P.G., Michael G.E. and Dawson M. (1992) Organic geochemistry of black shales, marlstones and oils of Middle Pennsylvanian rocks from the northern Denver and southeastern Powder River Basins, Wyoming, Nebraska and Colorado. *U.S. Geol. Sur. Bull.*, 1917-K, pp. 1-44
- Clezy P.S. and Mirza A.H. (1982) The chemistry of pyrolic compounds. XLIX. Further observations on the chemistry of the benzoporphyrins. *Aust. J. Chem.*, **35**, 197-209
- Cline J.D. and Kaplan I.R. (1975) Isotopic fractionation of dissolved nitrate during denitrification in the Eastern Tropical North Pacific. *Marine Chemistry.*, **3**, 271-299
- Coccioni R., Franchi R., Nesci O., Wezel C.F., Battistini F. and Pallecchi P. (1989) Stratigraphy and mineralogy of the Selli level (early Aptian) at the base of the Marne a Fucoidi in the Umbrian-Marchean Apennines (Italy). In *Cretaceous of the Western Tethys, 3<sup>rd</sup> International Symposium. Tübingen 1987* (Ed: Wiedmann J.), pp. 563-584 (Schweizerbart, Stuttgart)
- Coccioni R., Nesci O., Tramontana M., Wezel C.F. and Moretti E. (1987) Descrizione di un livello guida "Radiolaritico-Bituminoso-Ittiolitico" alla base delle Marne a Fucoidi nell'Appennino Umbro-Marchigiano. *Bollettino della Società Geologica Italiana.*, **106**, 183-192
- Coccioni R., Erba E. and Premoli-Silva I. (1992) Barremian-Aptian calcereous plankton biostratigraphy from the Gorgo Cerbara section (Marche, central Italy) and implications for plankton evolution. *Cret. Res.*, **13**, 517-537
- Cool T.E. (1982) Sedimentological evidence concerning the paleocenography of the Cretaceous western North Atlantic Ocean. *Palaeo., Palaeo., Palaeo.* **39**, 1-35
- Corwin A.H. (1960) Petroporphyrins, proc. 5<sup>th</sup> world petr. Congr. 1959, New York, paper V-10, 119
- Courtot C., Gannat É. and Wendling E. (1972) Le bassin potassique de Mulhouse et ses environs. Etude du Tertiaire. *Sci. Géol. Bull.*, **25**, 69-91
- Covey T.R., Lee E.D., Bruins A.P. and Henion J.D. (1986) Liquid chromatography-mass spectrometry. *Anal. Chem.*, **58**, 1451A-1461
- Curiale J.A., Cameron D. and Davis D.V. (1985) Biological marker distribution and significance in oils and rocks of the Monterey Formation, California. *Geochim. Cosmochim. Acta.*, **49**, 271-288
- Dean R.A. and Whitehead E.V. (1963) The composition of high boiling petroleum distillates and residues. *Proc. 6<sup>th</sup> world Petroleum Congr.*, sect. V, 261-279
- Dean W.E., Arthur M.A. and Stow D.A.V. (1984a) Origin and geochemistry of Cretaceous deep-sea black shales and multicoloured claystones, with emphasis on Deep Sea Drilling Project Site 530, Southern Angola Basin. *Init. Repts. DSDP*, **75** (Eds: Hay W.W. et al.), 819-844
- Dean W.E., Claypool G.E. and Thiede J. (1981) Origin of organic-carbon rich mid-Cretaceous limestones, mid-Pacific Mountains and southern Hess Rise. *Init. Repts. DSDP.*, **62**, 877-890. Washington D.C.: US Govt. Printing Office.
- Dean W.E. and Gardener J.V. (1982) Origin and geochemistry of redox cycles of Jurassic to Eocene age, Cape Verde Basin (DSDP site 367), continental margin of north-west Africa. See Schlanger and Cita, 1982, pp. 55-75

- Dean W.E., Arthur M.A. and Claypool G.E. (1986) Depletion of  $^{13}\text{C}$  in Cretaceous marine organic matter: source, diagenetic or environmental signal? *Mar. Geol.*, 70, 119-157
- de Boer P.L. and Wonders A.A.H. (1984) Astronomically induced rhythmic bedding in Cretaceous pelagic sediments near Moria (Italy). In: *Milankovitch and Climate*. (Eds. Berger A. et al.) Riedel, Hingham, Mass. Pp. 177-190
- de Boer P.L. (1982) Cyclicality and the storage of organic matter in middle-Cretaceous pelagic sediments. In: *Cyclic and event stratification* (Eds. Einsele G. and Seilacher A.), Springer-Verlag, Berlin., pp. 456-475
- de Boer P.L. (1986) Changes in the organic carbon burial during the Early Cretaceous. See Summerhays and Shackleton., pp. 321-331
- de Boer P.L. (1991) Pelagic black shale-carbonate rhythms: orbital forcing and oceanographic response. See Einsele et al., 1991 pp. 63-78
- Degens E.T. and Ross D.A. (1974) The Black Sea, geology, chemistry and biology: *AAPG Memoir*, 20, 633
- Degens E.T., Emeis K.C., Mycke B. and Wiesner M.G. (1986) Turbidites, the principal mechanism yielding black shales in the early deep Atlantic Ocean. See Summerhays and Shackleton (1986) pp. 361-376
- de Graciansky P.C., Brosse E., Deroo G., Herbin J.P., Montadert L., Muller C., Sigal J. and Schaaf A. (1982) Les formations d'âge Crétacé de l'Atlantique Nord et leur matière organique. Paléogéographie et milieux de dépôt. *Rev. Inst. Franç. Pétr.* 37, 275-336
- de Graciansky P.C., Deroo G., Herbin J.P., Montadert L., Müller C., Schaaf A. and Sigal J. (1984) Ocean wide stagnation episode in the late Cretaceous., *Nature*, 308, 346-349
- de Graciansky P.C. Deroo G., Herbin J.P., Jacquin T., Magniez F., Montadert L., Müller C., Ponsot C., Schaaf A. and Sigal J. (1986) Ocean-wide stagnation episodes in the Late Cretaceous., *Geol. Rund.*, 75, 17-41
- Demaison G.J. and Moore G.T. (1980) Anoxic environments and oil source bed genesis., *Org. Geochem.*, 2, 9-31
- Demaison G.J. (1991) Anoxia vs. productivity: what controls the formation of organic-carbon-rich sediments and sedimentary rocks: Discussion. *AAPG Bull.*, 75, 498-499
- Deroo G., Herbin J.P., Roucache J. and Tissot B. (1977) Organic geochemistry of some Cretaceous black shales from sites 367 and 368; leg 41, Eastern North Atlantic. In: *Init. Rept. DSDP*, 41 p. 865-877
- Deuser W.G. (1975) Reducing environments. In: *Chemical oceanography*. (Eds: Riley J.P. and Chester R.), 3, 1-37
- de Wit R. (1992) Sulphide-containing environments. In: *Encyclopaedia of Microbiology*, 4, 105-121
- de Wit R. and Caumette P. (1995) An overview of the brown-coloured isorenieratene- containing green sulphur bacteria (Chlorobiaceae). *Organic Geochemistry: developments and applications to energy, environment and human history*, 908-909
- Dias-Brito D. (1987) A bacia de Campos no Meso-Cretáceo: uma contribuição à palaeoceanografia do Atlântico Sul primitivo. *Rev. Bras. Geoc.*, 17(2), 162-167
- Dickman M. (1985) Seasonal succession and microlamina formation in a meromict lake displaying varved sediments. *Sedimentology.*, 34, 109-118
- Didyk B., Alturki Y.I.A., Pillinger C.T. and Eglinton G. (1975) The petroporphyrins of a Cretaceous oil. *Chem. Geol.*, 15, 193-208
- Didyk B.M., Simoneit B.R.T., Brassell S.C. and Eglinton G. (1978) Geochemical indicators of palaeoenvironmental conditions of sedimentation. *Nature.*, 272, 216-222
- Disnar J.R., Le Strat P., Farjanel G. and Fikri A. (1996) Organic matter sedimentation in the northeast of the Paris Basin: consequences on the deposition of the lower Toarcian black shales. *Chem. Geol.*, 131, 15-35
- Duffin K.L., Wachs T. and Heinon J.D. (1992) *Anal. Chem.*, 64, 61-68
- Dugdale R.C., Goering J.J., Barber R.T., Smith R.L. and Packard T.T. (1977) Denitrification and hydrogen sulphide in the Peru upwelling region during 1976. *Deep Sea Research.*, 24, 601-608
- Eckardt C.B., Wolf M. and Maxwell J.R. (1989) Iron porphyrins in the Permian Kupferschiefer of the lower Rhine Basin, N.W. Germany. *Org. Geochem.*, 14, 659-666
- Eckardt C.B., Carter J.F. and Maxwell J.R. (1990) *Energy & Fuels*, 4, 741-747
- Eckardt C.B., Keely B.J., Waring J.R., Chicarelli M.L. and Maxwell J.R. (1991) Preservation of chlorophyll-derived pigments in sedimentary organic matter. *Phil. Trans. R. Soc. Lond. B.*, 333, 339-348
- Eglinton G., Hajibrahim S.K., Maxwell J.R. and Quirke J.M.E. (1980) Petroporphyrins: structural elucidation and the application of HPLC fingerprinting to geochemical problems. In: *Advances in*

- Organic Geochemistry*, 1979. (Eds: A.G. Douglas and J.R. Maxwell) Pergamon Press, Oxford, pp. 193-203
- Eglinton G., Evershed R.P. and Gill J.P. (1984) Computerised GC-MS examination of petroporphyrins. *Org. Geochem.*, 6, 157-165
- Ehrmann W.U. and Thiede J. (1985) History of Mesozoic and Cenozoic sediment fluxes to the North Atlantic Ocean. *Contrib. Sedimentol.*, 15, 109
- Einsele G. and Seilacher A. (1982) Cyclic and Event Stratification. Berlin: Springer.
- Einsele G., Ricken W. and Seilacher A. (1991) Cycles and events in stratigraphy. Springer-Verlag, Berlin
- Ekstrom A., Fookes C.J.R., Hambley T., Loech H.J., Miller S.a. and Taylor J.C. (1983) Determination of the crystal structure of a petroporphyrin isolated from oil shale. *Nature*, 306, 173-174
- Ellsworth R.K. and Aronoff S. (1968) Purification and mass spectra of maleimides from the oxidation of chlorophyll and related compounds. *Archives of Biochemistry and Biophysics.*, 124, 358-364
- Ellsworth R.K. (1970) Gas chromatographic determination of some maleimides produced by the oxidation of haeme and chlorophyll a. *J. Chromatog.*, 50, 131-134
- Erbacher J. (1994) Entwicklung und Paläoozeanographische mittelkretazischer Radiolarien der westlichen Tethys (Italien) und des Nordatlantiks: Tübinger Mikropaläontologische Mitteilungen., 12, 120
- Erbacher J., Thurow J. and Littke R. (1996) Evolution patterns of radiolaria and organic matter variations: A new approach to identify sea-level changes in mid-Cretaceous pelagic environments. *Geology.*, 24(6), 499-502
- Erbacher J. and Thurow J. (1997) Influence of oceanic anoxic events on the evolution of mid-Cretaceous radiolaria in the North Atlantic and western Tethys. *Mar. Micropal.*, 30, 139-158
- Eugster H.P. (1985) Oil shales, evaporites, and ore deposits. *Geochim. Cosmochim. Acta.*, 49, 619-635
- Eugster H.P. and Hardie L.A. (1978) Saline lakes. In *Geochemistry, Geology and Physics of Lakes* (Ed: Lerman A.), pp. 237-293. Springer, New York.
- Evans R. and Kirkland D.W. (1988) Evaporitic environments as a source of petroleum. In *Evaporites and Hydrocarbons* (Ed: Schreiber B.B.), pp. 256-299. Columbia Univ. Press, New York.
- Fahrbach E. and Meincke J. (1979) Some observations on the variability of the Cabo Frio upwelling. *CUEA Newsletter.*, 8, 13-18
- Farrimond P.F. (1987) Toarcian and Cenomanian/Turonian oceanic anoxic events. PhD Thesis. University of Bristol.
- Farrimond P., Eglinton G., Brassel S.C. and Jenkyns H.C. (1988) The Toarcian black shale event in northern Italy. *Adv. Org. Geochem.* 1987., 13(4-6), 823-832
- Farrimond P., Eglinton G., Brassel S.C. and Jenkyns H.C. (1989) Toarcian anoxic event in Europe: an organic geochemical study. *Mar. Petrol. Geol.*, 6, 136-147
- Farrimond P., Eglinton G., Brassell S.C. and Jenkyns H.C. (1990) The Cenomanian/Turonian anoxic event in Europe: an organic geochemical study. *Mar. Pet. Geol.*, 7, 75-89
- Farrimond P., Stoddart D.R. and Jenkyns H.C. (1994) An organic geochemical profile of the Toarcian anoxic event in northern Italy. *Cehm. Geol.*, 111, 17-33
- Fischer A.G. and Arthur M.A. (1977) Secular variations in the pelagic realm. *Spec. Publ. Soc. Econ. Paleont. Miner.*, 25, 19-50
- Fischer A.G. (1981) Climatic oscillations in the biosphere. In: *Biotic crisis in ecological and evolutionary time*. Academic Press., pp. 103-131
- Fischer A.G., Premoli Silva I. and de Boer P.L. (1990) In: *Cretaceous resources, events and rhythms* (Eds: Ginsburg R.N. and Beaudoin B.), pp. 139-172 (Kluwer Academic Press, Dordrecht)
- Fleet A.J., Clayton C.J., Jenkyns H.C. and Parkinson D.N. (1987) Liassic source-rock deposition in Western Europe. In: *Petroleum geology of North West Europe* (Eds: Brooks J. and Glennie K.W.) Graham and Trotman, London. Pp. 59-70
- Föllmi K.B., Weissert H. and Lini A. (1993) Nonlinearities in phosphogenesis and phosphate-carbon coupling and their implications for global change. In: *Interactions of the C, N, P and S Biogeochemical Cycles and Global Change*. (Eds. Wollast R., Mackenzie F.T. and Chou L.) Springer-Verlag, New York, pp. 447-474
- Fookes C.J.R. (1983) *J. Chem. Soc., Chem. Comm.*, 1472-1473
- Frakes L.A. (1979) *Climates through geological time*: Amsterdam, Elsevier. p. 310.
- Freeman K.H., Wakeham S.G. and Hayes J.M. (1994) Predictive isotopic biogeochemistry: Hydrocarbons from anoxic marine basins. *Org. Geochem.*, 21, 629-644

- Fry B., Jannasch H., Molyneaux S.J., Wirsén C., Muramoto J. and King S. (1991) Stable isotope studies of the carbon, nitrogen and sulphur cycles in the Black Sea and Cariaco Trench. *Deep-Sea Res.*, 38, Suppl.2, S1003-1020
- Funnell B.M. (1987) Anoxic non-events: alternative explanations. See Brooks and Fleet, 1987. pp. 421-422
- Gale A.S., Jenkyns H.C., Kennedy W.J. and Cornfield R.M. (1993) Chemostratigraphy versus biostratigraphy: data from around the Cenomanian-Turonian boundary. *J. Geol. Soc. Lon.*, 150, 29-32
- Géczy B. (1984) Provincialism of Jurassic ammonites: Examples from Hungarian faunas: *Acta. Geol. Hungarica.*, 27, 379-389
- Gibbison R. (1996) Porphyrins and 1*H*-pyrrole-2,5-diones (maleimides) as indicators of anoxygenic photosynthesis in palaeowater columns. Ph.D. Thesis, University of Bristol.
- Gibbison R., Peakman T.M. and Maxwell J.R. (1995) Novel porphyrins as molecular fossils for anoxygenic photosynthesis. *Tet. Lett.*, 36(49), 9057-9060
- Gibson D.L. (1985) Pyrite-organic matter relationships: Current Bush Limestone, Georgina Basin, Australia. *Geochim. Cosmochim. Acta.*, 49, 989-992
- Gill J.P., Evershed R.P. and Eglinton G. (1986) Comparative computerised gas chromatographic-mass spectrometric analysis of petroporphyrins. *J. Chrom.*, 369, 281-312
- Glen C.R. and Arthur M.A. (1984) Sedimentary and geochemical indicators of productivity and oxygen contents in modern and ancient basins: the Holocene Black Sea as the "type" anoxic basin. *Chem. Geol.*
- Görlü N. (1991) Aptian-Albian palaeogeography of Neo-Tethyan domain. *Palaeo. Palaeo. Palaeo.*, 87, 267-288
- Grantham P.J., Posthuma J. and de Groot K. (1980) Variation and significance of the C<sub>27</sub> and C<sub>28</sub> triterpane content of a North Sea core and various North Sea crude oils. In: *Adv. Org. Geochem 1979* (eds: Douglas A.G. and Maxwell J.R.) Pergamon Press, Oxford, pp. 29-38
- Grice K. (1995) Distributions and stable carbon isotopic compositions of individual biological markers from the Permian Kupferschiefer (Lower Rhine Basin, N.W. Germany). Ph.D. Thesis. University of Bristol.
- Grice K., Gibbison R., Atkinson J.E., Schwark L., Eckardt C.B. and Maxwell J.R. (1996a) Maleimides (1*H*-pyrrole-2,5-diones) as molecular indicators of anoxygenic photosynthesis in ancient water columns. *Geochim. Cosmochim. Acta.*, 60(20), 3913-3924
- Grice K., Schaeffer P., Schwark L. and Maxwell J.R. (1996b) Molecular indicators of palaeoenvironmental conditions in an immature Permian shale (Kupferschiefer, Lower Rhine Basin, N.W. Germany) from free and S-bound lipids. *Org. Geochem.*, 25(3/4), 131-147
- Grice K., Schaeffer P., Schwark L. and Maxwell J.R. (1997) Changes in palaeoenvironmental conditions during deposition of the Permian Kupferschiefer (Lower Rhine Basin, northwest Germany) inferred from molecular and isotopic compositions of biomarker components. *Org. Geochem.*, 26(11-12), 677-690
- Guthrie J.M. and Pratt L.M. (1995) Geochemical character and origin of oils in Ordovician reservoir rock, Illinois and Indiana, USA. *A.A.P.G. Bull.*, 79, 1631-1649
- Habermehl G.C. and Springer G. (1982) *Naturwissenschaften*, 69, 543
- Habermehl G.C., Springer G. and Frank M.H. (1984) *Naturwissenschaften*, 71, 261-263
- Habib D. (1979) Sedimentary origin of North Atlantic Cretaceous palynofacies. In: *Deep drilling results in the Atlantic Ocean. Continental margins and palaeoenvironments*. (Eds. Talwani M., Hay W. and Ryan W.B.F.), *Am. Geophys. Union*, Maurice Ewing Series 3, 420-437
- Habib D. (1982) Sedimentation of black clay organic facies in a Mesozoic oxic North Atlantic. In: *Proc. Third North Amer. Paleont. Conv.*, 1, 217-220
- Hajibrahim S.K., Tibbetts P.J.C., Watts C.D., Maxwell J.R., Eglinton G., Colin H. and Guiochon G. (1978) Analysis by HPLC of carotenoid and porphyrin pigments of geochemical interest. *Anal. Chem.*, 50, 549-553
- Hajibrahim S.K. (1981) Development of high pressure liquid chromatography (HPLC) for fractionation and fingerprinting of petroporphyrin mixtures. *J. Liq. Chrom.*, 4, 749-764
- Hallam A. (1975) Jurassic environments. Cambridge University Press, Cambridge
- Hallam A. (1981) A revised sea-level curve for the Early Jurassic. *Geol. Soc. Lon. Journ.*, 138, 735-743
- Hallam A. (1985) A review of Mesozoic climates. *J. Geol. Soc. Lon.*, 142, 433-445
- Hallam A. (1987a) Mesozoic marine organic-rich shales. See Brooks and Fleet, 1987., pp. 251-261
- Hallam A. (1987b) Radiations and extinctions in relation to environmental change in the marine Lower Jurassic of north west Europe: *Palaeobiol.*, 3, 58-73

- Haq B.U., Hardenbol J. and Vail P.R.** (1987) The chronology of fluctuating sea level since the Triassic. *Science.*, 269, 483-489
- Harland W.B., Cox A.V., Llewellyn P.G., Pickton C.A.G., Smith A.G. and Walters R.** (1982). *A Geological Time Scale*. Cambridge Univ. Press, Cambridge
- Hartgers W.A., Sinninghe Damsté J.S., Requejo A.G., Allan J., Hayes J.M., Ling Y., Xie T.-M., Primack J. and de Leeuw J.W.** (1994) A molecular and carbon isotopic study towards the origin and diagenetic fate of diaromatic carotenoids. In *Advances in Organic Geochemistry 1993* (Eds: Telnaes N., van Grass G. and Oygard K.), *Org. Geochem.*, 22, 703-725
- Hartnett H.E., Keil R.G., Hedges J.L. and Devol A.H.** (1998) Influence of oxygen exposure time on organic carbon preservation in continental margin sediments. *Nature.*, 391, 572-574
- Hattin D.E.** (1975) Stratigraphy and depositional environment of Greenhorn limestone (Upper Cretaceous) Kansas. *Kansas Geol. Sur. Bull.*, 209, 128
- ten Haven H.L., de Leeuw J.W., Peakman T.M. and Maxwell J.R.** (1986) Anomalies in steroid and hopanoid maturity indices. *Geochim. Cosmochim. Acta.*, 50, 853-855
- ten Haven H.L., Eglinton G., Farrimond P., Kohnen M.E.L., Poynter J.G., Rullkötter J. and Welte D.H.** (1992) See Summerhayes *et al.* (1992), pp. 229-246
- Hay W.W. and Brock J.C.** (1992) See Summerhays *et al.* (1992) pp. 463-497
- Hayes D.E., Pimm A.C., *et al.***, (1972) *Init. Rept. DSDP.*, 14, Washington (U.S. Govt. Printing Office).
- Hayes J.M., Takigiku R., Ocampo R., Callot H.J. and Albrecht P.** (1987) Isotopic compositions and probable origins of organic molecules in the Eocene Messel oil shale., *Nature*, 39, 48-51
- Hays J.D. and Pitman W.C.** (1973) Lithospheric plate motion, sea level changes and climatic and ecological consequences. *Nature*, 246, 18-22
- Hedges J.L. and Keil R.G.** (1995) Sedimentary organic matter preservation: An assessment and speculative synthesis. *Mar. Chem.*, 49, 81-115
- Henrichs S.M. and Reeburgh W.S.** (1987) Anaerobic mineralisation of marine organic matter: Rates and the role of anaerobic processes in the oceanic carbon economy. *J. Geomicrobiol.*, 5, 191-237
- Herbert T.D. and Fischer A.G.** (1986) Milankovitch climatic origin of Mid-Cretaceous black shale rhythms in central Italy. *Nature.*, 321, 739-743
- Herbin J.P. and Deroo G.** (1982) Sédimentologie de la matière organique dans les formations du Mésozoïque de l'Atlantique Nord., *Bull. Soc. Géol. France.*, 7(24), 497-510
- Herbin J.P., Montadert L., Müller C., Gomez R., Thurow J. and Wiedmann J.** (1986) Organic-rich sedimentation at the Cenomanian-Turonian boundary in oceanic and coastal basins in the North Atlantic and Tethys. In: Summerhays and Shackleton, 1986., 389-422
- Hilbrecht H., Frieg C., Tröger K.A., Voigt S. and Voigt T.** (1996) Shallow water facies during the Cenomanian-Turonian anoxic event: bio-events, isotopes and sea-level in southern Germany. *Cret. Res.*, 17, 229-253
- Hodgson G.W., Strosher M. and Casagrande D.J.** (1971) Geochemistry of porphyrins: Analytical oxidation to maleimides. In: *Advances in Organic Geochemistry* (Eds: Gaertner H.R.V. and Wehner H.), Pergamon Press, Oxford, pp. 151-161
- Hoefs M.J.L., Sinninghe Damsté J.S. and De Leeuw J.W.** (1995) Organic geochemistry of Arabian Sea surface sediments: Palaeoenvironmental implications. *Proc. 17th International Conference Org. Geochem.*, 158-160
- Hofmann P.** (1992) *Sedimentary facies, Organic Facies and Hydrocarbon Generation in Evaporite Sediments of the Mulhouse Basin, France*. Berichte des Forschungszentrums Jülich No. 2664
- Hofmann P., Huc A.Y., Carpentier B., Schaeffer P., Albrecht P., Keely B.J., Maxwell J.R., Sinninghe Damsté J.S., de Leeuw J.W. and Leythaeuser D.** (1993) Organic matter of the Mulhouse Basin, France: a synthesis. *Org. Geochem.*, 20, 1105-1123
- Hofmann P., Ricken W., Leythaeuser D. and Schwark L.** (1997) Processes controlling the accumulation of organic matter in high frequency sedimentary cycles of Albian age in the North Atlantic Ocean. *Absts. 18<sup>th</sup> Meeting Org. Geochem.*, 143-144
- Hollander D.J., Bessereau G., Belin S., Huc A.Y. and Houzay J.P.** (1991) Organic matter in the Early Toarcian shales, Paris Basin, France: A response to environmental changes. *Rev. Inst. Franc. Petrol.*, 46(5), 543- 562
- Hollander D.J., Sinninghe-Damsté J.S., Hayes J.M., de Leeuw J.W. and Huc A.Y.** (1993a) Molecular and bulk isotopic analyses of organic matter in marls of the Mulhouse Basin (Tertiary, Alsace, France), *Org. Geochem.*, 20, 1253-1263
- Hsü *et al*** (1973)



- Hollander D.J., McKenzie J.A., Hsu K.J. and Huc A.Y. (1993b) Application of an eutrophic lake model to the origin of ancient organic-carbon-rich sediments. *Global Biogeochemical Cycles.*, 7(1), 157-179
- Huang E.C., Wachs T., Conboy J.J. and Henion J.D. (1990) Atmospheric pressure ionisation mass spectrometry. *Anal. Chem.*, 62, 713A-725A
- Huc A.Y. (1976) Mise en évidence de provinces géochimiques dans les schistes bitumineux du Toarcien de l'est du Bassin de Paris. Etude de la fraction organique soluble. *Rev. Inst. Franc. Petrol.*, 31, 933-953
- Huc A.Y. (1988) Sedimentology of organic matter. In: *Humic Substances and Their Role in the Environment* (Eds: Frimmel F.H. and Christmann R.F.), pp. 215-243. Wiley, Chichester.
- Huseby B. and Ocampo R. (1995) Study of porphyrins released from the Messel oil shale kerogen by selective chemical degradation. *Organic Geochemistry: developments and application to energy, climate, environment and human history*, 997-998
- Huseby B. (1996) A study of porphyrins in petroleum source rocks. *PhD Thesis*. University of Bergen, Norway
- Ibach L.E. (1982) Relationship between sedimentation rate and total organic carbon in ancient marine sediments. *Am. Ass. Pet. Geol. Bull.*, 66, 170-188
- Ikonomu M.G., Blades A.T. and Kerbarle P. (1991) *Anal. Chem.*, 63, 1989-1998
- Jackson A.H. (1976) Structure, properties and distribution of chlorophylls. In: *Chemistry and biochemistry of plant pigments*. (Eds. Vernon, L.P. and Seely G.R.) Academic Press, New York, 111
- Ingall E.D. and Jahnke R.A. (1994) Evidence for enhanced phosphorous regeneration from marine sediments overlain by oxygen-depleted waters. *Geochim. Cosmochim. Acta.*, 58, 2571-2575
- Ingle J.C., Jr. (1980) Cenozoic palaeobathymetry and depositional history of selected sequences within the southern California borderland. In: *Memorial to Orville L. Bandy*: Cushman Foundation special publication 19, 163-195
- Ingram B.L., Coccioni R., Montanari A. and Richtert F.M. (1994) Strontium isotopic composition of Mid-Cretaceous seawater. *Science.*, 264, 546-550
- Irving E., North T.K. and Couillard R. (1974) Oil, climate and tectonics., *Can. J. Earth Sci.*, 11, 1-15
- Ivanenkov V.N. and Rozanov A.G. (1961) Hydrogen sulphide contamination of the intermediate waters of the Arabian Sea and the Bay of Bengal. *Okenologia*, 1, 443-449
- Jahnke R.A. (1990) Early sediment diagenesis and recycling of biogenic debris in a deep continental basin. *J. Mar. Res.*, 48, 413-436
- Jarvis I., Carson G., Cooper M.K.E., Hart M., Leary P. and Tocher B., Horne D. and Rosenfeld A. (1988) Microfossil assemblages and the Cenomanian-Turonian (Late Cretaceous) Oceanic Anoxic Event. *Cret. Res.*, 9, 3-103
- Javor B. (1989) *Hypersaline Environments: Microbiology and Biogeochemistry*. Springer, Berlin.
- Jen J.J. and MacKinney G. (1970) On the photodecomposition of chlorophyll in vitro-I. Reaction rates. *Photochem. and Photobiol.*, 11, 297-302
- Jenkyns H.C. (1980) Cretaceous anoxic events: from continents to oceans. *J. Geol. Soc. Lond.*, 137, 171-188
- Jenkyns H.C. (1985) The Early Toarcian and Cenomanian anoxic events in Europe: comparisons and contrasts. *Geol. Rund.*, 74, 505-518
- Jenkyns H.C. and Clayton C.J. (1986) Black shales and carbon isotopes in pelagic sediments from the Tethyan Lower Jurassic. *Sedimentology.*, 33, 87-106
- Jenkyns H.C. (1991) Impact of the Cretaceous sea level rise and anoxic events on the Mesozoic carbonate platform of Yugoslavia. *Bull. Am. Ass. Pet. Geol.*, 75, 1007-1017
- Jenkyns H.C., Géczy B. and Marshall J.D. (1991) Jurassic manganese carbonates of central Europe and the early Toarcian anoxic event. *J. Geol.*, 99, 137-149
- Jenkyns H.C., Gale A.S. and Cornfield R.M. (1994) Carbon- and oxygen-isotope stratigraphy of the English Chalk and Italian Scaglia and its palaeoclimatic significance. *Geol. Mag.*, 134, 1-34
- Jenkyns H.C. and Clayton C.J. (1997) Lower Jurassic epicontinental carbonates and mudstones from England and Wales: chemostratigraphic signals and the early Toarcian anoxic event. *Sedimentology.*, 44, 687-706
- Jones C.E., Jenkyns H.C., Coe A.L. and Hesselbo S.P. (1994) Strontium isotope variations in Jurassic and Cretaceous seawater. *Geochim. Cosmochim. Acta.*, 58(14), 3061-3074
- Karuso P., Bergquist P.R., Buckleton J.S., Cambie R.C., Clark R.C. and Rickard C.E.F. (1986) 13,17-cyclopheophorbide enol, the first porphyrin isolated from a sponge. *Tet. Lett.*, 27, 2177-2178
- Katz B.J. and Elrod L.W. (1983) Organic geochemistry of DSDP site 467, offshore California, Middle Miocene to Lower Pliocene strata. *Geochim. Cosmochim. Acta.*, 47, 389-396

- Katz B.J.** (1995) The Schistes Carton – the Lower Toarcian of the Paris Basin. In: *Petroleum Source Rocks* (Ed Katz B.J.), pp. 89-110. Springer, Berlin.
- Kauffman E.G.** (1977) Geological and biological overview: Western Interior Cretaceous Basin. *Mount. Geol.*, **14**, 75-99
- Kauffman E.G.** (1981) Ecological reappraisal of the German Posidonienschiefer (Toarcian) and the stagnant basin model. In: *Communities of the Past*. (eds; Gray J. et al.) Hutchinson Ross, Stroudsburg., pp. 11-381
- Kaur S., Chicarelli M.I. and Maxwell J.R.** (1986) Naturally occurring benzoporphyrins: bacterial marker pigments? *J. Am. Chem. Soc.*, **108**, 1347-1348
- Keely B.J., Prowse W.G. and Maxwell J.R.** (1990) The Treibs hypothesis: an evaluation based on structural studies. *Energy and Fuels*, **4**, 628-634
- Keely B.J., Sinninghe Damsté J.S., Betts S.E., Yeu L., de Leeuw J.W. and Maxwell J.R.** (1993) A molecular stratigraphic approach to palaeoenvironmental assessment and the recognition of changes in source inputs in marls of the Mulhouse Basin (Alsace, France). *Org. Geochem.*, **20**, 1165-1186
- Keely B.J., Harris P.G., Popp B.N., Hayes J.M., Meischner D. and Maxwell J.R.** (1994) Porphyrin and chlorin distributions in a Late Pliocene lacustrine sediment. *Geochim. Cosmochim. Acta.*, **58**, 3691-3701
- Keely B.J., Blake S.R., Schaeffer P. and Maxwell J.R.** (1995) Distributions of pigments in the organic matter of marls from the Vena del Gesso evaporitic sequence. *Org. Geochem.*, **23**, 527-539
- Kelts K. and Hsü K.J.** (1978) Freshwater carbonate sedimentation. In: *Lakes: Chemistry, Geology, Physics* (Ed: Lerman A.), pp. 295-323. Springer New York
- Kemper E.** (1987) Das Klima der Kreide-Zeit. *Geol. Jahrbuch.*, **96A**, 1-185
- Kenig F., Sinninghe-Damsté J.S., Frewin N.L., Hayes J.M. and de Leeuw J.W.** (1995) Molecular indicators for palaeoenvironmental change in a Messinian evaporitic sequence (Vena del Gesso, Italy). II: High-resolution variations in abundances and <sup>13</sup>C contents of free and sulphur-bound carbon skeletons in a single marl bed. *Org. Geochem.*, **23**, 485-526
- Kirkland D.W., Bradbury J.P. and Dean W.E.** (1983) The heliothermic lake- a direct method of collecting and storing of solar energy. *Arch. Hydrobiol. Supp.*, **65**, 181-190
- Kohnen M.E.L., Schouten S., Sinninghe Damsté J.S. and de Leeuw J.W.** (1991a) Biases from natural sulphurisation in palaeoenvironmental reconstruction based on hydrocarbon biomarker distributions. *Nature*, **349**, 775-778
- Kohnen M.E.L., Sinninghe Damsté J.S., Kock-Dalen A.C. and de Leeuw J.W.** (1991b) Di- or polysulphide- bound biomarkers in sulphur-rich geomacromolecules as revealed by selective chemolysis. *Geochim. Cosmochim. Acta.*, **55**, 1375-1394
- Kohnen M.E.L., Schouten S., Sinninghe Damsté J.S., de Leeuw J.W., Merritt D.M. and Hayes J.M.** (1992a) The combined application of organic sulphur and isotope geochemistry to assess multiple sources of palaeobiochemicals with identical carbon skeletons. In: *Advances in Organic Geochemistry 1991* (Eds: Eckardt C.B., Maxwell J.R., Larter S.R. and Manning D.A.C.), *Org. Geochem.*, **19**, 403-419
- Kohnen M.E.L., Schouten S., Sinninghe Damsté J.S., de Leeuw J.W., Merritt D.M. and Hayes J.M.** (1992b) Recognition of palaeobiochemicals by a combined molecular sulphur and isotope geochemical approach. *Science*, **256**, 358-362
- Kominz M.A.** (1984) Oceanic ridge volumes and sea level change: an error analysis. In: *Interregional Unconformities and Hydrocarbon Accumulation*. *Am. Ass. Petrol. Geol. Mem.*, **36**, 109-127
- Koopmans M.P., Koster J., van Kaam-Peters H.M.E., Kenig F., Schouten S., Krane J., Skjetne T. and Telnaes N.** (1983) NMR spectroscopy of petroporphyrins. *Tetrahedron*, **39**, 4109-4119
- Hartgers W.A., de Leeuw J.W. and Sinninghe Damsté J.S.** (1996) Diagenetic and catagenic products of isorenieratene: Molecular indicators for photic zone anoxia. *Geochim. Cosmochim. Acta.*, **60**, 4467-4496
- Koopmans M.P., de Leeuw J.W. and Sinninghe Damsté J.S.** (1997) Novel cyclised aromatised diagenetic products of  $\beta$ -carotene in the Green River Shale. *Org. Geochem.*
- Koutsoukos E.A.M.** (1987) Palaeobatimetria da margem continental do Brasil durante o Albiano. *Rev. Bras. Geoc.*, **17**(2), 86-91
- Koutsoukos E.A.M. and Merrick K.A.** (1986) Foraminiferal palaeoenvironments from the Barremian to Maastrichtian of Trinidad, West Indies. *Trans. 1<sup>st</sup> Geol. Con. Geol. Soc. Trinidad and Tobago*, **1985**, pp. 85-101

- Kuhn-Schnyder E. (1974) Die Triasfauna der Tessiner Kalkalpen. Neujahrsblatt Naturforschenden Gesellschaft Zürich, Verlag Leemann, Zürich.
- Kuhnt W., Thurow J., Wiedmann J. and Herbin J.P. (1986) Oceanic anoxic conditions around the Cenomanian/Turonian boundary and the response of the biota. *Mitt. Geol. Pal. Inst. Univ. Hamburg.*, 60, 205-246
- Kuhnt W., Herbin J.P., Thurow J. and Wiedmann J. (1990) Distribution of Cenomanian-Turonian organic facies in the western Mediterranean and along the adjacent Atlantic margin. In: *Deposition of Organic Facies*. (Ed: Huc A.Y.) *Am. Ass. Pet. Geol. Stud. Geol.*, 3, pp. 133-160
- Küspert W. (1982) Environmental changes during oil shale deposition as deduced from stable isotope ratios. In: *Cyclic and Event Stratification*. (Eds: Einsele G. and Seilacher A.) Springer-Verlag, Berlin., pp.482-501
- Küspert W. (1983) Faciestypen des Posidonienschiefers (Toarcium, Süddeutschland) Eine isotopengeologische, organisch-chemische und petrographische studie. PhD Thesis, University of Tübingen.
- Lancelot Y., Seibold *et al.*, (1977) Site 368: Cape Verde Rise. In: *Init. Rept. DSDP*, 41, US Govt. Print. Off., Washington DC., pp. 233-286
- Larson R.L. (1991) Latest pulse of the Earth: Evidence for a mid-Cretaceous superplume. *Geology.*, 19, 547-550
- Leckie R. (1984) Mid-Cretaceous planktonic foraminiferal biostratigraphy off central Morocco, DSDP leg 79, Sites 545 and 547. *Init. Repts. DSDP.*, 79, 579-620
- Leventhal J.S. (1983) An interpretation of carbon and sulphur relationships in Black Sea sediments as indicators of environments of deposition. *Geochim. Cosmochim. Acta.*, 47, 133-137
- Lewan M.D. (1984) Factors controlling the proportionality of vanadium to nickel in crude oils. *Geochim. Cosmochim. Acta.*, 48, 2231-2238
- Lewan M.D. and Maynard J.B. (1982) Factors controlling the enrichment of vanadium and nickel in the bitumen of organic sedimentary rocks. *Geochim. Cosmochim. Acta.* 46, 2547-2560
- Lisitzin A.P. (1971) Distribution of siliceous microfossils in suspension and in bottom sediments. In: *Micropalaeontology of oceans*. (Eds: Funnell B.M. and Riedel W.R.), pp. 173-195
- Littke R., Rotzal H., Leythaeuser D. and Baker D.R. (1991a) Lower Toarcian Posidonia shale in Southern Germany (Schwäbische Alb). Organic facies, depositional environment and maturity. *Wissenschaft Technik. Sci. Technol.*, 44(11), 407-414
- Littke R., Baker D.R., Leythaeuser D. and Rullkötter J. (1991b) Keys to the depositional history of the Posidonia Shale (Toarcian) in the Hils Syncline, northern Germany. See Tyson and Pearson, 1991 pp. 311-333
- Loh H., Maul B., Prass M. and Rigel W. (1986) Primary production, maceral formation and carbonate species in the Posidonia shale of NW Germany. In: *Biogeochemistry of Black Shales*. (Eds: Degens *et al.*), Hamburg, *Mitt. Geol. Paläont. Inst. Univ. Hamburg.*, 60, 397-421
- MacKenzie A.S., Patience R.L. and Maxwell J.R. (1980a) Molecular parameters of maturation in the Toarcian shales, Paris Basin, France-I. Changes in the configurations of acyclic isoprenoid alkanes, steranes and triterpanes. *Geochim. Cosmochim. Acta.*, 44, 1709-1721
- MacKenzie A.S., Quirke J.M.E. and Maxwell J.R. (1980b) Molecular parameters of maturation in the Toarcian shales, Paris Basin, France-II. Evolution of metalloporphyrins. *Adv. Org. Geochem.* 1979. (Eds. Douglas A.G. and Maxwell J.R.) Pergamon Press, Oxford, pp. 239-248
- Maikovskiy V. (1941) Contribution à l'étude paléontologique et stratigraphique du bassin potassique d'Alsace. *Mem. Serv. Carte Géol. Als. Lorr.*, 6, 1-192
- Martens S.M. and Klump J.V. (1984) Biogeochemical cycling in an organic-rich coastal basin 4. An organic carbon budget for sediments dominated by sulphate reduction and methanogenesis. *Geochim. Cosmochim. Acta.*, 48, 1987-2004
- Mattioli E. (1997) Nannoplankton productivity and diagenesis in the rhythmically bedded Toarcian-Aalenian Fiuminata section (Umbria-Marche Apennine, central Italy). *Palaeo. Palaeo. Palaeo.*, 130, 113-133
- Maxwell J.R., Quirke J.M.E. and Eglinton G. (1980) Aspects of modern porphyrin geochemistry and the Treibs hypothesis. In: *Internationales Alfred-Treibs-Symposium Munich 1979*. (ed. Prashnowsky A.A.), pp. 37-55. Universität Würzburg
- McFadden W.H., Bradford D.C., Eglinton G., Hajibrahim S.K. and Nicolaides N.J. (1979) Application of combined liquid chromatography/mass spectrometry (LC/MS): analysis of petroporphyrins and meibomian gland waxes. *J. Chrom. Sci.*, 17, 518-522
- Mello M.R., Koutsoukas E.A.M., Hart M.B., Brassel S.C. and Maxwell J.R. (1989) Late Cretaceous anoxic events in the Brazilian continental margin. *Org. Geochem.*, 14(5), 529-542

- Meyers P.A., Dunham K.W. and Dunham P.L. (1986) Organic geochemistry of Cretaceous organic-carbon-rich shales and limestones from the western North Atlantic Ocean. See Summerhayes and Shackleton, 1986. pp. 333-345
- Meyers P.A. (1989) Sources and deposition of organic matter in Cretaceous passive margin deep sea sediments: A synthesis of organic geochemical studies from Deep Sea Drilling Project 603, outer Hatteras Rise. *Marine and Petroleum Geology*, 6, 182-189
- Meyers P.A. (1997) Organic geochemical proxies of palaeoceanographic, palaeolimnologic, and palaeoclimatic processes. *Org. Geochem.*, 27(5/6), 213-250
- Millero F.J. (1996) Chemical Oceanography, 2<sup>nd</sup> edition., CRC Press, Boca Raton.
- Mitchum R.K. and Korfmacher W.A. (1983) *Anal. Chem.*, 55, 1485A
- Moldowan J.M., Sundararaman P. and Schoell M. (1986) Sensitivity of biomarker properties to depositional environment and/or source input in the Lower Toarcian of SW-Germany. *Org. Geochem.*, 10, 915-926
- Montesinos E., Guerrero R., Abella C. and Esteve I. (1983) Ecology and physiology of the competition for light between *Chlorobium limicola* and *Chlorobium phaeobacteroides* in natural habitats. *Applied and Environmental Microbiology*, 4, 1007-1016
- Morse J.W. and Emeis K.C. (1992) Carbon/sulphur/iron relationships in upwelling sediments. See Summerhayes *et al.* (1992) pp. 247-255
- Müller P. and Suess E. (1979) Productivity, sedimentation rate, and sedimentary organic matter in the oceans-I. Organic matter preservation. *Deep Sea Res.*, 26A, 1347-1362
- Naylor C.C. (1997) Early oxidative transformation products of chlorophyll in contemporary environments. PhD Thesis, University of York
- Naylor C.C. and Keely B.J. (1997) Oxidative transformation products of chlorophylls: Structures, formation and significance. *Absts, 18<sup>th</sup> Int. Meet. Org. Geochem.*, 22-26 September, 1997, Maastricht, Netherlands., pp. 91-92
- North F.K. (1980) Episodes of source-sediment deposition (2). The episodes in individual close-up: *J. Pet. Geol.*, 2, 323-338
- Ohkouchi *et al.*, 1997
- Ocampo R., Callot H.J., Albrecht P. and Kintzinger J.P. (1984) A novel chlorophyll c related petroporphyrin in oil shale. *Tet. Lett.*, 25, 2589-2592
- Ocampo R., Callot H.J. and Albrecht P. (1985a) Identification of polar porphyrins in oil shale. *J.Chem.Soc., Chem.Comm.*, 198-200
- Ocampo R., Callot H.J. and Albrecht P. (1985b) Occurrence of bacterioporphyrins in oil shale. *J.Chem.Soc., Chem.Comm.*, 200-201
- Ocampo R., Callot H.J. and Albrecht P. (1987) Evidence for porphyrins of bacterial and algal origin in oil shale. In *Metal Complexes in Fossil Fuels* (Edited by Filby R.H. and Branthaver J.F.) *Am. Chem. Soc. Symp. Ser.* 1987, 344, pp.68-73
- Ocampo R., Callot H.J. and Albrecht P. (1989) Different isotope compositions of C<sub>32</sub> DPEP and C<sub>32</sub> etioporphyrin III in oil shale. *Naturwissenschaften*, 76, 419-421
- Ocampo R., Bauder C., Callot H.J. and Albrecht P. (1992). Porphyrins from the Messel oil shale (Eocene, Germany): Structure elucidation, geochemical significance and distribution as a function of depth. *Geochim. Cosmochim. Acta*. 56, 745-761
- Packard T.T., Dugdale R.C., Goering J.J. and Barber R.T. (1978) Nitrate reductase activity in the subsurface waters of the Peru Current., *J. Mar. Res.*, 36, 59-76
- Packard T.T., Blasco D. and Dugdale R.C. (1984) Coastal upwelling: A synopsis of its physical, chemical and biological characteristics. In: (Eds: Haq B. and Milliman J.) pp. 339-350
- Palacas, J.G. (1984) *Petroleum Geochemistry and Source Rock Potential of Carbonate Rocks* (Ed: by Palacas J.G.), AAPG Studies in Geology 18, pp. vii-viii. American Association of Petroleum Geologists, Tulsa.
- Palliani R.B., Cirilli S. and Mattioli E. (1998) Phytoplankton response and geochemical evidence of the lower Toarcian relative sea level rise in the Umbria-Marche basin (Central Italy). *Palaeo. Palaeo. Palaeo.*, 142, 33-50
- Palmer S. and Baker E.W. (1978) Copper porphyrins in deep sea sediments: a possible indicator of oxidised terrestrial organic matter. *Science*, 201, 49-51
- Palmisano A.C., Cronin S.E. and des Marias D.J. (1989a) Distribution and survival of lipophilic pigments from a phototrophic microbial mat community near Guerrero Negro, Mexico. In: *Microbial Mats: Physiological Ecology of Benthic Microbial Communities*. (Eds: Cronin Y. and Rosenberg E.) *Am. Soc. Microbiol.* Washington D.C., pp. 138-152

**Page  
missing**

- Quirke J.M.E. (1987) In: *Metal complexes in Fossil Fuels*, (Eds: Filby R.H. and Branthaver J.F.) American Chemical Society, Washington, 1987, p. 308
- Quirke M.J.E., Dale T., Britton E.D., Yost R.A., Trichet J. and Belayoni H. (1990) Preliminary characterisation of porphyrins from the Gafsa Basin, Tunisia: Evidence for metal-free benzo-porphyrins from an immature sediment. *Org. Geochem.* 15, 169-177.
- Putschew A., Schaeffer P., Schaeffer-Reis C. and Maxwell J.R. (1998) Carbon isotopic characteristics of the diaromatic carotenoid, isorenieratene (intact and sulfide bound) and a novel isomer in sediments. *Org. Geochem.*, 29, 1849-1856
- Rau G.H., Arthur M.A. and Dean W.E. (1987)  $^{15}\text{N}/^{14}\text{N}$  variations in Cretaceous Atlantic sedimentary sequences: Implications for past changes in marine nitrogen biogeochemistry. *Earth and Plan. Sci. Letts.*, 82, 269-279
- Raiswell R. and Berner R.A. (1985) Pyrite formation in euxinic and semi-euxinic sediments. *Am. J. Sci.*, 285, 710-724
- Rankin G.J. and Czernuszewicz R.S. (1993) Fingerprinting petroporphyrin structures with vibrational spectroscopy: resonance Raman spectra of nickel and vanadyl etioporphyrins I and III. *Org. Geochem.*, 20(5), 521-538
- Repeta D.J. and Gagosian R.B. (1987) Carotenoid diagenesis in recent marine sediments-I. The Peru continental shelf (15°S, 75°W)., *Geochim. Cosmochim. Acta.*, 51, 1001-1009
- Repeta D.J., Simpson D.J., Jorgensen B.B. and Jannasch H.W. (1989) Evidence for anoxygenic photosynthesis from the distribution of bacteriochlorophylls in the Black Sea., *Nature*, 342, 69-72
- Repeta D.J. (1990) Carotenoid diagenesis in Pleistocene to Miocene sediments from the Peru margin. *Procs. ODP. Sci. Reslts.*, 112, 567-571
- Repeta D.J., McCaffrey M.A. and Farrington J.W. (1992) Organic geochemistry as a tool to study upwelling systems: recent results from the Peru and Namibian shelves. In: *Upwelling Systems: Evolution since the Early Miocene*. (Eds. Summerhays et al.), Geological Society Special Publication., 64, 257-272
- Repeta D.J. (1993) A high resolution record of Holocene anoxygenic primary production in the Black Sea. *Geochim. Cosmochim. Acta.*, 57, 4337-4342
- Requejo A.G., Allan J., Creany S., Gray N.R. and Cole K.S. (1992) Aryl isoprenoids and diaromatic carotenoids in Paleozoic source rocks and oils from the Western Canada and Williston basins. *Org. Geochem.*, 23, 205-222
- Requejo A.G., Sassen R., Kennicutt II M.C., Kvedchuk L., McDonald T., Denoux G., Comet P. and Brooks J.M. (1995) Geochemistry of oils from the northern Timan-Pechora Basin, Russia. *Org. Geochem.*, 23, 205-222
- Rhoads D.C. and Morse J.M. (1971) Evolutionary and ecological significance of oxygen-deficient marine basins. *Lethaia*, 4, 413-428
- Ricken W. (1985) Epicontinental marl-limestone alterations: Event deposition and diagenetic bedding (Upper Jurassic, southwest Germany). In: *Sedimentary and evolutionary cycles*. (Eds: Bayer U. and Seilacher A.) Springer, Berlin. Pp. 127-162
- Rieber H. (1973) Ergebnisse Paläontologisch-stratigraphischer Untersuchungen in der Grenzbitumenzone (Mittlere Trias) des Monte San Giorgio (Kanton Tessin, Schweiz). *Ecologiae Geol. Helv.*, 66, 667-685
- Rieber H. (1975) Die Posidonienschiefer (oberer Lias) von Holzmaden und die Grenzbitumenzone (Mittlere Trias) des Monte San Giorgio (Kanton Tessin, Schweiz). *Jh. Ges. Naturkde Württ.*, 130, 163-190
- Rieber H. (1982) The formation of bituminous layers of the Middle Triassic of Ticino. In: *Cyclic and Event Stratification* (Eds: Einsle G. and Seilacher A.), Springer-Verlag., p. 572
- Rieber H. and Sorbini L. (1983) Middle Triassic bituminous shales of Monte San Giorgio (Tessin, Switzerland). Field Trip guide to Excursion 11A. *First International Congress on Palaeoecology.*, 1983, Lyon, France
- Riegraf F., Werner G. and Lörcher F. (1984) Der Posidonienschiefer. Biostratigraphie, Fauna und Fazies des südwestdeutschen Untertoarciums (Lias ε): Stuttgart. F. Enke., p.195
- Robertson A.H.F. and Bliefnick D.M. (1983) Sedimentology and origin of lower Cretaceous pelagic carbonates and redeposited clastics, Blake-Bahama Formation. Deep Sea Drilling Project Site 534, western Equatorial Atlantic. *Init. Repts. DSDP*, 76, 795-828
- Rontani J.F., Baillet G. and Aubert C. (1991) Production of acyclic isoprenoid compounds during the photodegradation of chlorophyll a in sea water. *J. Photochem. Photobiol. A. Chem.*, 59, 369-377
- Rosenberg R. (1977) Benthic macrofaunal dynamics, production and dispersion in an oxygen-deficient estuary of west Sweden. *J. Exp. Mar. Biol. Ecol.*, 26, 107-133
- Rosell-Melé A. and Maxwell J.R. (1996) Rapid characterisation of metallo porphyrin classes in natural extracts by gel permeation chromatography/ atmospheric pressure chemical ionisation/ mass spectrometry. *Rapid communications in mass spectrometry.*, 10, 209-213

- Rosell-Melé A., Carter J.F. and Maxwell J.R. (1996) High-performance liquid chromatography-mass spectrometry of porphyrins by using an atmospheric pressure interface. *J. Am. Soc. Mass Spectrom.*, 7, 965-971
- Rossignol-Strick M., Nesteroff W., Olive P. and Vergnaud-Grazzini C. (1982) After the deluge: Mediterranean stagnation and sapropel formation. *Nature*, 295, 105-110
- Roth P.H. (1978) Cretaceous nannoplankton biostratigraphy and oceanography of the northwestern Atlantic Ocean. *Init. Repts. DSDP.*, 44, 731-759
- Roth P.H. (1981) Mid-Cretaceous calcareous nannoplankton from the central Pacific: Implications for palaeoceanography. *Init. Repts. DSDP.*, 62, 471-489
- Roth P.H. (1986) Mesozoic palaeoceanography of the North Atlantic and Tethys Oceans. See Summerhays and Shackleton (1986), pp. 299-320
- Roth P.H. (1987) Mesozoic calcareous nannofossil evolution: relation to palaeoceanographic events. *Palaeoceanography*, 2, 601-611
- Rullkötter J., Cornford C. and Welte D.H. (1982) Geochemistry and petrography of organic matter in Northwest African continental margin sediments: Quality, provenance, depositional environment and temperature history. In: *Geology of the Northwest African continental margin*. (Eds: von Rad et al.), pp. 686-703. Springer, Heidelberg.
- Ryan W.B.F. and Cita M.B. (1977) Ignorance concerning episodes of ocean-wide stagnation. *Mar. Geol.*, 23, 197-215
- Sakata K., Yamamoto K., Ishikawa H., Yagi A., Etoh H. and Ina K. (1990) Chlorophyllone a, a new pheophorbide a related compound isolated from rudistaphis philippinarum as an antioxidative compound. *Tet. Lett.*, 31, 1165-1168
- Salaj J. (1978) The geology of the Pelagian Block: The eastern Tunisian Platform. In: *The ocean basins and margins, 4B, the Western Mediterranean*, (Nairn A.E.M., Kanes W.H. and Stehli F.G.), pp. 361-416
- Saltzman E.S. and Barron E.J. (1982) Deep circulation in the late Cretaceous: Oxygen isotope palaeotemperatures from Inoceramus remains in DSDP cores., *Palaeogeogr. Palaeoclimatol. Palaeoecol.*, 40, 167-181
- Sarmiento J.L., Herbert T.D. and Toggweiler J.R. (1988) Causes of anoxia in the world ocean: *Global Biogeochem. Cycles*, 2, 115-128
- Schaeffer P., Ocampo R., Callot H.J. and Albrecht P. (1993) Extraction of bound porphyrins from sulphur-rich sediments and their use for reconstruction of palaeoenvironments. *Nature*, 364, 133-136
- Schaeffer P., Ocampo R., Callot H.J. and Albrecht P. (1994) Structure determination by deuterium labelling of a sulphur-bound petroporphyrin. *Geochim. Cosmochim. Acta.*, 58, 4247-4252
- Schaeffer P., Harrison, W.N., Keely B.J. and Maxwell J.R. (1995) Product distributions from chemical degradation of kerogens from a marl from a Miocene evaporitic sequence (Vena del Gesso, N. Italy). *Org. Geochem.*, 23(6), 541-554
- Schaefflé J., Ludwig B., Albrecht P. and Ourisson G. (1977) Hydrocarbures aromatiques d'origine géologique. II. Nouveaux caroténoïdes aromatiques fossiles. *Tet. Lett.*, 41, 3673-3676
- Scheer H. (1991) Structure and occurrence of chlorophylls. In: *Chlorophylls*, 3-30
- Schelske C.L. and Hodell D.A. (1991) Recent changes in productivity and climate of Lake Ontario detected by isotopic analysis of sediments. *Limnology and Oceanography*, 36, 961-975
- Schlanger S.O. and Jenkyns H.C. (1976) Cretaceous anoxic events: causes and consequences., *Geol. Mijn.*, 55, 179-184
- Schlanger S.O., Jenkyns H.C. and Premoli-Silva L. (1981) Volcanism and vertical tectonics in the Pacific Basin related to the global Cretaceous transgression. *Earth Plan. Sci. Letts.*, 52, 435-449
- Schlanger S.O. and Cita M.B. (1982) Eds. *Nature and origin of Cretaceous carbon-rich facies*. Academic Press, New York.
- Schlanger S.O., Arthur M.A., Jenkyns H.C. and Scholle P.A. (1987) The Cenomanian-Turonian oceanic anoxic event, I. Stratigraphy and distribution of organic carbon-rich beds and the marine  $\delta^{13}\text{C}$  excursion. See Brooks and Fleet, 1987., pp. 371-400
- Scholle P.A. and Arthur M.A. (1980) Carbon isotopic fluctuations in pelagic limestones: Potential stratigraphic and petroleum exploration tool. *Bull. Am. Ass. Petrol. Geol.*, 64, 67-89
- Schmid J.C., Connan J. and Albrecht P. (1987) Identification of long-chain dialkylthiacyclopentanes in petroleum. *Nature*, 329, 54-56
- Schmidt K. (1980) A comparative study on the composition of chlorosomes (chlorobium vesicles) and cytoplasmic membranes from *Chloroflexus aurantiacus* strain Ok-70-fl and *Chlorobium limicola* f. *thiosulphatophilum* strain 623. *Arch. Microbiol.*, 124, 21-31
- Schreiber B.C. and Hsü K.J. (1980) Evaporites. In *Developments in Petroleum Geology II* (Ed: Hobson G.D.), pp. 87-138. Applied Science, London

- Schuler M., Blanc-Valleron M.M., Gely J.P. and Ansart M. (1991) Matière organique et palynofaciès de l'Oligocène inférieur évaporitique du bassin potassique de Mulhouse (France). *Palynosciences.*, 1, 41-58
- Schwark L. and Puttmann W. (1990) Aromatic hydrocarbon composition of the Permian Kupferschiefer in the Lower Rhine Basin, N.W. Germany. *Org. Geochem.*, 16, 749-761
- Schwark L. (1992) Geochemische Fazies-Charakterisierung des Basalen Zechsteins unter besonderer Berücksichtigung der Palaosalinität und des Redoxpotentials Diss, RWTH Aachen
- Schwarzacher W. and Fischer A.G. (1982) Limestone shale bedding and perturbations of the earth's orbit. In: *Cyclic and event stratification* (Eds. Einsele G. and Seilacher A.), Springer-Verlag, 72-95
- Sclater J.G. and Francheteau J. (1970) The implications of terrestrial heat flow observations on current tectonics and geochemical models of the crust and upper mantle of the earth. *Geophys. J. Roy. Astronom. Soc.*, 20, 509-542
- Sclater J.G., Hellinger S. and Tapscott C. (1977) The palaeobathymetry of the Atlantic Ocean from Jurassic to the present: *J. Geol.*, 85, 504-552
- Scotese and Summerhayes, 1986
- Seilacher A. (1982) Ammonite shells as habitats in the Posidonia shales of Holzmaden – floats or benthic island? *Neus Jahrbuch für Geologie und Paläontologie Monatshefte.*, 98-114
- Sellwood B.W., Price G.D. and Valdes P.J. (1994) *Nature.*, 370, 453-455
- Sheridan R.E. (1986) Pulsation tectonics controlling North Atlantic Palaeoceanography. See Summerhays and Shackleton, 1996 pp. 255-275
- Shearman D.J. (1963) Recent anhydrite, gypsum, dolomite and halite from the coastal flats of the Arabian shore of the Persian Gulf. *Proc. Geol. Soc. London.*, 1607, 63-65
- Shipboard Scientific Party (1972) Sites 143 and 144. 283-303 See Hays and Pimm., *et al.*, (1972) *Init. Rept. DSDP.*, 14, Washington (U.S. Govt. Printing Office).
- Shipboard Scientific Party (1977a) Site 367: Cape Verde Basin. See Lancelot and Seibold *et al.*, (1977) pp. 163-202
- Shipboard Scientific Party (1977b) Site 368: Cape Verde Rise. See Lancelot and Seibold *et al.*, (1977) pp. 233- 286
- Simoneit B.R.T. (1978) The organic chemistry of marine sediments. *Chemical Oceanography* (Eds. Riley J.P. and Chester R.), 2<sup>nd</sup> edn, 7, New York, Academic Press. Pp. 233-311
- Simoneit B.R.T. (1980) Terrigenous and marine organic markers and their input to marine sediments. *Proceedings of Symposium on Organic Geochemistry of Deep Sea Drilling Project Sediments.* (Ed. Baker E.W.), Princeton: Science Press.
- Simoneit B.R.T. and Stuermer D.H. (1982) Organic geochemical indicators for sources of organic matter and palaeoenvironmental conditions of Cretaceous oceans: See Schlanger and Cita, 1982. Pp. 145-164
- Sinninghe Damsté J.S., Rijpstra W.I.C., de Leeuw J.W. and Schenck P.A. (1988) Origin of organic sulphur compounds and sulphur containing high molecular weight substances in sediments and immature crude oils. In *Advances in Organic Geochemistry 1987* (Edited by L. Mattavelli and L. Novelli), *Org. Geochem.* 13, 593-606
- Sinninghe Damsté J.S. and de Leeuw J.W. (1990) Analysis, structure and geochemical significance of organically-bound sulphur in the geosphere: State of the art and future research. *Org. Geochem.* 16, 1077-1011
- Sinninghe Damsté J.S., Wakeham S.G., Kohnen M.E.L., Hayes J.M. and de Leeuw J.W. (1993a) A 6,000 year sedimentary record of chemocline excursions in the black sea. *Nature*, 362, 827-829
- Sinninghe-Damsté J.S. Betts S., Ling Y., Hofmann P. and de Leeuw J.W. (1993b) Hydrocarbon biomarkers of different lithofacies of the Salt IV Formation of the Mulhouse Basin, France. *Org. Geochem.*, 20, 1187-1200
- Sinninghe-Damsté J.S., Hartgers W.A., Baas M. and de Leeuw J.W. (1993c) Characterisation of high molecular weight organic matter in marls of the Salt IV Formation of the Mulhouse Basin. *Org. Geochem.*, 20, 1237-1251
- Sinninghe-Damsté J.S., Keely B.J., Betts S., Maxwell J.R. and de Leeuw J.W. (1993d) Variations in the abundances and distributions of isoprenoid chromans and long chain alkylbenzenes in sediments from the Mulhouse Basin: a molecular sedimentary record of palaeosalinity. *Org. Geochem.*, 20, 1201-1215
- Sinninghe-Damsté J.S., Frewin N.L., Kenig F. and de Leeuw J.W. (1995) Molecular indicators for palaeoenvironmental change in a Messinian evaporitic sequence (Vena del Gesso, Italy). I: Variations in extractable organic matter of ten cyclically deposited marl beds. *Org. Geochem.*, 23, 471-483

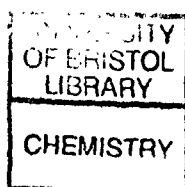


- Sinninghe Damsté J.S. and Köster J. (1998) A euxinic southern North Atlantic Ocean during the Cenomanian/Turonian oceanic anoxic event. *Earth Planet. Sci. Letts.*, **158**, 165-173
- Sirevåg R. and Ormerod J.G. (1970) Carbon dioxide fixation in green sulphur bacteria. *J. Biochem.*, **120**, 399-408
- Sirevåg R., Buchanan B.B., Berry J. and Troughton J.H. (1977) Mechanisms of CO<sub>2</sub> fixation in bacterial photosynthesis studied by the carbon isotope technique. *Arch. Microbiol.*, **112**, 35-38
- Sloan L.C. and Barron E.J. (1990) "Equable" climates during Earth history? *Geology*, **18**, 489-492
- Smith K.M. (1975) In: Porphyrins and Metalloporphyrins pp.21 (Elsevier: Amsterdam)
- Smith K.M. and Bobe F.W. (1987) Light adaption of bacteriochlorophyll d producing bacteria by enzymic methylation of their antenna pigments. *J. Chem. Soc., Chem. Commun.*, 276-277
- Southam J.R., Peterson W.H. and Brass G.W. (1982) Dynamic of anoxia. *Palaeogeog. Palaeocl. Palaeoecol.*, **40**, 183-198
- Southam J.R., Peterson W.H. and Brass G.W. (1984) A model of the coupled carbon, oxygen phosphorous system and anoxia in the deep sea. *Deep sea Res.*
- Stein R. (1986) Organic carbon and sedimentation rate – further evidence for anoxic deep water conditions in the Cenomanian/Turonian Atlantic Ocean. *Mar. Geol.*, **72**, 199-209
- Stein R., Rullkötter J. and Welte D.H. (1986) Accumulation of organic-carbon-rich sediments in the Late Jurassic and Cretaceous Atlantic Ocean – a synthesis. *Chem. Geol.*, **56**, 1-32
- Still W.C., Kahn M. and Mitra A. (1978) Rapid chromatographic technique for preparative separations with moderate resolution. *J. Org. Chem.*, **43**, 2923-2925
- Stow D.A.V. and Dean W.E. (1984) Middle Cretaceous black shale at Sites 530 in the southeastern Angola Basin. *Init. Repts. DSDP.*, **75**, 809-817
- Sturmfels E. (1943) Das Kalisalzager von Buggingen (Südbaden). *N. Jb. Miner. Geol. Pal., Abh.*, **78A**, 131-216
- Suess E. *et al.* (1988) *Procs. Init. Repts. ODP.*, **112**, College Station ODP.
- Summerhays C.P. (1981) Organic facies of middle Cretaceous black shales in deep North Atlantic. *Bull. Am. Ass. Petrol. Geol.*, **65**, 2364-2380
- Summerhays C.P. (1983) Sedimentation of organic matter in upwelling regimes. In: *Coastal upwelling, part B*. (Eds. Thiede J. and Suess E.) Plenum, London. 29-72
- Summerhays C.P. (1986) Organic rich Cretaceous sediments from the North Atlantic. See Brooks and Fleet, 1986, pp. 301-316
- Summerhays C.P. and Masran T.C. (1983) Organic facies of Cretaceous and Jurassic sediments from DSDP Site 534 in the Blake-Bahama Basin, western North Atlantic. *Init. Repts. DSDP.*, **76**, 469-480
- Summerhays C.P. and Shackleton N.J. (1986) (Eds.) North Atlantic Palaeoceanography., Geological society special publication no. 21.
- Summerhays C.P., Prell W.L. and Emeis K.C. (1992) Upwelling Systems: Evolution Since the Early Miocene. *Geological Society Special Publication*. No. 63.
- Summons R.E. and Powell T.G. (1987) Identification of aryl isoprenoids in source rocks and crude oils: Biological markers for the green sulphur bacteria. *Geochim. Cosmochim. Acta.*, **51**, 557-566
- Summons R.E., Volkman J.K. and Boreham C.J. (1987) Dinosterane and other steroidal hydrocarbons of dinoflagellate origin in sediments and petroleum. *Geochim. Cosmochim. Acta.*, **51**, 3075-3082
- Sundararaman P. (1985) High performance liquid chromatography of vanadyl porphyrins. *Anal. Chem.*, **57**, 2204-2206
- Sundararaman P., Biggs W.R., Reynolds J.G. and Fetzer J.C. (1988) Vanadyl porphyrins, indicators of kerogen breakdown and generation of petroleum. *Geochim. Cosmochim. Acta.*, **52**, 2337-2341
- Sundararaman P. (1992) Comparison of natural and laboratory simulated maturation of vanadyl porphyrins. In: *Biological markers in sediments and Petroleum* (Eds: Moldowan J.M., Albrecht P. and Philp R.P.), pp. 313-319. Prentice Hall, Englewood Cliffs, New Jersey.
- Sundararaman P. and Boreham C.J. (1993) Comparison of nickel and vanadyl porphyrin distributions of sediments. *Geochim. Cosmochim. Acta.*, **57**, 1367-1377
- Sundararaman P., Schoell M., Littke R., Baker D.R., Leythaeuser D. and Rullkötter J. (1993) Depositional environment of Toarcian shales from northern Germany as monitored with porphyrins. *Geochim. Cosmochim. Acta.*, **57**, 4213-4218
- Sundararaman P. and Vestel C. (1993) *Org. Geochem.*, **20**, 1099-1104
- Thomas D.W. and Blumer M. (1964) Porphyrin pigments of a Triassic sediment. *Geochim. Cosmochim. Acta.* **28**, 1147-1154

- Thomas J.B., Marshall J., Mann A.L., Summons R.E. and Maxwell J.R. (1993) Dinosterane (4,23,24-trimethylsteranes) and other biological markers in dinoflagellate-rich marine sediments of Rhaetian age. *Org. Geochem.*, 20, 91-104
- Thiede J. (1979) History of the North Atlantic Ocean: evolution of an asymmetric zonal palaeoenvironment in a latitudinal ocean basin. In: *Deep Drilling Results in the Atlantic Ocean: Continental Margins and Palaeoenvironment*. (Eds: Talwani *et al.*) *Am. Geophys. Union., Washington D.C., M. Ewing Ser.*, 3, 275-296
- Thiede J. and van Andel T.H. (1977) The paleoenvironment of anaerobic sediments in the late Mesozoic South Atlantic Ocean. *Earth Planet. Science Lett.*, 33, 301-309
- Thiede J. and Suess E. (1983) Coastal upwelling and its sediment record, part B, Sedimentary records of ancient coastal upwelling. Plenum, New York.
- Thiede J. and Jünger B. (1992) See Summerhays *et al.* (1992) pp. 47-76
- Thierstein H.R. (1979) Palaeoceanographic implications of organic carbon and carbonate distribution in Mesozoic deep sea sediments. In: *Deep Drilling Results in the Atlantic Ocean; Continental Margins and Palaeoenvironment*, (Eds. Talwani M., Hay W. and Ryan W.B.F.), Maurice Ewing Series 3, *Am. Geophys. Union.* Washington, D.C., 249-274
- Thierstein H.R. and Berger W.H. (1978) Injection events in ocean history. *Nature Lond.*, 276, 461-466
- Thierstein H.R. (1989) The mid-Cretaceous enigma. In: *Productivity of the Ocean: Present and Past*. (Eds: Berger W.H. *et al.*) Wiley, Chichester, pp. 355-375
- Treibs A. (1934) Chlorophyll und Haminderivate in bitumens Gesteinen, Erdölen, Erdwachsen und Asphalten. *Liebigs Ann.*, 510, 42-62
- Treibs A. (1936) Chlorophyll- und haminderivate in organischen mineralstoffen. *Angewandte Chemie*, 49, 682-686
- Thurrow J., Kuhnt W. and Wiedmann J. (1982) Zeitlicher und Paläogeographischer Rahmen der Phthanit und Black Shale- Sedimentation in Marokko., *N. Jb. Geol. Paläont.*, 165, 147-176
- Thurrow J., Brumsack H.J., Littke R., Meyers P.A. and Rullkötter J. (1992) Mid-Cretaceous events in the Indian Ocean – A key to understanding the global picture. In: *Indian Ocean Synthesis Volume*. (Eds: Duncan R., Kidd R., Rea D.K., von Rad U. and Weissel J.), pp. 253-273. *Am. Geophys. Union.*, Washington
- Tissot B., Califet-Debyser Y., Deroo G. and Oudin J.L. (1971) Origin and evolution of hydrocarbons in early Toarcian shales. *Am. Assoc. Pet. Geol. Bull.*, 55, 2177-2193
- Tissot B. (1979) Effects on prolific petroleum source rocks and major coal deposits caused by sea level changes. *Nature*, 277, 463-465
- Tissot B., Demaison G., Masson P., Delteil J.R. and Combaz A. (1980) Palaeoenvironment and petroleum potential of middle Cretaceous black shales in Atlantic Basin., *Bull. Am. Ass. Petrol. Geol.*, 64, 2051-2063
- Trüper H.G. and Pfennig N. (1992) The Family Chlorobiaceae. In: *Prokaryotes: a handbook on the biology of bacteria*. Vol. 4 (Ed: Balows A.), pp. 3583-3592
- Tucholke B.E. and Vogt P.R. (1979) Western North Atlantic: sedimentary evolution and aspects of tectonic history. In: *Initial reports of the deep sea drilling project*, 23 (Eds. Tucholke B.E. Vogt P.R.), Washington (US Government printing office), pp.791-825
- Tyson R.V. (1987) The genesis and palynofacies characteristics of marine petroleum source rocks. See Brooks and Fleet, 1987. Pp. 47-67
- Tyson R.V. and Pearson T.H. (Eds.) (1991) Modern and ancient continental shelf anoxia *Geol. Soc. Spec. Publ.*, No. 58
- Vai G.B. and Ricci Lucchi F. (1977) Algal crust, autochthonous and clastic gypsum in a cannibalistic evaporite basin: a case history from the Mesinian of Northern Appenines. *Sedimentology.*, 24, 211-244
- Vail P.R., Mitchum R.M. and Thompson S. (1977) Global cycles of relative changes of sea-level. *A.A.P.G. Mem.*, 26, 83-98
- van Andel T.J.H., Heath G.R. and Moore T.C. (1975) Cenozoic history and palaeoceanography of the central equatorial Pacific. *Geol. Soc. Am., Mem. No.143*, 134
- van Breemen R.B., Vanjura F.L. and Schwartz S.J. (1991) *J. Chrom.*, 542, 373-383
- Van Cappellen P. and Canfield D.E. (1993) Comment on "Lack of evidence for enhanced preservation of sedimentary organic matter in the oxygen minimum of the Gulf of California" by Calvert S.E., Bustin R.M. and Pederson T.F. *Geology.*, 21, 570-571
- Van Cappellen P. and Ingall E.D. (1994) Benthic phosphorous regeneration, net primary production and ocean anoxia: A model of the coupled marine biogeochemical cycles of carbon and phosphorous. *Palaeoceanography*, 9(5), 677-692

- Vandenberg J., Klootwijk C.T. and Wonders A.A.H. (1978) Late Mesozoic and Cenozoic movements of the Italian Peninsula: Further palaeomagnetic data from the Umbrian sequence. *Geol. Soc. Am. Bull.*, 89(1), 133-150
- van Graas G., Viets T.C., de Leeuw J.W. and Schenck P.A. (1983) A study of the soluble and insoluble organic matter from the Livello Bonarelli, a Cretaceous black shale deposit in Central Apennines, Italy., *Geochim. Cosmochim. Acta.*, 47, 1051-1059
- van Kaam-Peters H.M.E., Schouten S., de Leeuw J.W. and Sinninghe Damsté J.S. (1995) The Kimmeridge clay formation: Biomarker and molecular stable carbon isotope analyses. *Proc. 17th International Conference Org. Geochem.*, 216-218
- van Kaam-Peters H.M.E. (1997) Biomarker and compound-specific stable carbon isotope analysis of the Early Toarcian shales in SW Germany. In: *The depositional environment of Jurassic organic-rich sedimentary rocks in NW Europe. A biomarker approach*. PhD Thesis, University of Utrecht, pp. 191-216
- Vaughan D.J., Sweeny M., Diedel G.F.R. and Haranczyk C. (1989) The Kupferschiefer: An overview with an appraisal of the different types of mineralisation. *Econ. Geol.*, 84, 1003-1027
- Verne-Mismer J., Ocampo R., Callot H.J. and Albrecht P. (1986) Identification of a novel C<sub>33</sub> DPEP petroporphyrin from Boscan crude oil: evidence for geochemical reduction of carboxylic acids. *Tet. Letts.*, 37, 5257-5260
- Verne-Mismer J., Ocampo R., Callot H.J. and Albrecht P. (1987) Isolation of a series of vanadyl-tetrahydrobenzopetroporphyrins from Trimahdit oil shale. Structure determination and total synthesis of the major constituent. *J. Chem. Soc., Chem. Commun.*, 1581-1583
- Verne-Mismer J., Ocampo R., Callot H.J. and Albrecht P. (1988) Molecular fossils of chlorophyll c of the 17-nor-DPEP series. Structure determination, synthesis, geochemical significance. *Tet. Lett.*, 29, 371-374
- Verne-Mismer J., Ocampo R., Callot H.J. and Albrecht P. (1990) New chlorophyll fossils from Moroccan oil shales. Porphyrins derived from chlorophyll c<sub>3</sub> or a related pigment? *Tet. Lett.*, 31, 1751-1754
- Verne-Mismer J., Ocampo R., Bauder C., Callot H.J. and Albrecht P. (1990b) *Energy & Fuels*, 4, 639-643
- Villanueva J., Grimalt J.O., de Wit R., Keely B.J. and Maxwell J.R. (1994a) Chlorophyll and carotenoid pigments in solar saltern microbial mats. *Geochim. Cosmochim. Acta.*, 58, 4703-4715
- Villanueva J., Grimalt J.O., de Wit R., Keely B.J. and Maxwell J.R. (1994b) Sources and transformations of chlorophylls and carotenoids in a monomictic sulphate-rich karstic lake environments. *Org. Geochem.*, 22, 739-757
- Vogt P.R. (1989) Volcanogenic upwelling of anoxic, nutrient-rich water: a possible factor in carbonate-bank/reef demise and benthic faunal extinctions? *Geol. Soc. Am. Bull.*, 101, 1225-1245
- von Damm K.L., Edmund J.M., Grant B., Measures C.L., Walden B. and Weiss R.F. (1985) Chemistry of submarine hydrothermal solutions at 21°N. East Pacific Rise. *Geochim. Cosmochim. Acta.*, 49, 2197-2220
- von Kühn and Roth (1979) Beiträge zur Kenntnis der Salzlagertstätte am Oberrhein. *Z. Geol. Wiss.*, 7, 953-966
- von Rad U., Schulz H. and Sonne 90 scientific party. (1995). Sampling the oxygen-minimum zone off Pakistan: glacial-interglacial variations of anoxia and productivity (preliminary results, Sonne 90 cruise).
- Wakeham S.G., Sinninghe Damsté J.S., Kohnen M.E.L. and de Leeuw J.W. (1995) Organic sulphur compounds formed during early diagenesis in Black Sea sediments. *Geochim. Cosmochim. Acta.*, 59, 521-533
- Walker J.C.G. (1986) Global biogeochemical cycles of carbon, sulphur and oxygen., *Mar. Geol.*, 70, 159-174
- Waples D.W. (1983) A reappraisal of anoxia and organic richness, with emphasis on Cretaceous of North Atlantic., *A.A.P.G. Bull.*, 67, 963-978
- Waring J.R. (1991) Sedimentary porphyrins: their significance in depositional environment assessment. PhD Thesis, University of Bristol.
- Warren, J.K. (1986) Shallow water evaporitic environments and their source rock potential. *J. Sediment. Pet.*, 56, 442-454
- Warren J.K. (1989) *Evaporitic Sedimentology: Importance in Hydrocarbon Accumulation*. Prentice Hall, Englewood Cliffs, New Jersey.
- Watanabe N., Yamamoto K., Ishikawa H. and Yagi A. (1993) New chlorophyll a- related compounds isolated as antioxidants from marine bivalves. *J. Nat. Prod.*, 56, 305-317

- Watts A.B. and Steckler M.S.** (1979) Subsidence and eustasy at the continental margins of eastern North America. In: *Deep Sea Drilling Results in the Atlantic Ocean: continental margins and palaeoenvironment*. (Eds: Talwani M., et al.). *Am. Geophys. Union. Maurice Ewing Series.*, 3, 218-239
- Wedepohl K.H.** (1964) Untersuchungen am Kupferschiefer in Nordwestdeutschland: Ein Beitrag zur Deutung der Genese bituminöser Sedimente. *Geochim. Cosmochim. Acta.*, 28, 305-364
- Wedepohl K.H.** (1971) "Kupferschiefer" as a prototype of syngenetic sedimentary ore deposits. *Soc. Mining Geol. Japan (Spec. Issue)* 3, 268-273
- Weissert H., McKenzie J. and Hochuli P.** (1979) Cyclic anoxic events in the Early Cretaceous Tethys Ocean. *Geology*, 7, 147-151
- Weissert H.** (1981) The environment of deposition of black shales in the Early Cretaceous: an ongoing controversy. In: *Deep Sea Drilling Project: a decade of progress*. (Eds: Warme et al.) *Soc. Econ. Palaeontol. Mineral., Spec. Publ.*, 32, 547-560
- Weissert H.** (1989) C-isotope stratigraphy, a monitor of palaeoenvironmental change: a case study from the Early Cretaceous. *Surv. Geophys.*, 10, 1-61
- Weissert H.** (1990) Siliciclastics in the early Cretaceous Tethys and North Atlantic Oceans: Documents of periodic greenhouse climate conditions., *Mem. Soc. Geol. Ital.*, 44, 59-69
- Weissert H., Lini A., Föllmi K.B. and Kuhn O.** (1998) Correlation of Early Cretaceous carbon isotope stratigraphy and platform drowning events: a possible link? *Palaeo. Palaeo. Palaeo.*, 137, 189-203
- Wiedenmayer F.** (1980) Die Ammoniten der mediterranen Provinz im Pliensbachian und unteren Toarcian aufgrund neuer Untersuchungen im Generoso-Becken (Lombardische Alpen). – *Denkschr. Schweiz. Naturf. Ges.*, 93, 261
- Welte D.H. and Waples D.W.** (1973) Über die Bevorzugung geradzahliger *n*-Alkane in Sedimentgesteinen. *Naturwissenschaften* 60, 516-517
- Wilde P. and Berry W.B.N.** (1982) Progressive ventilation of the oceans potential for return to anoxic conditions in the post-Palaeozoic. See Schlanger and Cita, 1982., pp. 209-224
- Wolff G.A., Murray M., Maxwell J.R., Hunter B.K. and Sanders J.K.M.** (1983) 15,17-butano-3,8-diethyl-2,7,12,18-tetramethylporphyrin-a novel naturally occurring tetrapyrrole. *J. Chem. Soc., Chem. Commun.*, 922-924
- Woolley P.S., Keely B.J. and Hester R.E.** (1997) Surface enhanced resonance Raman spectroscopic identification of chlorophyll *a* allomers. *J. Chem. Soc., Perkin Trans. 2.*, 1731-1734
- Yen T.F., Boucher L.J., Dickie J.P., Tynan E.C. and Vaughan G., J.** (1969) *Inst. Pet., London*, 55, 87
- Ziegler P.A.** (1982) Geological atlas of Western and Central Europe. Published by Shell Int. Petr. Maatschap. B.V., Den Haag.
- Zimmerman H.B., Boersma A. and McCoy F.W.** (1986) Carbonaceous sediments and palaeoenvironment of the Cretaceous South Atlantic Ocean. See Brooks and Fleet.
- Zorn H.** (1971) Paläontologische stratigraphische und sedimentologische Untersuchungen des Salinatorredolomits (Mitteltrias) der Tessiner Kalkalpen. *Schweiz. Paläont. Abh.*, 91, 1-90



**ALMOST THE LAST PAGE**

THE END